Isomorphism, cold-adaptation, and phosphorylation of sarcomeric tropomyosin

by © A. Madhushika M. Silva, B.Sc. (Hons.)

A Thesis Submitted to the School of Graduate Studies in Partial Fulfillment of the Requirements for the Degree of

Doctor of Philosophy

Faculty of Science, Department of Biochemistry

Memorial University of Newfoundland

June 2021

St. John’s Newfoundland and Labrador

Abstract

Tropomyosin is a dimeric protein containing 284 amino acids per chain that is found, in association with F-actin and troponin, within the thin filament, a complex that regulates muscle contraction.

The thesis is composed of three results chapters:

i) The existence of beta tropomyosin (Tpm2) is demonstrated for the first time in fish (*Salmo salar*). Compared to the mammalian homologue, salmon Tpm2 has fewer cysteine (one per chain) and tyrosine (five per chain) residues. Tpm2 contributes half of the total tropomyosin in the jaw, tongue, and fin muscles. A Tpm1 isoform, either alpha-1 chain-like isoform X1 (cheek dark, jaw and tongue) or alpha (fin), accounts for the remainder. Salmon tropomyosins are distinguishable based on electrophoretic mobility, affinity for troponin-Sepharose, tryptic peptide mapping, and variable carboxyl-terminal regions (residues 276 - 284): beta (Tpm2), Leu-Ala-Leu-Asn-Asp-Met-Thr-Thr-Leu; alpha-1 chain-like isoform X1, His-Ala-Leu-Asn-Asp-Met-Thr-Ala-Ile, and alpha (Tpm1), Asn-Ala-Leu-Asn-Asp-Met-Thr-Ser-Ile.

ii) The relative instability of the most abundant isoform of Atlantic salmon, Tpm1, (20 substitutions vs. mammal) is due to a neutral 77th amino acid (Thr in salmon; Lys in rabbit), and glycines at 24 and 27 (Ala and Gln in rabbit). Incorporation of the respective mesophilic amino acid increases resistance to thermal unfolding as determined by calorimetry and chymotrypsin digestion at Leu-169, a site ~100 amino acids far away from residue-77. PyMOL indicates ion pairing between Lys-77 and Glu-82 in the opposite chain.

Binding of Tpm1 to troponin-Sepharose is influenced by N-terminal acetylation and the mutation of residues 24, 27, and 77. Furthermore, wild type Tmp1 displays a higher affinity for F-actin at 4 ^{o}C (K_D, ~ 0.1 µM) than 30 ^{o}C (K_D, ~ 1.6 µM). In contrast, the mesophilic homologue binds less tightly to actin at lower temperatures.

iii) Phosphorylation of serine 283 increases the susceptibility of mammalian Tpm1.1(α) to chymotrypsin (at Leu-169) and trypsin (at Arg-133), suggesting an induced opening of the center of the molecule >150 amino acids upstream, and shifts the corresponding portion of the circular dichroism unfolding profile. These results infer a change in exposure of actin-binding periods 4 (residues 124 - 147) and 5 (residues 166 - 189). The proposal is consistent with a two-fold increase in affinity for F-actin in co-sedimentation experiments.

Acknowledgments

I would like to express my deep and sincere gratitude to my research supervisor, Dr. David H. Heeley, for his immense knowledge, patience, motivation, guidance, and support during all this time. It was a great privilege and an honor to work and study under his guidance. Without his guidance and persistent support, this thesis would not have been possible.

I cannot express enough thanks to my supervisory committee members Drs. Sherri L. Christian and Martin E. Mulligan for the assistance, suggestions, guidance, and support throughout my project.

To all the staff of the Department of Biochemistry, thank you - for all the support you gave me throughout this entire period.

Finally, my loving family - mom, dad, sister, and my dearest friends, without all your love and support this thesis would not have been possible.

Table of Contents

List of Tables

List of Figures

List of abbreviations and symbols

ADP	Adenosine diphosphate
ATP	Adenosine triphosphate
C-	Carboxy terminal domain
CAPS	N-cyclohexyl-3-aminopropanesulfonic acid
C-cTnT	C-terminal region of human cardiac troponin
CNBr	Cyanogen bromide
cTnC	Cardiac TnC
C-TnC	C-domain of TnC
C-TnI	C-terminal region of TnI
C-TnT2	C-terminal region of TnT2
DTT	Dithiothreitol
EGTA	Ethylene glycol tetraacetic acid
EST	Expressed sequence tag
IPTG	Isopropyl beta-D-1-thiogalactopyranoside
MOPS	3-morpholinopropanesulfonic acid
myosin-S1	Myosin subfragment I
N-	Amino terminal domain
N-cTnI	Cardiac exclusive N-terminal domain of TnI
NMR	Nuclear magnetic resonance
NP40	Nonyl phenoxylpolyethoxylethanol40
N-TnC	N-domain of TnC
Pi	Inorganic phosphate
PMSF	Phenylmethylsulfonylfluoride
PVDF	Polyvinylidene difluoride
RCSB PDB	Structural Bioinformatics Protein Data Base

SDS-PAGE	Sodium dodecylsulfate polyacrylamide gel electrophoresis
T_m	Melting temperature
TnC	Troponin C
TnI	Troponin I
TnT	Troponin T
TnT1	N-terminal domain of TnT
TnT2	C-terminal domain of TnT
TPM	Tropomyosin gene
Tpm	Tropomyosin protein
UV	Ultraviolet

Appendix

Chapter 1. Introduction

1.1 Muscles in the body

Muscle tissue is specialized in contractions meaning it can shorten and generate pulling forces to enable movements in locomotion, heart contractions, blood circulation, breathing, and digestion (Nelson & Cox, 2017). The contractions of some muscles are voluntary whereas some are involuntary. Muscle tissue in the body can be divided mainly into smooth and striated muscles depending on the ultrastructure of the cells. Smooth muscle cells have no striations, do not function under voluntary control, contain only one nucleus per cell, and are tapered at both ends. These occur in the walls of hollow organs such as the intestines, stomach, urinary bladder, and around passages such as the respiratory tract and blood vessels. Striated muscles of the body on the other hand are highly organized and are distinguished by their ultrastructure with striation (Figure 1.1). These are comprised of skeletal and cardiac muscles. The skeletal muscles attach to bones and control contractions of physical activities such as locomotion, maintain posture, etc. Contractions by the skeletal muscle tissue are consciously controlled by the involvement of the somatic nervous system. Cardiac muscles make the walls of the heart and the contractions generated by this tissue are controlled involuntarily by the autonomous nervous system.

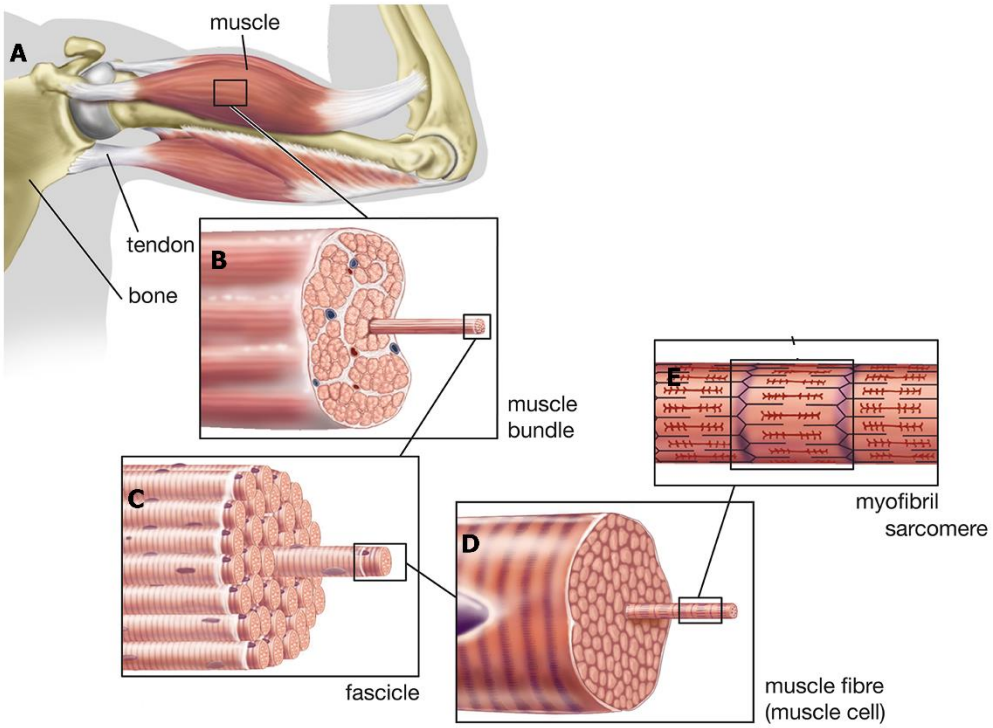
A
muscle
tendon
bone
B
muscle
bundle
C
fascicle
D
muscle fibre
(muscle cell)
E
myofibril
sarcomere

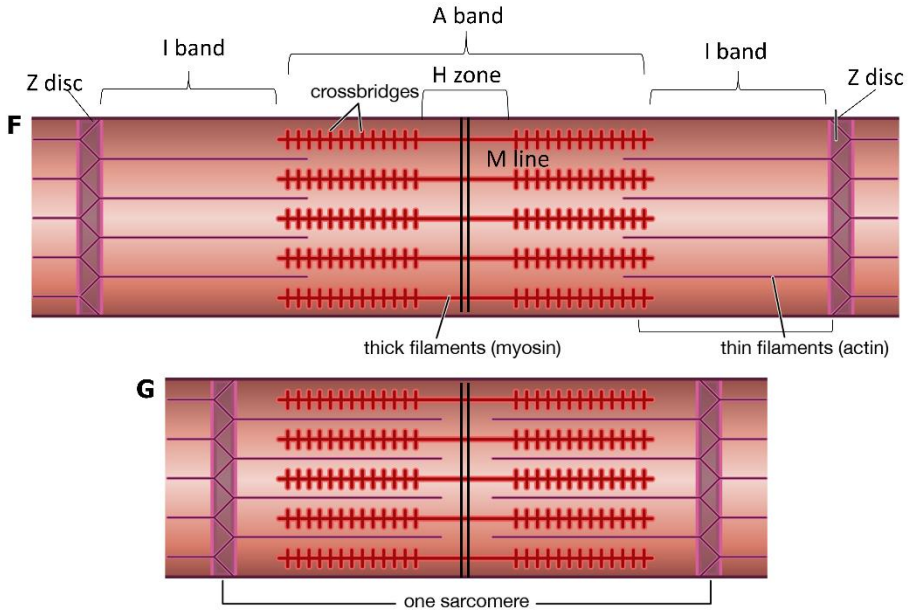
A band
I band
I band
Z disc
H zone
crossbridges
Z disc
F
M line
thick filaments (myosin)
thin filaments (actin)
G
one sarcomere

Figure 1.1. The organization of striated muscles. (A) Schematic presentation of skeletal muscles. (B) Muscle bundle. (C) Muscle fascicle. (D) Muscle fiber (cell). (E) Sarcomere. (F) Ultra-structure of the sarcomere. Horizontal lines: Purple - thin filaments rich in actin and Red - thick filaments rich in myosin. Crossbridges- Myosin heads. Z-discs - anchoring points for thin filaments and demarcation of the sarcomere. I-band - zone of thin filaments. A-band - zone of thin and thick filaments (length is equal to the length of thick filaments). H-zone - the region of thick filaments. M-line - demarcation of the middle of the thin filament (G) Shortened sarcomere during contraction showing reduced I-band length with unchanged A-band length. Adapted from Encyclopedia Brittanica with permission.

1.2 Striated muscles

While being structurally and functionally similar, depending on the contractile and metabolic phenotypes, the striated muscles are further categorized as slow-oxidative/Type I, fast-oxidative/Type IIa, and fast-glycolytic/Type IIb (Peter et al., 1972, Ruegg, 1988). The primary metabolic pathway used by the muscle type determines whether to be categorized as an oxidative or anaerobic form. The slow oxidative muscle reaches maximum tension relatively slowly and uses oxidative phosphorylation to produce adenosine triphosphate (ATP). These muscles contain many structural adaptations to maximize ATP production through aerobic metabolism. They are smaller in diameter to prevent large tension, include more mitochondria, and contract for longer periods due to their ability to produce more ATP. This tissue has an extensive supply of blood to carry more oxygen and contains myoglobin giving the slow fibers its distinctive red color. Additionally, slow fibers are also capable of withstanding fatigue for a long period, hence becoming very useful in maintaining posture, producing isometric contractions, and stabilizing bones and joints. Fast glycolytic fibers generate fast contractions through anaerobic glycolysis and generate a fewer number of ATP molecules per cycle, which makes them highly susceptible to fatigue. These muscles are larger in diameter and contain large amounts of glycogen reserves. They contain a low number of mitochondria and a lower blood supply making the fibers attain a white color. Compared to both slow oxidative and fast glycolytic fibers, fast oxidative fibers possess intermediary characteristics. They contract faster while undergoing aerobic respiration to produce ATP, therefore, are capable of generating fast and strong powerful movements due to their ability to produce high

tension. Additionally, due to oxidative respiration, they do not fatigue quickly. The percentage of these three fiber types in mammalian skeletal muscles is variable and human muscles contain a mix of all three. But in certain vertebrates such as fish (i.e., Salmonidae family), there are distinguishable anatomical regions in the skeletal muscles that are composed of one specific fiber type. For example, the main trunk muscle of Atlantic salmon (*Salmo salar*) is made of fast oxidative fibers whereas a stripe along the lateral line consists of slow oxidative fibers making salmon an ideal model to obtain these muscle fibers separately (Bone et al., 1995).

1.3 Striated muscle functional unit "the sarcomere"

The skeletal muscles in the body are attached to the bones (Figure 1.1A) via tendons and are made of bundles (Figure 1.1B) of muscle fibers named fascicules (Figure 1.1C). In both skeletal and cardiac muscle cells, the muscle fibers (Figure 1.1D) are filled with myofibrils (Figure 1.1E), which are filaments containing contractile proteins that occupy ~85% of the intracellular space (Macdougall et al., 1982; Alway et al., 1988). The remaining 15% accounts for the sarcoplasm that contains the organelles such as sarcoplasmic reticulum, mitochondria, and ribosomes (Claassen et al., 1989). The striated muscles get their name due to the ultrastructure under the microscope owing to the presence of sarcomeres (Figure 1.1E inset), which are the functional contractile units of myofibrils (muscle cells). A sarcomere is a defined area that is contained between Z-discs and consists of a central anisotropic dark region rich with myosin identified as A-bands composed of thick filaments that stretch towards Z-discs from the centers (Hanson & Huxley, 1953 and as reviewed in

Luther, 2009) (Figure 1.1F). The thick filaments are anchored to the middle of the sarcomere (M-line) via myomesin (Figure 1.1F). Two actin-dominated light isotropic regions, identified as I-bands are found on either side of the A-band (Huxley, 1953) consists of thin filaments and attach to the Z-line via alpha-actinin (Figure 1.1F). The H-zone in the middle of the A-band is comparatively lighter due to the existence of only thick filaments (Figure 1.1F). An identical set of proteins make up the sarcomeres of cardiac, slow oxidative, and fast oxidative skeletal muscles, but the existence of different isoforms (Bandman, 1992) gives rise to the unique properties of each muscle. In 1954 scientists described the molecular basis of contraction using high-resolution microscopy (Huxley & Niedergerke, 1954; Huxley & Henson, 1954). According to this study, they observed A-band rich in myosin remains its length relatively constant where the I-band rich in actin shortens during contractions (Figure 1.1G) leading to the sliding filament theory (Huxley & Simmons, 1971) which states the sliding of actin filaments past myosin during muscle contraction. Coupled with the energy from ATP hydrolysis (Lorand, 1953; Davies, 1964) the two filaments slide past each other by a mechanical force generated by the cyclic interaction of actin and myosin (Huxley, 1969).

1.4 The thin filaments

Selective extraction of I-bands (Figure 1.1F and G) from the muscle fibers demonstrated the release of tropomyosin along with actin suggesting that they are components in the thin filaments (Corsi & Perry, 1958). Filamentous actin (F-actin) appears as a slowly twisted double-strand of actin monomers (G-actin) (Figure 1.2). In the actin filament, there are 13

actin monomers per full turn (Fujii et al., 2010). The tropomyosin dimers in the thin filament interact via end-to-end (N- to C-terminal) to form two long continuous helical cables that wrap around the F-actin (Hanson & Lowy, 1964; Li et al., 2011) (Figures 1.2). In a 2015 study, von der Ecken showed that the tropomyosin-binding groove on F-actin is lined with positively charged side-chains (von der Ecken et al., 2015). One tropomyosin molecule spans seven actin monomers and interacts with one molecule of the troponin complex.

Troponin is a complex that consists of three subunits: troponin C (TnC) which binds Ca^{2+}, troponin T (TnT) which interacts with tropomyosin, and troponin I (TnI) which carries out an inhibitory function (Figure 1.2). Troponin is distributed at regular intervals along the entire length of thin filaments with no physical connection between two neighboring molecules (Ohtsuki et al., 1967; Ohtsuki, 1974). The various subunits form a globular core domain that is made of TnC, TnI, and C-terminal domain of TnT (TnT2), and an extended tail formed by the N-terminal domain of TnT (TnT1) (Figure 1.2). TnT provides binding sites for tropomyosin notably at two sites. TnT1 attaches to either side overlap region of the tropomyosin (binding site 1) (Figure 1.2) and TnT2 binds to the central region close to cysteine-190 (binding site 2) (Figure 1.2) (Ohtsuki, 1979; Pearlstone & Smillie, 1982; Tanokura et al., 1983; Morris & Lehrer, 1984; Heeley et al., 1987; White et al., 1987; Yamada et al., 2020 and Oda et al., 2020). Additionally, the actin–tropomyosin interfaces of the troponin complex include the inhibitory region of TnI, the C-terminal region of TnI (C-TnI), and the C-terminal region of TnT2 (C-TnT2) (Takeda et al., 2003). Recent cryo-EM structures (Yamada et al 2020 and Oda et al 2020) have shown that similar to tropomyosin, the troponin complex also spans seven actin monomers. The entire troponin

complex is extremely elongated, on the actin filament, the upper four units of one strand are bound by C-TnI and troponin core while TnT1-linker extends across the actin filaments down towards the N-terminus of tropomyosin spanning three actin units of the opposite strand (Figure 1.2). The N-terminal residues of TnT1 form the terminal α-helix that interacts with the head-to-tail junction of tropomyosin in an anti-parallel manner (Yamada et al., 2020 and Oda et al., 2020). Each component of the thin filament will be now discussed in detail in the upcoming sub-sections.

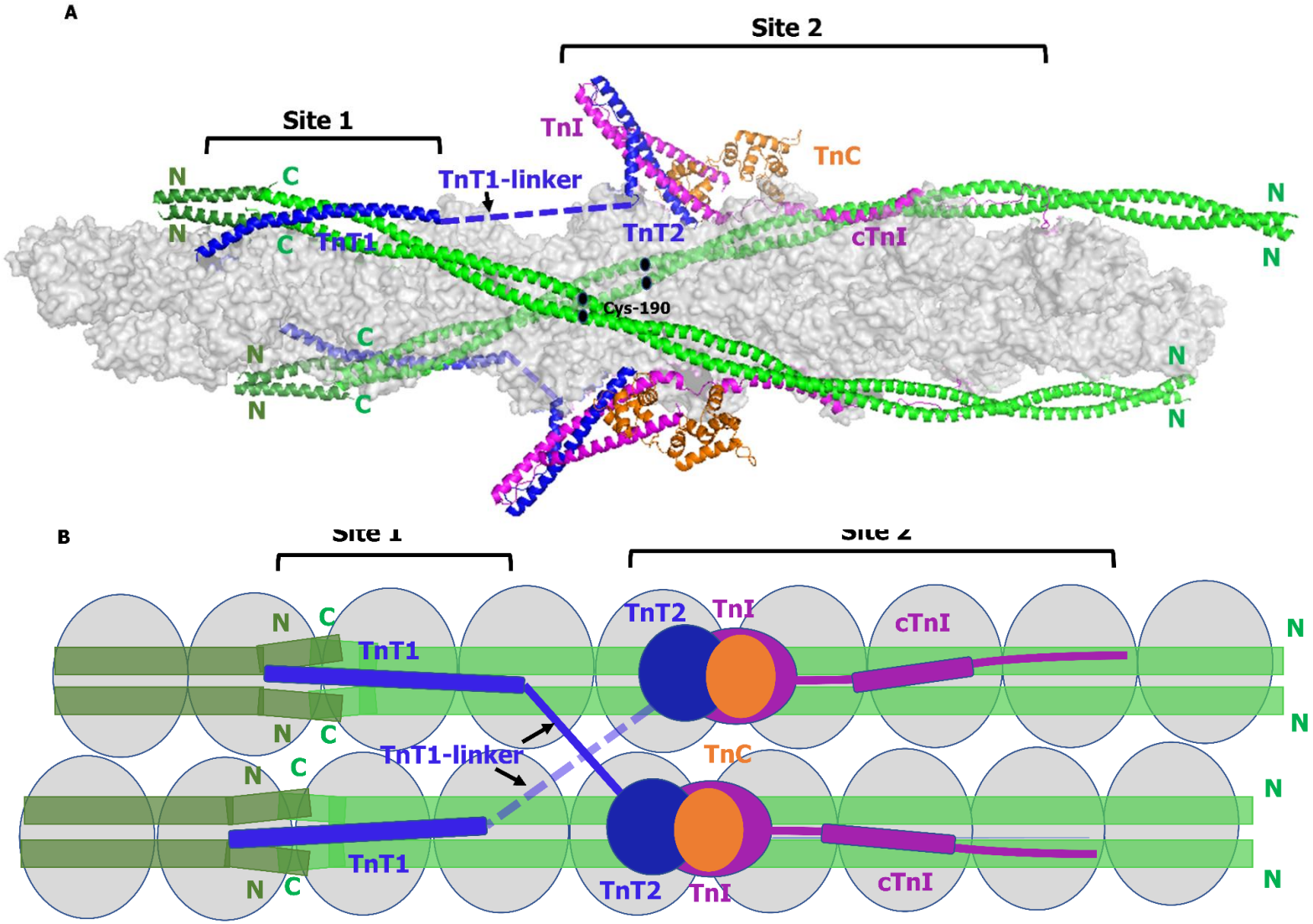
A
Site 2
Site 1
TnI
TnC
TnT1-linker
N
C
N
C
TnT1
TnT2
cTnI
N
N
Cys-190
C
N
C
N
C
N
N
B
Site 1
Site 2
N
C
TnT1
TnT2
TnI
cTnI
N
N
C
TnT1-linker
TnC
N
C
N
TnT1
N
C
TnT2
TnI
cTnI
N
N

Figure 1.2. The organization of thin filament complex in the Ca^{2+} free state. Ash - F-actin. Green - Tropomyosin coiled-coiled positioning along the grooves of F-actin as a continuous cable via head-to-tail interactions. N- N-terminal end of tropomyosin. C- C-terminal end of tropomyosin. Orange - TnC, Magenta - TnI. Blue - TnT. Black - Cys-190. A) Cryo-EM structure, PDB ID: 6KN7. Seven actin monomers interact with one tropomyosin dimer and one heterotrimeric troponin complex. The TnT1 binds to site 1 at the head-to-tail overlap region and TnT2 binds to site 2 near Cys-190 of tropomyosin. The entire troponin complex is extremely elongated. On the actin filament, the upper four units of one strand are bound to the troponin core (TnC, TnI, and TnT2) and C-TnI while the bottom three of the opposite strand are bound by TnT1 that extends to the head-to-tail overlap region of tropomyosin in an anti-parallel manner. B) Comparative schematic representation of the thin filament.

1.4.1 Tropomyosin

1.4.1.1 Discovery

Identified in the contractile apparatus of skeletal muscle, tropomyosin was initially recognized as an asymmetric protein and a prototype of myosin due to its similarity in both amino acid composition and physical properties giving it the name tropomyosin (Bailey, 1946; Bailey, 1948). The isoelectric range is between 4.2 - 4.6 and precipitation occurs with 50 - 60 % ammonium sulfate. At low ionic solutions, it shows an enormous viscosity due to spontaneous aggregation. The variants of the protein that exist in the muscle thin filament are made of two alpha-helical subunits of 284 amino acids of ~ 33 kDa arranged in a coiled-coil structure (Astbury et al., 1948; Woods, 1966; Frank Woods, 1967; Hodges et al., 1972; Sodek et al., 1972; Smillie, 1979).

1.4.1.2 Genes and isoforms

The vertebrate classes namely: fish, amphibians, avians, and mammals use four distinct tropomyosin genes namely: TPM1, TPM2, TPM3, and TPM4. These genes produce more than 40 isoforms via alternative promotors, alternative splicing of exons, and with different C-termini (Lees-Miller & Helfman, 1991; Pittenger et al., 1994; Perry, 2001; Gunning et al., 2005). Each of these genes is named when first identified and described after the protein they encoded. The first two isoforms which are also the predominant types, identified from striated muscles of rabbit (284 amino acids) were alpha (α-tropomyosin) coded by TPM1 and beta (β-tropomyosin) coded by TPM2, were given Greek letters as identifiers

(Cummins & Perry, 1973, 1974; Stone & Smillie, 1978; Mak et al., 1980; Pato et al., 1981). TPM3 and TPM4, referred to as gamma and delta respectively were named after fibroblast tropomyosins (MacLeod et al., 1985; Lees-Miller et al., 1990). Isoforms of tropomyosin are termed in accordance with their gene of origin, namely Tpm1 through Tpm4 (Geeves et al., 2015). The tropomyosin genes are highly conserved in terms of exon-intron structural organization (Figure 1.3) and were generated by duplication of an ancestral gene. The different exons are named 1a, 1b, 2a, 2b, 3, 4, 5, 6a, 6b, 7, 8, 9a, 9b, 9c and 9d. The transcription is initiated at either exon 1a or 1b. Among all tropomyosins exons 3, 4, 5, 6, 7, 8, and 9 are expressed. Exons 2 and 6 are expressed as a spliced variant, either 2a or 2b and 6a or 6b. The C-terminus is encoded by the choice of a different exon 9. Traditionally tropomyosin was also classified as high molecular weight (HMW) containing 284 amino acids and low molecular weight (LMW) with 248 amino acids, which differ in the N-terminus with HMW having exons 1a and 2 and LMW having only exon 1b (Cohen & Cohen, 1972; Fine & Blitz, 1975; Potter, 1982; Lewis et al., 1983; Pittenger et al., 1994).

In mammals (*Mus musculus*) TPM1 has the most complex gene structure comprising 15 exons. The use of two alternative promoters 1a and 1b combined with alternatively spliced exons 2a, 2b, and 6a, 6b, and the C-terminal exons 9a, 9b, 9c, and 9d (Figure 1.3A) (Ruiz-Opazo & Nadal-Ginard, 1987; Wieczorek et al., 1988; Lees-Miller et al., 1990) gives rise to skeletal muscle, smooth muscle and cytoskeletal isoforms (Wieczorek et al., 1988; Lees-Miller et al., 1990; Goodwin et al., 1991). Exon 2a is found only in smooth muscle tropomyosin (Ruiz-Opazo et al., 1985) whereas exon 9c is restricted to brain cytoskeletal isoforms that consist of less than 284 amino acids (Lees-Miller et al., 1990) and which are

involved in the development and plasticity of the nervous system (Stamm et al., 1993). In birds (*Gallus gallus*), the TPM1 gene is structurally similar to that in mammals with 15 exons and the brain-specific exon 9c (Figure 1.3A) (Lindquester et al., 1989; Lemonnier et al., 1991). A striking difference is the existence of exon 2a which only gets expressed in an embryonic heart isoform (Zajdel et al., 2003). Compared to the mammalian and avian counterparts, amphibian (*Xenopus laevis*) TPM1 lacks the aforementioned exon 9c (Hardy et al., 1991; Gaillard et al., 1998a; Gaillard et al., 1998b) (Figure 1.3A). In species such as pufferfish (*Fugu rubripes*) and zebrafish (*Danio rerio*), TPM1 has been duplicated to generate paralogs TPM1-1 and TPM1-2 (Figure 1.3A) (Ikeda et al., 2003; Toramoto et al., 2004; Dube et al., 2017). TPM1-1 is structurally similar to that of avian and mammalian isoform with the only exception at C-terminus containing only three variations instead of four (Figure 1.3A). TPM1-2 differs from its paralog due to the absence of exons 2a and 6a (Toramoto et al., 2004) (Figure 1.3A). Another noticeable difference in the TPM1-1 and TPM1-2 to the avian and mammalian counterparts is the lack of exon 9c (Figure 1.3A). The Atlantic salmon (*Salmo salar*) TPM1 is not duplicated and is structurally similar to pufferfish and zebrafish TPM1-2. The protein product of this gene Tpm1, (accession number AAB36559) (Heeley et al., 1995) which is also called the alpha-fast tropomyosin is found in the fast skeletal (lighter) muscle (Silva et al., 2020c) which supports high-speed swimming (Bone et al., 1995).

Mammalian TPM2 gives rise to the skeletal and smooth muscle isoforms of beta tropomyosin (Helfman et al., 1986). The gene contains 11 exons. Some of the characteristics include a single promoter exon namely exon 1a, a single second exon

namely 2a, mutually spliced exon 6a or 6b, and 9a and 9d (Figure 1.3B). The amphibian TPM2 is analogous to the mammalian homolog in terms of its structure and the types of isoforms generate (Hardy & Thiebaud, 1992; Gaillard et al., 1999) (Figure 1.3B). The major difference between avian and mammalian TPM2 is the existence, in the former, of the alternative promoter 1b that gives rise to cytoskeletal isoform (248 amino acids) (Libri et al., 1989; Forry-Schaudies et al., 1990) (Figure 1.3B). As shown in mammals, the TPM2 of avians also gives rise to skeletal and smooth muscle isoforms (Fatigati & Murphy, 1984; Forry-Schaudies et al., 1990; Xie et al., 1991). Fish TPM2 unlike other vertebrates does not contain exon 6a (Toramoto et al., 2004) (Figure 1.3B). Although cDNA evidence suggests the existence of beta isoform in fish, it had not been documented at the protein level prior to the research described in Chapter 2 of this thesis and Silva et al., 2020c.

TPM3 of mammals contains 14 exons with the two promoters, exon 2b, a single mutually spliced exon 6a or 6b, and four C-terminal exons which code for slow skeletal muscle and LMW cytoskeletal isoforms (Clayton et al., 1988; Dufour et al., 1998) (Figure 1.3C). In amphibians, although isoforms from TPM3 are not recorded, expressed sequence tag (EST sequences) cDNA evidence shows a TPM3 correspondent that codes for LMW tropomyosin with the accession number BC043980 (Mori et al., 2020) (Figure 1.3C). Details of the amphibian TPM3 lack to this date. Similar to amphibians, EST sequences demonstrate bird TPM3 to consist as several isoforms (226 - 332 amino acids) with at least 12 exons, no internal alternatively spliced exons, and three C-terminal exons (Figure 1.3C). The Tpm3 variant (accession number H9L3K0) of chicken (*Gallus gallus*) consists of 1a, 2b, 3, 4, 5, 6b, 7, 8, and 9a exons. The pufferfish and Zebrafish TPM3 gene compared to

the mammalian counterpart contains no duplication. It contains a single promoter, no internally mutually spliced exons, and two C-terminal exons (Toramoto et al., 2004; Dube et al., 2017) (Figure 1.3C). In early studies, Atlantic salmon was thought to contain a single alpha-slow (Tpm3, Z66490) (Heeley & Hong, 1994; Heeley et al., 1995; Jackman et al., 1996) isoform which is restricted to the slow skeletal (darker) muscle along the lateral line (which supports low-speed cruising) (Bone et al., 1995). In a recent survey (Silva et al., 2020c) two paralogs of Atlantic salmon TPM3 were identified in slow skeletal muscle having the same exon structure (Figure 1.3C) and which encode isoforms Tpm3-1 and Tpm3-2 (accession numbers XP_014016883 and XP_013997720 respectively). The Atlantic salmon TPM3 is different from zebrafish and pufferfish due to the existence of alternative promoter exon 1b (Figure 1.3C).

TPM4 of mammals encodes for cardiac tropomyosin and a cytoskeletal isoform that is composed of 248 amino acids (Yamawaki-Kataoka & Helfman, 1987; Lees-Miller et al., 1990). The rodent gene, which comprises 8 exons, lacks alternatively spliced exons 2a, 6a, 9a, 9b, and 9c (Figure 1.3D). In humans, although exon 9a is present, no isoform is reported to carry this exon. The avian and amphibian TPM4s have 11 exons with the two alternative promotors, exons 2a and 6b, and C-terminal encoding exons 9a and 9d carrying the possibility to code for smooth muscle isoforms (Lindquester et al., 1989; Hardy et al., 1995) (Figure 1.3D). Similar to that of the TPM1, the TPM4 gene in zebrafish and pufferfish is also duplicated generating the two paralogs TPM4-1 and TPM4-2 (Ikeda et al., 2003; Toramoto et al., 2004; Dube et al., 2017) which are structurally similar to the avian and amphibian gene with the two promotors, two alternatively spliced exons and two alternative

C-terminal exons (Figure 1.3D). Similar to TPM1 in Atlantic salmon, TPM4 is also not duplicated. Salmon TPM4 which codes for the variant in the heart, Tpm4 (accession number Z66527, Jackman et al., 1996) contains exons 1a, 2b, 3, 4, 5, 6b, 7, 8, and 9a.

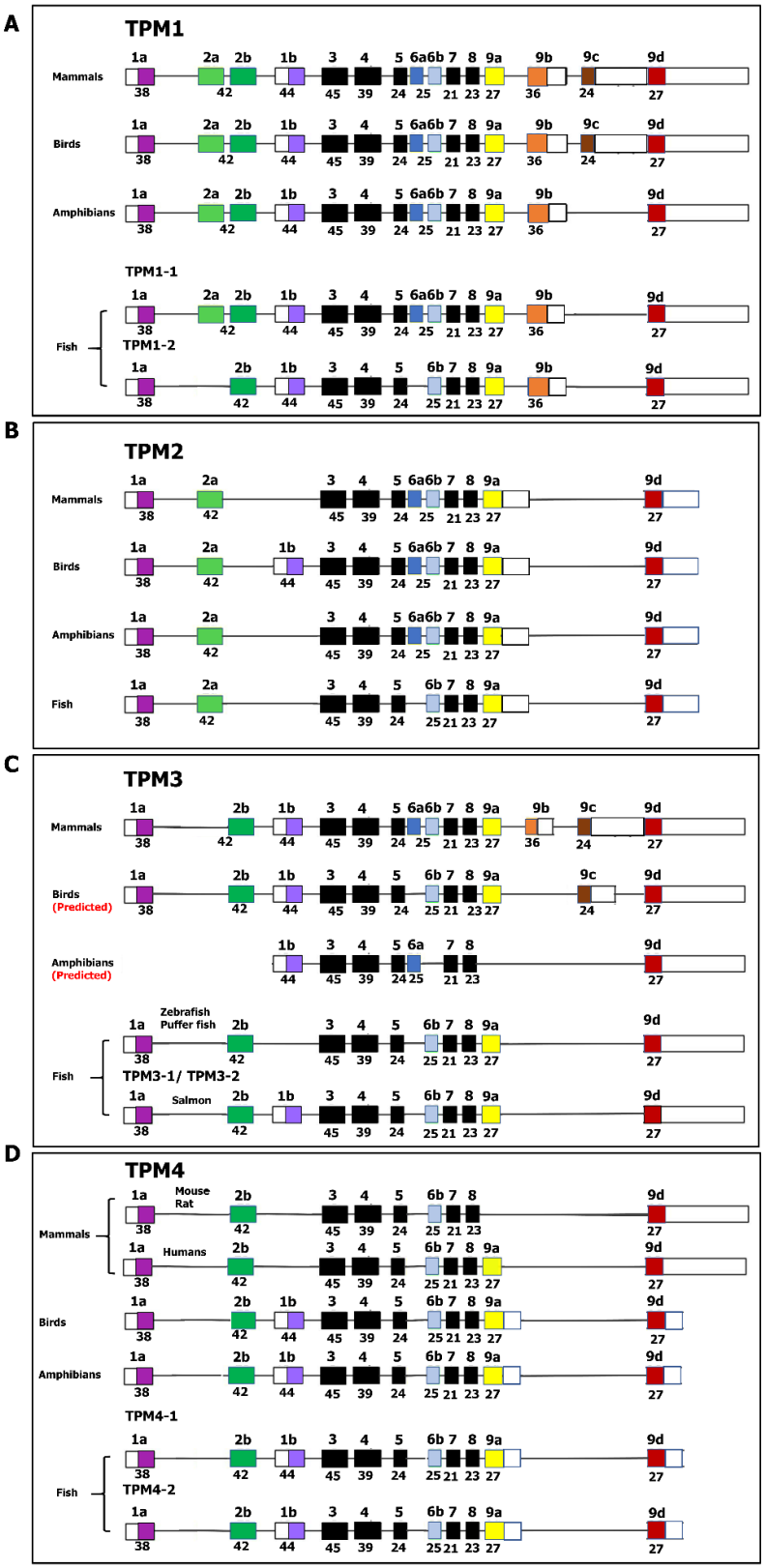
A
TPM1
Mammals
Birds
Amphibians
TPM1-1
Fish
TPM1-2
B
TPM2
Mammals
Birds
Amphibians
Fish
C
TPM3
Mammals
Birds
(Predicted)
Amphibians
(Predicted)
Zebrafish
Puffer fish
Fish
TPM3-1/ TPM3-2
Salmon
D
TPM4
Mouse
Rat
Mammals
Humans
Birds
Amphibians
TPM4-1
Fish
TPM4-2

Figure 1.3. Summary of TPM1, TPM2, TPM3, and TPM4 gene structures in vertebrates. Representative species for each vertebrate class: Mammals - House mouse, rat, and human. Amphibians - African clawed frog. Birds - Chicken. Fish - Puffer fish, zebrafish, and Atlantic salmon. The name of the vertebrate class appears on the left of each row. Exons are presented as boxes for each class out of the total 15 exons (1a, 1b, 2a, 2b, 3, 4, 5, 6, 7, 8, 9a, 9b, 9c, and 9d) and exon numbers are included above each exon. The number of amino acids coded by each exon is indicated below. The 3' and 5' non-coding regions of each exon are indicated in white. Purple- alternate promotors (1a and 1b). Green (2a and 2b) and Blue (6a and 6b) - internally spliced exons. Black - conserved exons (3, 4, 5, 7, and 8). Yellow (9a), Orange (9b), Brown (9c) and Red (9d) - C-terminal exons. (A) TPM1 gene structure. Duplicated TPM1 genes in fish (puffer fish and zebrafish) - TPM1-1 and TPM1-2. (B) TPM2 gene structure. (C) TPM3 gene structure. Predicted gene structures are indicated for bird and amphibian classes. TPM3 is not duplicated in puffer fish and zebrafish. Duplicated TPM3 genes in Atlantic salmon - TPM3-1 and TPM3-2. (D) TPM4 gene structure. The gene structure of humans varies from that of house mouse and rat due to the presence of exon 9a. Duplicated TMP4 genes in fish (puffer fish and zebrafish) - TPM4-1 and TPM4-2.

1.4.1.3 Tropomyosin structure and function

Following its first identification by Bailey in 1946, X-ray crystallography studies revealed tropomyosin to belong to the alpha-helical class of proteins (Astbury et al., 1948). Later it was suggested that tropomyosin contains a repeating heptad of amino acid sequences that enables the formation of a supercoiled structure. The amino acids of the heptad sequence were assigned to an alphabetical letter: a, b, c, d, e, f, and g. (Figure 1.4A). The "a" and "d" positions are occupied by non-polar side chains that fit as knobs into holes holding the two chains together to form the supercoil (Crick, 1953) which later found out to make an adhesive seam along the molecule facilitating the dimerization as well as forming of the core (Figure 1.4B) (Greenfield & Hitchcock-DeGregori, 1995). The "e" and "g" positions occupied by charged residues, provide extra cohesion through electrostatic interactions to opposing helices (Figure 1.4A) (Parry, 1975; McLachlan et al., 1975). The tropomyosin structure deduced using the primary amino acid sequence (Sodek et al., 1972; Stone & Smillie, 1978) of rabbit skeletal tropomyosin confirmed the structure proposed by Crick, 1953 and demonstrated that identical helices can pack in a parallel orientation containing an uninterrupted coiled-coil structure. Tropomyosin molecules polymerize to make a filamentous structure via end-to-end interactions involving 8 to 9 residues of the overlap region. The first high-resolution structure of tropomyosin at 7 Å resolution revealed it to be 20 Å in diameter, 400 Å long, and to contain approximately 3 full turns per molecule (Whitby & Phillips, 2000). More recently, the X-ray crystallography structure of the N-terminal 81 amino acid fragment at 2 Å resolution revealed that the two-fold symmetry of the identical sequences of the molecule is broken by 1.2 Å of an axial stagger and an axial

register allowing bends that ultimately enables the molecule to adopt a conformation with multiple bends (Brown et al., 2001). Despite its continuous alpha-helical coiled-coil structure, tropomyosin contains non-canonical regions with atypical amino acids occurring in heptad positions (explained further in section 1.4.1.4) along its length which have shown to be important in maintaining the flexibility which is critical for binding to the actin, troponin, or to another binding partner. Additionally, the comparison of different tropomyosin isoforms has revealed the flexibility varies from one to the other (Swenson & Stellwagen, 1989).

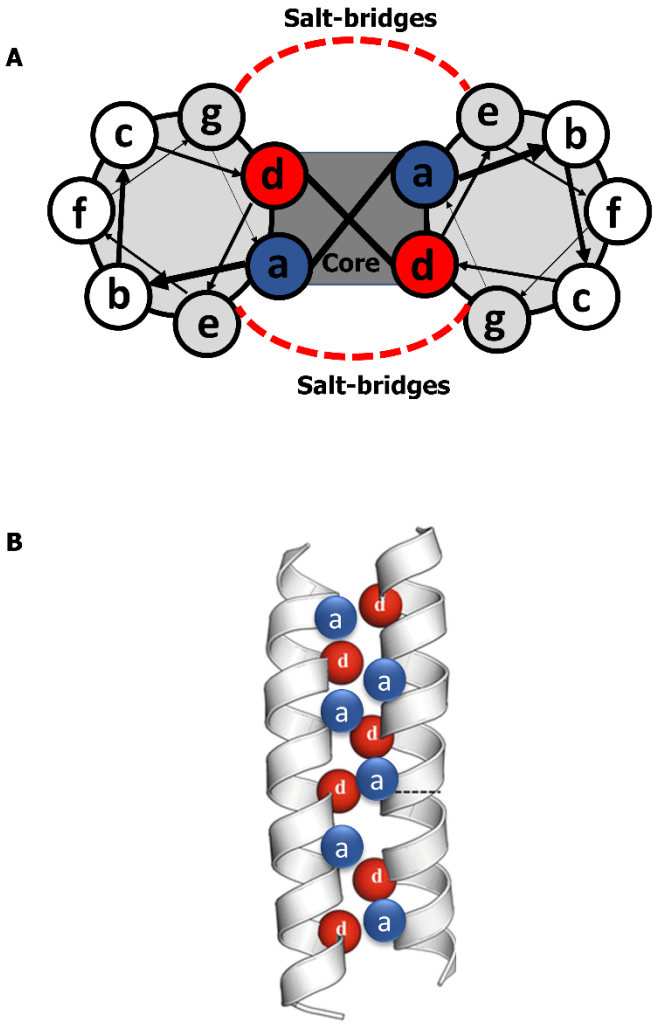

Figure 1.4. Tropomyosin coiled-coil structure. (A) Arrangement of the amino-acid heptad repeats. The core of the coiled-coil is formed by the interactions of hydrophobic residues in "a" and "d" positions. The "e" and "g" positions are occupied by charged residues, hence capable of forming salt bridges (red). (B) "Knobs into holes" arrangement of core residues and formation of the adhesive seam along the core facilitating the dimerization.

1.4.1.4 Tropomyosin flexibility

Tropomyosin requires flexibility to optimize binding to its targets and the basis of this was demonstrated with the first atomic structure (Brown et al., 2001).

Local flexibilities of tropomyosin are generated with the help of amino acids that are atypical for certain regions in the interface. These flexible regions contain three or more consecutive core residues of either stabilizing hydrophobic or bulky residues (Leu, Ile, Val, Met, Phe, and Tyr), destabilizing small side chains (Gly, Ala, and Ser) or larger non-hydrophobic side chains (Thr, Asn, Gln, Asp, Glu, His, Arg, Lys, and Trp), and intervening regions that consist of both stabilizing and destabilizing residues in the hydrophobic core (Kwok & Hodges, 2004).

An unusual feature of the tropomyosin molecule is the high occurrence of alanines (Brown et al., 2001) that can occupy the "a" and "d" positions (Conway & Parry, 1990). These alanines provide more space due to the small size of the R-group granting more freedom to move and accommodate bends, enabling tropomyosin to maintain contact with F- actin during contraction and relaxation. These closely-grouped alanines are also referred to as destabilizing clusters (Brown et al. 2001), spread throughout the entire molecule their spacing coinciding with the seven actin-binding periods. In the 2 Å structure of tropomyosin (Brown et al., 2001), it was observed that the coiled-coil radius is narrower at the Ala clusters compared to the canonical regions. Additionally, these regions showed axial stagger (i.e., the shift between the two tropomyosin strands) of 1.2 Å, poor packing, and are closer by nearly 2 Å at the interface than regions with canonical leucine and valine. It is concluded the alanine clusters are de facto "skips", and the bends that are formed

provide the necessary flexibility for the molecule to wind around actin. Mutagenesis studies demonstrate the replacement of Ala-74, Ala-78, and Ala-81 from 2nd and Ala-179, and 183 from 5th actin-binding periods with a larger non-polar side-chain can decrease F-actin affinity, by affecting chain stability (Singh & Hitchcock-DeGregori, 2003; Singh & Hitchcock-Degregori, 2006). The occurrence of Lys-15(a) and Lys-29(a) within the first alanine cluster (Brown et al., 2001) creates an unstable segment near to the N-terminus, specifically Lys-15(a)-Ala18(d)-Ala-22(a)-Ala-25(d)-Lys-29(a)-Ala-32(d)-Ser-36(a) (Figure 1.5) (Brown et al. 2001). A dramatic effect of the non-canonical amino acids is found in the final 31 residues. Starting at Gln-263(d) to Tyr-267(a), the two strands deviate from the alpha-helical structure and are splayed apart (Figure 1.5) (Li et al., 2002). Mutagenic replacement of Gln-263 to Leu stabilizes the core while weakening association with TnT (Greenfield et al., 2002). Another region of tropomyosin, from residues 176 - 284 (7 Å resolution) and which interacts with troponin at the binding site contains a global bend (Nitanai et al., 2007). Within this section, Tyr-214(d)-Glu-218(a)-Tyr-221(d) (Figure 1.5) demonstrates poor packing and increased interhelical distance compared to canonical hydrophobic bulky residue interface (Nitanai et al., 2007). A study of 2 Å structures from residues 176 - 273 reveals the hydrophobic core disrupted by three holes around Leu-207(d)-Ala-211(a)-Tyr-214(d), Glu-218(a)-Tyr-221(d), and Gln-263(d)-Tyr-267(a) (Figure 1.5) (Minakata et al., 2008). According to both studies (Nitanai et al., 2007; Minakata et al., 2008), it was also concluded that the higher negative charge of Glu-218 in the core "a" position helps to further destabilize the region, which coincides with an alanine cluster and caters for the docking of troponin to the mid-region (White et al., 1987). Destabilization of the core was also observed at Asp-137(d) at 2.3 Å resolution in a portion

of tropomyosin containing residues 89 - 208 (Figure 1.5) (Brown et al., 2005). The proximity of Asp-137 to large Met-127(a) and Met-141(a) causes poor packing and increases the susceptibility of tropomyosin to trypsin at peptide bond between Arg-133-Ala-134 (Pato et al., 1981; Ueno, 1984; Sumida et al., 2008). The region between Asp-137 and Tyr-214 contains an important actin-binding site (Brown & Cohen, 2005; Hitchcock-DeGregori et al., 2002; Singh & Hitchcock-Degregori, 2006)

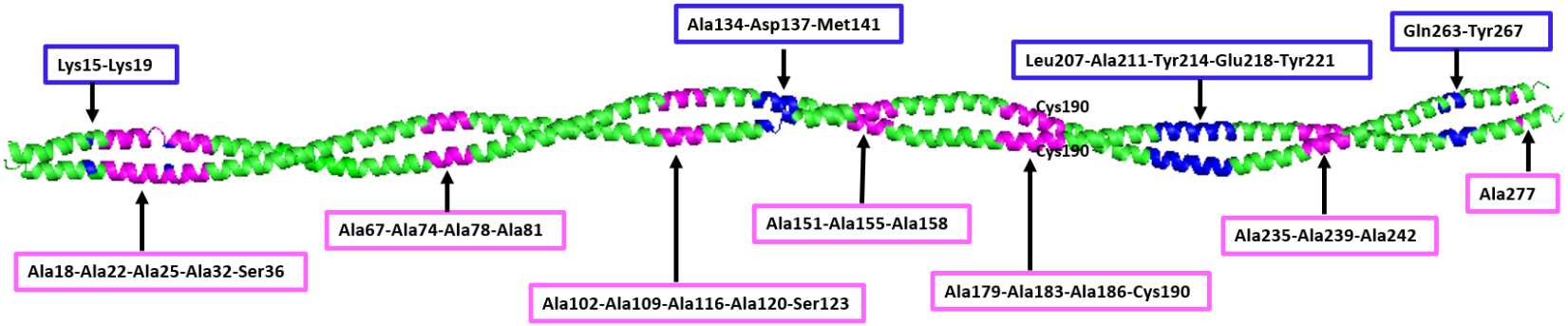

Figure 1.5. Schematic representation of destabilized regions on tropomyosin. The residues involved in "a" and "d" core positions are indicated in the boxes. Magenta - Localization of alanine clusters along the tropomyosin molecule. Blue – The positions where the hydrophobic core is broken due to the occurrence of atypical amino acids**.**

1.4.1.5 Regions of variable stabilities

Numerous biochemical studies (Phillips et al., 1980; Potekhin & Privalov, 1982; Betteridge & Lehrer, 1983; Ishii et al., 1992; Singh & Hitchcock-Degregori, 2006; Hodges et al., 2009; Kirwan & Hodges, 2010) provide evidence for sections of different stabilities and intrinsically flexible regions within tropomyosin. This is seen especially near to the C-terminus of tropomyosin which unfolds at a temperature less than the physiological temperature (Phillips et al., 1980) and in the mid-region. For example, attachment of fluorescent moieties on Cys-190 and monitoring the changes in emission during thermal denaturation has demonstrated that residue 190 is located in a locally unstable region which contributes to a pretransition that is observed before the main unfolding event (Betteridge & Lehrer, 1983). Tropomyosin containing a stabilizing fusion peptide at N-terminus revealed the middle unfolded region acts as a boundary allowing the independent unfolding of the C- and N-terminal domains (Ishii et al., 1992). The attachment of a fluorescence tag has also been shown to decrease the end-to-end polymerizability suggesting a long-range conformational coupling between Cys-190 and the C-terminal region (Graceffa & Lehrer, 1980) and affinity for F-actin (Ishii & Lehrer, 1985). Tryptic digestion also reveals the existence of instability in the center of the molecule. The proteolytic susceptibility is greater at low ionic strengths, at elevated temperatures, and with the introduction of a disulfide bond at Cys-190 (Ueno, 1984). In addition, the deletion and introduction of mutations to alter interface packing of the actin-binding periods, have been shown to affect the actin affinity highlighting the importance of local structure and stability of the coiled-coil (Hitchcock-DeGregori et al., 2002; Singh & Hitchcock-Degregori, 2006).

Analysis of tropomyosin fragments of various lengths has identified the region between residues 97 and 118, as a “stability control region” which is important for the overall stability of the molecule (Hodges et al., 2009). Fragments of tropomyosin lacking this region demonstrated significantly lower stabilities compared to the fragments that contained it. Two electrostatic clusters encompassing residues 97 - 104 (Glu-Glu-Leu-Asp-Arg-Ala-Gln-Glu) and residues 112 - 118 (Lys-Leu-Glu-Glu-Ala-Glu-Lys), with the potential of multiple intra- and inter-chain salt bridges were identified in this region. Interestingly, it is evident that all the above-mentioned charged residues stay outside “a” and “d” core positions (Hodges et al., 2009). Furthermore, a third site was identified from residues 105 - 111 (Arg-Leu-Ala-Thr-Ala-Leu-Gln) that contains a critical and unusual hydrophobic interaction by Leu-110(e) that maintains stability (Kirwan & Hodges, 2010).

1.4.1.6 Additional modes of destabilization of coiled-coil as cold adaptations

The importance of destabilized regions within tropomyosin as binding sites (Hitchcock-DeGregori & Singh, 2010) is emphasized by tropomyosin from psychrophiles (organisms that live < 15 ^{o}C) (Hayley et al., 2011; Fudge & Heeley, 2015). Atlantic salmon is a suitable model in this regard due to its low ambient temperature. The isoform in the fast skeletal muscle of the trunk, which is the biggest contributor to the body mass (Bone et al., 1995), has relatively few (~ 20) amino acid substitutions compared to the mesophilic (rabbit) counterparts (Heeley et al., 1995) (Chapter 3 Table 3.1). All of the non-canonical amino acids discussed above that occur in mammalian tropomyosin are conserved in the Atlantic salmon, as is the stability control region of tropomyosin (residues 97 - 118) (Hodges et al., 2009; Kirwan & Hodges, 2010) with a few exceptions, for example: 111(d) Thr (salmon), Gln (mammal) and 179(a) Thr (salmon), Ala (mammal). Other interesting differences are a pair of glycines (Gly-24 and 27) located within a major destabilizing cluster (Lys-15(a)-Ala18(d)-Ala-22(a)-Ala-25(d)-Lys-29(a)-Ala-32(d)-Ser-36(a) (Figure 1.5), and two substitutions that affect charge at neutral pH, namely residue 77(g) (Thr in salmon, Lys in mammal and bird (Stone & Smillie, 1978), and residue 276(c) (Asn in salmon, His in mammal and bird). Due to partial protonation of histidine at neutrality (Edwards & Sykes, 1981) the only substitution that will alter the net charge by a full unit is Thr77(g)Lys. Also, since the "e" positions in the next heptad units (of the same and opposite strands of the coiled-coil) are occupied by glutamates (Glu-75 and Glu-82), there is the potential for a change in ion pairing. Also, residue 77 falls in an alanine cluster that, as mentioned above, is known to be important for thin filament formation. For example, the replacement of Ala

74(d), 78(a), and 81(d) with a bulkier group (leucine and valine) increases the melting temperature of mammalian tropomyosin and weakens its interaction with actin by at least two orders of magnitude (Singh & Hitchcock-DeGregori, 2003).

From the results of previous studies, mesophilic tropomyosins are broadly divided into an N-domain of higher stability and a C-domain of lower stability (Woods, 1977; Edwards and Sykes, 1980; Phillips et al., 1980; Smillie et al., 1980; Morris & Lehrer, 1984; Ishii & Lehrer, 1986) which is demonstrated in the difference between the melting temperatures of the respective CNBr fragments, ΔT_m = 15 ^oC (Williams & Swenson, 1981). On the contrary, the N-domain and C-domain of salmon tropomyosin exhibit a much narrower ΔT_m (Goonasekara & Heeley, 2008) pointing towards the destabilizing effects of Gly-24, Gly-27, Thr-77, and Thr-111. Considering the issue of cold-adaptation and chain flexibility, Gly is known to play an important role as an entropic determinant in enzymes that function at low temperatures (Matthews et al., 1987; Deniz, 2018; Saavedra et al., 2018). In addition to that membrane-bound proteins from psychrophilic bacteria show increased occurrence of helix-breaking, destabilizing amino acids, and an avoidance of the helix-forming amino acid in the amino acid composition compared to mesophilic bacteria (Kahkle & Thorvaldsen, 2012). Analysis of membrane lipids demonstrates an increased ratio of unsaturated fatty acyl residues, cis double bonds, chain shortening, and methyl branching (Russell, 1997; Russell, 2008).

1.4.1.7 The end-to-end interaction

Self-polymerization is one of the intrinsic properties of tropomyosin (Bailey, 1948). The process, which involves a merger of the ends of the molecule, C-termini to N-termini, forms a long continuous cable (Figure 1.2). In the crystalline complexes, tropomyosin coiled coil length is measured shorter than that of 284 (423 Å) amino acids giving an effective length of 275 (410 Å) amino acids, suggesting an overlap of 9 residues (McLachlan et al., 1975; Phillips et al., 1979; Smillie, 1979). Removal of residues of 282 - 284 from rabbit cardiac tropomyosin using carboxypeptidase has no effect on the polymerizability whereas the removal of residue Met-281 significantly weakens it (Johnson & Smillie, 1977). Genetic deletion of residues 1 - 9 from the N-terminus causes the loss of tropomyosin function by preventing binding to actin in the absence of troponin (Cho et al., 1990). Exhaustive carboxypeptidase treatment, which stops at Glu-273, has a similar effect (Mak & Smillie, 1981; Dabrowska et al., 1983). Removal of the N-terminal half of the overlap is more deleterious than that of the C-terminal half (Cho et al., 1990).

The electrostatic nature of the overlap was indicated by its sensitivity to ionic strength (Bailey, 1948) and from the amino acid sequence of tropomyosin (Stone & Smillie, 1978). Specifically, the end regions of tropomyosin are enriched in lysine (N-terminus) and carboxylates (C-terminus). Early models predicted a salt bridge between Lys-7 and the C-terminal alpha-carboxylate (Johnson & Smillie, 1977). Consistent with this prediction acetylation of Lys-7 was found to diminish polymerization (Johnson & Smillie, 1977). Non-polar interactions are also thought to be important. For example, in their NMR study

Greenfield et al., 2006 showed that Met-8 participates in a hydrophobic interaction with Met-281.

In the crystal structure of the first 80 amino acids of tropomyosin, residues 1 - 4 are not in a helical conformation (Figure 1.6A) (Brown et al., 2001). The NMR analysis of a C-terminal fragment reveals that residues 270 - 279 are arranged as parallel linear helices, while the last five residues are disordered (Figure 1.6B) (Greenfield et al., 2003). In a subsequent study, Gln-263, Tyr-267, and Ile-270 cause the C-terminal region of tropomyosin to splay apart (Figure 1.6B) (Greenfield et al., 2006). Formation of the overlap is characterized by the N-terminal 11 amino acids inserting into the cleft (Figure 1.6C) (Li et al., 2002; Nitanai et al., 2007) such that the N- and C-termini are rotated 90^{o} compared to each other (Figure 1.6D) (Greenfield et al., 2006).

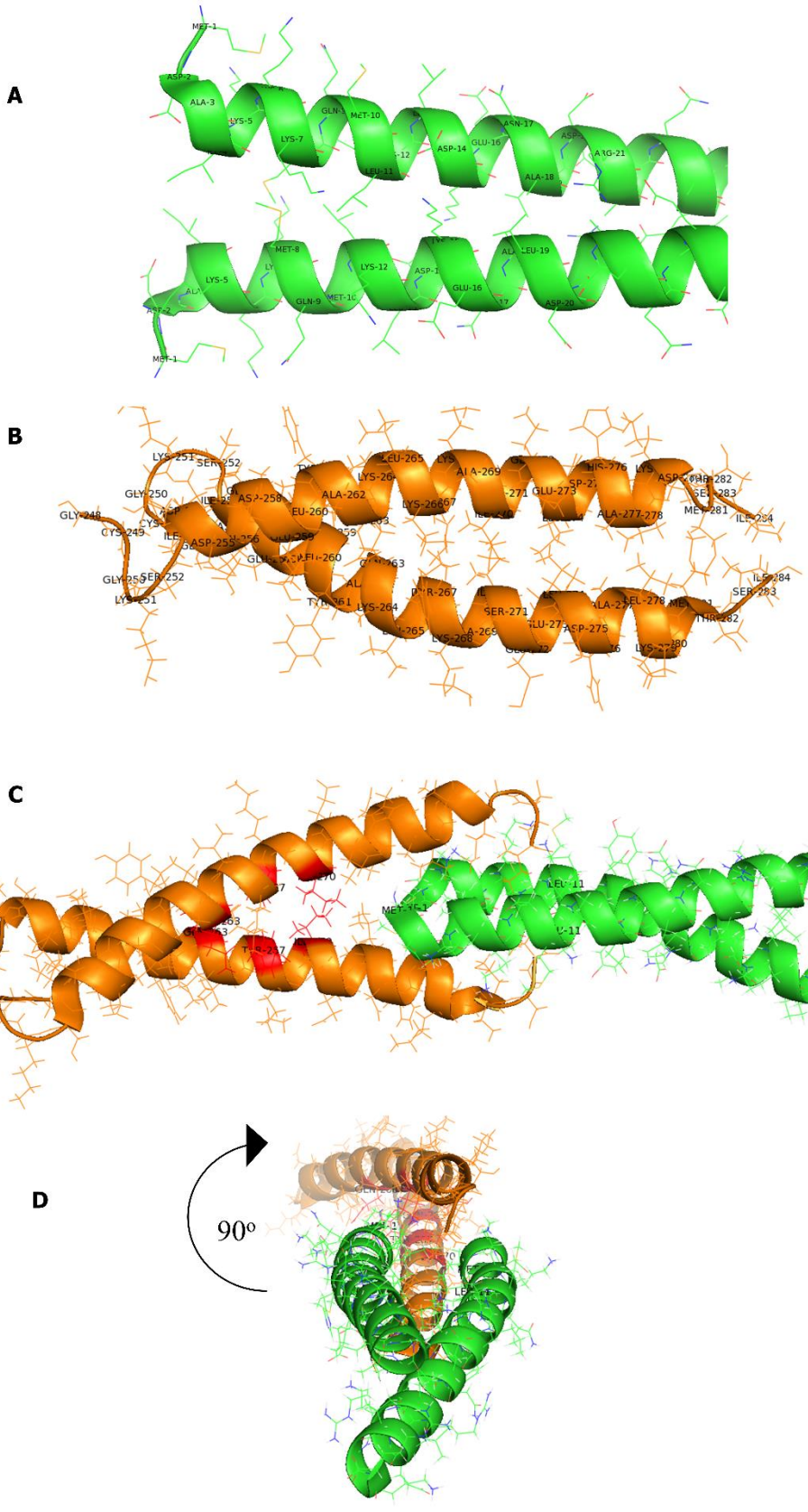
A
B
C
D
90º

Figure 1.6. Tropomyosin overlap region. Green - N-terminal segment. Orange - C-terminal segment. (A) N-terminal 26 residues of chicken alpha tropomyosin, PDB ID: 1IC2. Residues 1-Met-2-Asp-3-Ala-4-Ile are not organized into the alpha-helical conformation. (B) C-terminal fragment of rat striated tropomyosin, PDB ID: 1MV4. The parallel linear helical formation of residues 270-Ile-Ser-Glu-Glu-Leu-Asp-His-Ala-Leu-Lys-279 and non-helical arrangement of residues 279-Asp-Met-Thr-Ser-Ile-284 at the C-terminus. (C) C- and N- terminal overlap region of rat striated tropomyosin, PDB ID: 2G9J). The insertion of 11 residues from the N-terminal coiled-coil into the C-terminal region. Red- Residues Gln-263, Tyr-267, and Ile-270 causing the splaying of the C-terminus disrupting the coiled-coil structure. (D) The 90^{o} rotation of the two termini compared to each other.

1.4.1.8 Actin binding sites on tropomyosin

The seven-fold and fourteen-fold repeats on sarcomeric tropomyosin (284 amino acids) were initially proposed to be associated with actin-binding (Parry, 1975; McLachlan et al., 1975; McLachlan & Stewart, 1976). The weak periodicity of fourteen bands along the molecule contains a narrow zone of net positively charged residues and a broader zone of negatively charged residues. Overlapping every positive zone is a hydrophobic zone that always contains at least one non-polar group on the outer surface (McLachlan & Stewart, 1976). Further, seven pairs of alternative sets of alpha and beta sites are thought to bind equivalently to complementary groups of sites on seven actins in the "relaxed" and "active" states of muscle, respectively. The negative zones are envisaged to attach to actin by magnesium bridges and the hydrophobic zone by direct contact with the narrow outer edge of the actin filament. The crystalline structure by von der Ecken et al., 2015 confirms the early postulation by demonstrating that negatively charged tropomyosin interacts with a positively charged groove on F-actin. In addition, the functional contributions of individual actin-binding periods were studied with mutants, where periods 2 - 6 were singly deleted from rat striated muscle alpha-tropomyosin or replaced by a leucine zipper sequence (Hitchcock-DeGregori et al., 2002). When the mutants were tested for actin binding, regulation of the actomyosin ATPase with troponin, myosin S1 binding to reconstituted thin filaments, and thermal stability, tropomyosin was found to be relatively insensitive to deletion of period 2. In contrast, complete deletion of period 5 (residues 166 - 207) or partial deletion (residues 166 - 188) was detrimental to actin and myosin S1 affinity and (Singh & Hitchcock-DeGregori, 2007). Period 6 (residues 208 - 242), which constitutes part of the

troponin binding site, is required for full inhibition of the actomyosin ATPase at low Ca^{2+} concentration. The replacement of alanine in the 2nd and 5th actin-binding periods with leucine and valine resulted in an increase in melting temperature and a decrease in the actin-binding ability (Singh & Hitchcock-DeGregori, 2003; Singh & Hitchcock-Degregori, 2006). Tropomyosin chimeras containing a leucine zipper sequence (from transcription factor GCN4) in actin binding periods 2 (residues 47 - 60), 3 (residues 89 - 102), and the C-terminal half of 5 (residues 189 - 213) all bound actin with similar affinity (Hitchcock-DeGregori et al., 2002). The effects of deletion of each period increased towards the C-terminus. Loss of function upon deletion of each periodic repeat was found to be in the order of $2 < 3 \sim 4 \sim 6 \leq 5$ (Hitchcock-DeGregori et al., 2002). Therefore, actin binding periods 1 (included in the overlap complex) and 5 are considered the primary acting binding sites on the tropomyosin molecule (Singh & Hitchcock-DeGregori, 2007).

1.4.1.9 Post-translational modifications

There are primarily two types of post-translational modifications found in striated muscle tropomyosins namely: acetylation of N-terminal methionine and phosphorylation of serine-283.

1.4.1.9.1 Acetylation

The striated chicken alpha tropomyosin when expressed in *E.coli* is identical to the one expressed in muscle except at the N-terminus where the recombinant lacks the acetylation

of the initiating methionine (Hitchcock-DeGregori & Heald, 1987). These recombinant proteins have shown poor end-to-end polymerization, weak F-actin affinities, and inability to inhibit actomyosin ATPase activity compared to the muscle protein (Hitchcock-DeGregori & Heald, 1987; Heald & Hitchcock-DeGregori, 1988; Cho et al., 1990; Willadsen et al., 1992). The initiating methionine of tropomyosin occupies a hydrophobic core "a" position in the heptad repeat. The absence of an acetyl group, which is electrically neutral at pH 7, places a positive charge in the core. The two positively charged side chains in the unacetylated tropomyosin thereby destabilize the N-terminal region impairing its ability to associate end-to-end (Monteiro et al., 1994). The effect of unacetylation is overcome by adding amino acids to the N-terminus. The fusion of peptides of different lengths to the unacetylated N-terminus has been shown to rescue polymerizability and binding properties of tropomyosin. The fusion of 2-mer (Ala-Ser), 3-mer (Ala-Ala-Ser) and 17-mer (Ala- Ser- Met-Tyr-Gly-Gly-Glu-Glu-Met-Gly-Arg-Gly-Ser-Ile-Gln-Gly-Arg) amino acids to the N-terminus of *E.coli* proteins have been shown to restore head to tail polymerization, capacity to inhibit actomyosin ATPase, and actin-binding (Monteiro et al., 1994). The 17-mer showed increased polymerizability and decreased ATPase inhibitory activity compared to the 2- and 3-mers. The fusion of Ala-Ser-Arg to the N-terminus of recombinant tropomyosin has demonstrated a 10 fold increase in the actin affinity compared to the muscle expressed form containing the N-terminal acetylation (Urbancikova & Hitchcock-DeGregori, 1994). It has been demonstrated that longer fusions with 80 amino acids of a non-structural influenza virus protein to tropomyosin impaired the head-to-tail association without affecting actin-binding (Hitchcock-DeGregori and Heald, 1987). Even though certain of these fusions demonstrated similar functions to the

wild type muscle form they were not identical. Acetylated muscle tropomyosin produced in insect cells displays the same actin affinity as the wild type (Urbancikova & Hitchcock-DeGregori, 1994). Several acetyltransferase enzymes were identified as responsible for the acetylation of tropomyosin (Polevoda et al., 2003; Skoumpla et al., 2007). In contrast to the alpha tropomyosin in skeletal muscles, alpha tropomyosin from smooth muscles is capable of binding to actin without an N-terminal modification where as beta tropomyosins from skeletal and smooth muscles are observed to show mixed results (Pittenger et al., 1995; Coulton et al., 2006).

1.4.1.9.2 Phosphorylation

Phosphorylation of tropomyosin, in contrast, appears to be linked to regulation of function. Studies with alpha and beta isoforms isolated from adult rabbit and frog skeletal and cardiac muscles revealed phosphorylation to occur at Ser-283 (Mak et al., 1978). Both isoforms are phosphorylated to a higher extent in fetal skeletal and cardiac muscles of mammals and birds compared to adults (Montarras et al., 1981; Heeley et al., 1982; Heeley et al., 1985). Taking rat heart, which mostly consists of Tpm1.1(α) (Lewis & Smillie, 1980; Muthuchamy et al., 1993) as an example, the level of phosphorylation decreases from 0.7 mole per mole early in development to ~ 0.3 in the mature heart (Heeley et al., 1982), with the exception of the auricular appendage that maintains high levels (~ 0.5 mole per mole) of phosphorylation throughout (Heeley, 2013). Additionally, it has also been shown that the extent of phosphorylation is dependent on the tissue type where heart > skeletal muscle, (Mak et al., 1978; Heeley et al., 1985). The decline of phosphorylation in birds (Montarras

et al., 1981) is attributed, at least in part, to a decrease in the amount of tropomyosin kinase (deBelle & Mak, 1987). Early biochemical studies revealed tropomyosin to be a non-suitable substrate for 3'5' cAMP-dependent protein kinases (Pratje & Heilmeyer, 1972; Perry & Cole, 1974). But studies using tropomyosin kinase (Montgomery & Mak, 1984) demonstrated that the rat and chicken skeletal alpha isoform is the preferred substrate compared to beta isoform (Watson et al., 1988). The development of chromatographic separation of endogenously phosphorylated tropomyosin using Q-Sepharose in the presence of urea also led to the pathway for biochemical characterization of phosphorylated tropomyosins (Heeley et al., 1989; Heeley, 1994). The samples generated by enzyme incubation, or by chromatography, were equivalent in F-actin binding properties and viscosities (Heeley et al., 1989). Consistent with previous reports, the kinase does not require Ca^{2+} or cyclic adenosine monophosphate (cAMP) activity and is unable to phosphorylate protein digested with carboxypeptidase (residues 1 - 273) (Montgomery & Mak, 1984). The observations from the biochemical investigations (Heeley et al., 1989) were in agreement with the developmental surveys (Heeley et al., 1982), in that phosphorylated Tpm1.1(α) showed comparatively increased ability for head-to-tail polymerization (Heeley et al., 1989). In addition, phosphorylation tightened the interaction of Tpm1.1(α) with troponin, as demonstrated by affinity chromatography (Heeley et al., 1989). Results showed that the F-actin binding was unaffected (Heeley et al., 1989). On the contrary, phosphorylation of cytoskeletal isoforms has revealed an association with actin remodeling (Naga Prasad et al., 2005; Houle & Huot, 2006) suggesting a possible role of phosphorylation in actin binding. This point is investigated in thesis Chapter 3.

The increased avidity for the end-to-end association of phosphorylated tropomyosin in the four chain overlap bundle is explained by ion-pairing between the phosphate moieties on opposite chains and protonated lysines at positions 5, 6, 7, and 12 with Lys-7 and 12 being of particular importance (Greenfield et al., 2006; Lehman et al., 2015). In addition, phosphorylation also has been shown to affect the troponin binding ability of tropomyosin. Affinity chromatography experiments involving soluble fragments of TnT (Heeley, 1994) showed that the C-terminal 100 amino acid fragment (TnT2) had a higher affinity for phosphorylated Tpm1.1(α) than unphosphorylated Tpm1.1(α). The observation was surprising given that TnT2 binds to a central region of tropomyosin, namely binding site 2 (Iwao Ohtsuki, 1979; Pearlstone & Smillie, 1982a; Tanokura et al., 1983; Morris & Lehrer, 1984) which is far removed from the site of phosphorylation. The affinity of the tail section of TnT (TnT1) for tropomyosin-Sepharose was shown to be insensitive to phosphorylation (Heeley, 1994) where TnT1, envisaged to arch over consecutive tropomyosins (binding site 1) (Mak & Smillie, 1981b; Brisson et al., 1986; Heeley e al., 1987; White et al., 1987; Goonasekara & Heeley, 2009). But TnT1 induced viscosity studies showed a significantly reduced effect when tropomyosin was fully phosphorylated (Heeley, 1994). (Heeley, 1994). In a reconstituted ATPase assay, thin filaments (pCa^{2+} 4) composed of phosphorylated tropomyosin activated myosin-S1 to a greater extent than the unphosphorylated control (Heeley et al., 1989; Heeley, 1994). Additionally, it was recently reported that phosphorylation increases the affinity of thin filaments for myosin-S1 in the presence of adenosine diphosphate (ADP) while not significantly affecting the cooperativity (Silva et al., 2020a).

The role of Ser-283 phosphorylation has been investigated using mutagenesis and in reconstituted protein mixtures (Sano et al., 2000; Nixon et al., 2013), myofibrils (Nixon et al., 2013), and transgenic animals (reviewed in Wieczorek, 2018). The results of pseudo-phosphorylation, specifically the replacement of Ser-283 with glutamate, demonstrated the importance of an electrostatic component in viscosity measurements and by inference the overlap interaction (Sano et al., 2000). The mutant Ser283Glu shows higher viscosity whereas the Ser283Lys shows lower viscosity when compared with the non-phosphorylated control. Thin filaments containing mutant Ser283Asp and fluorescently-labeled troponin-C exhibited comparatively slower rates of Ca^{2+} dissociation and prolonged myofibrillar force (Nixon et al., 2013). Transgenic mice carrying this mutation exhibited a severe dilated cardiomyopathy within 2 weeks postpartum (Wieczorek, 2018). Further, it was revealed that decreasing the level of phosphorylation by alanine replacement (i.e., Ser283Ala) protected against a familial hypertrophic cardiomyopathy mutation, namely Glu180Gly (Schulz et al., 2013; Wieczorek, 2018). Mouse lines synthesizing tropomyosin bearing the dilated cardiomyopathy disease mutation Glu54Lys have decreased levels of phosphorylation compared to the control (Warren et al., 2008). More recently, and again in a whole animal context, pseudo-phosphorylation (Ser283Asp) was found to be detrimental (post-birth) depending upon the proportions of the mutant and endogenous proteins (Rajan et al., 2019).

Studies have continued on the enzymology of tropomyosin phosphorylation, including that of cytoskeletal isoforms. This work has shown the involvement of more than one kinase (Naga Prasad et al., 2005; Houle et al., 2007; Wu & Solaro, 2007; Yuan et al.,

2008; Simoneau et al., 2012; Palani et al., 2019), with a particular interest in the casein kinase family (Nüesch & Rommelaere, 2007; Rajan et al., 2019).

1.4.1.10 Tropomyosin and human diseases

Tropomyosin is identified as being directly involved in four human disease conditions: 1) cancer, 2) cardiomyopathy, 3) nemaline myopathy, 4) and ulcerative colitis.

1.4.1.10.1 Cancer

The studies using chicken embryo fibroblasts cells infected with Rous sarcoma virus reveal that during oncogenic transformation, expression of HMW tropomyosin isoforms decreases (Hendricks & Weintraub, 1981, 1984). Similar results were observed with rat kidney epithelial cells infected with the Kirsten virus or Rous sarcoma virus and rat embryo cells infected with SV40 or adenovirus type 5 (Leonardi et al., 1982; Matsumura et al., 1983). It is assumed that the decrease in HMW tropomyosin is either involved in, or causes, rearrangement of stress fibers which may be responsible for morphological transformations. Analysis of metastatic Lewis carcinoma cells and v-Ha-ras-transformed NIH3T3 (pH1-3) cells revealed that expression of Tpm2 is significantly reduced in the metastatic cancer stage compared to that of the low metastatic cancer or the non-transformed cells (Takenaga et al., 1988a; Takenaga et al., 1988b).

In humans, breast carcinoma cells showed a less than 25 percent expression of Tpm1-3, or abolished expression (Tpm1) of HMW isoforms whereas at metastasis increased

expression of Tpm 1 was identified (Franzén et al., 1996; Raval et al., 2003; Varga et al., 2005). Similarly, human bladder cell carcinoma showed decreased expression of Tpm1, Tpm2, and Tpm3 isoforms (Pawlak et al., 2004). In contrast to the above observations, low-grade astrocytic tumors expressed HMW tropomyosins, while highly malignant central nervous system tumors of different origins did not (Hughes et al., 2003). Studies with human astrocytoma cells also revealed increased HMW tropomyosin expression in anaplastic cells compared to normal cells (Galloway et al., 1990). Interestingly in a study with transformed colon epithelial cells, it was demonstrated that expression of LMW tropomyosin is progressively increased (Lin et al., 2002).

1.4.1.10.2 Cardiomyopathies

This phenotype in humans is characterized by features such as enlarged heart and fibrosis (Maron et al., 2006; Wexler et al., 2009; Price et al., 2016). There are several tropomyosin mutations identified responsible for generating familial hypertrophic cardiomyopathy concentrated to three regions of the molecule. Seven mutations fall in the troponin binding region namely: Ile172Thr, Asp175Asn, Glu180Gly, Glu180Val, Leu185Arg, Glu192Lys, and Met281Thr (Thierfelder et al., 1994; Nakajima-Taniguchi et al., 1995; Yamauchi-Takihara et al., 1996; Jääskeläinen et al., 1998; van de Meerakker et al., 2013). Other mutations are Glu62Gln, Ala63Val, and Lys70Thr (Yamauchi-Takihara et al., 1996; Jongbloed et al., 2003) and finally Val95Ala in the mid-region of tropomyosin (Karibe et al., 2001). It is apparent that many of the above mentioned mutations result in a change in charge. Such substitutions have the potential to alter the stability of the molecule by

interfering with salt bridges as well as affecting the interactions to partner proteins such as actin (Olson et al., 2001; Kremneva et al., 2004)

1.4.1.10.3 Nemaline myopathy

This is a hereditary condition characterized by weak and reduced muscle strength. A defining feature of this condition is the appearance of rod-shaped structures in the nucleus. The most common reason for nemaline myopathy is the Met9Arg mutation in the TPM3 that causes alteration of an extremely conserved amino acid that falls into the overlap region (Laing et al., 1995). In very rare conditions it is also evident that mutations Gln147Pro, Glu117Lys, and Glu41Lys, (Donner et al., 2002; Tajsharghi et al., 2007), and Glu139deletion (Lehtokari et al., 2007; Clarke et al., 2009) in TPM2 are involved in causing nemaline myopathy.

1.4.1.10.4 Ulcerative colitis

This is categorized as a form of chronic inflammatory bowel disease that affects the mucosa of the colon. Analysis of blood samples of 95% of patients suffering from this condition revealed the presence of anti-tropomyosin antibodies (Das et al., 1993). Further studies demonstrated the primary target of these antibodies are HMW tropomyosins (Biancone et al., 1998; Geng et al., 1998).

1.4.2 Actin

Actin belongs to the same structural superfamily as sugar kinases and Hsp70 (Bork et al., 1992). Discovered during world war II (Straub, 1942) actin is one of the most ubiquitous and abundant proteins in the animal kingdom. Other hallmarks are the activation of myosin MgATPase and interconversion between monomer (G-actin) and polymer (F-actin). At low ionic conditions, actin stays as a globular monomer (42000 kDa) known as G-actin (Elzinga et al., 1973). With increasing ionic strength, the G-actin polymerizes forming F-actin. This process is reversible and provides the basis for actin isolation. Actin can bind to one molecule of ATP or ADP. When actin polymerizes to the F-actin form, ATP is transformed to ADP and inorganic phosphate (Pi) (Straub & Feuer, 1950; Wegner, 1977; Engel et al., 1977). Also it has a high affinity binding site for divalent cations such as Ca^{2+}, Mn^{2+}, Sr^{2+}, Ni^{2+}, Zn^{2+} or Mg^{2+} (Strzelecka-Gołaszewska, 1973; Strzelecka-Gołaszewska et al., 1978; Frieden et al., 1980). The divalent cation in complex with the nucleotide is important in maintaining the native structure of actin as well as maintaining its polymerization properties (Nagy & Jencks, 1962; Lehrer & Kerwar, 1972; Frieden et al., 1980; Estes et al., 1992). Since the cellular concentration of Mg^{2+} is in millimolar values (Kushmerick et al., 1986), under physiological conditions Mg^{2+} is found bound to actin compared to Ca^{2+} (Pollard et al., 2000).

Traditionally there are six isoforms of actin recognized in mammals (Pollard, 2001) named according to Greek symbols based on isoelectric focusing (Zechel & Weber, 1978) with alpha-actin having a pI 5.4. These are; alpha (α -skeletal, α -cardiac and α -vascular smooth), beta (β-cytoplasmic) and gamma (γ-enteric smooth and γ-cytoplasmic), encoded

by the genes *Actb, Actg1, Acta1, Actc1, Acta2,* and *Actg2,* respectively. A recent study (Witjes et al., 2019) indicates the existence of two additional actin groups in vertebrates, actin alpha 4 encoded from *Acta4* and epsilon 1 encoded from the *Acte1* gene. The same epsilon 1 actins in fish are identified as a unique isoform named slow skeletal actin (Silva & Heeley, 2021). Sarcomeric actins, following N-terminal processing, consist of 375 amino acids (Elzinga et al., 1973). Of the small number of amino acid changes, most occur near to the N-terminus (Herman, 1993).

The first high-resolution (~3 Å) structure of G-actin, reported in 1990, was in a complex with DNase I (Kabsch et al., 1990). Actin was shown to be made up of four subdomains namely 1, 2, 3, and 4 (Figure 1.7A). The subdomains 1 and 3 are larger and are suspected to risen from gene duplication whereas subdomains 2 and 4 are considered as insertions to domains 1 and 3 respectively. The two larger domains have very little contact between them resulting in two clefts. The upper cleft binds to ATP or ADP which in turn provides important linkages between the domains (Figure 1.7A). The lower cleft situated between domains 1 and 3 contains hydrophobic residues, hence is named the hydrophobic cleft (Figure 1.7A). It is a binding site for actin-binding proteins. The protein chain begins and ends in subdomain 1, which consists of three sections of the sequence (residues 1 - 32, 70 - 144, and 338 - 375) (Figure 1.7). Subdomain 2 (residues 33 - 69) is the smallest of the four. Subdomain 3 is composed of two stretches (residues 145 - 180 and 270 - 337), and subdomain 4 is contiguous (residues 181 - 269). The exposed areas of subdomains 1 and 3 are called barbed ends whereas in 2 and 4 they are called pointed ends which generate the polarity of the molecule. At the top of subdomain 2 (res 39 - 51) is disordered and

contains DNase I binding loop (or D-loop) (Figure 1.7A) and is considered to play an important role during filament formation. This breakthrough research by Kabsch et al., 1990 and other subsequent achievements (Schutt et al., 1993; Otterbein et al., 2001) helped to resolve the structure of the filamentous form of actin (Holmes et al., 1990; Chou & Pollard, 2019). F-actin is made of two right-handed helices (Holmes et al., 1990) (Figure 1.7B). Each strand contains nearly 13 molecules repeating every six (left-handed) turns with an axial distance of 35.9 nm. Since the rise per molecule is 2.76 nm and twist per molecule is 166 ^{o} (which is close to 180 ^{o}), the structure takes the appearance of a two-start right-handed helix (Fujii et al., 2010) (Figure 1.7B). The D-loop in F-actin acquires more of an open configuration and inserts into the target binding cleft of the immediately above unit (Figure 1.7B). Another classic feature of actin filaments is the formation of chevrons when decorated with rigor myosin heads (Moore et al., 1970).

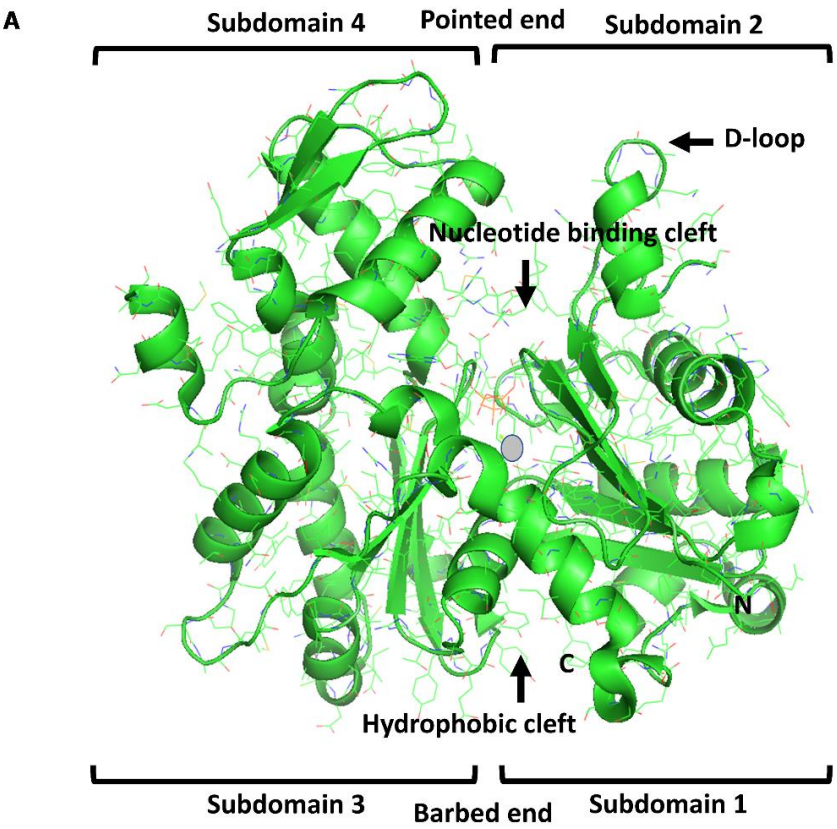
A
Subdomain 4
Pointed end
Subdomain 2
D-loop
Nucleotide binding cleft
N
C
Hydrophobic cleft
Subdomain 3
Barbed end
Subdomain 1

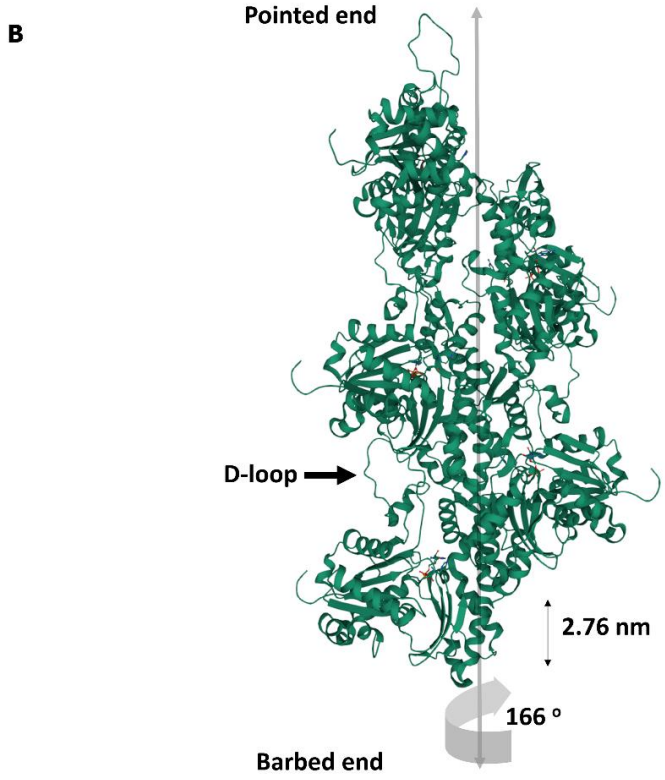
B
Pointed end
D-loop
2.76 nm
166 °
Barbed end

Figure 1.7. The structure of actin. (A) G-actin monomer, PDB ID: 4B1U(Mouilleron et al., 2012)**.** Subdomain 1, 2, 3, and 4 regions are depicted in brackets. N, N-terminal end; C, C-terminal end of actin in subdomain 1. Arrows indicating the central nucleotide binding-cleft, the hydrophobic-cleft, and the D-loop. Orange - ATP and the sphere divalent cation bound to the central cleft. (B) The helical structure of F-actin containing five G-actin units, PDB ID: 3MFP. The D-loop interacts with the hydrophobic cleft of the immediately above unit. The rise per molecule is 2.76 nm and the twist per molecule is 166 º.

1.4.3 Troponin

In the 1960s, it was speculated that contractions in striated muscle were regulated by a special protein complex located on actin filaments. This complex was identified as native tropomyosin (Ebashi et al., 1968) and consisted of tropomyosin (Bailey, 1946) and another component. This second component was named troponin. The early studies identify troponin as the Ca^{2+} binding component of the thin filament (Ebashi et al., 1968; Perry, 1979; Leavis & Gergely, 1984). Troponin is a heterotrimer of three components: troponin C (TnC), troponin I (TnI), and troponin T (TnT) which were so-named in 1972 (Greaser et al., 1973). These subunits are specialized for different functions. TnC is the Ca^{2+} binding component of troponin (Hartshorne & Mueller, 1968; Schaub & Perry, 1969). TnI inhibits actomyosin ATPase activity (Hartshorne & Mueller, 1968; Ebashi et al., 1971; Wilkinson et al., 1972; Eisenberg & Kielley, 1974; Eaton et al., 1975). TnT was assigned the symbol T owing to its interaction with tropomyosin (Greaser et al., 1973; Jackson et al., 1975). The troponin complex consists of a core (or the globular complex) domain and an extended tail. TnC and TnI together make up most of the core domain that binds tropomyosin near Cys-190 (binding site 2) while the N-terminal region of TnT (TnT1) forms the extended tail structure (Iwao Ohtsuki, 1979; Pearlstone & Smillie, 1982b; Tanokura et al., 1983; Morris & Lehrer, 1984). The core consists of two regions, the regulatory head made of the N-terminal region of TnC (residues 3 - 83) and TnI (residues 150 - 159) and the rigid coiled-coil domain 'IT arm' consisting of the C-terminal domain of TnT (TnT2 residues 203 - 271), N-terminal domain of TnC (residues 93 -161) and the C-terminal regions of TnI (residues 42 - 136) (Takeda et al., 2003). TnT2 also consists of regions that are part of the

globular domain of troponin that interacts with tropomyosin (Takeda et al., 2003). The TnT1 tail region spans across the head-to-tail joint of tropomyosin (binding site 1) (Mak & Smillie, 1981b; Brisson et al., 1986; Heeley, et al., 1987; White et al., 1987; Goonasekara & Heeley, 2009; Manning et al., 2012). In the thin filament, seven actin monomers interact with one tropomyosin dimer and one heterotrimeric troponin complex which is designated as a regulatory unit (Ohtsuki, 1979; Zot & Potter, 1987; Tobacman, 1996).

Recent cryoEM analyses of the cardiac thin filament, confirmed some of the previous theories of Takeda et al., 2003, specifically the potential of the TnI inhibitory region (residues 137 - 148), the final ~ 50 amino acids of TnI (residues 163 - 210), and the C-terminal portion of TnT2 (residues 272 - 288) to all form interfaces with actin-tropomyosin. In addition, cardiac troponin was shown to be extremely elongated such that the upper four actin units of one strand are bound by the C-terminal portion of TnI (residues 163 - 210) and troponin core, while the bottom three of the opposite strand are bound by TnT1 interacts with the head-to-tail overlap of tropomyosin (Oda et al., 2020; Yamada et al., 2020).

1.4.3.1 Troponin C (TnC)

TnC is the Ca^{2+} binding component of the trimeric complex and a member of the so-called EF-hand family that includes calmodulin, parvalbumin, and myosin light chains (Ikura, 1996). Two genes code for TnC isoforms in higher organisms. One codes for the fast skeletal isoform whereas the other codes for the cardiac / slow skeletal muscle isoform, abbreviated as cTnC (Wilkinson, 1980; Li & Hwang, 2015). All TnCs are characterized

low isoelectric points (pI 4.1 - 4.4) (Hartshorne and Dreizen, 1973), and a high proportion of phenylalanine relative to tyrosine (Elzinga et al., 1973; Van Eerd & Takahashi, 1976). The first crystal structure of TnC (fast skeletal) was reported in 1985 (Herzberg & James, 1985) and the NMR solution structure appeared ten years later (Slupsky & Sykes, 1995). These studies showed that TnC contains nine short alpha-helices named in alphabetical order (except for the first which is called N): N (residues 3 - 9), B (residues 14 - 25), C (residues 38 - 47), D (residues 74 - 85), E (residues 94 - 104), F (residues 114 - 123), G (residues 130 - 140) and H (residues 150 - 157) (Figure 1.8A). The short helices make four motifs known as EF-hands (EF-hand I residues 16 - 51, EF-hand II residues 52 - 87, EF-hand III residues 92 - 127, EF-hand IV residues 128 - 161) which consists of helix-loop-helix structures where the interconnected loops contain negatively charged residues that can bind to divalent cations (Figure 1.8A). EF-hands I and II in the N-terminal domain (N-TnC) have comparatively lower affinity for divalent metal ions (Figure 1.8A) (Potter & Gergely, 1975; Houdusse et al., 1997). Further, site I is inoperative in the case of the cardiac / slow isoform site I due to the insertion of valine-28 and two substitutions, Asp-29 to Leu-29 and Asp-31 to Ala (Van Eerd & Takahashi, 1976; Kawasaki & Kretsinger, 1994; Sia et al., 1997).

EF-hands III and IV that make up the C-terminal domain (C-TnC) have higher affinity and are permanently filled by Mg^{2+} under physiological conditions (Potter & Gergely, 1975). Thus, owing to the disparity in binding affinities, N-TnC is considered regulatory and C-TnC structural (Figure 1.8A) and the cardiac isoform possesses only one regulatory site (Kawasaki & Kretsinger, 1994). Interestingly, a recent report suggests that site II of human

cTnC is partially occupied by Mg^{2+} during rest, an observation that has ramifications for conditions that incur an elevation in resting [Mg^{2+}] (Rayani et al., 2021).

The two domains of TnC are connected by a flexible linker (residues 88 - 91) which is stabilized by several salt-bridges and thought to be involved in transducing conformational signals between them (Sundaralingam et al., 1985; Takeda et al., 2003). The structure of Ca^{2+} free N-domain significantly varies from the C-domain. This demonstrates its role as a Ca^{2+} sensor where troponin undergoes conformational upon binding Ca^{2+} from a "closed" to an "open" state (Herzberg & James, 1985). The EF-hand motifs move close together via an intervening beta-sheet motif that reorients the helices revealing a hydrophobic patch (residues 93 -161) that contains the binding site for TnI (Herzberg et al., 1986; Takeda et al., 2003).

Comparison of cTnCs from trout and mammal has demonstrated that the former possesses a higher affinity for Ca^{2+} at ambient temperature (Moyes et al., 1996; Gillis & Tibbits, 2002 and Gillis et al., 2005). Using a fluorescent mutant (Tyr27Trp) a two-fold difference was observed at site II (Gillis et al., 2000) as well as a weak interaction at site I (Gillis et al., 2003). The Ca^{2+} binding properties of salmonid cTnC are proposed to act as an evolutionary advantage to maintain heart function since the cardiac myofilament becomes less Ca^{2+} sensitive at a lower temperature (Gillis & Tibbits, 2002). Consistent with their having > 92 % sequence identity (Moyes et al., 1996), the conformation of the two cTnCs is similar as shown by NMR (Blumenschein et al., 2004). The NMR study also demonstrated that the salmonid form of the protein adopts a more compact structure at 7 ^{o}C compared to 30 ^{o}C (Blumenschein et al., 2004). It is assumed that the difference in Ca^{2+} sensitivity arises from substitutions that occur in the N-terminal (residues 1 - 41) region

especially due to residues 2 (Asn in trout, Asp in mammals), 28 (Ile in trout, Val in mammals), 39 (Gln in trout, Leu in mammals), and 30 (Asp in trout, Gly in mammals) (Gillis & Tibbits, 2002; Gillis et al., 2005) and interacting sequences of TnC with other components of the troponin complex situated elsewhere from the regulatory site (Moyes et al., 1996).

1.4.3.2 Troponin I (TnI)

TnI inhibits actomyosin ATPase activity (Perry et al., 1973; Eaton et al., 1975; Leavis & Gergely, 1984). The inhibitory activity is enhanced by tropomyosin interaction and is neutralized when TnC is saturated with Ca^{2+} (Head & Perry, 1974; Eaton et al., 1975; Perry, 1999). Three genes encode for three TnI isoforms. Two of the isoforms are found in fast and slow skeletal fibers, and one isoform is found in cardiac fibers (Dhoot & Perry, 1982; Perry, 1999). Depending on the source, TnI is made up of 181 - 210 amino acids with a molar mass of ~ 21- 24 kDa and consists of a large number of positive residues (Wilkinson & Grand, 1978). The cardiac isoform is larger due to the existence of 30 more amino acids in the N-terminus. Structurally there are several domains in the protein that are connected by structurally disordered regions. These domains are: cardiac exclusive N-terminal domain (N-cTnI), IT arm, switch peptide, inhibitory peptide, and C-terminal domain (C-TnI). The N-cTnI consists of an acidic region (residues 2 - 11) and a Xaa-Pro motif (residues 12 - 18) which forms an unstable helix (Marston & Zamora, 2020). The IT arm is a rigid coiled-coil structure made of C-terminal domains TnI (C-TnI) and TnT (TnT2). The IT arm is not known to have direct interactions with actin or tropomyosin and lies

perpendicular to the tropomyosin strand, but acts as a scaffold to bind to C-TnC (Takeda et al., 2003; Oda et al., 2020). The C-TnI consists of two anti-parallel alpha-helices H1 (residues 43 - 79) and H2 (residues 90 - 135) connected via a flexible U-turn (residues 80 - 89) (Figure 1.8B). The H1 helix and its amphiphilic portion (residues 43 - 65) bind to the C-domain of TnC (C-TnC). The H2 helix forms a parallel α-helical coiled-coil with (residues 226 - 271) of TnT2. The IT arm is less mobile and serves as an anchor for C-TnC. Inhibitory peptide (residues 137 - 148) containing basic residues is involved in the actomyosin ATPase inhibitory activity (Eyk et al., 1997). The switch peptide of C-TnI made of helix-H3 (residues 149 - 162) contains amphiphilic residues that interact with the hydrophobic cleft of the N-domain of TnC (N-TnC) (residues 93 - 161). The C-TnI from residues 163 - 210 interacts with the actin filament at low Ca^{2+} is important for anchoring the molecule onto the thin filament and reaches up to the third actin subunit on the N-terminal side of tropomyosin molecule from the actin subunit which is bound to N-TnC (Figure 1.2B) (Takeda et al., 2003; Yamada et al., 2020).

1.4.3.3 Troponin T (TnT)

The largest among the three subunits, TnT is an extended comma-shaped structure (Flicker et al., 1982) that participates in interactions with TnC, TnI, tropomyosin and actin (Fisher et al., 1995; Potter et al., 1995). The tissue-specific isoforms of TnT that exist in fast and slow muscles, as well as developmental isoforms, arise from splicing of multiple genes (Jin et al., 1992; Pan & Potter, 1992; Mesnard et al., 1993; Greig et al., 1994; Anderson et al., 1995; Perry, 1998). Depending on the isoform, the TnT subunit consists of 250 - 300 amino

acids and with a molecular weight of ~ 31 - 36 kDa (as reviewed in Perry, 1998). The TnT molecule is made of three structurally identifiable regions: N-terminal domain (TnT1), a linker domain, and C-terminal domain (TnT2) (Figure 1.8C and D) (Mak & Smillie, 1981b; Perry, 1998; Yamada et al., 2020). The TnT2 domain is further divided into distinguishable regions. According to Takeda et al., 2003, the C-terminal region of human cardiac troponin TnT2 (C-cTnT residues 278 - 288) binds close to cysteine-190 on tropomyosin (binding site 2) (Pearlstone & Smillie, 1982; Tanokura et al., 1983; Morris & Lehrer, 1984). The residues 204 - 220 of the TnT2 domain form the H1 α-helix, whereas residues 226 - 277 form the H2 α-helix (Figure 1.8C). Residues 226 - 271 of H2 helix interact with TnI (residues 90 - 135) by forming a coiled-coil on one side while the other side (residues 256 - 270) interacts with Ca^{2+} binding loops of TnC (EF-hands III and IV) (Figure 1.8C) (Takeda et al., 2003; Yamada et al., 2020; Risi et al., 2021). The TnT1 (residues 1 - 168) consists of an N-terminal alpha-helix (residues 87 - 150) (Figure 1.8D) that is protease resistant indicating the existence of a structural domain (Ohtsuki, 1979; Morris & Lehrer, 1984; Takeda et al., 2003; Yamada et al., 2020). The TnT1 linker region connects the troponin core to the N-terminal α-helix (Figure 1.8D) (Yamada et al., 2020).

TnT1 interacts with the head-to-tail overlap of tropomyosin (binding site 1) in an anti-parallel manner extending towards the N-terminal side of tropomyosin (Brisson et al., 1986; White et al., 1987; Goonasekara & Heeley, 2009; Manning et al., 2012). The remaining residues at the N-terminal tip of Tn-T1 are thought to bind to actin (Oda et al., 2020; Yamada et al., 2020).

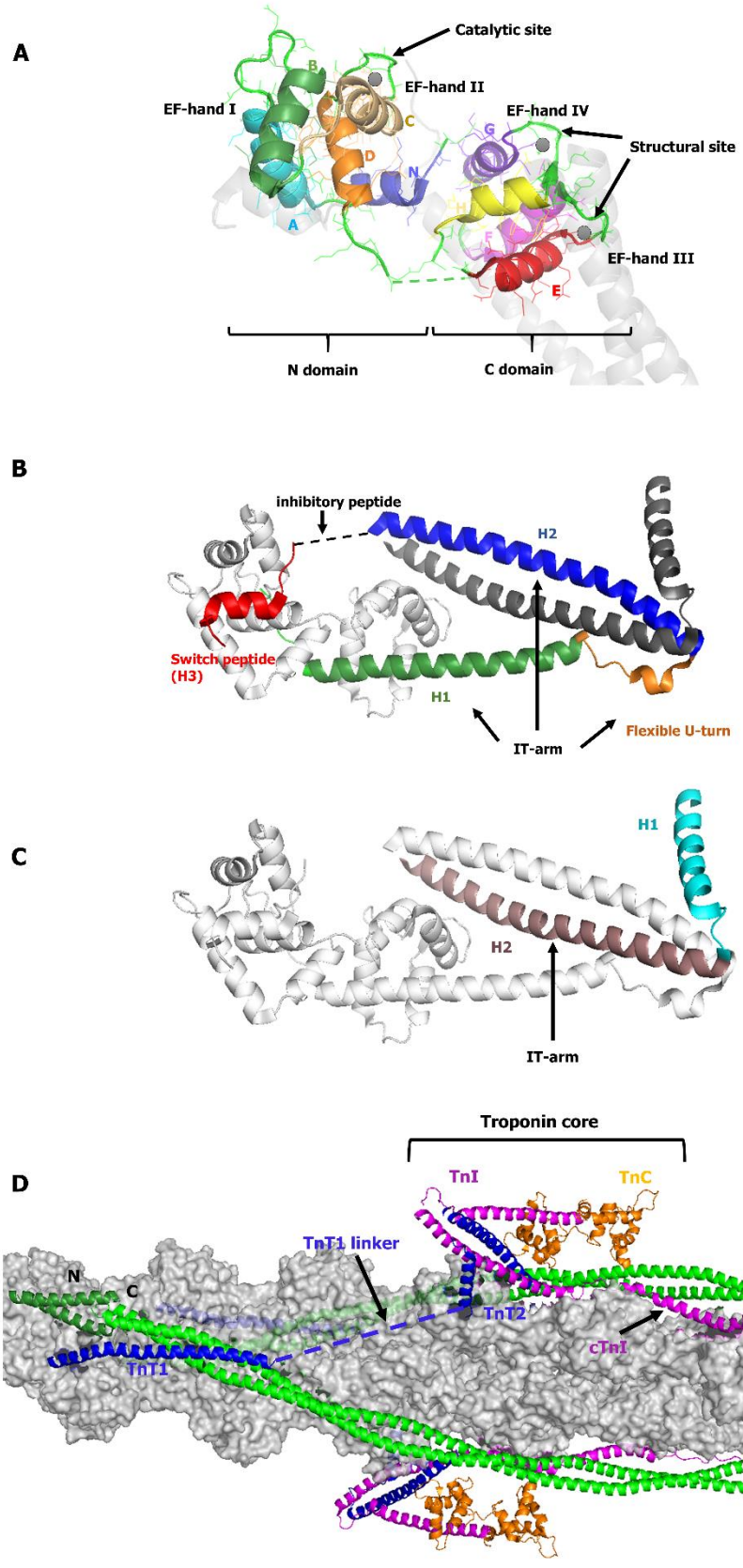
A
Catalytic site
EF-hand I
EF-hand II
EF-hand IV
Structural site
EF-hand III
N domain
C domain
B
inhibitory peptide
H2
Switch peptide
(H3)
H1
IT-arm
Flexible U-turn
C
H1
H2
IT-arm
D
Troponin core
TnI
TnC
TnT1 linker
T1
N
C
TnT2
cTnI
TnT1
T2

Figure 1.8. The structure of troponin. PDB ID: 1J1E. (A) Troponin C (TnC) subfragment color-coded in the troponin complex. The short helices: Cyan - A, Dark green - B, Brown - C, Orange - D, Red - E, Pink - F, Purple - G, Yellow - H and Dark purple - N. EF-hands: I, A-loop-B; II, C-loop-D (catalytic site); III, E- loop-F (structural site); IV, G-loop-H (structural site). Grey spheres - divalent metal ions. N- N-terminal domain. C- C-terminal domain. (B) Troponin I (TnI) subfragment is color-coded in the troponin complex. The IT arm regions of C-TnI contain Green - H1 helix, Blue - H2 helix, and Orange - flexible U-turn. Red - Switch peptide of C-TnI made of H3 helix. Black dotted line - inhibitory peptide region. (C) C-terminal domain of Troponin T(TnT2) color-coded in the troponin complex. Cyan - H1 helix. Brown - H2 helix of the IT arm. (D) Troponin complex interaction with thin filament partners, PDB ID: 6KN7. Green -tropomyosin, Ash - F actin, Orange - TnC, Magenta - TnI, and Blue - TnT. C - C-terminus. N - N-terminus of tropomyosin. Troponin core containing TnC, TnI, and TnT2 is located on tropomyosin (T1). The C-TnI interacts with actin at low Ca^{2+}. The Antiparallel extension of the TnT1 linker and the helix extends towards the C-terminus of the other tropomyosin (T2) dimer and interacts at the overlap.

1.5 Myosin and thick filament

Myosins are a superfamily of motor proteins that use energy from ATP hydrolysis first showed by Engelhardt & Liubimova, 1994 to displace actin filaments and generate force (Huxley, 1969). In humans, there are 39 myosin genes expressed (Heissler & Sellers, 2016). The different members of the myosin family are denoted by Roman numerals. The most abundant forms of myosins are type I, II, and V. In muscle cells, myosin II powers contractions, and in non-muscle cells provide the force to separate the two daughter cells during cytokinesis. Myosin I is involved in linking the actin cytoskeleton with the plasma membrane (Pollard & Korn, 1973) whereas myosin V uses its lipid binding domain to membrane vesicles and intracellular organelles (Johnston et al., 1991; Cheney et al., 1993).

Myosins are made up of different-sized subunits. For example, muscle myosins are hexameric; two heavy chains and four light chains (Figure 1.9A). The heavy chain contains three structurally distinctive domains: (i) the highly conserved N-terminal catalytic motor domain which is also known as the head (80 -100 kDa) and which contains the actin-binding and ATPase sites; (ii) the "lever-arm" region which is located between the head and the tail (see below) and which depending upon the isoform contains one to six IQ motifs (with amino acid sequence IQxxxRGxxxR) that bind to EF-hand proteins (e.g. myosin light chains or calmodulin) which can regulate the properties of myosin by phosphorylation (Perrie et al., 1973; Nishikawa et al., 1985; Scarff et al., 2020) and (iii) the hypervariable C-terminal tail that consists of an alpha-helical coiled-coil for dimerization. In myosin II the tails aggregate making the thick filament or A-band in the sarcomere region (Figure 1F and G). In some non-muscle myosins, the tail has a cargo binding domain (Figure 1.9A).

The head region can be cleaved off using proteases such as trypsin (Mueller & Perry, 1962) and chymotrypsin (Weeds & Taylor, 1975). The resulting fragment, myosin-S1, has a molar mass of ~ 120 kDa, is soluble, and retains actin-activated MgATPase activity (Margossian & Lowey, 1973a, 1973b). The first high-resolution structure of the motor domain has been described using chicken fast skeletal (myosin II) myosin-S1 in the absence of a nucleotide (Rayment et al., 1993; Gulick et al., 1997; Coureux et al., 2004). The myosin motor domain contains a seven stranded beta-sheet embedded in numerous alpha-helices (Figure 1.9B). It consists of a deep cleft of 50 kDa that separates it into two domains: the upper 50 kDa (U50) and, the lower 50 kDa (L50). The ATP-binding site is located at the bottom of the cleft and consists of a phosphate-binding loop (P-loop) (Figure 1.9B) that is characteristic of nucleotide-binding proteins (Rayment et al., 1993; Smith & Rayment, 1996). In the absence of ATP, the U50 and L50 bind to actin filaments and forms a tight (rigor) bond. Upon binding to actin, the cleft is found to stay closed (Rayment et al., 1993; Yengo et al., 1999; Volkmann et al., 2000; Holmes et al., 2003). The N-terminal portion of the head is anchored (via SH1 helix) to the "converter" region (Figure 1.9B), which is capable of rotating about 60^{o} in response to ATP binding and release of hydrolysis products. The converter is attached to the L50 domain via a helix (relay helix) and also provides anchoring for the "lever-arm" described above. The extended conformation of the lever is stabilized by the two light chains (Figure 1.9 A & B) (Rayment et al., 1993).

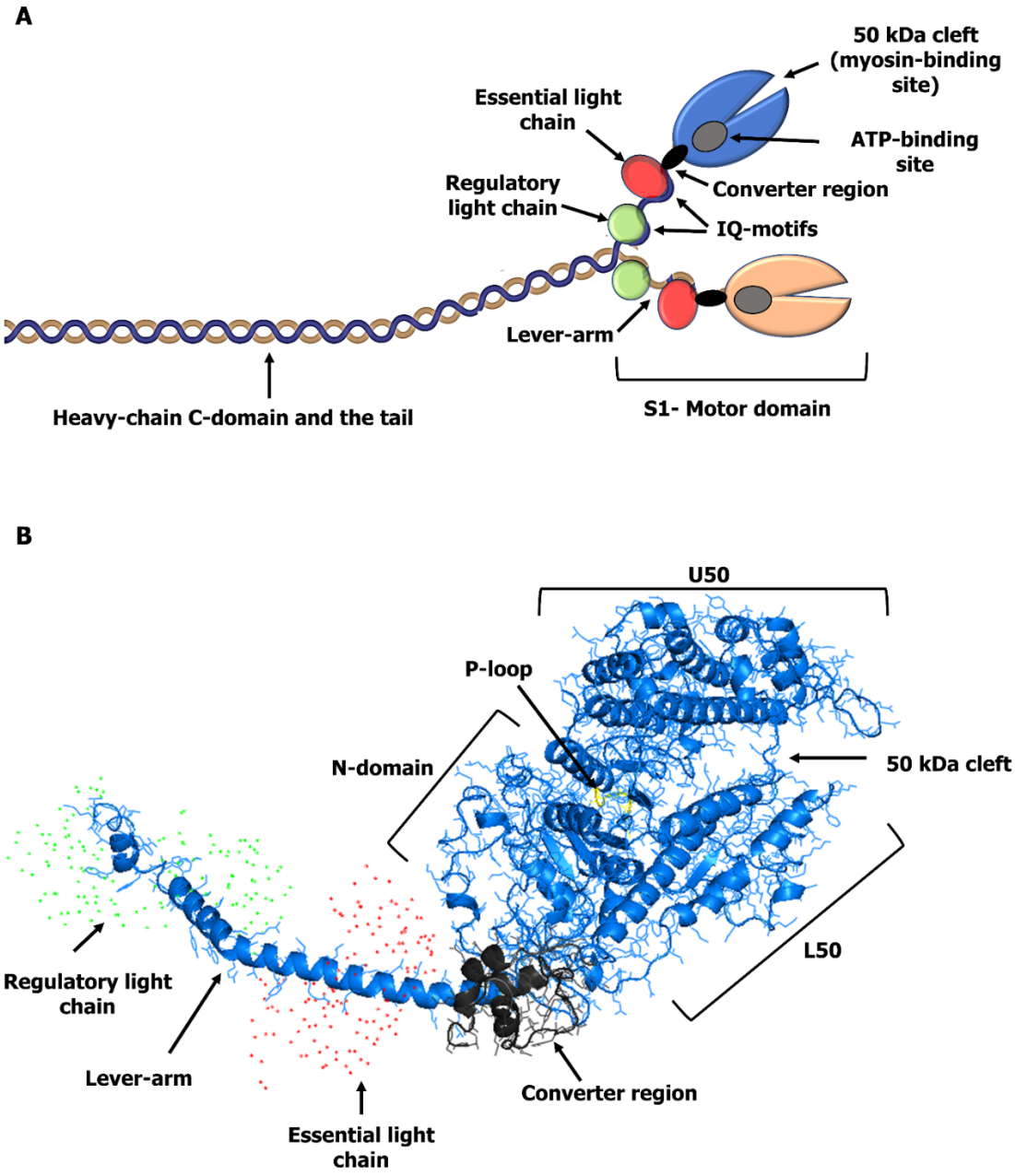
A
50 kDa cleft
(myosin-binding
site)
Essential light
chain
ATP-binding
site
Converter region
Regulatory
light chain
IQ-motifs
Lever-arm
Heavy-chain C-domain and the tail
S1- Motor domain
B
U50
P-loop
N-domain
50 kDa cleft
L50
Regulatory light
chain
Lever-arm
Converter region
Essential light
chain

Figure 1.9. The structure of myosin. Blue and Orange - myosin heavy chains. Red - regulatory light chain. Green - essential light chain. Black - converter region. (A) Schematic representation of myosin heavy chains. Brace - Myosin S1-motor domain consisting of one heavy chain and two light chains. The 50 kDa deep cleft in the S1-motor domain extends to the ATP-binding site (Ash circle). The converter domain provides anchoring for lever-arm with IQ-motifs that binds to regulatory or essential light chains. The C-terminal tail extends from the lever arm. (B) Myosin S1-motor domain, PDB ID: 2MYS. The motor-domain containing beta-sheets embedded in numerous alpha-helices. Yellow - P-loop located at the bottom of 50 kDa cleft. U50 - Upper 50 kDa domain. L50 - Lower 50 kDa domain. N - domain is anchored to the converter domain. The lever-arm consists of an extended alpha-helix extending from the flexible converter region.

1.6 Muscle contraction

In the sarcomere, troponin and tropomyosin control the interaction of F-actin with myosin thereby regulating contraction and relaxation. Early X-ray diffraction studies suggested that these processes involve the movement of tropomyosin on the grooves of F-actin (Parry & Squire, 1973; Haselgrove & Huxley, 1973) leading to the development of the steric blocking model. The model proposed that tropomyosin is able to take up two positions on actin. At low Ca^{2+} concentration, tropomyosin impedes myosin binding and actin is unable to activate myosin. Whereas, at high concentration, Ca^{2+} binding to troponin causes a shift in tropomyosin that exposes the myosin binding site that was previously covered. Myosin heads can now bind to actin, allowing activation of MgATPase (i.e. catalytic hydrolysis) and the production of force (Huxley, 1973; Haselgrove & Huxley, 1973). However, in its original form steric blocking was inconsistent with the fact that Ca^{2+} has a small effect on the affinity of myosin-S1 for thin filaments during steady-state ATP hydrolysis (Chalovich et al., 1981; Chalovich & Eisenberg, 1982). Subsequently, the discrepancy between binding and ATPase activity was accommodated in improved thin filament models (McKillop & Geeves, 1993; Chen et al., 2001).

1.6.1 The Ca^{2+} switch of thin filament regulation

The position of tropomyosin on the thin filament is controlled by the troponin complex in response to the changes in intracellular Ca^{2+} concentration (Ebashi et al., 1969; Gordon et al., 1997). Hence it is identified as the Ca^{2+} switch. At low Ca^{2+} concentration, the interactions made by both TnT (Heeley, 1994; Manning et al., 2012; Yamada et al., 2020) and TnI (Mudalige et al., 2009; Manning et al., 2011; Yamada et al., 2020) to tropomyosin, position tropomyosin on actin subdomains 1 and 2 where it prevents the strong (productive) binding of actin to myosin. More specifically, the C-TnI region binds to actin and the N-TnI binds to tropomyosin near the troponin core (C-TnI, TnC, and TnT2), covering the myosin head binding sites (Figure 1.10A). Hence, the system is turned off.

When the Ca^{2+} level increases, Ca^{2+} ions bind to the regulatory sites in N-TnC. This induces a conformational re-arrangement, which opens the hydrophobic patch in the N-domain of TnC exposing it to the switch peptide of TnI. The binding of this peptide moves the C-TnI away from actin which causes tropomyosin to azimuthally shift along the actin surface thereby revealing some of the myosin-binding site~~s~~ (Figure 1.10B). The displacement in tropomyosin is uniform ~10 Å along its length except near the head-to-tail junction (Yamada et al., 2020). In the Ca^{2+} bound state, tropomyosin occupies an intermediate position in which some of the surfaces of actin are exposed to myosin but not all. For the thin filament to be fully turned on, the attachment of rigor-myosin to the thin filament is required (McKillop & Geeves 1993).

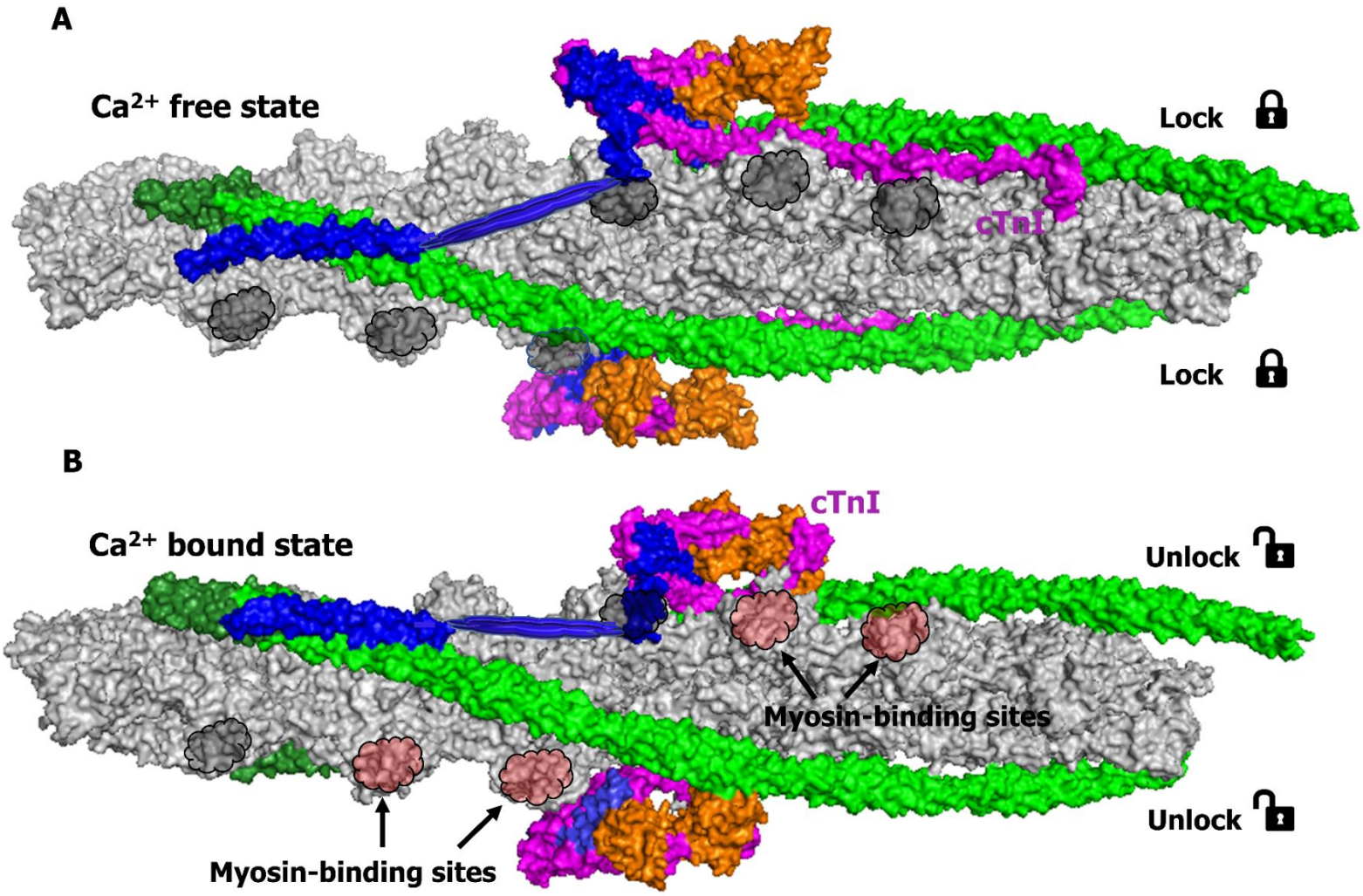
A
Ca2+ free state
Lock
cTnI
Lock
B
Ca2+ bound state
cTnI
Unlock
Myosin-binding sites
Unlock
Myosin-binding sites

Figure 2.10. The Ca^{2+} induced regulatory mechanism of muscle contraction. The structural changes between Ca^{2+} free and bound states are shown. Gray - F-actin. Green - Tropomyosin. Orange - TnC, Magenta - TnI. Blue - TnT. Dark gray - closed myosin-binding sites. Pink - open myosin-binding sites. (A) Ca^{2+} free state, PDB ID: 6KN7. The cTnI region binds to actin and N-TnI binds tropomyosin above the troponin core (C-TnI, TnC, and TnT2), covering the myosin head binding sites. Hence the thin filament acquires a locked state. (B) Ca^{2+} bound state, PDB ID: 6KN8. Binding of a Ca^{2+} ion to the EF-hand II of N-TnC causes the C-TnI to dissociates from the actin filament and bind to the N-TnC region. This causes tropomyosin to move around on the actin filament surface together with TnT1 near the head-to-tail junction exposing some of the myosin head binding sites.

1.6.2 The swinging cross-bridge cycle of muscle contraction

The first direct evidence for an alteration in myosin head position was obtained from a structural analysis of insect muscles at rest and in rigor (Reedy et al., 1965). These changes were used to formulate the swinging cross-bridge model (Huxley, 1969). In 1971 Lymn & Taylor explained this cycle (Figure 1.11) in terms of the kinetic properties of actomyosin. The details are as follows. In the absence of ATP, the myosin head forms a "rigor" bond with the actin filament (Figure 1.11). The binding of MgATP to the active site on the myosin leads to the rapid dissociation of the rigor complex (Figure 1.11). The next step in the cycle involves the hydrolysis of substrate and the conformational rearrangement in the lever arm. The myosin-MgADP-Pi complex then rebinds to actin. The myosin-MgATP and myosin-MgADP-Pi states are considered as ‘weak-binding’ or ‘pre-force generating’ intermediates that have low (micromolar) actin affinities that do not generate force (De La Cruz & Ostap, 2004). Myosin rebinding to actin triggers the release of Pi from myosin-MgADP-Pi and, in the absence of actin, this is slow (Yount et al., 1995; White et al., 1997). It is the dissociation of Pi from the active site that causes the lever arm to swing and drive the power stroke. A smaller swing in the lever arm is associated with the departure of MgADP (Figure 1.11). The release of ADP allows the binding of a new ATP molecule to myosin and the cycle starts again. For each turn of the cycle, changes in the conformation of the myosin cross-bridge move the actin filament approximately 10 nm (Yanagida et al., 1985; Spudich, 2001). Accordingly, in a muscle, the two filaments (A-band rich in myosin and I-band rich in actin) slide past each other (Huxley, 1969; Huxley & Simmons, 1971) coupled with the energy from ATP hydrolysis (Lorand, 1953; Davies, 1964).

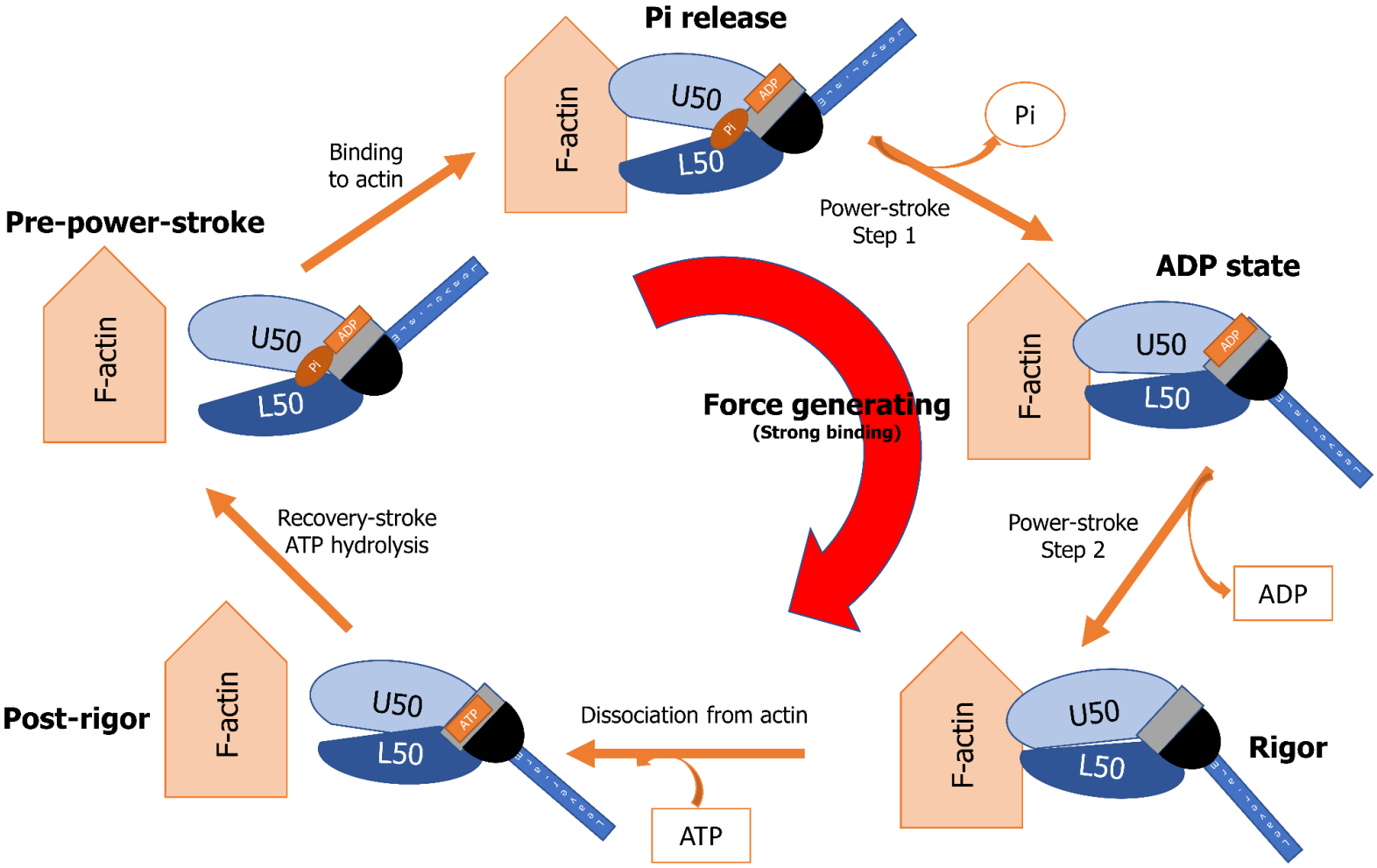
Pi release
F-actin
U50
ADP
Pi
L50
Pi
Binding
to actin
Power-stroke
Step 1
Pre-power-stroke
ADP state
F-actin
U50
ADP
Pi
L50
F-actin
U50
ADP
L50
Force generating
(Strong binding)
Recovery-stroke
ATP hydrolysis
Power-stroke
Step 2
ADP
Post-rigor
F-actin
U50
ATP
L50
Dissociation from actin
F-actin
U50
L50
Rigor
ATP

Figure 3.11. Schematic representation of the cross-bridge cycle with swinging lever arm. Orange - F-actin, Light blue - U50 domain, Dark blue - L50 domain and leaver arm, Ash - N-domain, and Black - converter region. The myosin heads at strong binding, and heads at the weak binding on actin filament during the ATPase cycle. The acto-myosin-MgADP and acto-myosin states are ‘strong-binding’ intermediates that attach to actin filaments with high (submicromolar) affinities. Lymn & Taylor 1971 cross-bridge cycle based on Wulf et al., 2016.

1.7 Results chapters of the thesis

Chapter 2. Demonstration of beta-tropomyosin (Tpm2) and alpha-1 chain-like X1 isoforms in Atlantic salmon (*Salmo salar*).

Chapter 3. Threonine-77 is a determinant of the low-temperature conditioning of the most abundant isoform of tropomyosin in Atlantic salmon.

Chapter 4. Further investigation into the biochemical effects of phosphorylation of tropomyosin Tpm1.1(α). Serine-283 is in communication with the mid-region.

1.8 Rationale and Objectives

Given the current state of knowledge concerning tropomyosin, my research focused on three major objectives:

1. The Atlantic salmon (*Salmo salar*) has a unique anatomy in regard to the distribution of different muscles which allows easy extraction of specific tropomyosin isoforms. The Heeley lab has identified and biochemically characterized the tropomyosin isoforms in the trunk (the major contributor to the muscle mass) and heart of Salmonidae fishes. These are alpha-fast (Tpm1, accession number AAB36559) the most abundant isoform and which is encoded by TPM1, alpha-slow (Tpm3, Z66490) encoded by TPM3, and cardiac (Tpm4, Z66527) encoded by TPM4 (Heeley et al., 1995; Jackman et al., 1996). The completion of the Atlantic salmon genome (Lien et al., 2016), reveals the presumed existence of numerous other tropomyosin isoforms including the TPM2 coded beta-tropomyosin although none of which have been documented at the protein level for any fish species. Therefore, the objective of this chapter is to identify and characterize the tropomyosin isoforms in the minor muscle tissues from head and fin regions, that have not been studied before for their potential to contain a novel isoform.

2. Flexibility is an important feature that is required for tropomyosin to bind to troponin and actin to maintain its regulatory function in the thin filament. Psychrophilic organisms (organisms that live < 15 ^{o}C) need additional flexibility to overcome cold-induced rigidity. In this regard, Atlantic salmon *(Salmo salar)* serves as a very good model due to its low ambient temperature and a relatively small number (~ 20) of amino acid substitutions in the most abundant tropomyosin isoform Tpm1 compared to the mesophilic homologs

(Tpm1.1(α)) such as rabbit (Heeley et al., 1995). Of the substitutions that are non-conservative one accounts for a full charge change; residue-77 (Thr salmon; Lys rabbit) while two others involve the presence of glycine, a known helix breaker (Richardson & Richardson, 1988), at residues-24 & 27 in salmon but not in rabbit. The residue-77 corresponds to a "g" heptad position (Stone & Smillie, 1978). Since the "e" positions in the next heptad units (of the same and opposite strands of the coiled-coil) are occupied by glutamates (Glu-75 and Glu-82), there is the potential for a change in ionic interactions at this location. Also, residue-77 falls into the 2nd alanine cluster among Ala-74(d), Ala-78(a), and Ala-81(d) a region that is known to be important for actin binding. Additionally, Gly-24 and 27 is in the segment Lys15-Ala18-Ala22-Ala25-Lys29-Ala32-Ser36 which is identified as a major destabilizing cluster at the N-terminal part of the molecule (Brown et al., 2001) which previous (Mak & Smillie, 1981; Pato et al., 1981; Brisson et al., 1986; Heeley et al., 1987; Goonasekara & Heeley, 2009; Manning et al., 2011) and recent (Oda et al., 2020; Yamada et al., 2020) researchers have shown to contain a binding site for TnT1. Therefore, the objective of this chapter is to determine the extent to which the non-conservative substitutions at residue-77 and Gly-24 and 27 contribute to the conformational flexibility of salmon tropomyosin.

3. The alpha form of tropomyosin in striated muscles in mammals and birds is phosphorylated at Ser-283 (Mak et al., 1978) and the levels change with the age of the animal (Heeley et al., 1982). The fetal skeletal and cardiac muscles tropomyosins are phosphorylated to a higher extent compared to that of the adult suggesting a prominent role in early development (Montarras et al., 1981; Heeley et al., 1982; Heeley et al., 1985). The

phosphorylation of alpha tropomyosin has been shown to increase the head-to-tail polymerizability (Heeley et al., 1989) and, troponin binding ability (Heeley, 1994) suggesting that it favors filament assembly. Although previous studies found no effect on F-actin binding (Heeley et al., 1989) phosphorylation of Ser-61 in cytoskeletal isoforms has revealed that it is associated with actin remodeling (Naga Prasad et al., 2005; Houle & Huot, 2006). Therefore, the objective of this chapter is to further understand the effect of phosphorylation on the properties of tropomyosin, specifically the conformational stability of the molecule as well as its interaction with F-actin.

1.9 Publications arising from this thesis

I. **Silva, A. M. M**., Kennedy, L. S., Hasan, S. C., Cohen, A. M., & Heeley, D. H. (2020). Demonstration of beta-tropomyosin (Tpm2) and duplication of the alpha-slow tropomyosin gene (TPM3) in Atlantic salmon Salmo salar. *Comparative Biochemistry and Physiology Part - B: Biochemistry and Molecular Biology*, *245*(January), 110439. https://doi.org/10.1016/j.cbpb.2020.110439

(The data presented in chapter 2 is used under copyright license from publisher Elsevier, with the copyright permission presented in appendix A).

This publication contains results that were generated by other second- authors. Only the results from experiments performed by the first-author, A.M.M Silva are presented in this thesis.

Author contributions

A.M.M.S., protein isolation, 1-D PAGE, 2-D PAGE, affinity chromatography, pairwise sequence alignments, phylogenetic analysis, and manuscript preparation.

L.S.K., 2-D PAGE.

S.C.H. 2-D PAGE.

A.M.C., tryptic peptide mass spectrometry.

D.H.H., protein isolation, end-group analysis, and manuscript preparation.

II. **Silva, A. M. M**., Ige, T., Goonasekara, C. L., & Heeley, D. H. (2020). Threonine-77 Is a Determinant of the Low-Temperature Conditioning of the Most Abundant Isoform of Tropomyosin in Atlantic Salmon. *Biochemistry*, *59*(31), 2859–2869. https://doi.org/10.1021/acs.biochem.0c00416

(The data presented in chapter 3 is used under copyright license from the publisher American Chemical Society, with the copyright permission presented in appendix A). This publication contains results that were generated by other second- authors. Only the results from experiments performed by the first-author, A.M.M Silva are presented in this thesis.

Author contributions

A.M.M.S., protein isolation, tryptic peptide mapping, limited proteolysis, calorimetry, troponin-Sepharose affinity chromatography, F-actin binding, PyMOl, and manuscript preparation.

T.I., site-directed mutagenesis.

C.L.G., protein isolation and

D.H.H., manuscript preparation.

III. **Silva, A. M. M**., Goonasekara, C. L., Hayley, M., & Heeley, D. H. (2020). Further Investigation into the Biochemical Effects of Phosphorylation of Tropomyosin Tpm1.1(α). Serine-283 Is in Communication with the Mid region. *Biochemistry*, *59*(50), 4725–4734. https://doi.org/10.1021/acs.biochem.0c00882

(The data presented in chapter 4 is used under copyright license from the publisher American Chemical Society, with the copyright permission presented in appendix A). This publication contains results that were generated by other second- authors. Only the results from experiments performed by the first-author, A.M.M Silva are presented in this thesis.

Author contributions

A.M.M.S., protein isolation, limited proteolysis, F-actin binding, circular dichroism, and manuscript preparation.

C.L.G., myosin-S1(ADP) binding.

M.H., circular dichroism.

D.H.H., protein isolation, fast-mixing stopped-flow experiments, tissue radiolabeling, and manuscript preparation.

1.10 Chapter 1 References

Alway S. E., Macdougall J. D., Sale D. G., Sutton J. R., Mccomas A. J. (1988). Functional and structural adaptations in skeletal muscle of trained athletes. *Journal of Functional and Applied Physiology.* 64 1114–1120. 10.1152/jappl.1988.64.3.1114

Astbury, W. T., Reed, R., & Spark, L. C. (1948). An X-ray and electron microscope study of tropomyosin. *Biochemical Journal*, *43*(2), 282–287. https://doi.org/10.1042/bj0430282

Bailey, K. (1946). Tropomyosin: a New Asymmetric Protein Component of Muscle. *Nature*, *157*(3986), 368–369. https://doi.org/10.1038/157368b0

Bailey, K. (1948). Tropomyosin: a new asymmetric protein component of the muscle fibril. *The Biochemical Journal*, *43*(2), 271–279. https://doi.org/10.1042/bj0430271

Bandman, E. (1992). Contractile protein isoforms in muscle development. *Developmental Biology*, *154*(2), 273–283. https://doi.org/10.1016/0012-1606(92)90067-q

Betteridge, D. R., & Lehrer, S. S. (1983). Two conformational states of didansylcystine-labeled rabbit cardiac tropomyosin. *Journal of Molecular Biology*, *167*(2), 481–496. https://doi.org/https://doi.org/10.1016/S0022-2836(83)80346-5

Biancone, L., Monteleone, G., Marasco, R., & Pallone, F. (1998). Autoimmunity to tropomyosin isoforms in ulcerative colitis (UC) patients and unaffected relatives. *Clinical and Experimental Immunology*, *113*(2), 198–205. https://doi.org/10.1046/j.1365-2249.1998.00610.x

Blumenschein, T. M. A., Gillis, T. E., Tibbits, G. F., & Sykes, B. D. (2004). Effect of temperature on the structure of trout troponin C. *Biochemistry*, *43*(17), 4955–4963. https://doi.org/10.1021/bi035504z

Bone, Q., Marshall, N. B., & Blaxter, J. H. S. (1995). *Biology of Fishes* (2nd ed.). Chapman & HaU in 1995. https://doi.org/10.1007/978-1-4615-2664-3

Bork, P., Sander, C., & Valencia, A. (1992). An ATPase domain common to prokaryotic cell cycle proteins, sugar kinases, actin, and hsp70 heat shock proteins. *Proceedings of the National Academy of Sciences of the United States of America*, *89*(16), 7290–7294. https://doi.org/10.1073/pnas.89.16.7290

Brisson, J. R., Golosinska, K., Smillie, L. B., & Sykes, B. D. (1986). Interaction of tropomyosin and troponin T: a proton nuclear magnetic resonance study. *Biochemistry*, *25*(16), 4548–4555. https://doi.org/10.1021/bi00364a014

Brown, J. H., & Cohen, C. (2005). Regulation of muscle contraction by tropomyosin and troponin: how structure illuminates function. *Advances in Protein Chemistry*, *71*, 121–159. https://doi.org/10.1016/S0065-3233(04)71004-9

Brown, J. H., Kim, K. H., Jun, G., Greenfield, N. J., Dominguez, R., Volkmann, N., Hitchcock-DeGregori, S. E., & Cohen, C. (2001). Deciphering the design of the tropomyosin molecule. *Proceedings of the National Academy of Sciences of the United States of America*, *98*(15), 8496–8501. https://doi.org/10.1073/pnas.131219198

Brown, J. H., Zhou, Z., Reshetnikova, L., Robinson, H., Yammani, R. D., Tobacman, L.

S., & Cohen, C. (2005). Structure of the mid-region of tropomyosin: bending and binding sites for actin. *Proceedings of the National Academy of Sciences of the United States of America*, *102*(52), 18878–18883. https://doi.org/10.1073/pnas.0509269102

Chalovich, J. M., Chock, P. B., & Eisenberg, E. (1981). Mechanism of action of troponin. tropomyosin. Inhibition of actomyosin ATPase activity without inhibition of myosin binding to actin. *The Journal of Biological Chemistry*, *256*(2), 575–578.

Chalovich, J. M., & Eisenberg, E. (1982). Inhibition of actomyosin ATPase activity by troponin-tropomyosin without blocking the binding of myosin to actin. *The Journal of Biological Chemistry*, *257*(5), 2432–2437. https://pubmed.ncbi.nlm.nih.gov/6460759

Chen, Y., Yan, B., Chalovich, J. M., & Brenner, B. (2001). Theoretical kinetic studies of models for binding myosin subfragment-1 to regulated actin: Hill model versus Geeves model. *Biophysical Journal*, *80*(5), 2338–2349. https://doi.org/10.1016/s0006-3495(01)76204-2

Cheney, R. E., O'Shea, M. K., Heuser, J. E., Coelho, M. V., Wolenski, J. S., Espreafico, E. M., Forscher, P., Larson, R. E., & Mooseker, M. S. (1993). Brain myosin-V is a two-headed unconventional myosin with motor activity. *Cell*, *75*(1), 13–23. https://doi.org/10.1016/S0092-8674(05)80080-7

Cho, Y. J., Liu, J., & Hitchcock-DeGregori, S. E. (1990). The amino terminus of muscle tropomyosin is a major determinant for function. *Journal of Biological Chemistry*,

265(1), 538–545. https://doi.org/https://doi.org/10.1016/S0021-9258(19)40264-0

Chou, S. Z., & Pollard, T. D. (2019). Mechanism of actin polymerization revealed by cryo-EM structures of actin filaments with three different bound nucleotides. *Proceedings of the National Academy of Sciences*, *116*(10), 4265 LP – 4274. https://doi.org/10.1073/pnas.1807028115

Claassen H., Gerber C., Hoppeler H., Luthi J. M., Vock P. (1989). Muscle filament spacing and short-term heavy-resistance exercise in humans. *The Journal of Physiology*. 409 491–495. 10.1113/jphysiol.1989.sp017509

Clarke, N. F., Domazetovska, A., Waddell, L., Kornberg, A., McLean, C., & North, K. N. (2009). Cap disease due to mutation of the beta-tropomyosin gene (TPM2). *Neuromuscular Disorders*, *19*(5), 348–351. https://doi.org/10.1016/j.nmd.2009.03.003

Clayton, L., Reinach, F. C., Chumbley, G. M., & MacLeod, A. R. (1988). Organization of the hTMnm gene: Implications for the evolution of muscle and non-muscle tropomyosins. *Journal of Molecular Biology*, *201*(3), 507–515. https://doi.org/https://doi.org/10.1016/0022-2836(88)90633-X

Cohen, I., & Cohen, C. (1972). A tropomyosin-like protein from human platelets. *Journal of Molecular Biology*, *68*(2), 383–387. https://doi.org/https://doi.org/10.1016/0022-2836(72)90220-3

Conway, J. F., & Parry, D. A. D. (1990). Structural features in the heptad substructure and longer range repeats of two-stranded α-fibrous proteins. *International Journal of*

Biological Macromolecules, *12*(5), 328–334. https://doi.org/https://doi.org/10.1016/0141-8130(90)90023-4

Corsi, A., & Perry, S. V. (1958). Some observations on the localization of myosin, actin, and tropomyosin in the rabbit myofibril. *The Biochemical Journal*, *68*(1), 12–17. https://doi.org/10.1042/bj0680012

Coulton, A., Lehrer, S. S., & Geeves, M. A. (2006). Functional homodimers and heterodimers of recombinant smooth muscle tropomyosin. *Biochemistry*, *45*(42), 12853–12858. https://doi.org/10.1021/bi0613224

Coureux, P. D., Sweeney, H. L., & Houdusse, A. (2004). Three myosin V structures delineate essential features of chemo-mechanical transduction. *EMBO Journal*, *23*(23), 4527–4537. https://doi.org/10.1038/sj.emboj.7600458

Crick, F. H. C. (1953). The packing of α-helices: simple coiled-coils. *Acta Crystallographica*, *6*(8), 689–697. https://doi.org/10.1107/s0365110x53001964

Cummins, P., & Perry, S. V. (1973). The subunits and biological activity of polymorphic forms of tropomyosin. *Biochemical Journal*, *133*(4), 765–777. https://doi.org/10.1042/bj1330765

Cummins, P., & Perry, S. V. (1974). Chemical and immunochemical characteristics of tropomyosins from striated and smooth muscle. *The Biochemical Journal*, *141*(1), 43–49. https://doi.org/10.1042/bj1410043

Dabrowska, R., Nowak, E., & Drabikowski, W. (1983). Some functional properties of nonpolymerizable and polymerizable tropomyosin. *Journal of Muscle Research and*

Cell Motility, *4*(2), 143–161. https://doi.org/10.1007/BF00712027

Das, K. M., Dasgupta, A., Mandal, A., & Geng, X. (1993). Autoimmunity to cytoskeletal protein tropomyosin. A clue to the pathogenetic mechanism for ulcerative colitis. *Journal of Immunology (Baltimore, Md. : 1950)*, *150*(6), 2487–2493.

Davies, R. E. (1964). Adenosine triphosphate breakdown during single muscle contractions. *Proceedings of the Royal Society of London. Series B, Biological Sciences*, *160*, 480–485. https://doi.org/10.1098/rspb.1964.0060

De La Cruz, E. M., & Ostap, E. M. (2004). Relating biochemistry and function in the myosin superfamily. *Current Opinion in Cell Biology*, *16*(1), 61–67. https://doi.org/10.1016/j.ceb.2003.11.011

deBelle, I., & Mak, A. S. (1987). Isolation and characterization of tropomyosin kinase from chicken embryo. *Biochimica et Biophysica Acta*, *925*(1), 17–26. https://doi.org/10.1016/0304-4165(87)90143-7

Deniz, A. A. (2018). Remote wiggling helps cold enzymes work seas affect each other. *Nature*, *558*(2016), 195–196.

Dhoot, G. K., & Perry, S. V. (1982). The effect of denervation on the distribution of the polymorphic forms of troponin components in fast and slow muscles of the adult rat. *Cell and Tissue Research*, *225*(1), 201–215. https://doi.org/10.1007/BF00216229

Donner, K., Ollikainen, M., Ridanpää, M., Christen, H.-J., Goebel, H. H., de Visser, M., Pelin, K., & Wallgren-Pettersson, C. (2002). Mutations in the beta-tropomyosin (TPM2) gene--a rare cause of nemaline myopathy. *Neuromuscular Disorders :*

NMD, *12*(2), 151–158. https://doi.org/10.1016/s0960-8966(01)00252-8

Dube, D. K., Dube, S., Abbott, L., Wang, J., Fan, Y., Alshiekh-Nasany, R., Shah, K. K., Rudloff, A. P., Poiesz, B. J., Sanger, J. M., & Sanger, J. W. (2017). Identification, characterization, and expression of sarcomeric tropomyosin isoforms in zebrafish. *Cytoskeleton (Hoboken, N.J.)*, *74*(3), 125–142. https://doi.org/10.1002/cm.21352

Dufour, C., Weinberger, R. P., Schevzov, G., Jeffrey, P. L., & Gunning, P. (1998). Splicing of two internal and four carboxyl-terminal alternative exons in nonmuscle tropomyosin 5 pre-mRNA is independently regulated during development. *The Journal of Biological Chemistry*, *273*(29), 18547–18555. https://doi.org/10.1074/jbc.273.29.18547

Eaton, B. L., Kominz, D. R., & Eisenberg, E. (1975). Correlation between the inhibition of the acto-heavy meromyosin ATPase and the binding of tropomyosin to F-actin: effects of Mg^{2+}, KCl, troponin I, and troponin C. *Biochemistry*, *14*(12), 2718–2725. https://doi.org/10.1021/bi00683a025

Ebashi, S, Kodama, A., & Ebashi, F. (1968). Troponin. I. Preparation and physiological function. *Journal of Biochemistry*, *64*(4), 465–477. https://doi.org/10.1093/oxfordjournals.jbchem.a128918

Ebashi, Setsuro, Endo, M., & Ohtsuki, I. (1969). Control of muscle contraction. *Quarterly Reviews of Biophysics*, *2*(4), 351–384. https://doi.org/DOI: 10.1017/S0033583500001190

Ebashi, Setsuro, Wakabayashi, T., & Ebashi, F. (1971). Troponin and its components.

Journal of Biochemistry, *69*(2), 441–445. https://doi.org/10.1093/oxfordjournals.jbchem.a129486

Edwards, B. F. P., and Sykes, B. D. (. (1980). Nuclear magnetic resonance evidence for the coexistence of several conformational states of rabbit cardiac and skeletal tropomyosins. *Biochemistry*, *19*, 2577 – 2583.

Edwards, B. F. P., & Sykes, B. D. (1981). Analysis of Cooperativity Observed in pH Titrations of Proton Nuclear Magnetic Resonances of Histidine Residues of Rabbit Cardiac Tropomyosin. *Biochemistry*, *20*(14), 4193–4198. https://doi.org/10.1021/bi00517a037

Eisenberg, E., & Kielley, W. W. (1974). Troponin tropomyosin complex. Column chromatographic separation and activity of the three active troponin components with and without tropomyosin present. *The Journal of Biological Chemistry*, *249*(15), 4742–4748. https://doi.org/10.1016/S0021-9258(19)42382-X

Elzinga, M., Collins, J. H., Kuehl, W. M., & Adelstein, R. S. (1973). Complete amino-acid sequence of actin of rabbit skeletal muscle. *Proceedings of the National Academy of Sciences of the United States of America*, *70*(9), 2687–2691. https://doi.org/10.1073/pnas.70.9.2687

Engel, J., Fasold, H., Hulla, F. W., Waechter, F., & Wegner, A. (1977). The polymerization reaction of muscle actin. *Molecular and Cellular Biochemistry*, *18*(1), 3–13. https://doi.org/10.1007/BF00215273

Engelhardt, W. A., & Liubimova, M. N. (1994). [Myosin and adenosine triphosphatase

(Nature, 144, 688, Oct. 14, 1939)]. *Molekuliarnaia biologiia*, *28*(6), 1229–1230.

Estes, J. E., Selden, L. A., Kinosian, H. J., & Gershman, L. C. (1992). Tightly-bound divalent cation of actin. *Journal of Muscle Research & Cell Motility*, *13*(3), 272–284. https://doi.org/10.1007/BF01766455

Fatigati, V., & Murphy, R. A. (1984). Actin and tropomyosin variants in smooth muscles. Dependence on tissue type. *The Journal of Biological Chemistry*, *259*(23), 14383–14388.

Fine, R. E., & Blitz, A. L. (1975). A chemical comparison of tropomyosins from muscle and non-muscle tissues. *Journal of Molecular Biology*, *95*(3), 447–454. https://doi.org/https://doi.org/10.1016/0022-2836(75)90202-8

Fisher, D., Wang, G., & Tobacman, L. S. (1995). NH2-terminal truncation of skeletal muscle troponin T does not alter the Ca^{2+} sensitivity of thin filament assembly. *The Journal of Biological Chemistry*, *270*(43), 25455–25460. https://doi.org/10.1074/jbc.270.43.25455

Flicker, P. F., Phillips, G. N., & Cohen, C. (1982). Troponin and its interactions with tropomyosin: An electron microscope study. *Journal of Molecular Biology*, *162*(2), 495–501. https://doi.org/https://doi.org/10.1016/0022-2836(82)90540-X

Forry-Schaudies, S., Maihle, N. J., & Hughes, S. H. (1990). Generation of skeletal, smooth and low molecular weight non-muscle tropomyosin isoforms from the chicken tropomyosin 1 gene. *Journal of Molecular Biology*, *211*(2), 321–330. https://doi.org/10.1016/0022-2836(90)90354-O

Franzén, B., Linder, S., Uryu, K., Alaiya, A. A., Hirano, T., Kato, H., & Auer, G. (1996). Expression of tropomyosin isoforms in benign and malignant human breast lesions. *British Journal of Cancer*, *73*(7), 909–913. https://doi.org/10.1038/bjc.1996.162

Frieden, C., Lieberman, D., & Gilbert, H. R. (1980). A fluorescent probe for conformational changes in skeletal muscle G-actin. *The Journal of Biological Chemistry*, *255*(19), 8991–8993.

Fudge, K. R., & Heeley, D. H. (2015). Biochemical characterization of the roles of glycines 24 and 27 and threonine 179 in tropomyosin from the fast skeletal trunk muscle of the Atlantic salmon. *Biochemistry*, *54*(17), 2769–2776. https://doi.org/10.1021/acs.biochem.5b00156

Fujii, T., Iwane, A. H., Yanagida, T., & Namba, K. (2010). Direct visualization of secondary structures of F-actin by electron cryomicroscopy. *Nature*, *467*(7316), 724–728. https://doi.org/10.1038/nature09372

Gaillard, C., Lerivray, H., Thézé, N., Cooper, B., Lepetit, D., Mohun, T., & Thiébaud, P. (1999). Differential expression of two skeletal muscle beta-tropomyosin mRNAs during *Xenopus laevis* development. *The International Journal of Developmental Biology*, *43*(2), 175–178.

Gaillard, C., Thézé, N., Hardy, S., Allo, M. R., Ferrasson, E., & Thiébaud, P. (1998). Alpha-tropomyosin gene expression in *Xenopus laevis*: differential promoter usage during development and controlled expression by myogenic factors. *Development Genes and Evolution*, *207*(7), 435–445. https://doi.org/10.1007/s004270050134

Gaillard, C., Thézé, N., Lerivray, H., Hardy, S., Lepetit, D., & Thiébaud, P. (1998). A novel tropomyosin isoform encoded by the Xenopus laevis alpha-TM gene is expressed in the brain. *Gene*, *207*(2), 235–239. https://doi.org/10.1016/s0378-1119(97)00634-3

Galloway, P. G., Likavec, M. J., & Perry, G. (1990). Tropomyosin isoform expression in normal and neoplastic astrocytes. *Laboratory Investigation; a Journal of Technical Methods and Pathology*, *62*(2), 163–170.

Geeves, M. A., Hitchcock-DeGregori, S. E., & Gunning, P. W. (2015). A systematic nomenclature for mammalian tropomyosin isoforms. *Journal of Muscle Research and Cell Motility*, *36*(2), 147–153. https://doi.org/10.1007/s10974-014-9389-6

Geng, X., Biancone, L., Dai, H. H., Lin, J. J., Yoshizaki, N., Dasgupta, A., Pallone, F., & Das, K. M. (1998). Tropomyosin isoforms in intestinal mucosa: production of autoantibodies to tropomyosin isoforms in ulcerative colitis. *Gastroenterology*, *114*(5), 912–922. https://doi.org/10.1016/s0016-5085(98)70310-5

Gillis, T. E., Blumenschein, T. M. A., Sykes, B. D., & Tibbits, G. F. (2003). Effect of Temperature and the F27W Mutation on the Ca^{2+} Activated Structural Transition of Trout Cardiac Troponin C. *Biochemistry*, *42*(21), 6418–6426. https://doi.org/10.1021/bi0340494

Gillis, T. E., Liang, B., Chung, F., & Tibbits, G. F. (2005). Increasing mammalian cardiomyocyte contractility with residues identified in trout troponin C. *Physiological Genomics*, *22*(29), 1–7.

https://doi.org/10.1152/physiolgenomics.00007.2005

Gillis, T. E., Marshall, C. R., Xue, X. H., Borgford, T. J., & Tibbits, G. F. (2000). Ca(2+) binding to cardiac troponin C: effects of temperature and pH on mammalian and salmonid isoforms. *American Journal of Physiology. Regulatory, Integrative and Comparative Physiology*, *279*(5), R1707-15. https://doi.org/10.1152/ajpregu.2000.279.5.R1707

Gillis, T. E., & Tibbits, G. F. (2002). Beating the cold: The functional evolution of troponin C in teleost fish. *Comparative Biochemistry and Physiology - A Molecular and Integrative Physiology*, *132*(4), 763–772. https://doi.org/10.1016/S1095-6433(02)00046-6

Goodwin, L. O., Lees-Miller, J. P., Leonard, M. A., Cheley, S. B., & Helfman, D. M. (1991). Four fibroblast tropomyosin isoforms are expressed from the rat alpha-tropomyosin gene via alternative RNA splicing and the use of two promoters. *The Journal of Biological Chemistry*, *266*(13), 8408–8415.

Goonasekara, C. L., & Heeley, D. H. (2008). Conformational properties of striated muscle tropomyosins from some salmonid fishes. *Journal of Muscle Research and Cell Motility*, *29*(2–5), 135–143. https://doi.org/10.1007/s10974-008-9148-7

Goonasekara, C. L., & Heeley, D. H. (2009). Effect of Removing the Amino-Terminal Hexapeptide of Tropomyosin on the Properties of the Thin Filament. *Biochemistry*, *48*(15), 3538–3544. https://doi.org/10.1021/bi802004j

Gordon, A. M., LaMadrid, M. A., Chen, Y., Luo, Z., & Chase, P. B. (1997). Calcium

regulation of skeletal muscle thin filament motility in vitro. *Biophysical Journal*, *72*(3), 1295–1307. https://doi.org/10.1016/S0006-3495(97)78776-9

Graceffa, P., & Lehrer, S. S. (1980). The excimer fluorescence of pyrene-labeled tropomyosin. A probe of conformational dynamics. *Journal of Biological Chemistry*, *255*(23), 11296–11300. https://doi.org/https://doi.org/10.1016/S0021-9258(19)70290-7

Greaser, M. L., & Yamaguchi, M. C. B. (1973). Troponin Subunits and Their Interactions. *Cold Spring Harb Symp Quant Biol*, *37*, 235–244.

Greenfield, N. J., & Hitchcock-DeGregori, S. E. (1995). The Stability of Tropomyosin, a Two-Stranded Coiled-Coil Protein, Is Primarily a Function of the Hydrophobicity of Residues at the Helix-Helix Interface. *Biochemistry*, *34*(51), 16797–16805. https://doi.org/10.1021/bi00051a030

Greenfield, N. J., Huang, Y. J., Swapna, G. V. T., Bhattacharya, A., Rapp, B., Singh, A., Montelione, G. T., & Hitchcock-DeGregori, S. E. (2006). Solution NMR Structure of the Junction between Tropomyosin Molecules: Implications for Actin Binding and Regulation. *Journal of Molecular Biology*, *364*(1), 80–96. https://doi.org/10.1016/j.jmb.2006.08.033

Greenfield, N. J., Palm, T., & Hitchcock-DeGregori, S. E. (2002). Structure and interactions of the carboxyl terminus of striated muscle α-tropomyosin: It is important to be flexible. *Biophysical Journal*, *83*(5), 2754–2766. https://doi.org/10.1016/S0006-3495(02)75285-5

Greenfield, N. J., Swapna, G. V. T., Huang, Y., Palm, T., Graboski, S., Montelione, G. T., & Hitchcock-DeGregori, S. E. (2003). The structure of the carboxyl terminus of striated α-tropomyosin in solution reveals an unusual parallel arrangement of interacting α-helices. *Biochemistry*, *42*(3), 614–619. https://doi.org/10.1021/bi026989e

Greig, A., Hirschberg, Y., Anderson, P. A., Hainsworth, C., Malouf, N. N., Oakeley, A. E., & Kay, B. K. (1994). Molecular basis of cardiac troponin T isoform heterogeneity in rabbit heart. *Circulation Research*, *74*(1), 41–47. https://doi.org/10.1161/01.res.74.1.41

Gulick, A. M., Bauer, C. B., Thoden, J. B., & Rayment, I. (1997). X-ray structures of the MgADP, MgATPgammaS, and MgAMPPNP complexes of the *Dictyostelium discoideum* myosin motor domain. *Biochemistry*, *36*(39), 11619–11628. https://doi.org/10.1021/bi9712596

Gunning, P. W., Schevzov, G., Kee, A. J., & Hardeman, E. C. (2005). Tropomyosin isoforms: divining rods for actin cytoskeleton function. *Trends in Cell Biology*, *15*(6), 333–341. https://doi.org/10.1016/j.tcb.2005.04.007

Hanson, J., & Huxley, H. E. (1953). Structural basis of the cross-striations in muscle. *Nature*, *172*(4377), 530–532. https://doi.org/10.1038/172530b0

Hanson, J., & Lowy, J. (1964). The structure of actin filaments and the origin of the axial periodicity in the I-substance of vertebrate striated muscle. *Proceedings of the Royal Society of London. Series B, Biological Sciences*, *160*, 449–460.

https://doi.org/10.1098/rspb.1964.0055

Hardy, S., Fiszman, M. Y., Osborne, H. B., & Thiebaud, P. (1991). Characterization of muscle and non muscle *Xenopus laevis* tropomyosin mRNAs transcribed from the same gene: Developmental and tissue-specific expression. *European Journal of Biochemistry*, *202*(2), 431–440. https://doi.org/10.1111/j.1432-1033.1991.tb16392.x

Hardy, S, & Thiebaud, P. (1992). Isolation and characterization of cDNA clones encoding the skeletal and smooth muscle *Xenopus laevis* beta tropomyosin isoforms. *Biochimica et Biophysica Acta*, *1131*(2), 239–242. https://doi.org/10.1016/0167-4781(92)90087-g

Hardy, S., Thézé, N., Lepetit, D., Allo, M. R., & Thiebaud, P. (1995). The *Xenopus laevis* TM-4 gene encodes non-muscle and cardiac tropomyosin isoforms through alternative splicing. *Gene*, *156*(2), 265–270. https://doi.org/https://doi.org/10.1016/0378-1119(94)00929-M

Hartshorne, D. J., Dreizen, P. (1973). Studies on the Subunit Composition of Troponin. *Cold Spring Harbor Symposia on Quantitative Biology*, *37*, 225–234.

Hartshorne, D. J., & Mueller, H. (1968). Fractionation of troponin into two distinct proteins. *Biochemical and Biophysical Research Communications*, *31*(5), 647–653. https://doi.org/https://doi.org/10.1016/0006-291X(68)90610-4

Haselgrove, J. C., & Huxley, H. E. (1973). X-ray evidence for radial cross-bridge movement and for the sliding filament model in actively contracting skeletal muscle. *Journal of Molecular Biology*, *77*(4), 549–568. https://doi.org/10.1016/0022-

2836(73)90222-2

Hayley, M., Chevaldina, T., & Heeley, D. H. (2011). Cold adaptation of tropomyosin. *Biochemistry*, *50*(30), 6559–6566. https://doi.org/10.1021/bi200327g

Head, J. F., & Perry, S. V. (1974). The interaction of the calcium-binding protein (troponin C) with bivalent cations and the inhibitory protein (troponin I). *Biochemical Journal*, *137*(2), 145–154. https://doi.org/10.1042/bj1370145

Heald, R. W., & Hitchcock-DeGregori, S. E. (1988). The structure of the amino terminus of tropomyosin is critical for binding to actin in the absence and presence of troponin. *The Journal of Biological Chemistry*, *263*(11), 5254–5259. https://doi.org/10.1016/s0021-9258(18)60708-2

Heeley, D.H., Bieger, T., Waddleton, D.M., Hong, C., Jackman, D.M., McGowan, C., Davidson, W.S. and Beavis, R. C. (1995). Characterisation of fast, slow and cardiac muscle tropomyosin from salmonid fish. *European Journal of Biochemistry.*, *232*, 226 – 234.

Heeley, D.H., Golosinska, K., Smillie, L. B. (1987). The effects of troponin-T fragments T1 and T2 on the binding of non-polymerisable tropomyosin to F-actin in the presence and absence of troponins -I and -C. *The Journal of Biological Chemistry*, *262*, 9971 –9978.

Heeley, D. H., Moir, A. J. G., & Perry, S. V. (1982). Phosphorylation of tropomyosin during development in mammalian striated muscle. *FEBS Letters*, *146*(1), 115–118. https://doi.org/10.1016/0014-5793(82)80716-3

Heeley, D. H. (1994). Investigation of the effects of phosphorylation of rabbit striated muscle αα-tropomyosin and rabbit skeletal muscle troponin-T. *European Journal of Biochemistry*, *221*(1), 129–137. https://doi.org/10.1111/j.1432-1033.1994.tb18721.x

Heeley, D. H., Watson, M. H., Mak, A. S., Dubord, P., & Smillie, L. B. (1989). Effect of phosphorylation on the interaction and functional properties of rabbit striated muscle αα-tropomyosin. *The Journal of Biological Chemistry*, *264*(5), 2424–2430. https://doi.org/10.1016/S0021-9258(19)81630-7

Heeley, D. H. (1994). Investigation of the effects of phosphorylation of rabbit striated muscle tropomyosin and rabbit skeletal troponin- T. *European Journal of Biochemistry*, *221*, 129 – 137.

Heeley, D. H., Bieger, T., Waddleton, D. M., Hong, C., Jackman, D. M., McGowan, C., Davidson, W. S., & Beavis, R. C. (1995). Characterisation of fast, slow and cardiac muscle tropomyosins from salmonid fish. *European Journal of Biochemistry*, *232*(1), 226–234. https://doi.org/10.1111/j.1432-1033.1995.tb20803.x

Heeley, D. H., Dhoot, G. K., & Perry, S. V. (1985). Factors determining the subunit composition of tropomyosin in mammalian skeletal muscle. *The Biochemical Journal*, *226*(2), 461–468. https://doi.org/10.1042/bj2260461

Heeley, D. H., & Hong, C. (1994). Isolation and characterization of tropomyosin from fish muscle. *Comparative Biochemistry and Physiology. Biochemistry and Molecular Biology*, *108*(1), 95–106. https://doi.org/10.1016/0305-0491(94)90169-4

Heeley, D. H. (2013). Phosphorylation of tropomyosin in striated muscle. *Journal of*

Muscle Research and Cell Motility, *34*(3), 233–237. https://doi.org/10.1007/s10974-013-9351-z

Heissler, S. M., & Sellers, J. R. (2016). *Myosins*, pp. 597–607). Academic Press. https://doi.org/https://doi.org/10.1016/B978-0-12-394447-4.20059-X

Helfman, D. M., Cheley, S., Kuismanen, E., Finn, L. A., & Yamawaki-Kataoka, Y. (1986). Nonmuscle and muscle tropomyosin isoforms are expressed from a single gene by alternative RNA splicing and polyadenylation. *Molecular and Cellular Biology*, *6*(11), 3582–3595. https://doi.org/10.1128/mcb.6.11.3582

Hendricks, M., & Weintraub, H. (1981). Tropomyosin is decreased in transformed cells. *Proceedings of the National Academy of Sciences*, *78*(9), 5633 LP – 5637. https://doi.org/10.1073/pnas.78.9.5633

Hendricks, M., & Weintraub, H. (1984). Multiple tropomyosin polypeptides in chicken embryo fibroblasts: differential repression of transcription by Rous sarcoma virus transformation. *Molecular and Cellular Biology*, *4*(9), 1823–1833. https://doi.org/10.1128/mcb.4.9.1823

Herman, I. M. (1993). Actin isoforms. *Current Opinion in Cell Biology*, *5*(1), 48–55. https://doi.org/10.1016/s0955-0674(05)80007-9

Herzberg, O., Moult, J., & James, M. N. G. (1986). A model for the Ca^{2+}-induced conformational transition of troponin C. A trigger for muscle contraction. *The Journal of Biological Chemistry*, *261*(6), 2638–2644. https://doi.org/10.1016/s0021-9258(17)35835-0

Herzberg, O., & James, M. N. G. (1985). Structure of the calcium regulatory muscle protein troponin-C at 2.8 Å resolution. *Nature*, *313*(6004), 653–659. https://doi.org/10.1038/313653a0

Hitchcock-DeGregori, S. E., & Heald, R. W. (1987). Altered actin and troponin binding of amino-terminal variants of chicken striated muscle alpha-tropomyosin expressed in *Escherichia coli*. *The Journal of Biological Chemistry*, *262*(20), 9730–9735.

Hitchcock-DeGregori, S. E., & Singh, A. (2010). What makes tropomyosin an actin binding protein? A perspective. *Journal of Structural Biology*, *170*(2), 319–324. https://doi.org/10.1016/j.jsb.2009.12.013

Hitchcock-DeGregori, S. E., Song, Y., & Greenfield, N. J. (2002). Functions of Tropomyosin's Periodic Repeats†. *Biochemistry*, *41*(50), 15036–15044. https://doi.org/10.1021/bi026519k

Hodges, R.S., Sodek, J., Smillie, L.B. and Jurasek, L. (1972). Tropomyosin: Amino acid sequence and coiled-coil structure. *Cold Spring Harbor Symp. Quant. Biol.*, *37*, 299 – 310.

Hodges, R. S., Mills, J., McReynolds, S., Kirwan, J. P., Tripet, B., & Osguthorpe, D. (2009). Identification of a Unique "Stability Control Region" that Controls Protein Stability of Tropomyosin: A Two-stranded α-Helical Coiled-coil. *The Journal of Molecular Biology*, *392*(3), 747–762. https://doi.org/10.1016/j.jmb.2009.07.039

Holmes, K. C., Angert, I., Jon Kull, F., Jahn, W., & Schröder, R. R. (2003). Electron cryo-microscopy shows how strong binding of myosin to actin releases nucleotide.

Nature, *425*(6956), 423–427. https://doi.org/10.1038/nature02005

Holmes, K. C., Popp, D., Gebhard, W., & Kabsch, W. (1990). Atomic model of the actin filament . *Nature*, *347*(6288), 44–49. https://doi.org/10.1038/347044a0

Houdusse, A., Love, M. L., Dominguez, R., Grabarek, Z., & Cohen, C. (1997). Structures of four Ca^{2+}-bound troponin C at 2.0 Å resolution: Further insights into the Ca^{2+}-switch in the calmodulin superfamily. *Structure*, *5*(12), 1695–1711. https://doi.org/10.1016/S0969-2126(97)00315-8

Houle, F., & Huot, J. (2006). Dysregulation of the endothelial cellular response to oxidative stress in cancer. *Molecular Carcinogenesis*, *45*(6), 362–367. https://doi.org/https://doi.org/10.1002/mc.20218

Houle, F., Poirier, A., Dumaresq, J., & Huot, J. (2007). DAP kinase mediates the phosphorylation of tropomyosin-1 downstream of the ERK pathway, which regulates the formation of stress fibers in response to oxidative stress. *Journal of Cell Science*, *120*(20), 3666 LP – 3677. https://doi.org/10.1242/jcs.003251

Hughes, J. A. I., Cooke-Yarborough, C. M., Chadwick, N. C., Schevzov, G., Arbuckle, S. M., Gunning, P., & Weinberger, R. P. (2003). High-molecular-weight tropomyosins localize to the contractile rings of dividing CNS cells but are absent from malignant pediatric and adult CNS tumors. *Glia*, *42*(1), 25–35. https://doi.org/10.1002/glia.10174

Huxley, H., & Hanson, J, (1954). Changes in the Cross-Striations of Muscle during Contraction and Stretch and their Structural Interpretation. *Nature, 973. 4412*, 973–

976.

Huxley, A. F., & Niedergerke, R. (1954). Structural changes in muscle during contraction. *Nature*, *4412*(4412), 971–973.

Huxley, A. F., & Simmons, R. M. (1971). Proposed mechanism of force generation in striated muscle. *Nature*, *233*(5321), 533–538. https://doi.org/10.1038/233533a0

Huxley, H. E. (1953). Electron microscope studies of the organisation of the filaments in striated muscle. *Biochimica et Biophysica Acta*, *12*(3), 387–394. https://doi.org/10.1016/0006-3002(53)90156-5

Huxley, H. E. (1969). The Mechanism of Muscular Contraction. *Science*, *164*(3886), 1356 LP – 1366. https://doi.org/10.1126/science.164.3886.1356

Huxley, H. E. (1973). Structural Changes in the Actin- and Myosin-eontaining Filaments during Contraction. *Cold Spring Harb Symp Quant Biol*, *37*, 361–376.

Ikeda, D., Toramoto, T., Ochiai, Y., Suetake, H., Suzuki, Y., Minoshima, S., Shimizu, N., & Watabe, S. (2003). Identification of novel tropomyosin 1 genes of pufferfish (*Fugu rubripes*) on genomic sequences and tissue distribution of their transcripts. *Molecular Biology Reports*, *30*(2), 83–90. https://doi.org/10.1023/A:1023995208279

Ikura, M. (1996). Calcium binding and conformational response in EF-hand proteins. *Trends in Biochemical Sciences*, *21*(1), 14–17.

Ishii, Y., & Lehrer, S. S. (1985). Fluorescence studies of the conformation of pyrene-labeled tropomyosin: effects of F-actin and myosin subfragment 1. *Biochemistry*,

24(23), 6631–6638. https://doi.org/10.1021/bi00344a050

Ishii, Y., & Lehrer, S. S. (1986). Effects of the state of the succinimido-ring on the fluorescence and structural properties of pyrene maleimide-labeled alpha alpha-tropomyosin. *Biophysical Journal*, *50*(1), 75–80. https://doi.org/10.1016/S0006-3495(86)83440-3

Ishii, Yoshiharu, Hitchcock-Degregori, S., Mabuchi, K., & Lehrer, S. S. (1992). Unfolding domains of recombinant fusion αα-tropomyosin. *Protein Science*, *1*(10), 1319–1325. https://doi.org/10.1002/pro.5560011011

Jääskeläinen, P., Soranta, M., Miettinen, R., Saarinen, L., Pihlajamäki, J., Silvennoinen, K., Tikanoja, T., Laakso, M., & Kuusisto, J. (1998). The cardiac beta-myosin heavy chain gene is not the predominant gene for hypertrophic cardiomyopathy in the Finnish population. *Journal of the American College of Cardiology*, *32*(6), 1709–1716. https://doi.org/10.1016/s0735-1097(98)00448-3

Jackman, D. M., Waddleton, D. M., Younghusband, B., & Heeley, D. H. (1996). Further characterisation of fast, slow and cardiac muscle tropomyosins from salmonid fish. *European Journal of Biochemistry*, *242*(2), 363–371. https://doi.org/10.1111/j.1432-1033.1996.0363r.x

Jackson, P., Amphlett, G. W., & Perry, S. V. (1975). The primary structure of troponin T and the interaction with tropomyosin. *Biochemical Journal*, *151*(1), 85–97. https://doi.org/10.1042/bj1510085

Jin, J. P., Huang, Q. Q., Yeh, H. I., & Lin, J. J. (1992). Complete nucleotide sequence and

structural organization of rat cardiac troponin T gene. A single gene generates embryonic and adult isoforms via developmentally regulated alternative splicing. *Journal of Molecular Biology*, *227*(4), 1269–1276. https://doi.org/10.1016/0022-2836(92)90540-z

Johnson, P, & Smillie, L. B. (1977). Polymerizability of rabbit skeletal tropomyosin: effects of enzymic and chemical modifications. *Biochemistry*, *16*(10), 2264–2269. https://doi.org/10.1021/bi00629a035

Johnson, P., & Smillie, L. B. (1977). Polymerizability of Rabbit Skeletal Tropomyosin: Effects of Enzymic and Chemical Modifications. *Biochemistry*, *16*(10), 2264–2269. https://doi.org/10.1021/bi00629a035

Johnston, G. C., Prendergast, J. A., & Singer, R. A. (1991). The Saccharomyces cerevisiae MYO2 gene encodes an essential myosin for vectorial transport of vesicles. *Journal of Cell Biology*, *113*(3), 539–551. https://doi.org/10.1083/jcb.113.3.539

Jongbloed, R. J., Marcelis, C. L., Doevendans, P. A., Schmeitz-Mulkens, J. M., Van Dockum, W. G., Geraedts, J. P., & Smeets, H. J. (2003). Variable clinical manifestation of a novel missense mutation in the alpha-tropomyosin (TPM1) gene in familial hypertrophic cardiomyopathy. *Journal of the American College of Cardiology*, *41*(6), 981–986. https://doi.org/10.1016/s0735-1097(02)03005-x

Kabsch, W., Mannherz, H. G., Suck, D., Pai, E. F., & Holmes, K. C. (1990). Atomic structure of the actin: DNase I complex . *Nature*, *347*(6288), 37–44.

https://doi.org/10.1038/347037a0

Kahlke, T., & Thorvaldsen, S. (2012). Molecular characterization of cold adaptation of membrane proteins in the Vibrionaceae core-genome. *PloS one*, 7(12), e51761. https://doi.org/10.1371/journal.pone.0051761

Karibe, A., Tobacman, L. S., Strand, J., Butters, C., Back, N., Bachinski, L. L., Arai, A. E., Ortiz, A., Roberts, R., Homsher, E., & Fananapazir, L. (2001). Hypertrophic cardiomyopathy caused by a novel alpha-tropomyosin mutation (V95A) is associated with mild cardiac phenotype, abnormal calcium binding to troponin, abnormal myosin cycling, and poor prognosis. *Circulation*, *103*(1), 65–71. https://doi.org/10.1161/01.cir.103.1.65

Kawasaki, H., & Kretsinger, R. H. (1994). Calcium-binding proteins. 1: EF-hands. *Protein Profile*, *1*(4), 343–517. http://europepmc.org/abstract/MED/8528904

Kirwan, J. P., & Hodges, R. S. (2010). Critical interactions in the stability control region of tropomyosin. *Journal of Structural Biology*, *170*(2), 294–306. https://doi.org/10.1016/j.jsb.2010.01.020

Kremneva, E., Boussouf, S., Nikolaeva, O., Maytum, R., Geeves, M. A., & Levitsky, D. I. (2004). Effects of two familial hypertrophic cardiomyopathy mutations in alpha-tropomyosin, Asp175Asn and Glu180Gly, on the thermal unfolding of actin-bound tropomyosin. *Biophysical Journal*, *87*(6), 3922–3933. https://doi.org/10.1529/biophysj.104.048793

Kushmerick, M. J., Dillon, P. F., Meyer, R. A., Brown, T. R., Krisanda, J. M., &

Sweeney, H. L. (1986). 31P NMR spectroscopy, chemical analysis, and free Mg^{2+} of rabbit bladder and uterine smooth muscle. *The Journal of Biological Chemistry*, *261*(31), 14420–14429.

Kwok, S. C., & Hodges, R. S. (2004). Stabilizing and destabilizing clusters in the hydrophobic core of long two-stranded α-helical coiled-coils. *The Journal of Biological Chemistry*, *279*(20), 21576–21588. https://doi.org/10.1074/jbc.M401074200

Laing, N. G., Wilton, S. D., Akkari, P. A., Dorosz, S., Boundy, K., Kneebone, C., Blumbergs, P., White, S., Watkins, H., & Love, D. R. (1995). A mutation in the alpha tropomyosin gene TPM3 associated with autosomal dominant nemaline myopathy. *Nature Genetics*, *9*(1), 75–79. https://doi.org/10.1038/ng0195-75

Larry, S.T. (1996). Thin Filament-Mediated Regulation of Cardiac Contraction. *Annual Review of Physiology*, 58:447-481.

Leavis, P. C., & Gergely, J. (1984). Thin filament proteins and thin filament-linked regulation of vertebrate muscle contraction. *CRC Critical Reviews in Biochemistry*, *16*(3), 235–305. https://doi.org/10.3109/10409238409108717

Lees-Miller, J. P., Goodwin, L. O., & Helfman, D. M. (1990). Three novel brain tropomyosin isoforms are expressed from the rat alpha-tropomyosin gene through the use of alternative promoters and alternative RNA processing. *Molecular and Cellular Biology*, *10*(4), 1729–1742. https://doi.org/10.1128/mcb.10.4.1729

Lees-Miller, J. P., & Helfman, D. M. (1991). The molecular basis for tropomyosin

isoform diversity. *BioEssays : News and Reviews in Molecular, Cellular and Developmental Biology*, *13*(9), 429–437. https://doi.org/10.1002/bies.950130902

Lees-Miller, J. P., Yan, A., & Helfman, D. M. (1990). Structure and complete nucleotide sequence of the gene encoding rat fibroblast tropomyosin 4. *Journal of Molecular Biology*, *213*(3), 399–405. https://doi.org/10.1016/S0022-2836(05)80202-5

Lehman, W., Medlock, G., Li, X. E., Suphamungmee, W., Tu, A.-Y., Schmidtmann, A., Ujfalusi, Z., Fischer, S., Moore, J. R., Geeves, M. A., & Regnier, M. (2015). Phosphorylation of Ser283 enhances the stiffness of the tropomyosin head-to-tail overlap domain. *Archives of Biochemistry and Biophysics*, *571*, 10–15. https://doi.org/10.1016/j.abb.2015.02.026

Lehrer, S. S., & Kerwar, G. (1972). Intrinsic fluorescence of actin. *Biochemistry*, *11*(7), 1211–1217. https://doi.org/10.1021/bi00757a015

Lehtokari, V. L., Ceuterick-de Groote, C., de Jonghe, P., Marttila, M., Laing, N. G., Pelin, K., & Wallgren-Pettersson, C. (2007). Cap disease caused by heterozygous deletion of the βtropomyosin gene TPM2. *Neuromuscular Disorders*, *17*(6), 433–442. https://doi.org/10.1016/j.nmd.2007.02.015

Lemonnier, M., Balvay, L., Mouly, V., Libri, D., & Fiszman, M. Y. (1991). The chicken gene encoding the alpha isoform of tropomyosin of fast-twitch muscle fibers: organization, expression and identification of the major proteins synthesized. *Gene*, *107*(2), 229–240. https://doi.org/10.1016/0378-1119(91)90323-4

Leonardi, C. L., Warren, R. H., & Rubin, R. W. (1982). Lack of tropomyosin correlates

with the absence of stress fibers in transformed rat kidney cells. *Biochimica et Biophysica Acta*, *720*(2), 154–162. https://doi.org/10.1016/0167-4889(82)90007-6

Lewis, W. G., Cote, G. P., Mak, A. S., & Smillie, L. B. (1983). Amino acid sequence of equine platelet tropomyosin. Correlation with interaction properties. *FEBS Letters*, *156*(2), 269–273. https://doi.org/10.1016/0014-5793(83)80511-0

Lewis, W. G., & Smillie, L. B. (1980). The amino acid sequence of rabbit cardiac tropomyosin. *The Journal of Biological Chemistry*, *255*(14), 6854–6859. https://doi.org/10.1016/S0021-9258(18)43652-6

Li, M. X., & Hwang, P. M. (2015). Structure and function of cardiac troponin C (TNNC1): Implications for heart failure, cardiomyopathies, and troponin modulating drugs. *Gene*, *571*(2), 153–166. https://doi.org/10.1016/j.gene.2015.07.074

Li, X. E., Tobacman, L. S., Mun, J. Y., Craig, R., Fischer, S., & Lehman, W. (2011). Tropomyosin position on F-actin revealed by EM reconstruction and computational chemistry. *Biophysical Journal*, *100*(4), 1005–1013. https://doi.org/10.1016/j.bpj.2010.12.3697

Li, Y., Mui, S., Brown, J. H., Strand, J., Reshetnikova, L., Tobacman, L. S., & Cohen, C. (2002). The crystal structure of the C-terminal fragment of striated-muscle alpha-tropomyosin reveals a key troponin T recognition site. *Proceedings of the National Academy of Sciences of the United States of America*, *99*(11), 7378–7383. https://doi.org/10.1073/pnas.102179999

Libri, D., Lemonnier, M., Meinnel, T., & Fiszman, M. Y. (1989). A single gene codes for

the beta subunits of smooth and skeletal muscle tropomyosin in the chicken. *The Journal of Biological Chemistry*, *264*(5), 2935–2944.

Lien, S., Koop, B. F., Sandve, S. R., Miller, J. R., Kent, M. P., Nome, T., Hvidsten, T. R., Leong, J. S., Minkley, D. R., Zimin, A., Grammes, F., Grove, H., Gjuvsland, A., Walenz, B., Hermansen, R. A., von Schalburg, K., Rondeau, E. B., Di Genova, A., Samy, J. K. A., … Davidson, W. S. (2016). The Atlantic salmon genome provides insights into rediploidization. *Nature*, *533*(7602), 200–205. https://doi.org/10.1038/nature17164

Lin, J. L. C., Geng, X., Bhattacharya, S. Das, Yu, J.-R., Reiter, R. S., Sastri, B., Glazier, K. D., Mirza, Z. K., Wang, K. K., Amenta, P. S., Das, K. M., & Lin, J. J.-C. (2002). Isolation and sequencing of a novel tropomyosin isoform preferentially associated with colon cancer. *Gastroenterology*, *123*(1), 152–162. https://doi.org/10.1053/gast.2002.34154

Lindquester, G. J., Flach, J. E., Fleenor, D. E., Hickman, K. H., & Devlin, R. B. (1989). Avian tropomyosin gene expression. *Nucleic Acids Research*, *17*(5), 2099–2118. https://doi.org/10.1093/nar/17.5.2099

Lorand, L. (1953). 'Adenosine Triphosphate–Creatine Transphosphorylase' as Relaxing Factor of Muscle. *Nature*, *172*(4391), 1181–1183. https://doi.org/10.1038/1721181a0

Luther, P. K. (2009). The vertebrate muscle Z-disc: Sarcomere anchor for structure and signalling. *Journal of Muscle Research and Cell Motility*, *30*(5–6), 171–185.

https://doi.org/10.1007/s10974-009-9189-6

Lymn, R. W., & Taylor, E. W. (1971). Mechanism of adenosine triphosphate hydrolysis by actomyosin. *Biochemistry*, *10*(25), 4617–4624. https://doi.org/10.1021/bi00801a004

Macdougall J. D., Sale D. G., Elder G. C., Sutton J. R. (1982). Muscle ultrastructural characteristics of elite powerlifters and bodybuilders. *European Journal of Appl. Physiology and Occupational Physiology*. 48 117–126. 10.1007/bf00421171

MacLeod, A. R., Houlker, C., Reinach, F. C., Smillie, L. B., Talbot, K., Modi, G., & Walsh, F. S. (1985). A muscle-type tropomyosin in human fibroblasts: evidence for expression by an alternative RNA splicing mechanism. *Proceedings of the National Academy of Sciences of the United States of America*, *82*(23), 7835–7839. https://doi.org/10.1073/pnas.82.23.7835

Mak, A.S., Smillie, L. B., & Bárány, M. (1978). Specific phosphorylation at serine-283 of alpha tropomyosin from frog skeletal and rabbit skeletal and cardiac muscle. *Proceedings of the National Academy of Sciences of the United States of America*, *75*(8), 3588–3592. https://doi.org/10.1073/pnas.75.8.3588

Mak, A. S., Smillie, L. B., & Stewart, G. R. (1980). A comparison of the amino acid sequences of rabbit skeletal muscle alpha- and beta-tropomyosins. *Journal of Biological Chemistry*, *255*(8), 3647–3655. https://doi.org/https://doi.org/10.1016/S0021-9258(19)85753-8

Mak, A. S., & Smillie, L. B. (1981a). Non-polymerizable tropomyosin: Preparation, some

properties and F-actin binding. *Biochemical and Biophysical Research Communications*, *101*(1), 208–214. https://doi.org/https://doi.org/10.1016/S0006-291X(81)80032-0

Mak, A. S., & Smillie, L. B. (1981b). Structural interpretation of the two-site binding of troponin on the muscle thin filament. *Journal of Molecular Biology*, *149*(3), 541–550. https://doi.org/https://doi.org/10.1016/0022-2836(81)90486-1

Manning, E. P., Tardiff, J. C., & Schwartz, S. D. (2011). A model of calcium activation of the cardiac thin filament. *Biochemistry*, *50*(34), 7405–7413. https://doi.org/10.1021/bi200506k

Manning, E. P., Tardiff, J. C., & Schwartz, S. D. (2012). Molecular Effects of Familial Hypertrophic Cardiomyopathy-Related Mutations in the TNT1 Domain of cTnT. *Journal of Molecular Biology*, *421*(1), 54–66. https://doi.org/https://doi.org/10.1016/j.jmb.2012.05.008

Margossian, S. S., & Lowey, S. (1973). Substructure of the myosin molecule. III. Preparation of single-headed derivatives of myosin. *Journal of Molecular Biology*, *74*(3). https://doi.org/10.1016/0022-2836(73)90375-6

Maron, B. J., Towbin, J. A., Thiene, G., Antzelevitch, C., Corrado, D., Arnett, D., Moss, A. J., Seidman, C. E., & Young, J. B. (2006). Contemporary definitions and classification of the cardiomyopathies: An American Heart Association Scientific Statement from the Council on Clinical Cardiology, Heart Failure and Transplantation Committee; Quality of Care and Outcomes Research and Function.

Circulation, *113*(14), 1807–1816. https://doi.org/10.1161/CIRCULATIONAHA.106.174287

Marston, S., & Zamora, J. E. (2020). Troponin structure and function: a view of recent progress. *Journal of Muscle Research and Cell Motility*, *41*(1), 71–89. https://doi.org/10.1007/s10974-019-09513-1

Matsumura, F., Lin, J. J., Yamashiro-Matsumura, S., Thomas, G. P., & Topp, W. C. (1983). Differential expression of tropomyosin forms in the microfilaments isolated from normal and transformed rat cultured cells. *The Journal of Biological Chemistry*, *258*(22), 13954–13964. https://doi.org/10.1016/S0021-9258(17)44009-9

Matthews, B. W., Nicholson, H., & Becktel, W. J. (1987). Enhanced protein thermostability from site-directed mutations that decrease the entropy of unfolding. *Proceedings of the National Academy of Sciences of the United States of America*, *84*(19), 6663–6667. https://doi.org/10.1073/pnas.84.19.6663

McKillop, D. F., & Geeves, M. A. (1993). Regulation of the interaction between actin and myosin subfragment 1: evidence for three states of the thin filament. *Biophysical Journal*, *65*(2), 693–701. https://doi.org/10.1016/S0006-3495(93)81110-X

McLachlan, A. D., & Stewart, M. (1976). The 14-fold periodicity in alpha-tropomyosin and the interaction with actin. *Journal of Molecular Biology*, *103*(2), 271–298. https://doi.org/10.1016/0022-2836(76)90313-2

McLachlan, A. D., Stewart, M., & Smillie, L. B. (1975). Sequence repeats in α-tropomyosin. *Journal of Molecular Biology*, *98*(2), 281–291.

https://doi.org/https://doi.org/10.1016/S0022-2836(75)80118-5

Mesnard, L., Samson, F., Espinasse, I., Durane, J., Neveux, J. Y., & Mercadier, J. J. (1993). Molecular cloning and developmental expression of human cardiac troponin T. *FEBS Letters*, *328*(1–2), 139–144. https://doi.org/10.1016/0014-5793(93)80981-Y

Minakata, S., Maeda, K., Oda, N., Wakabayashi, K., Nitanai, Y., & Maéda, Y. (2008). Two-crystal structures of tropomyosin C-terminal fragment 176-273: Exposure of the hydrophobic core to the solvent destabilizes the tropomyosin molecule. *Biophysical Journal*, *95*(2), 710–719. https://doi.org/10.1529/biophysj.107.126144

Montarras, D., Fiszman, M. Y., & Gros, F. (1981). Characterization of the tropomyosin present in various chick embryo muscle types and in muscle cells differentiated in vitro. *The Journal of Biological Chemistry*, *256*(8), 4081–4086. https://doi.org/10.1016/s0021-9258(19)69568-2

Monteiro, P. B., Lataro, R. C., Ferro, J. A., & Reinach, F. D. C. (1994). Functional α-tropomyosin produced in *Escherichia coli*. A dipeptide extension can substitute the amino-terminal acetyl group. *The Journal of Biological Chemistry*, *269*(14), 10461–10466. https://doi.org/10.1016/s0021-9258(17)34082-6

Montgomery, K., & Mak, A. S. (1984). In vitro phosphorylation of tropomyosin by a kinase from chicken embryo. *The Journal of Biological Chemistry*, *259*(9), 5555–5560.

Moore, P. B., Huxley, H. E., & DeRosier, D. J. (1970). Three-dimensional reconstruction

of F-actin, thin filaments and decorated thin filaments. *Journal of Molecular Biology*, *50*(2), 279–295. https://doi.org/10.1016/0022-2836(70)90192-0

Mori, T., Kitani, Y., Hatakeyama, D., Machida, K., Goto-Inoue, N., Hayakawa, S., Yamamoto, N., Kashiwagi, K., & Kashiwagi, A. (2020). Predation threats for a 24-h period activated the extension of axons in the brains of *Xenopus* tadpoles. *Scientific Reports*, *10*(1), 1–15. https://doi.org/10.1038/s41598-020-67975-7

Morris, E. P., & Lehrer, S. S. (1984). Troponin-Tropomyosin Interactions. Fluorescence Studies of the Binding of Troponin, Troponin T, and Chymotryptic Troponin T Fragments to Specifically Labeled Tropomyosin. *Biochemistry*, *23*(10), 2214–2220. https://doi.org/10.1021/bi00305a018

Mouilleron, S., Wiezlak, M., O'Reilly, N., Treisman, R., & McDonald, N. Q. (2012). Structures of the phactr1 RPEL domain and RPEL motif complexes with g-actin reveal the molecular basis for actin binding cooperativity. *Structure*, *20*(11), 1960–1970. https://doi.org/10.1016/j.str.2012.08.031

Moyes, C. D., Borgford, T., LeBlanc, L., & Tibbits, G. F. (1996). Cloning and expression of salmon cardiac troponin C: Titration of the low-affinity Ca^{2+} binding site using a tryptophan mutant. *Biochemistry*, *35*(36), 11756–11762. https://doi.org/10.1021/bi9607057

Mudalige, W. A. K. A., Tao, T. C., & Lehrer, S. S. (2009). Ca^{2+} dependent photocrosslinking of tropomyosin residue 146 to residues 157-163 in the C-terminal domain of troponin I in reconstituted skeletal muscle thin filaments. *Journal of*

Molecular Biology, *389*(3), 575–583. https://doi.org/10.1016/j.jmb.2009.04.027

Mueller, H., & Perry, S. V. (1962). The degradation of heavy meromyosin by trypsin. *The Biochemical Journal*, *85*(3), 431–439. https://doi.org/10.1042/bj0850431

Muthuchamy, M., Pajak, L., Howles, P., Doetschman, T., & Wieczorek, D. F. (1993). Developmental analysis of tropomyosin gene expression in embryonic stem cells and mouse embryos. *Molecular and Cellular Biology*, *13*(6), 3311–3323. https://doi.org/10.1128/mcb.13.6.3311

Naga Prasad, S. V., Jayatilleke, A., Madamanchi, A., & Rockman, H. A. (2005). Protein kinase activity of phosphoinositide 3-kinase regulates beta-adrenergic receptor endocytosis. *Nature Cell Biology*, *7*(8), 785–796. https://doi.org/10.1038/ncb1278

Nagy, B., & Jencks, W. P. (1962). Optical rotatory dispersion of G-actin. *Biochemistry*, *1*, 987–996. https://doi.org/10.1021/bi00912a008

Nakajima-Taniguchi, C., Matsui, H., Nagata, S., Kishimoto, T., & Yamauchi-Takihara, K. (1995). Novel missense mutation in alpha-tropomyosin gene found in Japanese patients with hypertrophic cardiomyopathy. *Journal of Molecular and Cellular Cardiology*, *27*(9), 2053–2058. https://doi.org/10.1016/0022-2828(95)90026-8

Nelson, D. L., & Cox, M. M. (2017). *Lehninger principles of biochemistry* (7th ed.). W.H. Freeman.

Nishikawa, M., Shirakawa, S., & Adelstein, R. S. (1985). Phosphorylation of smooth muscle myosin light chain kinase by protein kinase C. Comparative study of the phosphorylated sites. *Journal of Biological Chemistry*, *260*(15), 8978–8983.

https://doi.org/10.1016/s0021-9258(17)39445-0

Nitanai, Y., Minakata, S., Maeda, K., Oda, N., & Maéda, Y. (2007). Crystal structures of tropomyosin: flexible coiled-coil. *Advances in Experimental Medicine and Biology*, *592*, 137–151. https://doi.org/10.1007/978-4-431-38453-3_13

Nixon, B. R., Liu, B., Scellini, B., Tesi, C., Piroddi, N., Ogut, O., Solaro, R. J., Ziolo, M. T., Janssen, P. M. L., Davis, J. P., Poggesi, C., & Biesiadecki, B. J. (2013). Tropomyosin Ser-283 pseudo-phosphorylation slows myofibril relaxation. *Archives of Biochemistry and Biophysics*, *535*(1), 30–38. https://doi.org/10.1016/j.abb.2012.11.010

Nüesch, J. P. F., & Rommelaere, J. (2007). A viral adaptor protein modulating casein kinase II activity induces cytopathic effects in permissive cells. *Proceedings of the National Academy of Sciences of the United States of America*, *104*(30), 12482–12487. https://doi.org/10.1073/pnas.0705533104

Oda, T., Yanagisawa, H., & Wakabayashi, T. (2020). Cryo-EM structures of cardiac thin filaments reveal the 3D architecture of troponin. *Journal of Structural Biology*, *209*(3), 107450. https://doi.org/10.1016/j.jsb.2020.107450

Ohtsuki, I. (1974). Localization of Troponin in Thin Filament and Tropomyosin Paracrystal. *The Journal of Biochemistry*, *75*(4), 753–765. https://doi.org/10.1093/oxfordjournals.jbchem.a130448

Ohtsuki, I. (1979). Molecular arrangement of troponin-T in the thin filament. *The Journal of Biochemistry*, *86*(2), 491–497.

https://doi.org/10.1093/oxfordjournals.jbchem.a132549

Ohtsuki, I., Masaki, T., Nonomura, Y., & Ebashi, S. (1967). Periodic distribution of troponin along the thin filament. *The Journal of Biochemistry*, *61*(6), 817–819. https://doi.org/10.1093/oxfordjournals.jbchem.a128619

Olson, T. M., Kishimoto, N. Y., Whitby, F. G., & Michels, V. V. (2001). Mutations that alter the surface charge of alpha-tropomyosin are associated with dilated cardiomyopathy. *Journal of Molecular and Cellular Cardiology*, *33*(4), 723–732. https://doi.org/10.1006/jmcc.2000.1339

Otterbein, L. R., Graceffa, P., & Dominguez, R. (2001). The crystal structure of uncomplexed actin in the ADP state. *Science*, *293*(5530), 708–711. https://doi.org/10.1126/science.1059700

Palani, S., Köster, D. V, Hatano, T., Kamnev, A., Kanamaru, T., Brooker, H. R., Hernandez-Fernaud, J. R., Jones, A. M. E., Millar, J. B. A., Mulvihill, D. P., & Balasubramanian, M. K. (2019). Phosphoregulation of tropomyosin is crucial for actin cable turnover and division site placement. *The Journal of Cell Biology*, *218*(11), 3548–3559. https://doi.org/10.1083/jcb.201809089

Pan, B. S., & Potter, J. D. (1992). Two genetically expressed troponin T fragments representing alpha and beta isoforms exhibit functional differences. *The Journal of Biological Chemistry*, *267*(32), 23052–23056. https://doi.org/10.1016/S0021-9258(18)50054-5

Parry, D. A. D. (1975). Analysis of the primary sequence of α-tropomyosin from rabbit

skeletal muscle. *The Journal of Molecular Biology, 98*(3), 519–535. https://doi.org/10.1016/S0022-2836(75)80084-2

Parry, D. A. D, & Squire, J. M. (1973). Structural role of tropomyosin in muscle regulation: analysis of the X-ray diffraction patterns from relaxed and contracting muscles. *The Journal of Molecular Biology*, *75*(1), 33–55. https://doi.org/10.1016/0022-2836(73)90527-5

Pato, M. D., Mak, A. S., & Smillie, L. B. (1981). Fragments of rabbit striated muscle α-tropomyosin. I. Preparation and characterization. *The Journal of Biological Chemistry, 256*(2), 593–601. https://doi.org/10.1016/s0021-9258(19)70014-3

Pawlak, G., McGarvey, T. W., Nguyen, T. B., Tomaszewski, J. E., Puthiyaveettil, R., Malkowicz, S. B., & Helfman, D. M. (2004). Alterations in tropomyosin isoform expression in human transitional cell carcinoma of the urinary bladder. *International Journal of Cancer*, *110*(3), 368–373. https://doi.org/10.1002/ijc.20151

Pearlstone, J.R., Smillie, L. B. (1982). Binding of troponin-T fragments to several types of tropomyosin. Sensitivity to Ca^{2+} in the presence of troponin-C. *The Journal of Biological Chemistry, 257*, 10587 – 10592. https://doi.org/10.1016/S0021-9258(18)33862-6

Perrie, W. T., Smillie, L. B., & Perry, S. V. (1973). A phosphorylated light-chain component of myosin from skeletal muscle. *Biochemical Journal*, *135*(1), 151–164. https://doi.org/10.1042/bj1350151

Perry, S. V. (1998). Troponin T: Genetics, properties and function. *Journal of Muscle*

Research and Cell Motility, *19*(6), 575–602. https://doi.org/10.1023/A:1005397501968

Perry, S. V. (1999). Troponin I: inhibitor or facilitator. *Molecular and Cellular Biochemistry*, *190*(1–2), 9–32.

Perry, S. V. (2001). Vertebrate tropomyosin: distribution, properties and function. *Journal of Muscle Research & Cell Motility*, *22*(1), 5–49. https://doi.org/10.1023/A:1010303732441

Perry, S. V. (1979). The Regulation of Contractile Activity in Muscle. *Biochemical Society Transactions*, *7*(4), 593–617. https://doi.org/10.1042/bst0070593

Perry, S. V., & Cole, H. A. (1974). Phosphorylation of troponin and the effects of interactions between the components of the complex. *The Biochemical Journal*, *141*(3), 733–743. https://doi.org/10.1042/bj1410733

Peter, J. B., Barnard, R. J., Edgerton, V. R., Gillespie, C. A., & Stempel, K. E. (1972). Metabolic Profiles of Three Fiber Types of Skeletal Muscle in Guinea Pigs and Rabbits. *Biochemistry*, *11*(14), 2627–2633. https://doi.org/10.1021/bi00764a013

Phillips, G. N., Fillers, J. P., & Cohen, C. (1980). Motions of tropomyosin. Crystal as metaphor. *Biophysical Journal*, *32*(1), 485–502. https://doi.org/10.1016/S0006-3495(80)84985-X

Phillips, G. N. J., Lattman, E. E., Cummins, P., Lee, K. Y., & Cohen, C. (1979). Crystal structure and molecular interactions of tropomyosin. *Nature*, *278*(5703), 413–417. https://doi.org/10.1038/278413a0

Pittenger, M. F., Kazzaz, J. A., & Helfman, D. M. (1994). Functional properties of non-muscle tropomyosin isoforms. *Current Opinion in Cell Biology*, *6*(1), 96–104. https://doi.org/10.1016/0955-0674(94)90122-8

Pittenger, M. F., Kistler, A., & Helfman, D. M. (1995). Alternatively spliced exons of the β tropomyosin gene exhibit different affinities for F-actin and effects with nonmuscle caldesmon. *Journal of Cell Science*, *108*(10), 3253–3265.

Polevoda, B., Cardillo, T. S., Doyle, T. C., Bedi, G. S., & Sherman, F. (2003). Nat3p and Mdm20p are required for function of yeast NatB Nalpha-terminal acetyltransferase and of actin and tropomyosin. *The Journal of Biological Chemistry*, *278*(33), 30686–30697. https://doi.org/10.1074/jbc.M304690200

Pollard, T D. (2001). Genomics, the cytoskeleton and motility. *Nature*, *409*(6822), 842–843. https://doi.org/10.1038/35057029

Pollard, T. D., & Korn, E. D. (1973). Acanthamoeba myosin. I. Isolation from Acanthamoeba castellanii of an enzyme similar to muscle myosin. *The Journal of Biological Chemistry*, *248*(13), 4682–4690.

Pollard, T. D., Blanchoin, L., & Mullins, R. D. (2000). Molecular Mechanisms Controlling Actin Filament Dynamics in Nonmuscle Cells. *Annual Review of Biophysics and Biomolecular Structure*, *29*:545-76. doi: 10.1146/annurev.biophys.29.1.545.

Potekhin, S. A., & Privalov, P. L. (1982). Co-operative blocks in tropomyosin. *The Journal of Molecular Biology*, *159*(3), 519–535. https://doi.org/10.1016/0022-

2836(82)90299-6

Potter, J. D. (1982). Preparation of troponin and its subunits. *Methods in Enzymology*, *85 Pt B*, 241–263. https://doi.org/10.1016/0076-6879(82)85024-6

Potter, J. D., & Gergely, J. (1975). The calcium and magnesium binding sites on troponin and their role in the regulation of myofibrillar adenosine triphosphatase. *The Journal of Biological Chemistry*, *250*(12), 4628–4633. https://doi.org/10.1016/S0021-9258(19)41347-1

Potter, J. D., Sheng, Z., Pan, B.S., & Zhao, J. (1995). A Direct Regulatory Role for Troponin T and a Dual Role for Troponin C in the Ca^{2+} Regulation of Muscle Contraction. *The Journal of Biological Chemistry*, *270*(6), 2557–2562. https://doi.org/10.1074/jbc.270.6.2557

Pratje, E., & Heilmeyer, L. M. G. (1972). Phosphorylation of Rabbit Muscle Troponin and Actin By A 3 ’, 5 ’ CAMP-Dependent Protein Kinase. *FEBS Letters*.*27*(1), 89–93.

Price, J. F., Jeewa, A., & Denfield, S. W. (2016). Clinical Characteristics and Treatment of Cardiomyopathies in Children. *Current Cardiology Reviews*. 85-98

Rajan, S., Jagatheesan, G., Petrashevskaya, N., Biesiadecki, B. J., Warren, C. M., Riddle, T., Liggett, S., Wolska, B. M., Solaro, R. J., & Wieczorek, D. F. (2019). Tropomyosin pseudo-phosphorylation results in dilated cardiomyopathy. *The Journal of Biological Chemistry*, *294*(8), 2913–5835. https://doi.org/10.1074/jbc.RA118.004879

Raval, G. N., Bharadwaj, S., Levine, E. A., Willingham, M. C., Geary, R. L., Kute, T., & Prasad, G. L. (2003). Loss of expression of tropomyosin-1, a novel class II tumor suppressor that induces anoikis, in primary breast tumors. *Oncogene*, *22*(40), 6194–6203. https://doi.org/10.1038/sj.onc.1206719

Rayment, I., Rypniewski, W. R., Schmidt-Bäse, K., Smith, R., Tomchick, D. R., Benning, M. M., Winkelmann, D. A., Wesenberg, G., & Holden, H. M. (1993). Three-dimensional structure of myosin subfragment-1: A molecular motor. *Science*, *261*(5117), 50–58. https://doi.org/10.1126/science.8316857

Rayani, K., Seffernick, J., Li, A. Y., Davis, J. P., Spuches, A. M., Van Petegem, F., Solaro, R. J., Lindert, S., & Tibbits, G. F. (2021). Binding of calcium and magnesium to human cardiac troponin C. *Journal of Biological Chemistry*, *296*, 100350. https://doi.org/https://doi.org/10.1016/j.jbc.2021.100350

Reedy, M. K., Holmes, K. C., & Tregear, R. T. (1965). Induced changes in orientation of the cross-bridges of glycerinated insect flight muscle. *Nature*, *207*(5003), 1276–1280. https://doi.org/10.1038/2071276a0

Richardson, J. S., & Richardson, D. C. (1988). Amino acid preferences for specific locations at the ends of alpha helices. *Science*, *240*(4859), 1648–1652. https://doi.org/10.1126/science.3381086

Risi, C. M., Pepper, I., Belknap, B., Landim-Vieira, M., White, H. D., Dryden, K., Pinto, J. R., Chase, P. B., & Galkin, V. E. (2021). The structure of the native cardiac thin filament at systolic Ca(2+) levels. *Proceedings of the National Academy of Sciences*

of the United States of America, *118*(13). https://doi.org/10.1073/pnas.2024288118

Ruiz-Opazo, N., & Nadal-Ginard, B. (1987). Alpha-tropomyosin gene organization. Alternative splicing of duplicated isotype-specific exons accounts for the production of smooth and striated muscle isoforms. *The Journal of Biological Chemistry*, *262*(10), 4755–4765.

Ruiz-Opazo, N., Weinberger, J., & Nadal-Ginard, B. (1985). Comparison of alpha-tropomyosin sequences from smooth and striated muscle. *Nature*, *315*(6014), 67–70. https://doi.org/10.1038/315067a0

Rüegg, J. (1988). Calcium in Muscle Activation.

Russell N.J. Psychrophilic bacteria--molecular adaptations of membrane lipids. *Comparative Biochemistry and Physiology A.* 1997 Nov;118(3):489-93. doi: 10.1016/s0300-9629(97)87354-9. PMID: 9406431.

Russell N.J. (2008) Membrane Components and Cold Sensing. In: Margesin R., Schinner F., Marx JC., Gerday C. (eds) Psychrophiles: from Biodiversity to Biotechnology. S*pringer, Berlin, Heidelberg*. https://doi.org/10.1007/978-3-540-74335-4_11

Perry, S. V., Cole, H. A., & Head, J. F. (1973). Localization and Mode of Action of the Inhibitory Protein Component of the Troponin Complex. *Cold Spring Harb Symp Quant Biol*, *37*, 251–262.

Saavedra, H. G., Wrabl, J. O., Anderson, J. A., Li, J., & Hilser, V. J. (2018). Dynamic allostery can drive cold adaptation in enzymes. *Nature*, *558*(7709), 324–328. https://doi.org/10.1038/s41586-018-0183-2

Sano, K., Maeda, K., Oda, T., & Maéda, Y. (2000). The effect of single residue substitutions of serine-283 on the strength of head-to-tail interaction and actin binding properties of rabbit skeletal muscle alpha-tropomyosin. *The Journal of Biochemistry*, *127*(6), 1095–1102. https://doi.org/10.1093/oxfordjournals.jbchem.a022703

Scarff, C. A., Carrington, G., Casas-Mao, D., Chalovich, J. M., Knight, P. J., Ranson, N. A., & Peckham, M. (2020). Structure of the shutdown state of myosin-2. *Nature*, *588*(7838), 515–520. https://doi.org/10.1038/s41586-020-2990-5

Schaub, M. C., & Perry, S. V. (1969). The relaxing protein system of striated muscle. Resolution of the troponin complex into inhibitory and calcium ion-sensitizing factors and their relationship to tropomyosin. *The Biochemical Journal*, *115*(5), 993–1004. https://doi.org/10.1042/bj1150993

Schulz, E. M., Wilder, T., Chowdhury, S. A. K., Sheikh, H. N., Wolska, B. M., Solaro, R. J., & Wieczorek, D. F. (2013). Decreasing tropomyosin phosphorylation rescues tropomyosin-induced familial hypertrophic cardiomyopathy. *The Journal of Biological Chemistry*, *288*(40), 28925–28935. https://doi.org/10.1074/jbc.M113.466466

Schutt, C. E., Myslik, J. C., Rozycki, M. D., Goonesekere, N. C. W., & Lindberg, U. (1993). The structure of crystalline profilin–β-actin. *Nature*, *365*(6449), 810–816. https://doi.org/10.1038/365810a0

Sia, S. K., Li, M. X., Spyracopoulos, L., Gagné, S. M., Liu, W., Putkey, J. A., & Sykes,

B. D. (1997). Structure of cardiac muscle troponin C unexpectedly reveals a closed regulatory domain. *The Journal of Biological Chemistry*, *272*(29), 18216–18221. https://doi.org/10.1074/jbc.272.29.18216

Silva, A. M. M., & Heeley, D. H. (2021). Existence in the actin world of a specialized slow skeletal muscle isoform. *Comparative Biochemistry and Physiology Part B: Biochemistry and Molecular Biology*, *254*, 110568. https://doi.org/https://doi.org/10.1016/j.cbpb.2021.110568

Silva, A. M. M., Kennedy, L. S., Hasan, S. C., Cohen, A. M., & Heeley, D. H. (2020c). Demonstration of beta-tropomyosin (Tpm2) and duplication of the alpha-slow tropomyosin gene (TPM3) in Atlantic salmon (*Salmo salar*). *Comparative Biochemistry and Physiology Part - B: Biochemistry and Molecular Biology*, *245*(January), 110439. https://doi.org/10.1016/j.cbpb.2020.110439

Simoneau, B., Houle, F., & Huot, J. (2012). Regulation of endothelial permeability and transendothelial migration of cancer cells by tropomyosin-1 phosphorylation. *Vascular Cell*, *4*(1), 18. https://doi.org/10.1186/2045-824X-4-18

Singh, A., & Hitchcock-Degregori, S. E. (2006). Dual requirement for flexibility and specificity for binding of the coiled-coil tropomyosin to its target, actin. *Structure*, *14*(1), 43–50. https://doi.org/10.1016/j.str.2005.09.016

Singh, A., & Hitchcock-DeGregori, S. E. (2003). Local Destabilization of the Tropomyosin Coiled Coil Gives the Molecular Flexibility Required for Actin Binding. *Biochemistry*, *42*(48), 14114–14121. https://doi.org/10.1021/bi0348462

Singh, A., & Hitchcock-DeGregori, S. E. (2007). Tropomyosin's periods are quasi-equivalent for actin binding but have specific regulatory functions. *Biochemistry*, *46*(51), 14917–14927. https://doi.org/10.1021/bi701570b

Skoumpla, K., Coulton, A. T., Lehman, W., Geeves, M. A., & Mulvihill, D. P. (2007). Acetylation regulates tropomyosin function in the fission yeast Schizosaccharomyces pombe *Journal of Cell Science*, *120*(9), 1635 LP – 1645. https://doi.org/10.1242/jcs.001115

Slupsky, C. M., & Sykes, B. D. (1995). NMR solution structure of calcium-saturated skeletal muscle troponin C. *Biochemistry*, *34*(49), 15953–15964. https://doi.org/10.1021/bi00049a010

Smillie, L B. (1979). Structure and functions of tropomyosins from muscle and non-muscle sources. *Trends in Biochemical Sciences*, *4*(7), 151–155. https://doi.org/https://doi.org/10.1016/0968-0004(79)90003-3

Smillie, L.B., Pato, M. D., Pearlstone, J. R., & Mak, A. S. (1980). Periodicity of α-helical potential in tropomyosin sequence correlates with alternating actin binding sites. *The Journal of Molecular Biology*, *136*(2), 199–202. https://doi.org/10.1016/0022-2836(80)90314-9

Smith, C. A., & Rayment, I. (1996). Active site comparisons highlight structural similarities between myosin and other P-loop proteins. *Biophysical Journal*, *70*(4), 1590–1602. https://doi.org/10.1016/S0006-3495(96)79745-X

Sodek, J., Hodges, R. S., Smillie, L. B., & Jurasek, L. (1972). Amino-acid sequence of

rabbit skeletal tropomyosin and its coiled-coil structure. *Proceedings of the National Academy of Sciences of the United States of America*, *69*(12), 3800–3804. https://doi.org/10.1073/pnas.69.12.3800

Spudich, J. A. (2001). The myosin swinging cross-bridge model. *Nature Reviews. Molecular Cell Biology*, *2*(5), 387–392. https://doi.org/10.1038/35073086

Stamm, S., Casper, D., Lees-Miller, J. P., & Helfman, D. M. (1993). Brain-specific tropomyosins TMBr-1 and TMBr-3 have distinct patterns of expression during development and in adult brain. *Proceedings of the National Academy of Sciences of the United States of America*, 90(21), 9857–9861. https://doi.org/10.1073/pnas.90.21.9857

Stone, D., & Smillie, L. B. (1978). The amino acid sequence of rabbit skeletal α-tropomyosin. The NH2-terminal half and complete sequence. *The Journal of Biological Chemistry*, *253*(4), 1137–1148. https://doi.org/10.1016/s0021-9258(17)38122-x

Straub, F. B. (1942). Actin. Studies of the Med. Inst. *Szeged*, *2*, *3*.

Straub, F. B., & Feuer, G. (1950). Adenosinetriphosphate the functional group of actin. *Biochimica et Biophysica Acta*, *4*, 455–470. https://doi.org/https://doi.org/10.1016/0006-3002(50)90052-7

Strzelecka-Gołaszewska, H. (1973). Relative affinities of divalent cations to the site of the tight calcium binding in G-actin. *Biochimica et Biophysica Acta (BBA) - Protein Structure*, *310*(1), 60–69. https://doi.org/https://doi.org/10.1016/0005-

2795(73)90008-1

Strzelecka-Gołaszewska, H., Pròchniewicz, E., & Drabikowski, W. (1978). Interaction of actin with divalent cations. 2. Characterization of protein-metal complexes. *European Journal of Biochemistry*, *88*(1), 229–237. https://doi.org/10.1111/j.1432-1033.1978.tb12442.x

Sumida, J. P., Wu, E., & Lehrer, S. S. (2008). Conserved Asp-137 imparts flexibility to tropomyosin and affects function. *The Journal of Biological Chemistry*, *283*(11), 6728–6734. https://doi.org/10.1074/jbc.M707485200

Sundaralingam, M., Drendel, W., & Greaser, M. (1985). Stabilization of the long central helix of troponin C by intrahelical salt bridges between charged amino acid side chains. *Proceedings of the National Academy of Sciences of the United States of America*, *82*(23), 7944–7947. https://doi.org/10.1073/pnas.82.23.7944

Swenson, C. A., & Stellwagen, N. C. (1989). Flexibility of smooth and skeletal tropomyosins. *Biopolymers*, *28*(5), 955–963. https://doi.org/10.1002/bip.360280504

Tajsharghi, H., Ohlsson, M., Lindberg, C., & Oldfors, A. (2007). Congenital Myopathy With Nemaline Rods and Cap Structures Caused by a Mutation in the β-Tropomyosin Gene (TPM2). *Archives of Neurology*, *64*(9), 1334–1338. https://doi.org/10.1001/archneur.64.9.1334

Takeda, S., Yamashita, A., Maeda, K., & Maéda, Y. (2003). Structure of the core domain of human cardiac troponin in the Ca^{2+}-saturated form. *Nature*, *424*(6944), 35–41. https://doi.org/10.1038/nature01780

Takenaga, K, Nakamura, Y., & Sakiyama, S. (1988). Differential expression of a tropomyosin isoform in low- and high-metastatic Lewis lung carcinoma cells. *Molecular and Cellular Biology*, *8*(9), 3934–3937. https://doi.org/10.1128/mcb.8.9.3934

Takenaga, Keizo, Nakamura, Y., & Sakiyama, S. (1988). Suppression of synthesis of tropomyosin isoform 2 in metastatic v-Ha-ras-transformed NIH3T3 cells. *Biochemical and Biophysical Research Communications*, *157*(3), 1111–1116. https://doi.org/https://doi.org/10.1016/S0006-291X(88)80988-4

Tanokura, M., Tawada, Y., Ono, A., & Ohtsuki, I. (1983). Chymotryptic subfragments of troponin t from rabbit skeletal muscle. interaction with tropomyosin, troponin I and troponin C1. *Journal of Biochemistry*, *93*(2), 331–337. https://doi.org/10.1093/oxfordjournals.jbchem.a134185

Thierfelder, L., Watkins, H., MacRae, C., Lamas, R., McKenna, W., Vosberg, H. P., Seidman, J. G., & Seidman, C. E. (1994). Alpha-tropomyosin and cardiac troponin T mutations cause familial hypertrophic cardiomyopathy: a disease of the sarcomere. *Cell*, *77*(5), 701–712. https://doi.org/10.1016/0092-8674(94)90054-x

Toramoto, T., Ikeda, D., Ochiai, Y., Minoshima, S., Shimizu, N., & Watabe, S. (2004). Multiple gene organization of pufferfish Fugu rubripes tropomyosin isoforms and tissue distribution of their transcripts. *Gene*, *331*, 41–51. https://doi.org/10.1016/j.gene.2004.01.013

Ueno, H. (1984). Local structural changes in tropomyosin detected by a trypsin-probe

method. *Biochemistry*, *23*(20), 4791–4798. https://doi.org/10.1021/bi00315a040

Urbancikova, M., & Hitchcock-DeGregori, S. E. (1994). Requirement of amino-terminal modification for striated muscle alpha-tropomyosin function. *The Journal of Biological Chemistry*, *269*(39), 24310–24315. http://europepmc.org/abstract/MED/7929088

van de Meerakker, J. B. A., Christiaans, I., Barnett, P., Lekanne Deprez, R. H., Ilgun, A., Mook, O. R. F., Mannens, M. M. A. M., Lam, J., Wilde, A. A. M., Moorman, A. F. M., & Postma, A. V. (2013). A novel alpha-tropomyosin mutation associates with dilated and non-compaction cardiomyopathy and diminishes actin binding. *Biochimica et Biophysica Acta*, *1833*(4), 833–839. https://doi.org/10.1016/j.bbamcr.2012.11.003

Van Eerd, J. P., & Takahashi, K. (1976). Determination of the complete amino acid sequence of bovine cardiac troponin C. *Biochemistry*, *15*(5), 1171–1180. https://doi.org/10.1021/bi00650a033

Van Eyk, J. E., Thomas, L. T., Tripet, B., Wiesner, R. J., Pearlstone, J. R., Farah, C. S., Reinach, F. C., & Hodges, R. S. (1997). Distinct regions of troponin I regulate Ca^{2+} dependent activation and Ca^{2+} sensitivity of the acto-S1-TM ATPase activity of the thin filament. *The Journal of Biological Chemistry*, *272*(16), 10529–10537. https://doi.org/10.1074/jbc.272.16.10529

Varga, A. E., Stourman, N. V, Zheng, Q., Safina, A. F., Quan, L., Li, X., Sossey-Alaoui, K., & Bakin, A. V. (2005). Silencing of the Tropomyosin-1 gene by DNA

methylation alters tumor suppressor function of TGF-beta. *Oncogene*, *24*(32), 5043–5052. https://doi.org/10.1038/sj.onc.1208688

Volkmann, N., Hanein, D., Ouyang, G., Trybus, K. M., DeRosier, D. J., & Lowey, S. (2000). Evidence for cleft closure in actomyosin upon ADP release. *Nature Structural Biology*, *7*(12), 1147–1155. https://doi.org/10.1038/82008

von der Ecken, J., Müller, M., Lehman, W., Manstein, D. J., Penczek, P. A., & Raunser, S. (2015). Structure of the F-actin-tropomyosin complex. *Nature*, *519*(7541), 114–117. https://doi.org/10.1038/nature14033

Anderson, P.A. W., Greig.A., Mark, T. M., Malouf, N. N., Oakeley, A.E., Ungerleider, R. M., Allen, P. D., and Kay, B.K. (1995). Molecular Basis of Human Cardiac Troponin T Isoforms Expressed in the Developing, Adult, and Failing Heart. *Circulation Research*, *76*(4), 681–686. https://doi.org/10.1161/01.RES.76.4.681

Warren, C. M., Arteaga, G. M., Rajan, S., Ahmed, R. P. H. H., Wieczorek, D. F., & Solaro, R. J. (2008). Use of 2-D DIGE analysis reveals altered phosphorylation in a tropomyosin mutant (Glu54Lys) linked to dilated cardiomyopathy. *Proteomics*, *8*(1), 100–105. https://doi.org/10.1002/pmic.200700772

Watson, M. H., Taneja, A. K., Hodges, R. S., & Mak, A. S. (1988). Phosphorylation of alpha alpha- and beta beta-tropomyosin and synthetic peptide analogues. *Biochemistry*, *27*(12), 4506–4512. https://doi.org/10.1021/bi00412a043

Weeds, A. G., & Taylor, R. S. (1975). Separation of subfragment-1 isoenzymes from rabbit skeletal muscle myosin. *Nature*, *257*(5521), 54–56.

https://doi.org/10.1038/257054a0

Wegner, A. (1977). The mechanism of ATP hydrolysis by polymer actin. *Biophysical Chemistry, 7*(1), 51–58. https://doi.org/https://doi.org/10.1016/0301-4622(77)87014-2

Wexler, R. K., Elton, T., Pleister, A., & Feldman, D. (2009). Cardiomyopathy: an overview. *American Family Physician*, *79*(9), 778–784. https://pubmed.ncbi.nlm.nih.gov/20141097

Whitby, F. G., & Phillips, G. N. (2000). Crystal structure of tropomyosin at 7 angstroms resolution. *Proteins: Structure, Function and Genetics*, *38*(1), 49–59. https://doi.org/10.1002/(SICI)1097-0134(20000101)38:1<49::AID-PROT6>3.0.CO;2-B

White, H. D., Belknap, B., & Webb, M. R. (1997). Kinetics of nucleoside triphosphate cleavage and phosphate release steps by associated rabbit skeletal actomyosin, measured using a novel fluorescent probe for phosphate. *Biochemistry*, *36*(39), 11828–11836. https://doi.org/10.1021/bi970540h

White, S. P., Cohen, C., & Phillips, G. N. J. (1987). Structure of co-crystals of tropomyosin and troponin. *Nature*, *325*(6107), 826–828. https://doi.org/10.1038/325826a0

Wieczorek, D. F. (2018). *The Role of Tropomyosin in Cardiac Function and Disease.* doi: http://dx.doi.org/10.5772/intechopen.81420

Wieczorek, D. F., Smith, C. W., & Nadal-Ginard, B. (1988). The rat alpha-tropomyosin

gene generates a minimum of six different mRNAs coding for striated, smooth, and nonmuscle isoforms by alternative splicing. *Molecular and Cellular Biology*, *8*(2), 679–694. https://doi.org/10.1128/mcb.8.2.679

Wilkinson, J. M. (1980). Troponin C from Rabbit Slow Skeletal and Cardiac Muscle Is the Product of a Single Gene. *European Journal of Biochemistry*, *103*(1), 179–188. https://doi.org/10.1111/j.1432-1033.1980.tb04302.x

Wilkinson, J. M., & Grand, R. J. A. (1978). Comparison of amino acid sequence of troponin I from different striated muscles. *Nature*, *271*(5640), 31–35. https://doi.org/10.1038/271031a0

Wilkinson, J. M., Perry, S. V, Cole, H. A., & Trayer, I. P. (1972). The regulatory proteins of the myofibril. Separation and biological activity of the components of inhibitory-factor preparations. *The Biochemical Journal*, *127*(1), 215–228. https://doi.org/10.1042/bj1270215

Willadsen, K. A., Butters, C. A., Hill, L. E., & Qll, L. S. T. (1992). Effects of the Amino-terminal Regions of Tropomyosin and Troponin T on Thin Filament Assembly. *The Journal of Biological Chemistry*, *267*(33), 23746–23752. https://doi.org/10.1016/S0021-9258(18)35901-5

Williams, D. L., & Swenson, C. A. (1981). Tropomyosin Stability: Assignment of Thermally Induced Conformational Transitions to Separate Regions of the Molecule. *Biochemistry*, *20*(13), 3856–3864. https://doi.org/10.1021/bi00516a029

Witjes, L., Van Troys, M., Vandekerckhove, J., Vandepoele, K., & Ampe, C. (2019). A

new evolutionary model for the vertebrate actin family including two novel groups. *Molecular Phylogenetics and Evolution*, *141*(April), 106632. https://doi.org/10.1016/j.ympev.2019.106632

Woods, E F. (1966). The dissociation of tropomyosin by urea. *Journal of Molecular Biology*, *16*(2), 581–584. https://doi.org/https://doi.org/10.1016/S0022-2836(66)80199-7

Woods, E F. (1967). Molecular Weight and Subunit Structure of Tropomyosin B. *Journal of Biological Chemistry*, *242*(12), 2859–2871. https://doi.org/https://doi.org/10.1016/S0021-9258(18)99585-2

Woods, E. F. (1977). Stability of Segments of Rabbit α-Tropomyosin. *Australian Journal of Biological Sciences*, *30*(6), 527–542. https://doi.org/10.1071/BI9770527

Wu, S. C., & Solaro, R. J. (2007). Protein kinase C zeta. A novel regulator of both phosphorylation and de-phosphorylation of cardiac sarcomeric proteins. *The Journal of Biological Chemistry*, *282*(42), 30691–30698. https://doi.org/10.1074/jbc.M703670200

Wulf, S. F., Ropars, V., Fujita-Becker, S., Oster, M., Hofhaus, G., Trabuco, L. G., Pylypenko, O., Sweeney, H. L., Houdusse, A. M., Schröder, R. R., & Vale, R. D. (2016). Force-producing ADP state of myosin bound to actin. *Proceedings of the National Academy of Sciences of the United States of America*, *113*(13), E1844–E1852. https://doi.org/10.1073/pnas.1516598113

Xie, L., Miyazaki, J., & Hirabayashi, T. (1991). Identification and distribution of

tropomyosin isoforms in chicken digestive canal. *Journal of Biochemistry*, *109*(6), 872–878. https://doi.org/10.1093/oxfordjournals.jbchem.a123473

Yamada, Y., Namba, K., & Fujii, T. (2020). Cardiac muscle thin filament structures reveal calcium regulatory mechanism. *Nature Communications*, *11*(1), 153. https://doi.org/10.1038/s41467-019-14008-1

Yamauchi-Takihara, K., Nakajima-Taniguchi, C., Matsui, H., Fujio, Y., Kunisada, K., Nagata, S., & Kishimoto, T. (1996). Clinical implications of hypertrophic cardiomyopathy associated with mutations in the α-tropomyosin gene. *Heart*, *76*(1), 63–65. https://doi.org/10.1136/hrt.76.1.63

Yamawaki-Kataoka, Y., & Helfman, D. M. (1987). Isolation and characterization of cDNA clones encoding a low molecular weight nonmuscle tropomyosin isoform. *The Journal of Biological Chemistry*, *262*(22), 10791–10800.

Yanagida, T., Arata, T., & Oosawa, F. (1985). Sliding distance of actin filament induced by a myosin crossbridge during one ATP hydrolysis cycle. *Nature*, *316*(6026), 366–369. https://doi.org/10.1038/316366a0

Yengo, C. M., Chrin, L., Rovner, A. S., & Berger, C. L. (1999). Intrinsic tryptophan fluorescence identifies specific conformational changes at the actomyosin interface upon actin binding and ADP release. *Biochemistry*, *38*(44), 14515–14523. https://doi.org/10.1021/bi991226l

Yount, R. G., Lawson, D., & Rayment, I. (1995). Is myosin a "back door" enzyme? *Biophysical Journal*, *68*(4 Suppl), 44S-47S; discussion 47S-49S.

Yuan, C., Sheng, Q., Tang, H., Li, Y., Zeng, R., & Solaro, R. J. (2008). Quantitative comparison of sarcomeric phosphoproteomes of neonatal and adult rat hearts. *American Journal of Physiology-Heart and Circulatory Physiology*, *295*(2), H647–H656. https://doi.org/10.1152/ajpheart.00357.2008

Zajdel, R. W., Denz, C. R., Lee, S., Dube, S., Ehler, E., Perriard, E., Perriard, J.-C., & Dube, D. K. (2003). Identification, characterization, and expression of a novel alpha-tropomyosin isoform in cardiac tissues in developing chicken. *Journal of Cellular Biochemistry*, *89*(3), 427–439. https://doi.org/10.1002/jcb.10504

Zechel, K., & Weber, K. (1978). Actins from mammals, bird, fish and slime mold characterized by isoelectric focusing in polyacrylamide gels. *European Journal of Biochemistry*, *89*(1), 105–112. https://doi.org/10.1111/j.1432-1033.1978.tb20901.x

Zot, A. S., & Potter, J. D. (1987). Structural Aspects of Troponin-Tropomyosin Regulation of Skeletal Muscle Contraction. *Annual Review of Biophysics and Biophysical Chemistry*, *16*(1), 535–559. https://doi.org/10.1146/annurev.bb.16.060187.002535

Chapter 2. Demonstration of beta-tropomyosin (Tpm2) and alpha-1 chain-like isoform X1 in Atlantic salmon (*Salmo salar*).

Abstract

The isoforms of the vertebrates' tropomyosin family arise from four genes namely: TPM1 (alpha), TPM2 (beta), TPM3 (alpha-slow), and TPM4 (cardiac). Although genome sequencing predicts the existence of these tropomyosin isoforms in fish, the current study is the first ever to demonstrate the existence of Tpm2 (beta) and alpha-1 chain-like isoform X1 at the protein level in any such species. Isolated tropomyosins are analyzed using electrophoresis, mass spectrometry, limited proteolysis, and troponin-affinity chromatography. The findings of this section are: (i) Tpm2 exists in the tongue, jaw, and fin muscles of Atlantic salmon whereas the alpha-1 chain-like isoform X1 is found in the tongue, jaw, and cheek dark, (ii) Salmon Tpm2 and alpha-1 chain-like isoform X1 have different electrophoretic mobilities compared to mammalian Tpm2, and salmon Tpm1 in the presence of anionic detergent, (iii) The two isoforms have unique carboxyl-terminal region from residues 276 - 284; Tpm2, Met-Thr-Thr-Leu and alpha-1 chain-like isoform X1, Met-Thr-Ala-Ile, iv) Salmon Tpm2 has a reduced content of cysteine (one per chain) and tyrosine (five per chain) compared to mammalian homologs and (v) Of the two isoforms in the tongue, Tpm2 displays a comparatively weaker affinity for troponin-Sepharose possibly due to the presence of two closely spaced glycines in the N-terminal region at residues 27 and 31. The results were published in Silva et al., 2020c.

2.1 Introduction

Tropomyosin is a coiled-coil, rod-shaped protein that is located in muscle and cytoskeleton where it has interrelated structural and regulatory roles (Perry, 2001). The isoforms of the tropomyosin family arise from the expression of multiple genes (four in mammals and birds), exon shuffling, and the use of more than one promoter. The first proof of the occurrence of isoforms came from denaturing polyacrylamide electrophoresis (PAGE). The first two isoforms identified were alpha and beta tropomyosin from striated muscles (They were given Greek letters as identifiers) (Cummins & Perry, 1973, 1974). These are the major forms of tropomyosin. Protein sequencing of rabbit tropomyosin showed that they contain the same number of amino acids: (Stone & Smillie, 1978; Mak et al., 1980). Nucleic acid sequencing of chicken and rat demonstrated four genes (MacLeod, 1982; Helfman et al., 1986; Ruiz-Opazo & Nadal-Ginard, 1987; Libri et al., 1989; Lees-Miller & Helfman, 1991) which have been named: TPM1 (alpha), TPM2 (beta), TPM3 (alpha-slow), and TPM4 (cardiac) (nomenclature as proposed in Geeves et al., 2015). The duplication of TPM1 and TPM4 in pufferfish and zebrafish has caused these particular species to have a total of six genes (Ikeda et al., 2003; Toramoto et al., 2004; Schevzov et al., 2011; Dube et al., 2017). More than forty years after their identification the alpha and beta tropomyosins in rabbit skeletal muscle were demonstrated to possess different biochemical properties (Heeley & Lohmeier-Vogel, 2016).

The Heeley lab has used the trunk musculature of Salmonidae fish (Figure 2.1), including Atlantic salmon (*Salmo salar*), as a source of tropomyosin (protein) for biochemical studies (Heeley et al., 1995; Jackman et al., 1996; Goonasekara & Heeley, 2008; Fudge & Heeley,

2015). The advantages of the Atlantic salmon are: its size which enables muscle samples to be obtained in sizeable quantities from a variety of anatomical zones, including the segregated fast and slow trunk muscles (Figure 2.1) and its year-round availability. Previous studies have shown that the slow skeletal (darker) muscle along the lateral line (which supports low-speed cruising) and the fast skeletal (lighter) muscle (which supports rapid bursts) (Bone et al., 1995) synthesize non-identical isoforms (Heeley & Hong, 1994; Heeley et al., 1995) specifically, alpha-fast (Tpm1, accession number AAB36559) and alpha-slow (Tpm3, Z66490) (Jackman et al., 1996). The 1996 study additionally recorded a unique variant in the heart, which is Tpm4, (Z66527). During these investigations (Heeley et al., 1995; Jackman et al., 1996) Tpm2 was not found. Since the completed Atlantic salmon genome (Lien et al., 2016) contains the Tpm2 gene, a reinvestigation has been carried out to find beta tropomyosin.

In this study, we have utilized protein electrophoresis, mass spectrometric tryptic peptide mapping, chromatography, limited proteolysis, and affinity chromatography in combination with the published genome (Lien et al., 2016) to further characterize the tropomyosin isoforms in Atlantic salmon. The results show the presence of Tpm2 (at protein level) in the jaw, tongue, pectoral fin, and the slow trunk muscle (Silva et al., 2020c). In these instances, Tpm2 is always found along with another isoform and contributes 50% of the total tropomyosin in the above mentioned anatomical regions, however, Tm2 is absent from the fast skeletal muscle that makes up the bulk of the trunk. Some of the distinctive characteristics of salmon Tpm2 include the number of cysteines (one vs. two in mammalian Tpm2) and tyrosines (five vs. six in mammalian Tpm2), and

the penultimate C-terminal amino acid: threonine rather than serine (Mak et al., 1978), giving salmon Tpm2 the unique Thr-283-Leu-284 C-terminus. Salmon Tpm2 also displays an altered electrophoretic mobility relative to mammal i.e., Tpm2. Salmon Tpm2 contains noticeable differences in the troponin binding regions compared to the isoform in the fast trunk muscle (AAB36559).

As mentioned, none of the salmon muscles analyzed in this work provides a pure source of Tpm2. In the cases of jaw, tongue, and cheek dark, a second isoform was identified, namely, alpha-1 chain-like isoform X1 (XP_013980250) which exists in equal proportion to Tpm2. Both Tpm2 and XP_013980250 contained lysine in the 77^{th} residue position, as opposed to the fast skeletal isoform which has threonine. The relevance of this isomorphism is explored in detail in Chapter 3. A final point, Tpm2 is not present in all of the head muscles of the Atlantic salmon. Cheek dark muscle comprises a 50:50 mixture of Tpm1 and alpha-1 chain-like isoform X1.

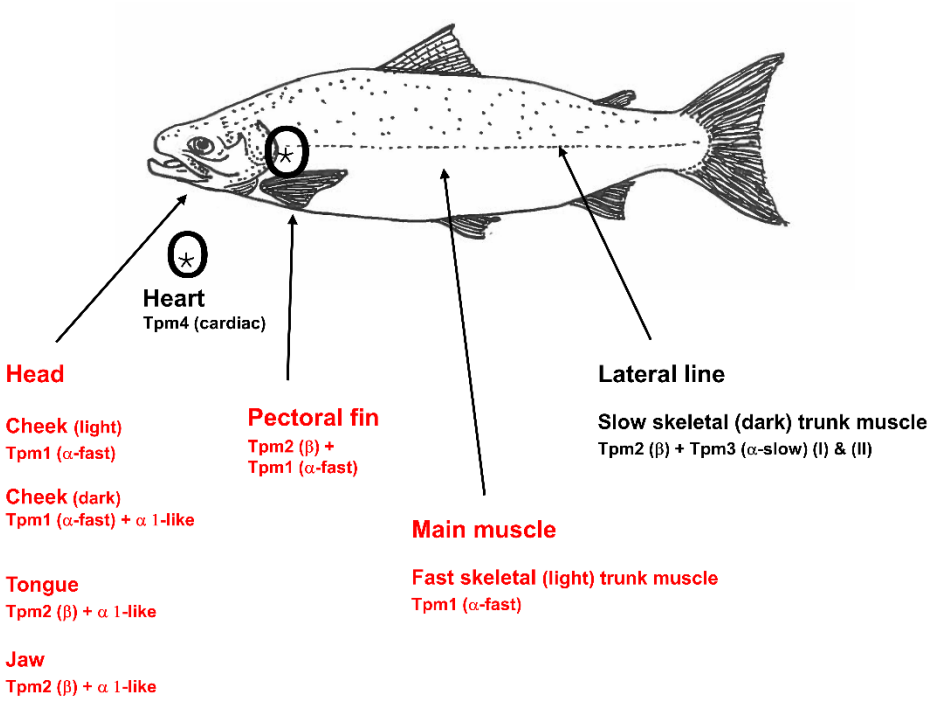

Figure 2.1. Distribution of tropomyosin isoforms in Atlantic salmon (*Salmo salar*). Indicated are the sites of the striated muscles showing the distribution of different isoforms. Red - The regions that are analyzed in the current study and their corresponding tropomyosin isoform composition. Adapted from Silva et al., 2020c.

2.2 Materials and Methods

2.2.1 Muscle tissue and sample extract preparation

Atlantic salmon was obtained from a local fishmonger, carefully dissected, and biopsies were taken from various anatomical regions: trunk, pectoral fin (adductor pectoral), cheek (adductor mandibulae), and tongue (sternohyoid) (No live specimens were harmed in this work). Muscle extracts for analyses were prepared by homogenizing 0.1 g of muscle biopsy in 1 mL of saturated urea (prepared each time freshly from solid) containing ~2 mM dithiothreitol (DTT) using a Kinematica Polytron pt. 10 - 35 (Brinkmann) at a medium speed for 30 s. The temperature was maintained at room temperature (~ 20 - 25 °C) during all steps. The homogenates were clarified by spinning in an Eppendorf 5415 centrifuge for 1 min at 15000 rpm and left to settle at room temperature for 5 - 10 min. The clarified supernatants were used for analyses. Rabbit fast skeletal muscle acetone powder was prepared as outlined in Smillie, 1982.

2.2.2 Electrophoresis

One-dimensional sodium dodecyl sulfate-polyacrylamide gel electrophoresis (SDS-PAGE) was performed using the method of Laemmli, 1970. Two dimensional PAGE (O'Farrell, 1975) consisted of isoelectric focusing in the first dimension which was performed in tube gels made with 9 M urea, (2 % (v/v) Ampholyte pH 4 - 6 Fluka; 4 % (m/v) acrylamide monomer (Bio-Rad), 0.25 % (m/v) N, N'-methyl-bis-acrylamide (Bio-Rad); 0.038 % (v/v) NP40; rod dimensions, (1.5 mm × 18 cm). Any persulfate remaining from the

polymerization reaction was depleted by a short pre-run (15 mins at 160 V). The clarified supernatant was loaded onto the tube gels. Sample loadings were varied over a fivefold range (3 - 15 μL) with lower loadings employed in the instances where isoforms migrated close to each other. The top tank consisted of 15 mM H_3PO_4 and the lower tank 4 mM NaOH. The isoelectric focusing step was carried out at 350 V overnight (total kVhr, 6.5 - 7). The tube gels were then placed on the second dimension gels in the presence of sample buffer. The second dimension was carried out using SDS-PAGE (Laemmli, 1970) containing no stacking gel phase. Acrylamide/ N, N-methylene-bis-acrylamide (BioRad) (m/v) ratio was 30: 0.8. The separating gel phase consisted of 12 % (m/v) acrylamide. Gels were run at 160 V (Running buffer; 0.083 M glycine, 0.020 M Tris) for one tracking dye length and then placed in 0.25% (m/v) Coomassie Brilliant Blue-R250 (Bio-Rad), 50% (v/v) ethanol, 10% (v/v) acetic acid for ~1 h for staining. The gels were then de-stained until clear using 10% (v/v) ethanol and 10% (v/v) acetic acid solution and stored in the cold still they were photographed using ImageQuant LAS400/chemiImager™. Protein spots of interest were carefully cut out of stained polyacrylamide gels using clean scalpels, dried in an evacuated desiccator, and were sent to the Proteomics and Mass Spectrometry Core Facility at Dalhousie for analysis.

2.2.3 Salmon tongue and rabbit fast skeletal isoforms purification

Atlantic salmon tongue tropomyosin isoforms were isolated from tongue muscle acetone powder as outlined in (Smillie, 1982). Following 0.1M NaCl extraction and isoelectric precipitation at pH 4.6, nucleic acids were removed by passage over the Q Sepharose Fast Flow column. Further enrichment was attained by loading fractions directly onto hydroxyapatite (Smillie, 1982). After exhaustive dialysis in the presence of β-mercaptoethanol and NH_4HCO_3 in a cold room, samples were freeze-dried and store at 8 ^oC till use. Tropomyosin concentration was determined by UV absorbance with A_{280} according to the formula $[tropomyosin] = \frac{A280nm - 1.5A320nm}{0.25}$ with 1.5 A_{320} scatter correction. When needed rabbit fast skeletal tropomyosin was also prepared using the same method as described above.

2.2.4 Troponin affinity chromatography

Whole troponin (TnT, TnC, and TnI) was obtained from rabbit skeletal muscle as described in (Potter, 1982) without the step involving Cibacron Blue-based chromatography. Troponin concentration was determined by UV absorbance with A_{280} according to the following formula $[troponin] = \frac{A280nm - 1.5A320nm}{0.47}$ with 1.5 A_{320} scatter correction.

A troponin-Sepharose 4B column was prepared by coupling rabbit skeletal troponin to CNBr-activated Sepharose 4B as per the instructions provided by the manufacturer (GE Health Care) (Heeley & Lohmeier-Vogel, 2016) (Column, 0.9 cm x 15 cm (volume, ~ 9.5

mL). Chromatography start buffer contained 10 mM imidazole, 1 mM EGTA, 0.01% (m/v) NaN_3, 1 mM dithiothreitol, pH 7.0. All column steps (load, wash, and elution) were carried out in a cold room (10 ^oC) (Linear salt gradient, 0 - 0.5 M NaCl; volume, 160 mL; flow rate, ~ 25 mL / hour; fraction size, ~ 1.8 mL). The conductivity measurements were made using a Radiometer CDM80 Conductivity Meter after warming up fractions to room temperature. The increase in conductivity per tube was 0.31 mS/cm. Tropomyosin-containing fractions were identified and quantified using Bradford reagent with absorbance at 595 nm (Bradford, 1976) followed by SDS-PAGE analysis. The two methods were in agreement in identifying the fraction containing the highest amount of protein and the conductivity of peak absorbance 595 nm fraction was noted.

2.2.5 Phylogenetic analysis

The amino acid sequences encoded by the common exons in vertebrates, namely 3, 4, 5, 6b, 7, and 8, in Tpm1, Tpm2, Tpm3, and Tpm4 isoforms were aligned using multiple sequence alignment ClustalW program for a selected set of animals. The tree was constructed using the neighbor-joining method (Saitou & Nei, 1987) in MEGA X (Kumar et al., 2018). Evolutionary distances were computed by Poisson correction (Zuckerkandl and Pauling, 1965) and internal branches were analyzed using 1000 bootstrap repeats (Felsenstein, 1985).

2.3 Results

2.3.1 Electrophoretic comparison of salmon and mammalian tropomyosins

In Figure 2.2A the relative mobilities of Atlantic salmon and rabbit tropomyosins are compared using one-dimensional Laemmli gel system. Tropomyosin prepared from salmon fast skeletal trunk muscle (Figure 2.2A, lane 1) migrates at a similar rate to rabbit skeletal beta-tropomyosin (Figure 2.2A, upper band lane 2). Conversely, tropomyosin from the slow skeletal trunk muscle (Figure 2.2A, lane 3) migrates nearer to rabbit alpha-tropomyosin from skeletal and cardiac extracts (Figure 2.2A, the lower band in lane 2 and lane 4). Salmon tongue tropomyosin yields a doublet (Figure 2.2A, lane 5) which straddles the mobility of rabbit alpha-tropomyosin (compare Figure 2.2A, lanes 5 and 6).

Next, in Figure 2.2B, the various salmon tropomyosins are compared with each other using the same gel system as in Figure 2.2A. In the case of the tongue, each band (Figure 2.2B lane 5) is well separated from that of fast trunk tropomyosin (Figure 2.2B lane 1). This is especially noticeable when the proteins are mixed and run in the same lane (Figure 2.2B lane 3). When a mixture of tropomyosins from the tongue and slow trunk muscle is run together the upper band thickness increases and more than one band is evident (Figure 2.2B, lane 4). In this instance, the fastest moving band is assumed to correspond to that of lower tongue tropomyosin. Fast trunk tropomyosin is the slowest moving out of those tested. Thus, the relative mobilities of the various tropomyosins increase in the order: fast trunk = rabbit beta < slow trunk = rabbit alpha = tongue upper < tongue lower.

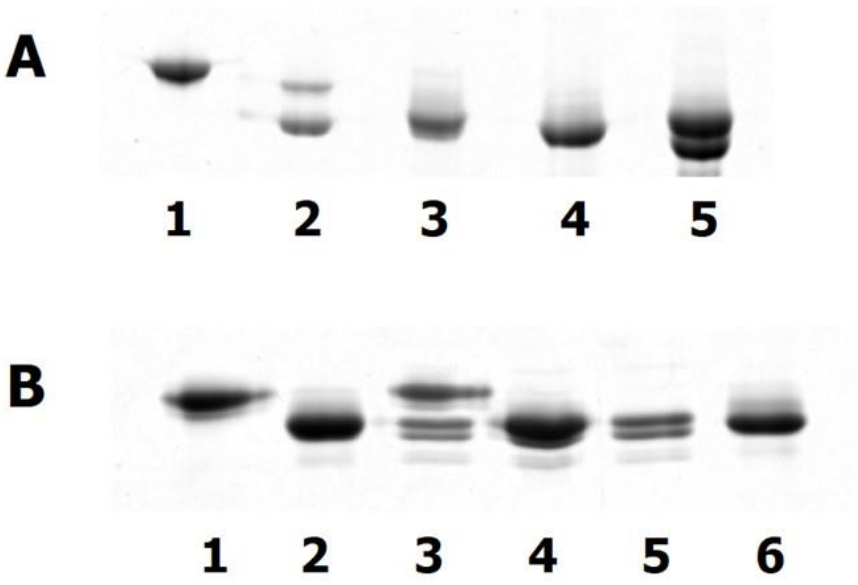

Figure 2.2. One-dimensional PAGE of Atlantic salmon striated muscle tropomyosins. Tropomyosins were isolated from separate muscles and analyzed by SDS-PAGE. The protein source is Salmo salar unless stated otherwise. There is a difference in enlargement between panels. (A) Comparison of salmon and rabbit tropomyosins. Lane 1, fast trunk muscle; lane 2, rabbit skeletal muscle (alpha Tpm1.1 + beta Tpm2.2); lane 3, slow trunk muscle; lane 4, rabbit heart (alpha, Tpm1.1 only) and lane 5, tongue (B) Comparison of Atlantic salmon tropomyosins. Lane 1, fast trunk; lane 2, slow trunk; lane 3, a mix of fast trunk + tongue; lane 4, a mix of slow trunk + tongue; lane 5, tongue and lane 6, slow trunk. Faint lower molecular weight bands in lanes 3,4 and 5 of B may be due to a slight breakdown of tongue tropomyosin. Reprinted from Silva et al., 2020c.

2.3.2 Fast skeletal trunk muscle is composed of a single form of tropomyosin

The lighter-toned muscle in the trunk is the main muscle, and most commercially important part, of the Atlantic salmon. It is composed of a single isoform that is classed as alpha-fast tropomyosin, (Heeley et al., 1995). There are 20 - 22 amino acid differences when compared to alpha-fast skeletal isotypes in chicken and rodent and twice as many when compared to beta isotypes. It is referred to herein as alpha-fast or Tpm1. The sequence of salmon Tpm1 (accession AAB36559) has been previously verified by measuring the masses of the isolated intact protein and fragments thereof (Heeley et al., 1995; Jackman et al., 1996). Unique features of the Tpm1 sequence are: a pair of glycines at residues 24 and 27 (Figure 2.4 arrows) and a neutral side-chain, threonine, in residue position 77, and which, therefore, provide an effective means of identification in PAGE (compared to rabbit homologue). When the two-dimensional electrophoretic analysis is repeated, a single spot is observed (Figure 2.3A), which is evidence of a lack of heterogeneity.

2.3.3 Beta and alpha-1 chain-like isoform X1 tropomyosin isoforms are present in the head and fin skeletal muscles.

Analysis of muscles from different regions of the head (tongue and cheek) and muscle lobes from pectoral fins reveals the existence of a variety of tropomyosin isoforms. In lighter sections of the cheek, one form of tropomyosin is apparent on the gel (Figure 2.3d). Since the peptide map included residues 22 - 49 (Table 1) which encompass Gly-24 and 27, it is concluded this corresponds to Tpm1 (alpha fast). By contrast, a second (major) isoform is

evident in darker sections of cheek muscle (Figure 2.3e). It is equivalent to the genome entry entitled alpha-1 chain-like isoform X1 (accession, XP_013996655; chromosome, ssa14). Since it contains Gly at residues 45 and 52. The C-terminal sequence, His-276-Ala-Leu-Thr-Asp-Met-Thr-Ala-Ile-284, also distinguishes it from other tropomyosin isoforms in this study. Unusual for a striated muscle tropomyosin, the 283rd residue is Ala. Surprisingly, in a pairwise alignment alpha-1 chain-like isoform X1, it is more closely related to Tpm4 (heart, Z66527 Jackman et al., 1996; accession, XP_014071189) than Tpm1 (alpha fast): 21 vs. 39 substitutions. This point is supplied as a cautionary note and is not investigated further. Two closely migrating spots, neither of which corresponds to the Tpm1 (alpha-fast) isoform are observed in the tongue (Figure 2.3f), a point that is also demonstrated by co-electrophoresis (Figure 2.3g). An identical spot pattern is observed for the tongue and jaw tropomyosin (Silva et al., 2020c). For example, when extracts of each muscle are loaded onto the same isoelectric focusing gel, the resulting electrophoretic pattern (Figure 2.3h) is the same for each sample separately (Silva et al., 2020c Figure 2.3), The results of two-dimensional PAGE are consistent with those of one-dimensional PAGE, where tongue tropomyosin resolved into two bands (Figure 2.2B lanes 3 and 5). The process of isoform identification was then performed as before. Peptides derived from tropomyosin contained within the upper spot match the sequence of Tpm2 (beta), coverage: 65 % (Figure 2.4 and Table 1). Those from the lower spot match XP_013996655, coverage: 73.5 % (Figure 2.4 and Table 1). The same isoform is identified in the darker tissue of the cheek.

Two prominent spots are detected in extracts of pectoral fin skeletal muscle (Figure 2.3b) indicating a minimum of two isoforms. Based on co-electrophoresis with the fast skeletal isoform (Figure 2.3c) and peptide mapping (Table 1) the upper spot is identified as Tpm1 (alpha-fast). The tryptic peptide map spans 88% of the sequence and includes Gly-24 and 27 (Figure 2.4). The lower intensely stained spot is characterized by a comparatively faster mobility in the SDS dimension and a higher isoelectric point (Figure 2.3b). This particular tropomyosin (sequence coverage: 79% and Table 1) corresponds to the genome entry named beta X1 (accession, XP_014000233; chromosome, ssa01). We refer to it here as beta tropomyosin or Tpm2 (Geeves et al., 2015). Some of the characteristics of Atlantic salmon beta tropomyosin, all of which are covered in the peptide map are: (i) one cysteine per chain (as opposed to two in other vertebrate homologs, Cys190Ser); (ii) five tyrosines per chain (as opposed to six, Tyr267Gly); (iii) closely-spaced glycines at residues 27 and 31 and (iv) the carboxyl-terminal sequence, Leu-276-Ala-Leu-Asn-Asp-Met-Thr-Thr-Leu-284, which lacks serine (Mak et al., 1978; Heeley, 2013). Further, salmon Tpm2 possesses seven methionines, one less than the counterpart in rabbit. Based on the sequence, the observed difference in mobility (Tpm1 vs. Tpm2) apparent in Figure 2.3g can be accounted for by the charge substitution, Lys-77 (in Tpm2) to Thr (in Tpm1) and is further analyzed in chapter 3.

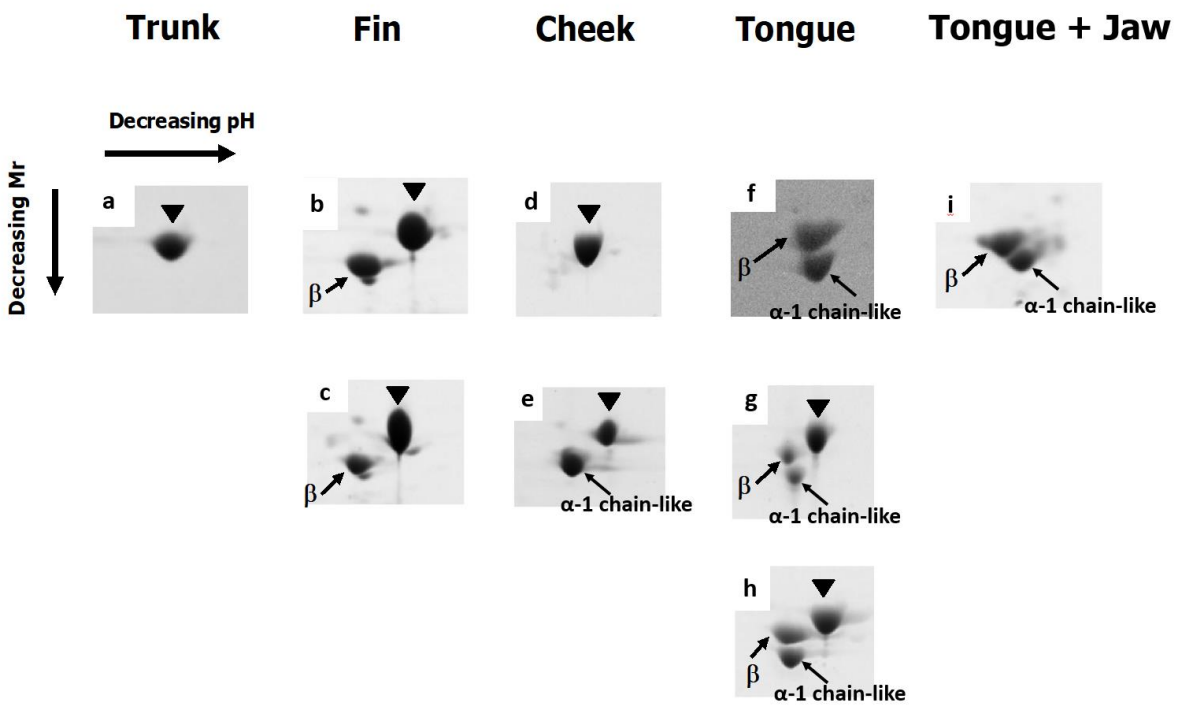

Figure 2.3. Two-dimensional PAGE of Atlantic salmon tropomyosins. The insets (a - i) are sections of second dimension gels, that contain the main isoforms of tropomyosin in terms of abundance. Chevrons indicate the spot corresponding to Tpm1 (alpha-fast). The spot corresponding to Tpm2 (beta) and alpha-1 chain-like isoform X1 are indicated by arrows. Mixing experiments (c, h, and i) were performed to confirm isoform positions. Minor spots (b and c) may correspond to additional (minor) isoforms or different proteins of similar electrophoretic mobility and isoelectric points. Small gel-to-gel differences are noticeable. Insets: (a) fast trunk muscle; (b) pectoral fin; (c) mix of pectoral fin + fast trunk; (d) cheek (light); (e) cheek (dark); (f) mix of jaw + tongue; (g), mix of tongue + fast trunk; (h) tongue and (i), mix of tongue + jaw (light). Adapted from Silva et al., 2020c.

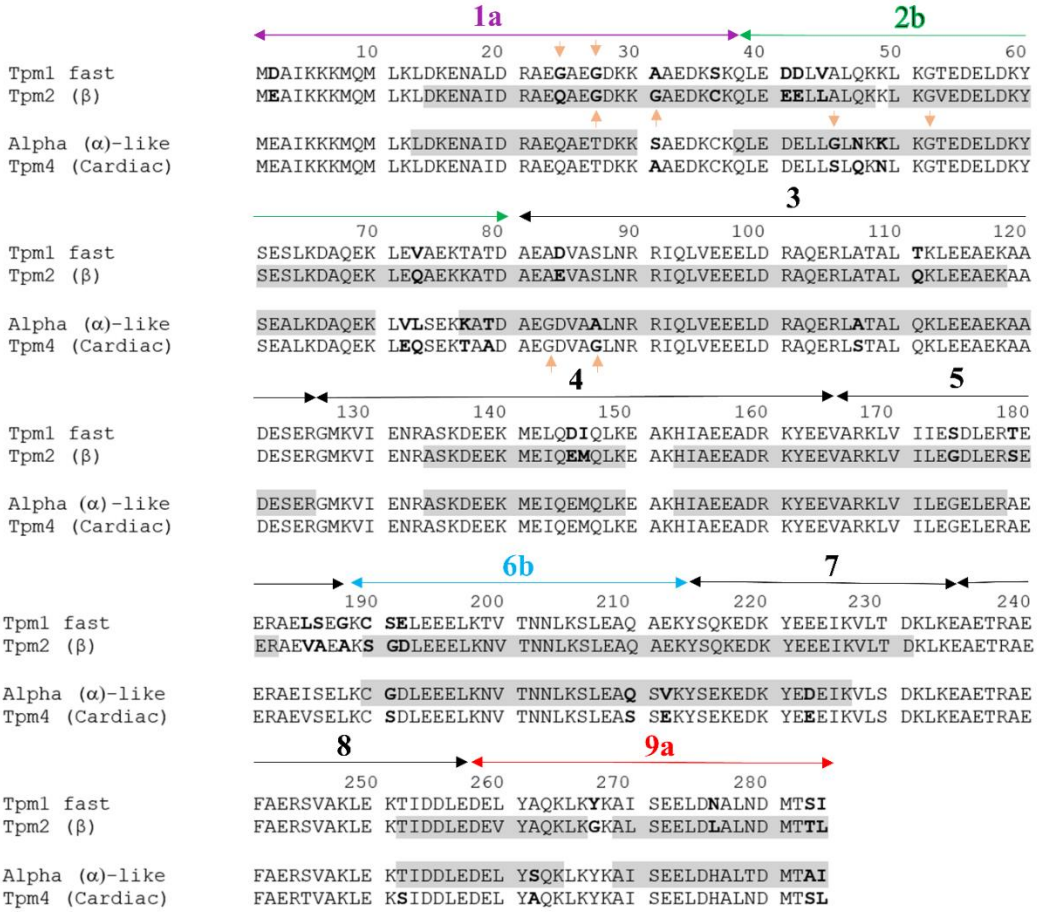

Figure 2.4. Amino acid sequences of Atlantic salmon tropomyosins and mass spectrometric tryptic peptide coverage. The abbreviated names and accession numbers of the tropomyosins in the figure are: Tpm1 (alpha fast) AAB36559; Tpm2 (beta) XP_014000233; Tpm4 (cardiac), XP_014071189 and alpha 1 chain-like isoform X1 (cheek/tongue), XP_013996655. Letters in bold correspond to positions of non-identity between the following pairings: alpha-fast vs. beta, 32 substitutions, and Tpm4 vs. alpha 1-like Tpm (cheek/tongue), 21 substitutions. Exons 1a, 2b, 3, 4, 5, 6b, 7, 8, and 9a coded regions are indicated above the sequence. Conserved exons 3, 4, 5, 7, and 8 are indicated in black. Orange color arrows - closely spaced double glycines in each isoform. The shaded sections of the sequence are confirmed herein by mass spectrometry (Table 1). In most instances, these sections are made up of adjoining smaller fragments. Adapted from Silva et al., 2020c.

Table 2. 1. Mass spectrometric tryptic peptide mapping of spots from 2D-PAGE.

Isoform	Fragment length	The sequence of the peptide
Tpm2 (beta) Pectoral fin coverage 79%	16-47	ENAIDRAEQAEGDKKGAEDKCKQLEEELLALQK
	50-90	LKGVEDELDKYSESLKDAQEKLEQAEKKATDAE AEVASLNR
	92-118	IQLVEEELDRAQERLATALQKLEEAEK
	134-149	ASKDEEKMEIQEMQLK
	153-182	HIAEEADRKYEEVARKLVILEGDLERSEER
	190-232	SGDLEEELKNVTNNLKSLEAQAEKYSQKEDKYEEEIKVL TDK
	252-266	TIDDLEDEVYAQKLK
	268-284	ALSEELDLALNDMTTL
Tpm1 (alpha-fast) Pectoral fin, coverage 88%	1-128	MDAIKKKMQMLKLDKENALDRAEGAEGDKKAAEDKSK QLEDDLVALQKKLKGTEDELDKYSESLKDAQEKLEVAE KTATDAEADVASLNRRIQLVEEELDRAQERLATATKLEE AEKAADESERGMK
	134-149	ASKDEEKMELQDIQLK
	153-161	HIAEEADRK
	168-182	KLVIIESDLERTEER
	190-205	CSELEEELKTVTNNLK
	214-233	YSQKEDKYEEEIKVLTDKLK
	252-264	TIDDLEDELYAQK
Alpha 1-like Tpm Tongue, coverage 73.5%	13-30	LDKENAIDRAEQAETDKK
	38-70	QLEDELLGLNKKLKGTEDELDKYSEALKDAQEK
	77-125	KATDAEGDVAALNRRIQLVEEELDRAQERLATALQKLEE AEKAADESER
	134-149	ASKDEEKMEIQEMQLK
	153-178	HIAEEADRKKYEEVARKLVILEGELER
	190-227	CGDLEEELKNVTNNLKSLEAQSVKYSEKEDKYEDEIK
	252-264	TIDDLEDELYSQK
	268-284	AISEELDHALTDMTAI
Tpm2 (beta Tongue,) coverage 65%	22-49	AEQAEGDKKGAEDKCKQLE EELLALQKK
	52-118	GVEDELDKYSESLKDAQEKLEQAEKKATDAEAEVASLN RRIQLVEEELDRAQERLATALQKLEEAEK
	134-149	ASKDEEKMEIQEMQLK
	153-161	HIAEEADRK
	168-182	KLVILEGDLERSE ER

	190-205	SGDLEEELKNVTNNLK
	214-233	YSQKEDKYEEEIKVLTDKLK
	252-264	TIDDLEDEVYAQK
Tpm1 (alpha fast) Cheek (light), coverage 60.2%	1-6	MDAIKK
	22-49	AEGAEGDKKAAEDKSKQLEDDLVALQKK
	77-125	TATDAEADVASLNRRIQLVEEELDRAQERLATALTKLEE AEKAADESER
	134-149	ASKDEEKMELQDIQLK
	153-182	HIAEEADRKYEEVARKLVIIESDLERTE ER
	248-284	KLE KTIDDLEDELYAQKLKYKAISEELDNALNDMTSI
Alpha 1-like Tpm Cheek (dark), coverage 67.5%	13-30	LDKENAIDRAEQAETDKK
	38-70	QLE DELLGLNKKLKGTEDELDKYSEALKDAQEK
	77-101	KATDAEGDVAALNRRIQLVEEELDR
	134-149	ASKDEEKMEIQEMQLK
	153-178	HIAEEADRKYEEVARKLVILEGELER
	190-277	CGDLEEELKNVTNNLKSLEAQSVKYSEKEDKYEDEIKVL SDKLKEAETRAEFAERSVAKLEKTIDDLEDELYSQKLKY KAISEELDHA
	245-264	VAKLEKTIDDLEDELYSQK
	269-284	AISEELDHALTDMTAI

2.3.4 Protein isolation

Figure 2.5A shows the Q Sepharose elution profile of salmon tongue tropomyosins. Protein peaks were identified by measuring absorbance at 280 nm and conductivity. Fractions identified as tropomyosin are highlighted in the boxed section of the elution profile. SDS-PAGE analysis reveals that the two isoforms (beta and alpha-1 chain-like isoform X1) elute in a single peak with conductivity centered at ~ 28 mS/cm. The tropomyosin-containing fractions were then passed over hydroxyapatite for further enrichment (Figure 2.5B). Following SDS-PAGE confirmation, fractions (Figure 2.5B boxed area in elution profile and gel inset box) are dialyzed, freeze-dried, and stored in a refrigerator. A yield of ~ 10 mg of tropomyosin is obtained from 100 g of tongue muscle.

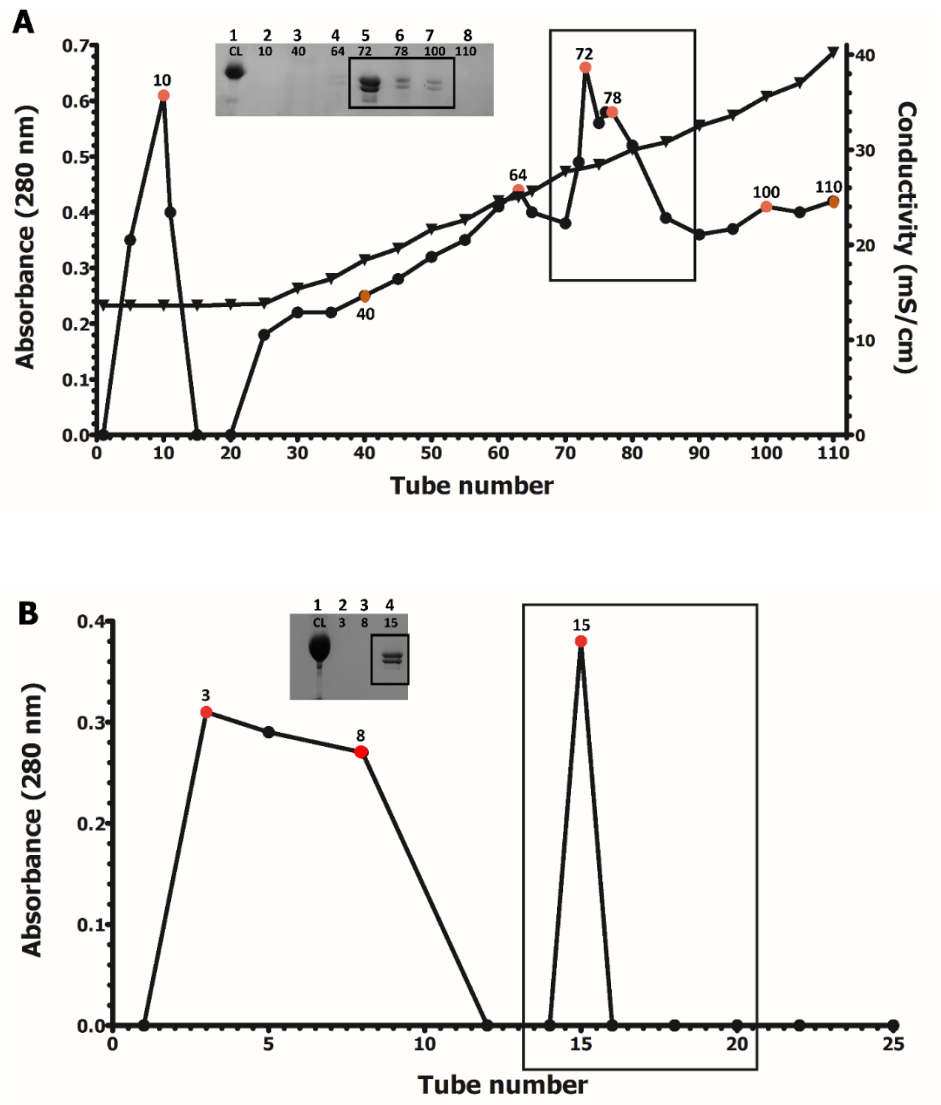

Figure 2.5. Chromatography of Atlantic salmon tongue tropomyosin. (A) Q Sepharose Fast Flow chromatography of extract of tongue acetone powder (column, 0.45 x 15 cm, volume, ~16 mL). Freshly prepared start buffer, contained 30 mM tris(hydroxymethyl)aminomethane (Tris), 50 mM NaCl, and 1 mM DTT, pH 8.0, (linear salt gradient, 0.05 - 0.5 M NaCl, volume 800 mL). Tropomyosin elution is centered at conductivity ~ 28 mS. Inset, SDS-PAGE with fraction number indicated. Lane 1 - column load (CL). Tropomyosin-containing fractions are indicated by boxes. (B) Hydroxyapatite chromatography of salmon tropomyosin fractions pooled from Q Sepharose. (Column, 0.45 x 15 cm, volume, ~ 16 mL). Tropomyosins are isocratically eluted with 60 (start) and 200 (end) mM phosphate pH 7.0 in the presence of 1 M NaCl and 1 mM DTT at room temperature, Inset, SDS-PAGE with fraction number indicated. Lane 1 - CL from Q column. Tropomyosin-containing fractions are indicated by boxes.

2.3.5 Troponin affinity chromatography of tongue tropomyosin

According to previous studies, troponin-T has been shown to bind to two sites on tropomyosin (Ohtsuki, 1979; Mak & Smillie, 1981; Pearlstone & Smillie, 1982; Tanokura et al., 1983; Morris & Lehrer, 1984; Brisson et al., 1986; White et al., 1987; Heeley et al., 1989; Goonasekara & Heeley, 2009). The elongated N-terminal portion of troponin T, TnT1, which consists of the first 160 amino acids, binds to sequences on either side of the overlap region of tropomyosin (binding site 1) (Figure 1.2). The C-terminal one third, TnT2, binds to the central region close to Cys-190 (binding site 2) (Figure 1.2). Therefore, this lays the path to investigate the functional effect of the sequence heterogeneity of the two isoforms that are present in tongue muscle (Figures 2.2A and 2.2B lanes 5 and Figure 2.3 h) on troponin binding (using affinity chromatography).

The affinity experiment carried out at 5 ^{o}C revealed the appearance of two peaks (Figure 2.6 A). Protein identities were confirmed with SDS-PAGE using tropomyosin standards. The conductivities of the highest (A_{595}) fraction are: ~ 8 mS/cm (Tpm2) compared to 14 mS/cm (alpha-1 chain-like isoform X1) (Figure 2.6A), which is equivalent to ten fractions in the NaCl gradient. Electrophoretic analysis (Figure 2.6B) shows that Tpm2 (e.g., Figure 2.6B lane 2), which corresponds to the upper band, is more prominent in the first peak (Figure 2.6B lane 2) indicating a weaker affinity for the column. In contrast, the later fractions contain comparatively more of the other isoform (in tongue) namely alpha-1 chain-like isoform X1, which corresponds to the lower band (Figure 2.6B lane 7). The observations can be explained by the presence of homodimers (i.e., ββ)) in tongue whose elution profiles overlap. While only partial separation of these species is achieved, the

results are consistent with alpha-1 chain-like isoform X1 binding more tightly to troponin-Sepharose than Tpm2.

The two forms of tropomyosin in the Atlantic salmon tongue muscle (Table 2.1) share 32 amino acid differences. Non-conservative substitutions (changes in charge underlined) are: Gly (in Tpm2) 27 Thr (in alpha-1 chain-like isoform X1); Gly31Ser; Ala45Gly; Val53Thr; Ser63Ala; Glu72Val; Gln73Leu; Ala74Ser; Ala83Gly; Ser87Ala; Ser179Ala; Ala186Ser; Ser190Cys; Ala211Ser; Glu212Val; Gln216Glu; Ala262Ser; Gly267Tyr; Leu276His; Asn279Thr and Thr283Ala.

Thus, is it apparent that the heterogeneity of the isoforms falls in both of the troponin-T binding sites on tropomyosin. Currently, it is not possible to weigh the relative effects of the various amino acid replacements, although changes in charge are expected to be more influential than others. Further, a given substitution may influence the interaction between the two proteins directly or indirectly, i.e., by causing a long-range change in the conformation of tropomyosin (Edwards and Sykes, 1980; Graceffa & Lehrer, 1980; Edwards & Sykes, 1981; Ly & Lehrer, 2012; Mamidi et al., 2013).

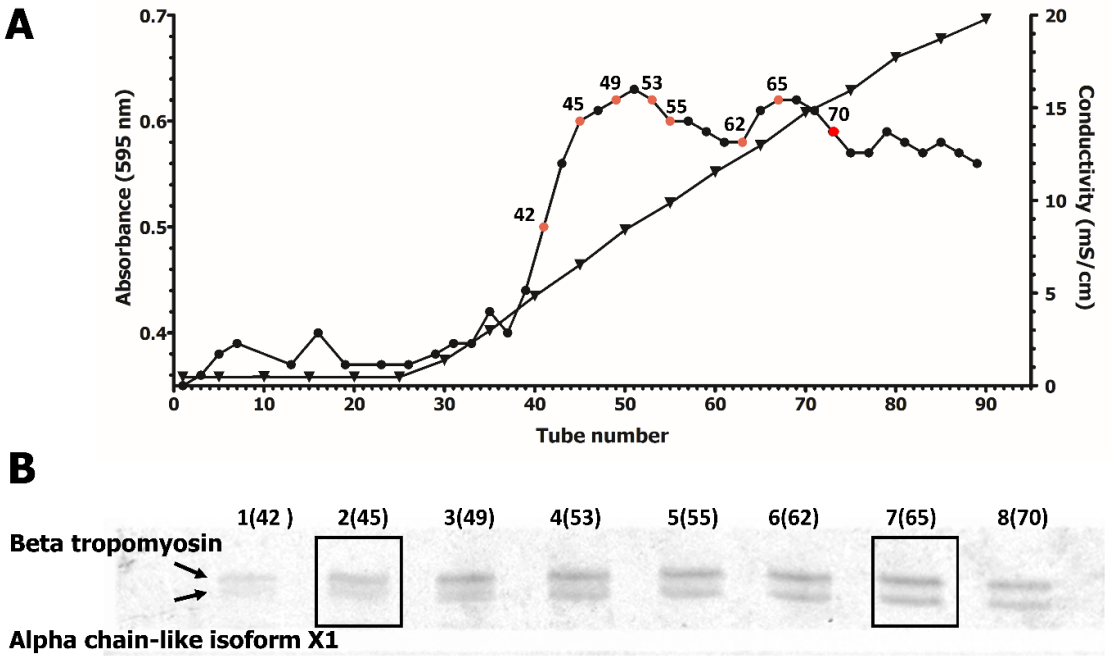

Figure 2.6. Comparison of binding of tongue tropomyosins to troponin-Sepharose 4B. (A) Chromatographic profile of tongue tropomyosin isoform elution. The column packed with rabbit skeletal troponin-Sepharose 4B was equilibrated in a low ionic strength buffer containing 1 mM EGTA. After loading, no tropomyosin is detected in the flow-through. Protein detection is by Bradford reagent. The slope of the NaCl gradient expressed as the conductivity at room temperature is 0.31 mS/cm per fraction. Isoform elution starts at the 37th fraction (Peak 1 highest A_{595} at conductivity, 8 mS/cm. Peak 2 highest A_{595} at conductivity, 14 mS/cm). Based on the peak absorbances, the displacement in elution is 6 mS/cm which is equivalent to 10 fractions or 18 mL (B) SDS-PAGE analyzed fractions of the elution profile are highlighted in red. There is good agreement between the fraction that yielded the thickest gel band after staining with Coomassie and the results of the Bradford assay. Lanes 1 - 3 (fractions 42, 45, and 49), earlier eluting fractions. Lanes 4 - 7 (fractions 53, 55, and 62), later eluting fractions. The highlighted lanes, 2 (fraction 45) and 7 (fraction 65) contain unequal (as per densitometry) proportions of the two isoforms, indicating dissimilar affinities.

2.3.6 Phylogenetic tree

A tree diagram of vertebrate striated muscle tropomyosins is presented in Figure 2.7. The most closely related group pairings are TPM1 and 3 on the one hand and TPM2 and 4 on the other as per Toramoto et al., 2004. In regard to Atlantic salmon, the diagram shows that Tpm3 (I) and (II) emerged post-speciation i.e., following genome enlargement. Surprisingly, the alpha 1 chain-like isoform X1 (XP_013996655), which exists in some head muscles (e.g., Figures 2.1, 2.3e, and 2.3i) groups with the TPM4 clade and not TPM1 as anticipated based on its designation as an alpha type-1 isoform. While this is a moot point, a Tpm4 transcript (nucleic acid) is expressed in pufferfish skeletal muscle (Toramoto et al., 2004).

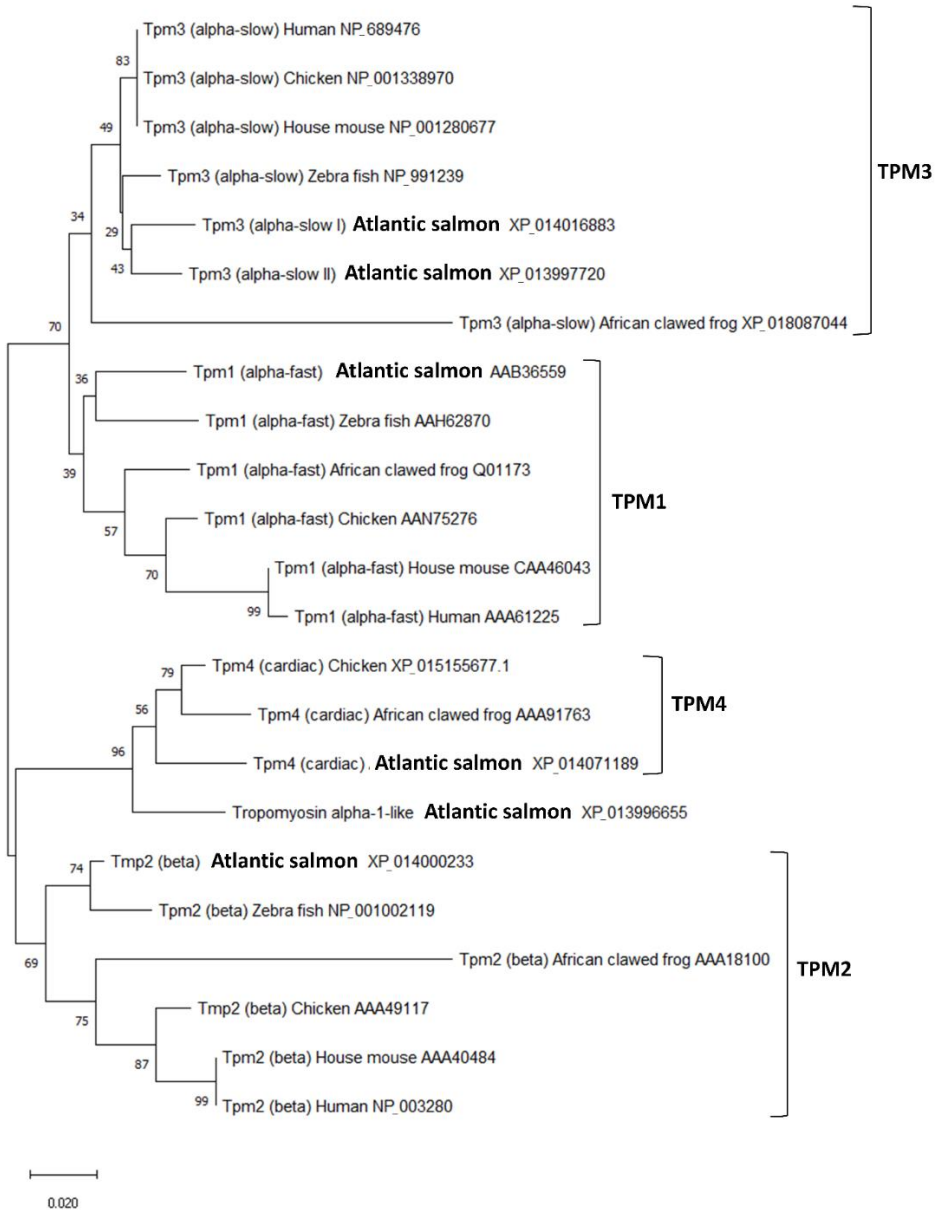

Figure 2.7. Phylogenetic analysis of vertebrate striated muscle tropomyosins. The tree was generated using a neighbor-joining algorithm (Saitou & Nei, 1987), and the amino acid sequences encoded in exons 3, 4, 5, 6b, 7, and 8. Tropomyosins that are present in the striated muscle of Atlantic salmon are highlighted in larger font (bold type). Accession numbers and TPM genes are indicated in the figure. Bootstrap percentages from 1000 repeats appear at the nodes. Reprinted from Silva et al., 2020c.

2.4 Chapter 2 Discussion

The existence of beta tropomyosin (Tpm2) is demonstrated at the protein level for the first time in a fish species. It is identified in the skeletal muscles of the tongue, jaw, and pectoral fin, as well as in the slow muscle in the trunk (Silva et al., 2020c) where it contributes to half of the total tropomyosin, collectively making it the second-most abundant isoform of tropomyosin after Tpm1. Surprisingly, Tpm2 is absent in the fast trunk muscle, the main muscle of the salmon.

Salmon Tpm2 contains 29 and 30 amino acid differences when compared to the homologs in chicken and rodent, respectively. Unique features of the salmonid beta isoform are a reduced number of cysteine (one vs. two) and tyrosine (five vs. six) residues (Figure 2.4). Additionally, there are differences in the C-terminal portion of the tropomyosin overlap region, specifically at residues 276, His (salmon) vs. Asn (rodent); residue-281, Met vs. Ile and residue-283, Thr vs. Ser. Thirty two amino acid differences exist between salmon Tpm2 (beta) and Tpm1 (alpha-fast), which is similar in scale to the mammalian homologs (Mak et al., 1980) which were the first isoforms of tropomyosin to be discovered (Cummins & Perry, 1973). Although Ser-283 is a site of phosphorylation in many vertebrate tropomyosins (Mak et al., 1978; Heeley, 2013), to date Ser-283 phosphorylation has not been detected in Salmonidae (Heeley & Hong, 1994; Heeley et al, 1995) which is also confirmed by the results from this chapter. A comparison of salmon Tpm2 with homologs in pufferfish and zebrafish, which are yet to be studied at the protein level, shows fewer than 10 substitutions.

Half of the 32 substitutions shared between Tpm1 and Tpm2 are located in the parts of tropomyosin that are implicated in troponin binding (Ohtsuki, 1979; Mak & Smillie, 1981; Pearlstone & Smillie, 1982; Flicker et al., 1982; Tanokura et al., 1983; Morris & Lehrer, 1984; Brisson et al., 1986; White et al., 1987; Heeley et al., 1987; Hammell & Hitchcock-DeGregori, 1996; Goonasekara & Heeley, 2009; Jin & Chong, 2010; Mamidi et al., 2013; Amarasinghe & Jin, 2015; Pavadai et al., 2020). Within this region, residues 54 - 72 (exon 2b), 85 - 110 (exon 3), 112 - 142 (exons 3 and 4), 147 - 171 (exon 5), and 200 - 259 (exons 7 and 8) are conserved and the majority of substitutions are found localized (Figure 2.4). A cluster of six differences is situated between residues 185 -192, a known site of troponin attachment. Additionally, the C-terminal residues 260 - 284 and N-terminal residues 19 - 52 (Figure 2.4) of each molecule, have a cluster of differences that has implications for end-to-end connectivity as well as for troponin-T binding. It is surprising that Atlantic salmon Tpm1 (alpha-fast) and Tpm2 (beta) exhibit the opposite of the mobility-isotype relationship that was originally reported by Cummins & Perry, 1973 for rabbit isoforms. The reason appears to largely due to the only charge substitution, Lys-77 in Tpm2 (faster migration) and Thr-77 in Tpm1 (slower migration), as illustrated by the behavior of a Lys-77-containing Tpm1 mutant (Chapter 3, Figure 2.2) and is a sharp reminder of the influence of charged groups on the complexation of tropomyosin with anionic detergent (Mak et al., 1980; Lau et al., 1985; Sanders & Smillie, 1985).

Considering the Tpm2 and alpha-1 chain-like isoform X1 (XP_013996655), there are thirty-two substitutions (Figure 2.4 legend), Moreover, there are consecutive replacements at residues 72 -74, including Val-72 to Glu (in Tpm2) and two additional charge changes

in the middle of the molecule, Val-212 to Glu (Tpm2) and Glu-216 to Gln (Tpm2). Further, there are alterations in side chain size (Gly-267 in Tpm2 vs. Tyr) and group charge (Leu-276 in Tpm2 vs. His).

What is the importance of the heterogeneity among isoforms? It is reasonable to hypothesize that the non-identity of the sequence is a functional adaptation to a physiological niche.

Considering the issue of cold-adaptation and chain flexibility, Gly is known to play an important role as an entropic determinant in enzymes that function at low temperature (Matthews et al., 1987; Deniz, 2018; Saavedra et al., 2018). A unique feature of a number of salmon tropomyosins is the presence of closely spaced pairs of Gly between residues 20 - 90 (Figure 2.4 arrows). Specifically, Gly-24 and Gly-27 in Tpm1 (alpha fast); Gly-27 and 31 in Tpm2 (beta); Gly-45 and Gly-52 in alpha-1 chain-like isoform X1 and Gly-83 and Gly-87 in Tpm4 (cardiac) found in major isoforms. Considering the troponin affinity results of Tpm2 and alpa-1 chain-like isoform X1, it is the Tpm2 isoform that has a comparatively lower affinity for troponin (Figure 2.6B).

As Gly-27 and Gly-31 of Tpm2 fall within a major destabilizing cluster Lys15-Ala18-Ala22-Ala25-Lys29-Ala32-Ser36, as opposed to Gly-45 and Gly-52 of alpha-1 chain-like isoform X1 isoform it is possible that this could have an effect on reducing the affinity for Troponin. As discussed in chapter 3 the double replacement of Gly-24 and Gly-27 in Tpm1 with alanine increases troponin affinity. Further, there is also an increase in both heat stability and resistance to proteolytic scission at the 6th and 11th peptide bonds (Fudge & Heeley, 2015; Silva et al., 2020b). These findings are in accordance with the psychrophilic

nature of the salmonid fishes. For example, how the muscle overcomes cold-induced rigidity. Within the thin filament, tropomyosin winds around actin and changes its physical position during contraction and relaxation. With all of these points in mind, it can be proposed that closely spaced glycines are a strategy to deal with a low temperature habitat that would otherwise hinder the function of the thin filament.

In summary, this chapter demonstrates the existence of fish Tpm2 and alpha-1 chain-like isoform X1 tropomyosins at the protein level. There are interesting changes in the molecule, including the sites of troponin attachment. The study also underlines the critical placement of glycine in achieving cold-adaptation in a dynamic coiled-coil of salmon tropomyosin allowing it to inhabit the polar niche in the ocean.

2.5 Chapter 2 Future directions

The recent completion of the Atlantic cod (*Gadus gadus*) genome has opened the door to perform a search for Tpm2 (protein) in a second fish species. Annotation of the genome predicts the existence of a Tpm2 (accession, XP_030210170.1). In a preliminary set of experiments, we surveyed the muscles from cheek red and white regions, tongue, jaw red and white regions, and tail using 2-D electrophoresis. The pattern of isoforms is different to that found in Atlantic salmon. The next step will be to analyze the protein spots as was done for salmon in this chapter. This approach is expected to establish whether Tpm2 exists at the protein level in Atlantic cod and map its anatomical distribution. Following that it will be of interest to conduct to phylogenetic and biochemical comparisons.

2.6 Chapter 2 References

Amarasinghe, C., & Jin, J.P. (2015). N-Terminal Hypervariable Region of Muscle Type Isoforms of Troponin T Differentially Modulates the Affinity of Tropomyosin-Binding Site 1. *Biochemistry*, *54*(24), 3822–3830. https://doi.org/10.1021/acs.biochem.5b00348

Bone, Q., Marshall, N. B., & Blaxter, J. H. S. (1995). *Biology of Fishes* (2nd ed.). Chapman & HaU in 1995. https://doi.org/10.1007/978-1-4615-2664-3

Bradford, M. M. (1976). A rapid and sensitive method for the quantitation of microgram quantities of protein utilizing the principle of protein-dye binding. *Analytical Biochemistry*, *72*(1), 248–254. https://doi.org/https://doi.org/10.1016/0003-2697(76)90527-3

Brisson, J. R., Golosinska, K., Smillie, L. B., & Sykes, B. D. (1986). Interaction of tropomyosin and troponin T: a proton nuclear magnetic resonance study. *Biochemistry*, *25*(16), 4548–4555. https://doi.org/10.1021/bi00364a014

Cummins, P., & Perry, S. V. (1973). The subunits and biological activity of polymorphic forms of tropomyosin. *Biochemical Journal*, *133*(4), 765–777. https://doi.org/10.1042/bj1330765

Cummins, P., & Perry, S. V. (1974). Chemical and immunochemical characteristics of tropomyosins from striated and smooth muscle. *The Biochemical Journal*, *141*(1), 43–49. https://doi.org/10.1042/bj1410043

Deniz, A. A. (2018). Remote wiggling helps cold enzymes work seas affect each other. *Nature*, *558*(2016), 195–196.

Dube, D. K., Dube, S., Abbott, L., Wang, J., Fan, Y., Alshiekh-Nasany, R., Shah, K. K., Rudloff, A. P., Poiesz, B. J., Sanger, J. M., & Sanger, J. W. (2017). Identification, characterization, and expression of sarcomeric tropomyosin isoforms in zebrafish. *Cytoskeleton (Hoboken, N.J.)*, *74*(3), 125–142. https://doi.org/10.1002/cm.21352

Edwards, B. F. P., & Sykes, B. D. (1980). Nuclear magnetic resonance evidence for the coexistence of several conformational states of rabbit cardiac and skeletal tropomyosins. *Biochemistry*, *19*, 2577 – 2583.

Edwards, B. F. P., & Sykes, B. D. (1981). Analysis of Cooperativity Observed in pH Titrations of Proton Nuclear Magnetic Resonances of Histidine Residues of Rabbit Cardiac Tropomyosin. *Biochemistry*, *20*(14), 4193–4198. https://doi.org/10.1021/bi00517a037

Felsenstein, J. (1985). Confidence Limits on Phylogenies: An Approach Using The Bootstrap. *Evolution; International Journal of Organic Evolution*, *39*(4), 783–791. https://doi.org/10.1111/j.1558-5646.1985.tb00420.x

Flicker, P. F., Phillips, G. N., & Cohen, C. (1982). Troponin and its interactions with tropomyosin: An electron microscope study. *Journal of Molecular Biology*, *162*(2), 495–501. https://doi.org/https://doi.org/10.1016/0022-2836(82)90540-X

Fudge, K. R., & Heeley, D. H. (2015). Biochemical characterization of the roles of glycines 24 and 27 and threonine 179 in tropomyosin from the fast skeletal trunk

muscle of the Atlantic salmon. *Biochemistry*, *54*(17), 2769–2776. https://doi.org/10.1021/acs.biochem.5b00156

Geeves, M. A., Hitchcock-DeGregori, S. E., & Gunning, P. W. (2015). A systematic nomenclature for mammalian tropomyosin isoforms. *Journal of Muscle Research and Cell Motility*, *36*(2), 147–153. https://doi.org/10.1007/s10974-014-9389-6

Goonasekara, C. L., & Heeley, D. H. (2008). Conformational properties of striated muscle tropomyosins from some salmonid fishes. *Journal of Muscle Research and Cell Motility*, *29*(2–5), 135–143. https://doi.org/10.1007/s10974-008-9148-7

Goonasekara, C. L., & Heeley, D. H. (2009). Effect of Removing the Amino-Terminal Hexapeptide of Tropomyosin on the Properties of the Thin Filament. *Biochemistry*, *48*(15), 3538–3544. https://doi.org/10.1021/bi802004j

Graceffa, P., & Lehrer, S. S. (1980). The excimer fluorescence of pyrene-labeled tropomyosin. A probe of conformational dynamics. *The Journal of Biological Chemistry*, *255*(23), 11296–11300. https://doi.org/https://doi.org/10.1016/S0021-9258(19)70290-7

Hammell, R. L., & Hitchcock-DeGregori, S. E. (1996). Mapping the functional domains within the carboxyl terminus of alpha-tropomyosin encoded by the alternatively spliced ninth exon. *The Journal of Biological Chemistry*, *271*(8), 4236–4242. https://doi.org/10.1074/jbc.271.8.4236

Heeley, D.H., Bieger, T., Waddleton, D.M., Hong, C., Jackman, D.M., McGowan, C., Davidson, W.S. and Beavis, R. C. (1995). Characterisation of fast, slow and cardiac

muscle tropomyosin from salmonid fish. *European Journal of Biochemistry, 232*, 226 – 234.

Heeley, D.H., Golosinska, K., Smillie, L. B. (1987). The effects of troponin-T fragments T1 and T2 on the binding of non-polymerisable tropomyosin to F-actin in the presence and absence of troponins - I and -C. *The Journal of Biological Chemistry, 262*, 9971 –9978.

Heeley, D. H., Watson, M. H., Mak, A. S., Dubord, P., & Smillie, L. B. (1989). Effect of phosphorylation on the interaction and functional properties of rabbit striated muscle αα-tropomyosin. *The Journal of Biological Chemistry*, *264*(5), 2424–2430. https://doi.org/10.1016/S0021-9258(19)81630-7

Heeley, D H, & Hong, C. (1994). Isolation and characterization of tropomyosin from fish muscle. *Comparative Biochemistry and Physiology. Biochemistry and Molecular Biology*, *108*(1), 95–106. https://doi.org/10.1016/0305-0491(94)90169-4

Heeley, D H, Smillie, L. B., & Lohmeier-Vogel, E. M. (1989). Effects of deletion of tropomyosin overlap on regulated actomyosin subfragment 1 ATPase. *The Biochemical Journal*, *258*(3), 831—836. https://doi.org/10.1042/bj2580831

Heeley, D. H. (2013). Phosphorylation of tropomyosin in striated muscle. *Journal of Muscle Research and Cell Motility*, *34*(3), 233–237. https://doi.org/10.1007/s10974-013-9351-z

Heeley, D. H., & Lohmeier-Vogel, E. M. (2016). Biochemical Comparison of Rabbit Skeletal Muscle Alpha and Beta Tropomyosin Isoforms. *Biophysical Journal*,

110(3), 276a. https://doi.org/10.1016/j.bpj.2015.11.1497

Helfman, D. M., Cheley, S., Kuismanen, E., Finn, L. A., & Yamawaki-Kataoka, Y. (1986). Nonmuscle and muscle tropomyosin isoforms are expressed from a single gene by alternative RNA splicing and polyadenylation. *Molecular and Cellular Biology*, *6*(11), 3582–3595. https://doi.org/10.1128/mcb.6.11.3582

Ikeda, D., Toramoto, T., Ochiai, Y., Suetake, H., Suzuki, Y., Minoshima, S., Shimizu, N., & Watabe, S. (2003). Identification of novel tropomyosin 1 genes of pufferfish (Fugu rubripes) on genomic sequences and tissue distribution of their transcripts. *Molecular Biology Reports*, *30*(2), 83–90. https://doi.org/10.1023/A:1023995208279

Jackman, D. M., Waddleton, D. M., Younghusband, B., & Heeley, D. H. (1996). Further characterisation of fast, slow and cardiac muscle tropomyosins from salmonid fish. *European Journal of Biochemistry*, *242*(2), 363–371. https://doi.org/10.1111/j.1432-1033.1996.0363r.x

Jin, J. P., & Chong, S. M. (2010). Localization of the two tropomyosin-binding sites of troponin T. *Archives of Biochemistry and Biophysics*, *500*(2), 144–150. https://doi.org/10.1016/j.abb.2010.06.001

Kumar, S., Stecher, G., Li, M., Knyaz, C., & Tamura, K. (2018). MEGA X: Molecular Evolutionary Genetics Analysis across Computing Platforms. *Molecular Biology and Evolution*, *35*(6), 1547–1549. https://doi.org/10.1093/molbev/msy096

Laemmli, U. K. (1970). 227680a0. *Nature*, *227*, 680–685.

Lau, S. Y., Sanders, C., & Smillie, L. B. (1985). Amino acid sequence of chicken gizzard

gamma-tropomyosin. *The Journal of Biological Chemistry*, *260*(12), 7257–7263.

Lees-Miller, J. P., & Helfman, D. M. (1991). The molecular basis for tropomyosin isoform diversity. *BioEssays : News and Reviews in Molecular, Cellular and Developmental Biology*, *13*(9), 429–437. https://doi.org/10.1002/bies.950130902

Libri, D., Lemonnier, M., Meinnel, T., & Fiszman, M. Y. (1989). A single gene codes for the beta subunits of smooth and skeletal muscle tropomyosin in the chicken. *The Journal of Biological Chemistry*, *264*(5), 2935–2944.

Lien, S., Koop, B. F., Sandve, S. R., Miller, J. R., Kent, M. P., Nome, T., Hvidsten, T. R., Leong, J. S., Minkley, D. R., Zimin, A., Grammes, F., Grove, H., Gjuvsland, A., Walenz, B., Hermansen, R. A., von Schalburg, K., Rondeau, E. B., Di Genova, A., Samy, J. K. A., … Davidson, W. S. (2016). The Atlantic salmon genome provides insights into rediploidization. *Nature*, *533*(7602), 200–205. https://doi.org/10.1038/nature17164

Ly, S., & Lehrer, S. S. (2012). Long-range effects of familial hypertrophic cardiomyopathy mutations E180G and D175N on the properties of tropomyosin. *Biochemistry*, *51*(32), 6413–6420. https://doi.org/10.1021/bi3006835

MacLeod, A. R. (1982). Distinct alpha-tropomyosin mRNA sequences in chicken skeletal muscle. *European Journal of Biochemistry*, *126*(2), 293–297. https://doi.org/10.1111/j.1432-1033.1982.tb06778.x

Mak, A. S., Smillie, L. B., & Bárány, M. (1978). Specific phosphorylation at serine-283 of alpha tropomyosin from frog skeletal and rabbit skeletal and cardiac muscle.

Proceedings of the National Academy of Sciences of the United States of America, *75*(8), 3588–3592. https://doi.org/10.1073/pnas.75.8.3588

Mak, A. S, Smillie, L. B., & Stewart, G. R. (1980). A comparison of the amino acid sequences of rabbit skeletal muscle alpha- and beta-tropomyosins. *The Journal of Biological Chemistry*, *255*(8), 3647–3655. https://doi.org/https://doi.org/10.1016/S0021-9258(19)85753-8

Mak, A. S., & Smillie, L. B. (1981). Structural interpretation of the two-site binding of troponin on the muscle thin filament. *Journal of Molecular Biology*, *149*(3), 541–550. https://doi.org/https://doi.org/10.1016/0022-2836(81)90486-1

Mamidi, R., Michael, J. J., Muthuchamy, M., & Chandra, M. (2013). Interplay between the overlapping ends of tropomyosin and the N terminus of cardiac troponin T affects tropomyosin states on actin. *FASEB Journal*, *27*(9), 3848–3859. https://doi.org/10.1096/fj.13-232363

Matthews, B. W., Nicholson, H., & Becktel, W. J. (1987). Enhanced protein thermostability from site-directed mutations that decrease the entropy of unfolding. *Proceedings of the National Academy of Sciences of the United States of America*, *84*(19), 6663–6667. https://doi.org/10.1073/pnas.84.19.6663

Morris, E. P., & Lehrer, S. S. (1984). Troponin-Tropomyosin Interactions. Fluorescence Studies of the Binding of Troponin, Troponin T, and Chymotryptic Troponin T Fragments to Specifically Labeled Tropomyosin. *Biochemistry*, *23*(10), 2214–2220. https://doi.org/10.1021/bi00305a018

O'Farrell, P. H. (1975). High Resolution of Proteins * Electrophoresis. *The Journal of Biological Chemistry*, *250*(10), 4007–4021. http://www.jbc.org/content/250/10/4007.short

Ohtsuki, I. (1979). Molecular arrangement of troponin-T in the thin filament. *Journal of Biochemistry*, *86*(2), 491–497. https://doi.org/10.1093/oxfordjournals.jbchem.a132549

Pavadai, E., Rynkiewicz, M. J., Ghosh, A., & Lehman, W. (2020). Docking Troponin T onto the Tropomyosin Overlapping Domain of Thin Filaments. *Biophysical Journal*, *118*(2), 325–336. https://doi.org/10.1016/j.bpj.2019.11.3393

Pearlstone, J. R., & Smillie, L. B. (1982). Binding of troponin-T fragments to several types of tropomyosin. Sensitivity to Ca^{2+} in the presence of troponin-C. *The Journal of Biological Chemistry*, *257*(18), 10587–10592. https://doi.org/10.1016/s0021-9258(18)33862-6

Perry, S. V. (2001). Vertebrate tropomyosin: distribution, properties and function. *Journal of Muscle Research & Cell Motility*, *22*(1), 5–49. https://doi.org/10.1023/A:1010303732441

Potter, J. D. (1982). Preparation of troponin and its subunits. *Methods in Enzymology*, *85 Pt B*, 241–263. https://doi.org/10.1016/0076-6879(82)85024-6

Ruiz-Opazo, N., & Nadal-Ginard, B. (1987). Alpha-tropomyosin gene organization. Alternative splicing of duplicated isotype-specific exons accounts for the production of smooth and striated muscle isoforms. *The Journal of Biological Chemistry*,

262(10), 4755–4765.

Saavedra, H. G., Wrabl, J. O., Anderson, J. A., Li, J., & Hilser, V. J. (2018). Dynamic allostery can drive cold adaptation in enzymes. *Nature*, *558*(7709), 324–328. https://doi.org/10.1038/s41586-018-0183-2

Saitou, N., & Nei, M. (1987). The neighbor-joining method: a new method for reconstructing phylogenetic trees. *Molecular Biology and Evolution*, *4*(4), 406–425. https://doi.org/10.1093/oxfordjournals.molbev.a040454

Sanders, C., & Smillie, L. B. (1985). Amino acid sequence of chicken gizzard beta-tropomyosin. Comparison of the chicken gizzard, rabbit skeletal, and equine platelet tropomyosins. *The Journal of Biological Chemistry*, *260*(12), 7264–7275. https://doi.org/https://doi.org/10.1016/S0021-9258(17)39602-3

Schevzov, G., Whittaker, S. P., Fath, T., Lin, J. J., & Gunning, P. W. (2011). Tropomyosin isoforms and reagents. *Bioarchitecture*, *1*(4), 135–164. https://doi.org/10.4161/bioa.1.4.17897

Silva, A. M. M., Ige, T., Goonasekara, C. L., & Heeley, D. H. (2020b). Threonine-77 Is a Determinant of the Low-Temperature Conditioning of the Most Abundant Isoform of Tropomyosin in Atlantic Salmon. *Biochemistry*, *59*(31), 2859–2869. https://doi.org/10.1021/acs.biochem.0c00416

Silva, A. M. M., Kennedy, L. S., Hasan, S. C., Cohen, A. M., & Heeley, D. H. (2020c). Demonstration of beta-tropomyosin (Tpm2) and duplication of the alpha-slow tropomyosin gene (TPM3) in Atlantic salmon (*Salmo salar*). *Comparative*

Biochemistry and Physiology Part - B: Biochemistry and Molecular Biology, *245*(January), 110439. https://doi.org/10.1016/j.cbpb.2020.110439

Smillie, L. B. (1982). Preparation and identification of alpha- and beta-tropomyosins. *Methods in Enzymology*, *85 Pt B*, 234–241. https://doi.org/10.1016/0076-6879(82)85023-4

Stone, D., & Smillie, L. B. (1978). The amino acid sequence of rabbit skeletal α-tropomyosin. The NH2-terminal half and complete sequence. *The Journal of Biological Chemistry*, *253*(4), 1137–1148. https://doi.org/10.1016/s0021-9258(17)38122-x

Tanokura, M., Tawada, Y., Ono, A., & Ohtsuki, I. (1983). Chymotryptic subfragments of troponin t from rabbit skeletal muscle. interaction with tropomyosin, troponin I and troponin C1. *Journal of Biochemistry*, *93*(2), 331–337. https://doi.org/10.1093/oxfordjournals.jbchem.a134185

Toramoto, T., Ikeda, D., Ochiai, Y., Minoshima, S., Shimizu, N., & Watabe, S. (2004). Multiple gene organization of pufferfish *Fugu rubripes* tropomyosin isoforms and tissue distribution of their transcripts. *Gene*, *331*, 41–51. https://doi.org/10.1016/j.gene.2004.01.013

White, S. P., Cohen, C., & Phillips, G. N. J. (1987). Structure of co-crystals of tropomyosin and troponin. *Nature*, *325*(6107), 826–828. https://doi.org/10.1038/325826a0

Zuckerkandl, E., & Pauling, L. (1965). Evolutionary divergence and convergence in

proteins. In: Bryson, V. and Vogel, H.J., Eds.,. *Evolving Genes and Proteins, Academic Press, New York*, 97–166.

Chapter 3. Threonine-77 is a determinant of the low-temperature conditioning of the most abundant isoform of tropomyosin in Atlantic salmon.

Abstract

The fast skeletal muscle of Atlantic salmon contains a single isoform Tpm1 (arising from TPM 1 gene family) that is >92% identical (20 substitutions) to the more conformationally stable mammalian homolog (rabbit). The basis of the relative instability of salmon tropomyosin is investigated by mutagenically reversing the only charge substitution, residue 77 (Thr in salmon; Lys in rabbit), which falls within a known destabilizing Ala cluster. Isolated recombinant whole protein and CNBr fragments of mutant-77 thereof are analyzed by electrophoresis, proteolytic digestion, Edman-sequencing, calorimetry, troponin affinity, F-actin binding, and PyMOL. The mutation (Thr-77 to Lys): i) produces an electrophoretic shift in the presence of either SDS or urea; ii) affects the two unfolding transitions are observed in calorimetry (0.1 M KCl, 1 mM dithiothreitol; pH 7.0), the mid-points (Tms) of which are ~5 ^{o}C higher for the mutant-77, 35 (minor) and 44 ^{o}C (major), vs. the recombinant control. Unfolding of fragment CNBr (CN1A, residues 11 - 127) is monophasic, Tms 53 (mutant-77) vs. 40 ^{o}C (recombinant control); iii) generates a marked resistance to chymotrypsin digestion (0.1M NaCl, pH 8.5; Temp 10 - 30 ^{o}C) in mutant-77 at peptide bonds 11 and 169. The main chymotryptic site (peptide bond between residues 88 - 89) of mutant CN1A, is also less susceptible to digestion; iv) indicates salt-bridges between Lys-77 to Glu-75 and Glu-82 in the adjacent chain; v) decreases the affinity for troponin. Furthermore, wild type salmon Tmp1 displays a higher affinity for F-actin

(30mM KCl, 5mM $MgCl_2$, pH 7.5) at 4 ^oC (K_D,~0.1 µM) than at 30 ^oC (K_D, ~0.5 µM). The evidence presented in this section indicates: (i) Loss of an ionic interaction is a critical factor in destabilizing a stretch of 150 amino acids in the molecule, thereby increasing the flexibility of the coiled-coil structure, (ii) the absence of an acetyl group (known to disrupt tropomyosin's N-terminal region) dramatically weakens its affinity for troponin, however, affinity is regained by removing the helix-breaking glycines, and (iii) the existence of a troponin binding site at one end of tropomyosin having possible regulatory significance.

3.1 Introduction

As mentioned in Chapter 1, tropomyosin is a flexible coiled-coil (Stone & Smillie, 1978) regulatory protein found in the thin filament of muscle fibers (Pirani et al., 2005; Risi et al., 2017). It contains a repeating heptad of amino acids assigned alphabetically: a, b, c, d, e, f, and g. The "a" and "d" positions are occupied by non-polar side chains (Crick, 1953) that make an adhesive seam facilitating dimerization and forming the core of the molecule (Greenfield & Hitchcock-DeGregori, 1995). The "e" and "g" positions are occupied by charged residues that provide additional cohesion through electrostatic interactions (Parry, 1975) between the opposing helices. Additionally, a key feature in tropomyosin is the clusters of alanine residues that occupy core positions. The small size of the alanine R group grants more freedom for the chains to bend which enables tropomyosin to maintain contact with F-actin during muscle contraction and relaxation. These closely-grouped alanines also referred to as destabilizing clusters (Kwok & Hodges, 2004), occur at regular intervals throughout the entire molecule and correspond to the seven actin-binding periods.

Tropomyosin also contains a small number of amino acids that are atypical in terms of their location in the heptad. Examples include charged Lys-15(a), Lys-29(a), Asp-137(d), Glu-218(a) and polar Tyr-214(d), Tyr-222(d), Gln-263(d) and Tyr-267(a) side-chains in positions "a" and "d". Such irregularities are now recognized to be structurally and functionally beneficial in terms of flexibility. For example, Asp-137(d), which destabilizes the flanking structure as evidenced by an enhanced rate of trypsinolysis at Arg-133 (Pato et al., 1981; Sumida et al., 2008) and Glu-218(a) creates an opening between the two strands (Minakata et al., 2008). Both of these residues, Arg-133 and Glu-218, cater to the docking

of troponin to the mid-region of tropomyosin (White et al., 1987; Oda et al., 2020; Yamada et al., 2020). According to X-ray structures, the region consisting of residues Lys15-Ala18-Ala22-Ala25-Lys29-Ala32-Ser36 is identified as a major destabilizing cluster at the N-terminal part of the molecule (Brown et al., 2001) which previous (Mak & Smillie, 1981; Pato et al., 1981; Brisson et al., 1986; Heeley et al., 1987; Goonasekara & Heeley, 2009; Manning et al., 2011) and recent (Oda et al., 2020; Yamada et al., 2020) studies have shown to contain a binding site for the tail region of troponin-T.

Replacement of Ala-74, Ala-78, and Ala-81 from the 2nd and Ala-179, and Ala-183 from the 5th actin-binding periods with a larger non-polar side-chain has been shown to decrease F-actin affinity, by affecting chain stability (Singh & Hitchcock-DeGregori, 2003; Singh & Hitchcock-Degregori, 2006). Further, the complexation of a tropomyosin C-terminal peptide and troponin-T is inhibited by replacing Gln-263 with Leu (Greenfield et al., 2002).

The importance of instability in mesophilic (mammalian and avian) tropomyosins (Hitchcock-DeGregori & Singh, 2010) is emphasized in tropomyosins from psychrophiles (organisms that live < 15 ^{o}C) (Hayley et al., 2011; Fudge & Heeley, 2015). In this context, Atlantic salmon (*Salmo salar*) is a suitable model for the study of tropomyosin stability. The trunk muscle, which is the biggest contributor to the body mass of salmon (Bone et al., 1995), consists of a single isoform of tropomyosin, Tpm1 (alpha-fast, accession AAB36559) (Chapter 2 and Silva et al., 2020c). There are relatively few (~ 20) amino acid substitutions in salmon tropomyosin compared to the mesophilic counterparts (Heeley et al., 1995) (Table 3.1). All of the aforementioned non-canonical amino acids that occur in mammalian tropomyosin are conserved, as is the stability control region of tropomyosin

(residues 97 - 118) (Hodges et al., 2009; Kirwan & Hodges, 2010), with two exceptions: Thr-111 (salmon), Gln-111 (mammal) and Thr-179 (salmon), Ala-179 (mammal). Other interesting differences are a pair of glycines (Gly-24 and Gly-27) and two substitutions that affect charge at neutral pH, namely residue-77 (Thr in salmon, Lys in mammal and bird), which corresponds to a "g" heptad position (Stone & Smillie, 1978), and residue-276 (Asn in salmon, His in mammal and bird). Since the histidine in question is partially protonated at neutrality (Edwards & Sykes, 1981) only one substitution will alter the net charge by a full unit, specifically Thr77(g)Lys. Since the "e" positions in the next heptad units (of the same and opposite strands of the coiled-coil) are occupied by glutamates (Glu-75 and Glu-82), there is potential for a change in ionic interactions at this location. Also, as mentioned above residue-77 falls in an alanine cluster that is known to be important for thin filament formation. For example, the replacement of Ala-74(d), Ala-78(a), and Ala-81(d) with a bulkier group (leucine and valine) increases the melting temperature of mammalian tropomyosin and weakens its interaction with actin by at least two orders of magnitude (Singh & Hitchcock-DeGregori, 2003).

Table 3. 1. Comparison of residue positions in the most abundant isoform of vertebrate sarcomeric tropomyosin.

Organism	Res-77(g)	Res-80(c)	Res-82(e)	Total number of substitutions
Atlantic salmon (AAB36559)	Thr	Asp	Glu	-
Zebra fish (AAH62870)	Lys	Asp	Glu	19
Puffer fish (BAC10576)	Lys	Asp	Glu	18
African clawed frog (Q01173)	Lys	Asp	Glu	21
Chicken (AAN75276)	Lys	Asp	Glu	21
Rabbit (AAB34957)	Lys	Asp	Glu	20
Bovine (BAD86590)	Lys	Asp	Glu	21
Human (AAA61225)	Lys	Asp	Glu	21

Residue	Salmon	Rabbit
24 (c)	Gly	Gln
27 (f)	Gly	Ala
35 (g)	Lys	Arg
42 (g)	Asp	Glu
45 (c)	Ala	Ser
63 (g)	Ser	Ala
73 (c)	Val	Leu
77 (g)	Thr	Lys
111 (f)	Thr	Gln
132 (f)	Asn	Ser
135 (b)	Ser	Gln
143 (c)	Leu	Ile
145 (e)	Asp	Glu
157 (c)	Glu	Asp
179 (d)	Thr	Ala
191 (b)	Ser	Ala
229 (e)	Thr	Ser
247 (b)	Ala	Thr
252 (g)	Thr	Ser
276 (c)	Asn	His

Amino acid sequences of alpha-fast skeletal tropomyosins were obtained from the NCBI database. Residues 77, 80, and 82 are putative ion-pairing groups. The total number of substitutions are compared to the Atlantic salmon tpm1. Right-hand side of table, 20 amino acid differences between salmon Tmp1 (Heeley et al., 1995) and rabbit Tpm1.1(alpha) (Stone & Smillie, 1978). "Reprinted with permission from Silva, A. M. M., Ige, T., Goonasekara, C. L., & Heeley, D. H. (2020a). Threonine-77 Is a Determinant of the Low-Temperature Conditioning of the Most Abundant Isoform of Tropomyosin in Atlantic Salmon. Biochemistry, 59(31), 2859–2869. https://doi.org/10.1021/acs.biochem.0c00416) Copyright (2021) American Chemical Society."

The focus of Chapter 3 is on understanding the effect of the charge substitution at residue position 77 in salmon Tpm1. Replacement of Thr-77 by Lys increases the melting temperature of both cooperative transitions that are observed during heat denaturation. The change also leads to a pronounced reduction in the proteolytic susceptibility of the 169th peptide bond, ~ 100 amino acids away from the mutation site, which is indicative of a long-range conformational rearrangement and which may extend through the 5th actin-binding period (N-terminal residues 165 - 188). Significantly, the 5th period is crucial for actin-binding (Hitchcock-DeGregori & Singh, 2010). In this regard, the affinity of native salmon Tpm1 for F-actin is stronger at 4 ^{o}C than 22 ^{o}C; the opposite of what has been long-known to be the case for the mammalian homolog (Drabikowski & Gergely, 1962). It is clear that a variety of adaptations enable tropomyosin to achieve optimum function in a low-temperature niche (Fudge & Heeley, 2015; Silva et al., 2020b) as documented for enzymes (Matthews et al., 1987; Davail et al., 1994; Cambillau & Claverie, 2000; D'Amico et al., 2002; Gianese et al., 2002; Greaves & Warwicker, 2009; Waage et al., 2017; Deniz, 2018; Saavedra et al., 2018). The current work shows that a neutral side-chain, Thr, as a replacement for Lys-77 has a strong influence on the cold adaptation of tropomyosin.

3.2 Materials and Methods

3.2.1 Protein isolation

3.2.1.1 Tropomyosin

Wild-type (Thr-77) and mutants of (Lys-77; Ala-24 and Ala-27) Atlantic salmon Tpm1 (alpha-fast, accession AAB36559, (Heeley et al., 1995) were expressed in *E. coli* BL21 cells as described (Fudge & Heeley, 2015). Expression was induced using Isopropyl beta-D-1-thiogalactopyranoside (IPTG) and tropomyosin was isolated without exposure to organic solvent or high temperature. Briefly, 4 L of induced bacterial culture was pelleted at low speed, resuspended in 200 mL of extraction buffer containing 0.2 M NaCl, 50 mM 3-morpholinopropanesulfonic acid (MOPS), 1 mM dithiothreitol (DTT), 0.01% (m/v) NaN_3 pH 7.0) and passed twice through a French press. The volume of the lysate was then increased to 500 mL and kept stirring for 1 h in the cold with periodic additions of the protease inhibitor phenylmethlsulfonylfluoride (PMSF) (0.5 mM final concentration). After removal of cellular debris, the tropomyosin-containing supernatant was purified using Q Sepharose Fast Flow followed by a Hydroxyapatite column step. The time from induction to freeze-drying was less than a week. Wild-type tropomyosin (acetylated alpha-fast) was isolated from Atlantic salmon and rabbit fast skeletal muscle acetone powder using 0.1M NaCl extraction and induced isoelectric precipitation at pH 4.6 followed by chromatographic separation steps (Smillie, 1982).

3.2.1.2 Cyanogen bromide (CNBr) cleavage and isolation of fragments

Tropomyosins were fragmented under the following conditions: 200-fold molar excess of CNBr reagent over methionine, 70 % (v/v) formic acid, overnight, in the dark at room temperature. The CNBr whole digests were then diluted > 10-fold with deionized water and lyophilized. The two large fragments, CN1A and CN1B (Hodges et al., 1972) were then separated by hydroxyapatite chromatography and isolated fragment identities were confirmed by electrophoretic mobility and, for some batches of CN1A, Edman-sequencing. Six cycles gave the partial sequence: Leu-Lys-Leu-Asp-Lys-Glu which corresponds to residues 11 - 16 of salmon Tpm1 (alpha-fast) and is consistent with methionine being in position 10 (Heeley et al., 1995).

3.2.1.3 Troponin

Whole troponin (TnT, TnC, and TnI) was prepared from rabbit fast skeletal muscles using the ammonium sulfate ($(NH_4)_2SO_4$) salting-out procedure without the step involving Cibacron Blue-based chromatography described by Potter, 1982.

3.2.1.4 Actin

Actin was prepared from rabbit skeletal muscle acetone powder by cycles of polymerization and depolymerization (Spudich & Watt, 1971). Sucrose was added to the final G-actin (final sugar concentration 2 mg/ml). The mixture was then freeze-dried, and

stored at -20 ^{o}C. For binding assays actin-sucrose was dissolved in a binding buffer containing 5 mM MOPS, 30 mM KCl, 1 mM $MgCl_2$, 0.1 mM EGTA, 1 mM DTT at pH 7.5 with 0.5 mM MgATP and dialyzed overnight. The stock solution was stored refrigerated and used within two weeks.

3.2.1.5 Concentration determination

Protein concentrations were measured by UV absorbance with A_{280} using the following formulae with appropriate correction for light scattering at A_{320}. Fragment concentrations were determined based on tyrosine content. F-actin concentration was determined by measuring UV absorbance at A_{290} in the presence of urea with appropriate correction for light scattering at A_{320}. (Houk & Ue, 1974).

$$[Full\ length\ tropomyosin] = \frac{A280nm - 1.5A320nm}{0.25}$$

$$[CN1A] = \frac{A280nm\ x\ Dilution\ Factor\ x\ \ (115\ \ X\ 13{,}340\frac{g}{mol})}{1280\ M^{-1}cm^{-1}}$$

$$[CN1B] = \frac{A280nm\ x\ Dilution\ Factor\ x\ \ (115\ \ X\ 15{,}295\frac{g}{mol})}{1280\ M^{-1}cm^{-1}\ X\ 5}$$

$$[troponin] = \frac{A280nm - 1.5A320nm}{0.47}$$

$$[F - actin] = \frac{A290nm - 1.34A320nm}{0.69}$$

3.2.2 Electrophoresis

Sodium dodecyl sulfate-polyacrylamide electrophoresis (SDS-PAGE) (Laemmli, 1970) and alkaline urea PAGE (Perrie & Perry, 1970) were carried out as described. Alkaline urea gels were briefly pre-ran (15 mins at 160 V) before sample loading. Polyacrylamide slabs were of 0.75 mm thickness and consisted of an acrylamide/ N, N'-methylene-bis-acrylamide (BioRad) (m/v) ratio of 30 : 0.8. The gels were photographed using a ImageQuant LAS400/chemiImager^{TM}. Transfer from a (duplicate) SDS gel to polyvinylidene difluoride (PVDF) membranes was performed using 10 mM cyclohexylaminopropanesulfonic (CAPS), 10% (v/v) methanol, pH 11.0 in a cold room at 60 V over night (total VH ~ 1000). The next day, the membrane was briefly stained with 0.025% (m/v) Coomassie Brilliant Blue R-250, 40% methanol, and destained with 50% ethanol and air-dried overnight.

3.2.3 Thermal Denaturation

Unfolding profiles were recorded using a Nano DSC differential scanning calorimeter (TA instruments). Ten mg of freeze-dried samples of full-length tropomyosin and CN1A, and CN1B fragments were prepared by dissolving in 1 mL of 0.1 M KCl, 20 mM phosphate, 1 mM DTT, pH 7.0 and dialyzed (500 mL of dialysis buffer per 1 mL of the sample) overnight in the cold against the same buffer, that had been degassed previously before adding DTT from the solid (where applicable). Unfolding was induced by a linear heat ramp of 1 ^{o}C per minute between 5 and 65 ^{o}C.

3.2.4 Proteolytic fragmentation

Digestion with chymotrypsin (Worthington) and trypsin (Worthington) followed the same procedure as described in Pato et al., 1981. Ten mg of the freeze-dried enzyme was dissolved in 2 mM HCl and stored in a refrigerator. The same stock solution was used for each side-by-side comparison. Digestion buffer consisted of 50 mM NH_4HCO_3, 0.1 M NaCl, 1mM DTT at pH 8.0. For 33,000 g/mol of Tpm1 (α) monomer the following enzyme: substrate mole ratios were used, chymotrypsin; 1:250 (5 ^oC), 1:500 (20 and 37 ^oC) and 1:1000 (25 ^oC) and trypsin; 1:500 (10 ^oC). For CN1A (residues 11-127) of Tpm1(α) a 1: 250 enzyme: substrate mole ratio was used at 25 ^oC. Samples of acetylated and recombinant tropomyosins were digested side-by-side at a concentration of 2 mg/mL. The reaction was initiated by the addition of the protease with immediate mixing. Aliquots were withdrawn at set times and quenched with 10 M urea containing 1 mM DTT. At the end of the experiment, the samples were analyzed all together by SDS-PAGE with the boiling step omitted. The intensity of the Coomassie-stained band corresponding to intact tropomyosin was measured using ImageJ 1.52a. Densitometric analyses were carried out by fitting data into the following equation for a single exponential process.

$$Y = (Yo - Plateau)^{\mathrm{T}(-K\mathrm{T}X)} + Plateau$$

Y^0, Y value when X (time) is zero.

Plateau, Y value at infinite times

K, the rate constant

T, time

Selected gel bands were excised from the gels using a new scalpel, dried in a desiccator, and sent to the Proteomics and Mass Spectrometry Core Facility at Dalhousie University for peptide mapping. Fragments of interest electroblotted onto PVDF were sent to SPARC BioCentre, Hospital for Sick Kids for Edman sequencing.

3.2.5 Troponin affinity chromatography

Troponin-Sepharose 4B was prepared by coupling rabbit skeletal troponin to CNBr-activated Sepharose 4B as per the instructions provided by the manufacturer (GE Health Care) (Heeley & Lohmeier-Vogel, 2016). Column, 0.9 cm x 15 cm (volume, ~ 9.5 mL). Chromatography start buffer contained 10 mM imidazole, 1 mM EGTA, 0.01% (m/v) NaN_3, 1 mM DTT, pH 7.0. All column steps (load, wash, and elution) were carried out in a cold room (10 ^oC) (Linear salt gradient, 0 - 0.5 M NaCl; volume, 160 mL; flow rate, ~ 25 mL / hour; fraction size, ~ 1.8 mL). The conductivity measurements were obtained by warming up fractions to room temperature. The increase in conductivity per tube was 0.34 mS/cm. Tropomyosin-containing fractions were identified and quantified by Bradford reagent at A_{595} measurement (Bradford, 1976) followed by SDS-PAGE analysis. Absorbance measurements and SDS-PAGE were in agreement in identifying the fraction containing the highest amount of protein. The conductivity of the highest A_{595} fraction was noted.

3.2.6 F-actin binding

Mixtures of F-actin and tropomyosin were sedimented at 4 ^{o}C using a 70Ti rotor (40,000 rpm) or at 22 ^{o}C in Beckman Airfuge A-100/30 Fixed-Angle six-slot rotor (25 psi) for 40 min. The binding buffer contained 5 mM MOPS, 30 mM KCl, 1 mM $MgCl_2$, 0.1 mM EGTA, 1 mM DTT, pH 7.5 set at room temperature. Actin was polymerized by dialysis against the binding buffer which also contained 0.2 mM MgATP and 0.01 % (m/v) NaN_3. A diluted sample of F-actin was prepared daily from the stock which was used within two weeks. Binding components were combined in the order tropomyosin (0.25 - 4 µM) > buffer > F-actin (10 µM) with gentle mixing using a P200 Gilson Pipetman with a truncated tip, and incubated for 1 hr at the respective temperature. Aliquots were taken both before and after sedimentation for analysis by SDS-PAGE. Each gel was stained using a standardized procedure consisting of 50 mL of 0.25% (m/v) unused Coomassie R-250 for 1hr with shaking and then destained until the background cleared. The intensity and the size of the tropomyosin-containing bands were estimated from gel photographs using densitometry as outlined below using ImageJ 1.52a (Rasband, 2018). After back-ground reduction, the moles of bound tropomyosin were determined by ImageJ 1.52a from the difference in band intensity of loaded (pre-sedimentation) and free-unbound (post-sedimentation supernatant) tropomyosin in conjunction with a calibration relationship of quantified area of the bands of known amounts of tropomyosin. Binding curves were generated using GraphPad Prism 5 using the Sigmoidal dose-response (variable slope) equation (below) to obtain the best fit curve. Binding curves were constructed from three separate experiments for each temperature.

$$Y = Bottom + \frac{(Top - Bottom)}{1 + 10^{(LogEC50 - X) - HillSlope}}$$

Bottom - Y value at the bottom plateau

Top - Y value at the top plateau

LogEC50 (K_D) - X value when the response is halfway between Bottom and Top

Hill Slope - Hill coefficient

3.2.7 Molecular visualization

The spatial arrangement of Lys-77(g) and neighboring carboxylates in the 7 Angstrom structure of porcine tropomyosin (Whitby & Phillips, 2000) DOI: 10.2210/pdb1C1G/pdb was viewed using PyMOL for education purposes V. 1.74 (DeLano Scientific, California). The structure was downloaded from the Research Collaboratory for Structural Bioinformatics Protein Data Base (RCSB PDB). The structure of the porcine tropomyosin was changed at 20 sites with the respective Atlantic salmon tropomyosin amino acid residues to obtain the salmon fast skeletal tropomyosin using the wizard → mutagenesis function. The distances between the interested residues (77(g) to Glu-82(e) and Asp-80(c) of the opposite strand) were measured using the wizard → measurement function. The spatial arrangement of Gly-24(c) and Gly-27(f) in the Lys15-Ala18-Ala22-Ala25-Lys29-Ala32-Ser36 region was viewed using the Atlantic salmon tropomyosin (the model was

built in SWISS-MODEL with Atlantic salmon tropomyosin alpha-fast (accession AAB36559) sequence using pdb1C1G as a template).

3.3 Results

3.3.1 Chromatography

Figure 3.1A depicts the typical chromatography profile of full-length salmon Tpm 1 (acetylated and recombinant proteins) separated using the Q Sepharose column with a NaCl gradient. Fractions identified as tropomyosin (boxed area on the elution profile) when analyzed by SDS-PAGE reveal the existence of a contaminant (gel image inset, lanes 7 - 9). Hence these fractions are pooled, sent through a hydroxyapatite column (Figure 3.1B), and eluted with a phosphate gradient. Fractions containing tropomyosin are highlighted on the elution profile with a box. The final enrichment is confirmed electrophoretically (Figure 3.1B gel inset). A yield of ~ 40 mg is typically obtained from 1 L of bacterial culture and ~ 50 mg from 100 g muscle acetone powder. A portion of wild-type and recombinant tropomyosin was taken for chemical cleavage using cyanogen bromide (CNBr). The resulting fragments are separated using a hydroxyapatite column as shown in Figure 3.1C. SDS-PAGE (Figure 3.1C gel inset) reveals that CN1A (residues 11 - 127) elutes in the early peak whereas the CN1B (residues 142 - 281) elutes in the later one. The difference in A_{280} of the two fragments is due to their unequal aromatic amino acid contents: CN1A (1 Tyr) vs. CN1B (5 Tyr). Fractions from each peak are pooled as indicated by the box on the elution profile. Yield is typically ~ 10 mg per 40 mg of total digest material.

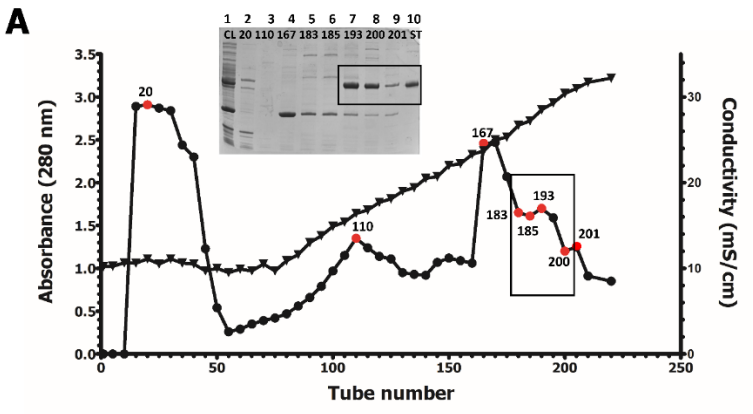
A
1 2 3 4 5 6 7 8 9 10
CL 20 110 167 183 185 193 200 201 ST
Absorbance (280 nm)
Conductivity (mS/cm)
Tube number
20
110
167
183
185
193
200
201

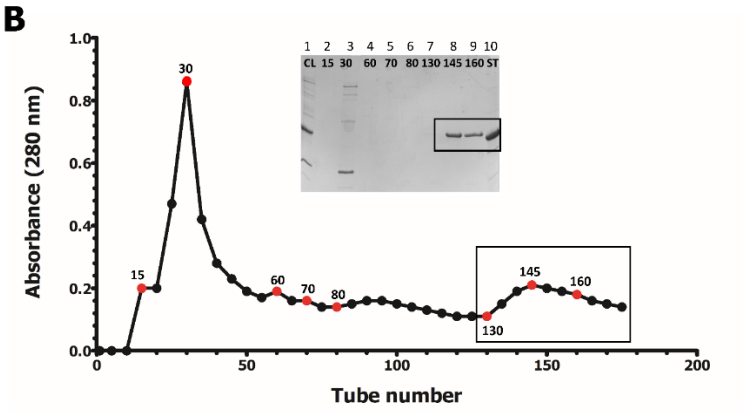
B
1 2 3 4 5 6 7 8 9 10
CL 15 30 60 70 80 130 145 160 ST
Absorbance (280 nm)
Tube number
15
30
60
70
80
130
145
160

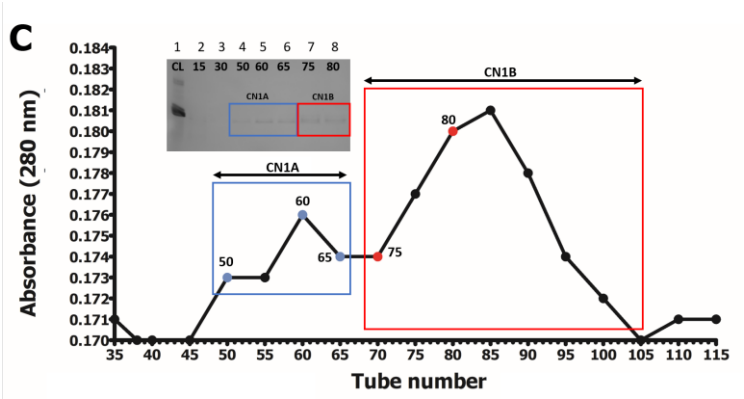
C
1 2 3 4 5 6 7 8
CL 15 30 50 60 65 75 80
CN1A
CN1B
Absorbance (280 nm)
Tube number
50
60
65
75
80

Figure 3.1. Chromatography profiles of acetylated and recombinant tropomyosins and CNBr fragments. Tropomyosin elution is detected using A_{280} measurements of each fraction followed by SDS-PAGE. (A) Tropomyosin was enriched, and the nucleic acid was removed using Q Sepharose Fast Flow chromatography (GE Healthcare) (column, 2.5 x 12 cm, volume, ~ 75 mL). Freshly prepared start buffer contained 30 mM tris(hydroxymethyl)aminomethane (Tris), 50 mM NaCl, and 1 mM DTT, pH 8.0 (linear salt gradient, 0.05 - 0.5 M NaCl, volume 800 mL). Tropomyosin elution centered at conductivity ~ 28 mS. Inset, SDS-PAGE with fraction number indicated. Lane 1 - column load (CL); Lane 10 - tropomyosin standard (ST). Tropomyosin-containing fractions are indicated by boxes. (B) Hydroxyapatite chromatography of tropomyosin fractions pooled from Q Sepharose. Further enrichment was attained by loading fractions directly onto the column (column, 2.5 x 12 cm, volume, ~ 75 mL). Start buffer contained 1 M NaCl, 60 mM phosphate, pH 7.0 at room temperature (linear phosphate gradient, 0.06 - 0.2 M phosphate, volume 800 mL). Inset, SDS-PAGE with fraction number indicated. Lane 1 - CL from Q column; Lane 10 - ST. Tropomyosin-containing fractions are indicated by boxes. (C) Hydroxyapatite chromatography of CNBr fragments (column, 1.25 x 8 cm, volume, ~ 40 mL). Start buffer contained 1 M NaCl, 50 mM phosphate, 1 mM DTT, pH 7.0 at room temperature (linear phosphate gradient, 50 - 200 mM phosphate, volume 400 ml, fraction size ~3 ml, flow rate 30 ml/hr). Fraction identity is indicated by box color, blue - CN1A and red - CN1B. Gel inset, SDS-PAGE analysis of the highlighted fractions in the profile with the number indicated. Lane 1 - CL of whole CNBr digest.

3.3.2 Electrophoresis

Chromatographically enriched full-length recombinant non-mutant (control, Thr-77) and mutant (Lys-77) salmon Tpm1s are electrophoretically analyzed in Figure 3.2. At alkaline pH in the presence of urea, control Tpm1 (Figure 3.2A, lane 1) migrates ahead of the mutant Tpm1 (Figure 3.2A, lane 2) towards the positive electrode. This is conclusively demonstrated by co-electrophoresis of control and mutant (Figure 3.2A, lane 3). In the presence of SDS detergent the mutant Tpm1 (Figure 3.2B, lane 1) migrates ahead of control Tpm1 (Figure 3.2B, lane 2) and in a mixture resolves into two bands (Figure 3.2B, lane 3). The shift illustrates the relationship between the charged group in tropomyosin and its complexation with anionic detergent.

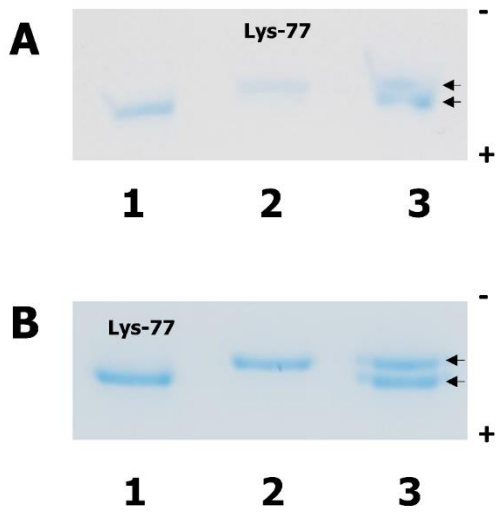

Figure 3.2. Electrophoretic analysis of Atlantic salmon Tpm1 (alpha-fast). (A) Alkaline urea PAGE. Lane 1, non-mutant control (Thr-77); lane 2, mutant (Lys-77) and lane 3, mixture. 10% (m/v) acrylamide monomer. (B) SDS-PAGE. Lane 1, mutant (Lys-77); lane 2, non-mutant control (Thr-77) and lane 3, 12% (m/v) acrylamide monomer. Arrowheads indicate the separated bands ((-) and (+)**,** the orientation of the electrodes). Reprinted with permission from Silva, A. M. M., Ige, T., Goonasekara, C. L., & Heeley, D. H. (2020a). Threonine-77 Is a Determinant of the Low-Temperature Conditioning of the Most Abundant Isoform of Tropomyosin in Atlantic Salmon. Biochemistry, 59(31), 2859–2869. https://doi.org/10.1021/acs.biochem.0c00416. Copyright (2021) American Chemical Society.

3.3.3 Thermal Denaturation

3.3.3.1 Full-length Tpm1s

In this section, the global unfolding of salmon Tpm1s is monitored using the first derivative of the calorimetry progress curve. The ionic conditions, 0.1 M KCl, 1 mM DTT, pH 7.0 are such that Tpm1s will exist as units of 66,000 g/mole (reduced monomeric form). Two transitions of unequal proportions are evident in all profiles. The main transition appears to center in the temperature gradient ~10 ^{o}C away from the minor (Figure 3.3A). The average melting temperatures (T_m), of the three proteins, are as follows: wild-type (acetylated), 30.5 ^{o}C minor and 40.1 ^{o}C main; recombinant control (Thr-77), 30.3 ^{o}C minor and 40 ^{o}C main; and mutant (Lys-77), 35.1 ^{o}C minor and 43.5 ^{o}C main (Figure 3.3A). The T_{ms} of wild-type and recombinant control are in close agreement with each other with one outstanding difference: the magnitude of the minor transition is less pronounced in the recombinant (indicated by an arrow in Figure 3.3A). The two transitions of mutant (Lys-77) tropomyosin show a rightward shift of ~ 5 ^{o}C for the minor transition and ~ 3.5 ^{o}C for the main transition (Figure 3.3A) compared to the control. Another noticeable feature of the mutant is that the minor and major transitions are sharper, compared to the same transitions exhibited by both the recombinant and the control. It is also apparent that nearly all of the unfolding profiles contain a positive slope before the first transition (Figure 3.3A). The extent to which this is contributed by an unsteady baseline (following the start-up hook) or by a co-operative unfolding step is uncertain (at the moment). Calculated enthalpy values (Table 3.2): mutant > wild-type > control agree with the observed differences in melting temperature. A second heat cycle is carried out following a cool down of 1 ^{o}C per min allowing gradual refolding.

In the reheating step the minor transition becomes less obvious in the mutant (Figure 3.2B) whereas almost or completely disappearing from control (Figure 3.2C) and acetylated wild-type (Figure 3.2D) Tpm1s. Comparison of the 1st and 2nd heating cycles shows that refolding of salmon tropomyosin is not fully reversible. Specifically, upon reheating the first transition is reduced in magnitude, demonstrating the presence of a region of low stability. The pronounced minor transition of acetylated wild-type compared to the control (Figure 3.3A vs. 3.3E and Table 3.3), is suggestive of the crucial role of N-terminal acetylation. The absence of acetylation from the recombinants resulting in a localized unfolding induced by the protonated alpha-amino group of Met-1(a) that falls in a core position (Monteiro et al., 1994). In addition, it is possible that the helical breaking Gly-24 and Gly-27 of salmon Tpm1 fall in the major destabilized cluster Lys15-Ala18-Ala22-Ala25-Lys29-Ala32-Ser36 (Brown et al., 2001) further destabilizes the coiled-coil while contributing to the minor transition. A double mutant with Gly-24 and Gly-27 replaced by Ala is used to further the understanding of the contribution of the N-terminal half of the molecule to the minor transition. The observed *Tms* 35.2 ^{o}C minor and 40.8 ^{o}C main transition (Figure 3.3E) indicate a shift of the minor transition in the temperature gradient ~ 5 ^{o}C away compared to the control (Figure 3.3A vs. 3.3E) suggesting that the minor transition possibly arises from the N-terminal half from the major destabilized cluster region Lys15-Ala18-Ala22-Ala25-Lys29-Ala32-Ser36 that additionally contain two Glys at residue-24 and residue-27 in Atlantic salmon. This highlights the need for the careful control of the temperature during isolation, especially in the case of tropomyosins from psychrophilic organisms. Averaged melting temperatures determined by calorimetry are summarized in Table 3.2.

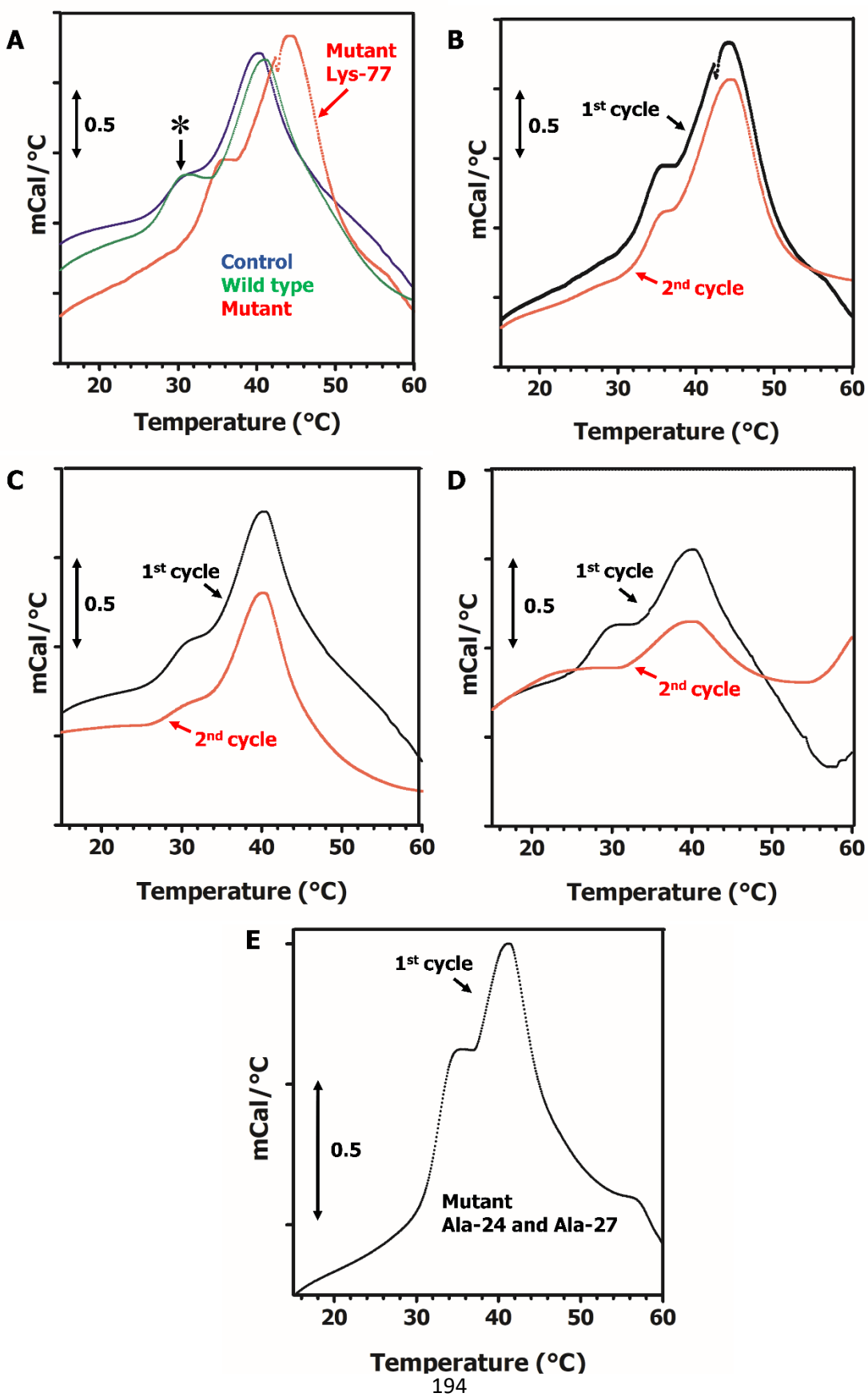
A
0.5
mCal/°C
Mutant
Lys-77
Control
Wild type
Mutant
20
30
40
50
60
Temperature (°C)
B
0.5
mCal/°C
1st cycle
2nd cycle
20
30
40
50
60
Temperature (°C)
C
0.5
mCal/°C
1st cycle
2nd cycle
20
30
40
50
60
Temperature (°C)
D
0.5
mCal/°C
1st cycle
2nd cycle
20
30
40
50
60
Temperature (°C)
E
0.5
mCal/°C
1st cycle
Mutant
Ala-24 and Ala-27
20
30
40
50
60
Temperature (°C)

Figure 3.3. Effect of mutagenesis of residues-24, 27, and 77 on the thermal stability of Atlantic salmon Tpm1 (alpha-fast). (A - E) Representative heat capacity profiles (Heat ramp, 1 ^{o}C / min, 5 - 65 ^{o}C. Protein concentrations, 2.7 - 3.6 mg / mL). (A) Recombinant control (Thr-77) Tpm1 (blue trace) T_{m1} = 30.3 ^{o}C, T_{m2} = 40 ^{o}C; enthalpy, 268 kcal / mol; recombinant mutant (Lys-77) Tpm1 (red trace) T_{m1} = 35.1 +/- 0.32 ^{o}C, T_{m2} = 43.5 +/- 0.56 ^{o}C; enthalpy, 311 kcal / mol and wild-type (acetylated) Tmp1 (green trace), T_{m1} = 30.5 +/- 0.56 ^{o}C, T_{m2} = 40.1 +/- 0.09 ^{o}C; enthalpy, 303 kcal / mol. The asterisk and arrow indicate a difference in the sharpness of the minor transition. (B) Mutant (Lys-77) Tpm1, 2nd heat cycle following a 1 h cooldown of 1 ^{o}C per minute. 1st heat cycle (from A). Note - the reason for the glitch that is evident during the 1st heat cycle is unknown (C) Control (Thr-77) Tpm1, 2nd heat cycle following a 1 h cooldown of 1 ^{o}C per minute. 1st heat cycle (from A). (D) Acetylated wild-type Tpm1, 2nd heat cycle following a 1 h cooldown of 1 ^{o}C per minute. (E) Mutant (Ala-24 and 27) T_{m1} = 35.2 +/- 0.2 ^{o}C, T_{m2} = 40.8 +/- 0.01 ^{o}C. More than one batch of each tropomyosin was analyzed. The upward trend that is observed following the main unfolding transition in some recordings is attributed to baseline drift. Adapted with permission from Silva, A. M. M., Ige, T., Goonasekara, C. L., & Heeley, D. H. (2020a). Threonine-77 Is a Determinant of the Low-Temperature Conditioning of the Most Abundant Isoform of Tropomyosin in Atlantic Salmon. Biochemistry, 59(31), 2859–2869. https://doi.org/10.1021/acs.biochem.0c00416. Copyright (2021) American Chemical Society.

3.3.3.2 CNBr fragments

The distribution of methionine in salmon Tpm1 (residues 1, 8, 10, 127, 141, and 281, which is identical to that in the mammalian homolog (Stone & Smillie, 1978)), permits the analysis of two large pieces of the Tpm1 molecule: CN1A (residues 11 - 127) that encompasses residue-77 and CN1B (residues 148 - 281). The identities of these CNBr fragments were established by Pato et al., 1981. The sectional analysis below illustrates the consequence of a neutral amino acid in position 77 of the N-terminal half of the molecule. It also illustrates the interdependency of the N- and C-termini. When unfolding is induced, mutant (Lys-77) CN1A exhibits a transition at ~ 53 ^{o}C (Figure 3.4A) which is a rightward shift of 13 ^{o}C relative to the recombinant control (Figure 3.4B). The minor element in the mid-20 ^{o}C region of Figure 3.4A must be viewed with caution owing to its small size and the harsh cleavage conditions (70% formic acid). The CN1B fragment exhibits a transition at ~ 41 ^{o}C which is close to that of control CN1A (Figure 3.4B inset), consistent with a previous study (Goonasekara & Heeley, 2008). Conversely, mammalian CN1A and CN1B (Williams & Swenson, 1981) reflect the generally accepted N-terminal to C-terminal decline in stability (Woods, 1977; Lehrer, 1978; Edwards and Sykes, 1980; Smillie et al., 1980; Phillips et al., 1980). As what is seen with the fragments, the main transition (Table 3.2, 40 ^{o}C) of mutant salmon Tmp1 (Lys-77) is 10 ^{o}C less than that of the mutant CN1A (Figure 3.4A). This can only mean that the CN1A portion is destabilized by connection to the rest of the protein. The averaged melting temperatures determined by calorimetry are summarized in Table 3.2.

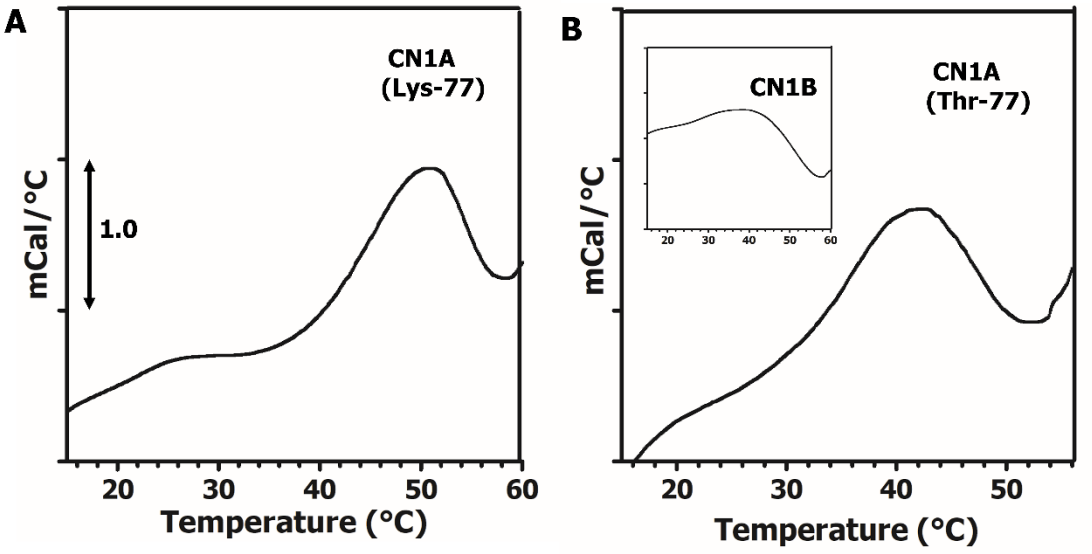

Figure 3.4. Effect of mutagenesis of residue-77 on melting properties of CN1A and CN1B fragments. Heat ramp, 1 ^{o}C / min, 5 - 65 ^{o}C. Protein concentrations, 2.7 - 3.6 mg / mL. (C) Mutant (Lys-77) CN1A, T_m = 52.8 +/- 0.05 ^{o}C. (D) Control (Thr-77) CN1A, T_m = 41.2 +/- 1 ^{o}C. Inset, fragment CN1B (residues 142 - 281), T_m = 37.8 ^{o}C. More than one batch of each tropomyosin was analyzed, except for CN1B. Adapted with permission from Silva, A. M. M., Ige, T., Goonasekara, C. L., & Heeley, D. H. (2020a). Threonine-77 Is a Determinant of the Low-Temperature Conditioning of the Most Abundant Isoform of Tropomyosin in Atlantic Salmon. Biochemistry, 59(31), 2859–2869. https://doi.org/10.1021/acs.biochem.0c00416. Copyright (2021) American Chemical Society.

Table 3. 2. Calculated melting temperatures of analyzed proteins.

		Melting temperature (°C)		Enthalpy (kcal / mol)
Figure 3.3				
A	Recombinant control (Thr-77) Tpm1 (blue trace)	T_{m1} = 30.3 ± 2.1	n≥2	268
		T_{m2} = 40 ± 2.0		
	Recombinant mutant (Lys-77) Tpm1 (red trace)	T_{m1} = 35.1 ± 0.32		311
		T_{m2} = 43.5 ± 0.56		
	Wild-type (acetylated) Tmp1 (green trace)	T_{m1} = 30.5 ± 0.56		303
		T_{m2} = 40.1 ± 0.09		
B	Recombinant mutant (Lys-77) Tpm1	*1st cycle (Heat) = same as A*	n≥2	
		2nd cycle (Re-heat) T_{m1} = 43.7 ± 0.67 T_{m2} = 36.3 ± 0.15		
C	Recombinant control (Thr-77) Tpm1	*1st cycle (Heat) = same as A*	n=2	
		2nd cycle (Re-heat) T_{m2} = 41.5 ± 1.50		
D	Wild-type (acetylated) Tmp1	*1st cycle (Heat) = same as A*	n=2	
		2nd cycle (Re-heat) T_{m2} = 40.0 ± 0.10		
E	Recombinant mutant (Gly-24 and Gly-27) Tpm1	T_{m1} = 35.2 ± 0.2	n=2	
		T_{m2} = 40.8 ± 0.01		
Figure 3.4				
A	Recombinant mutant (Lys-77) CN1A	52.8 ± 0.05	n=2	
B	Recombinant control (Thr-77) CN1A	41.2 ± 1	n=2	
	Inset, fragment CN1B (residues 142 - 281)	37.8	n=1	

Averaged melting temperatures. Protein batches are prepared without exposure to heat at any time in their histories unless otherwise stated. More than one batch of each tropomyosin is analyzed, except for the recombinant control (Thr-77) CN1A sample B. Enthalpy values for the unfolding profiles are determined by calculating the area under the curve with baseline correction. Tm1 - major transition and Tm2 - minor transition. Adapted with permission from Silva, A. M. M., Ige, T., Goonasekara, C. L., & Heeley, D. H. (2020a). Threonine-77 Is a Determinant of the Low-Temperature Conditioning of the Most Abundant Isoform of Tropomyosin in Atlantic Salmon. Biochemistry, 59(31), 2859–2869. https://doi.org/10.1021/acs.biochem.0c00416. Copyright (2021) American Chemical Society.

3.3.4 Limited proteolysis

Proteolytic susceptibility of different Tpm1s and CN1A fragments are compared in order to identify vulnerable sites within flexible regions. This approach is taken based on the assumption that the accessibility of a specific cleavage site increases with increasing chain flexibility. Digestion experiments are performed on batches of protein that were not exposed to organic solvents or elevated temperature throughout their preparation unless otherwise stated.

3.3.4.1 Chymotrypsin digestion on non-heat treated intact proteins

According to previous studies (Pato et al., 1981), Leu-169 is the preferred site of chymotryptic cleavage in rabbit Tpm1.1(α) followed by Leu-11. Analysis of salmon fast skeletal Tpm1 has shown that the primary cleavage site is shifted to Leu-11 (Fudge & Heeley, 2015), greatly due to the existence of a destabilizing double Gly-24 and Gly-27 close to the cleavage site and the lack of N-terminal acetylation in the recombinant proteins. In this regard, chymotrypsin is used to assess solvent exposure of both Leu-11 and Leu-169 residues in salmon Tpm1s: wild-type (acetylated), recombinant control (Thr-77), and recombinant mutant (Lys-77) to understand the effect of changes to residue-77.

The 5 ^{o}C (close to the native temperature of salmon) digestion (Figure 3.5A), carried out for 15 h, demonstrates that the change of Thr-77 to Lys is highly influential in the context of proteolytic susceptibility. The control (Thr-77) is extensively degraded leaving only the digested products at the bottom of the gel (Figure 3.5A, lane 3). Comparatively, this is a

clear-cut difference between the mutant and control (Long sections of mutant (Lys-77) still observed after 15 h (Figure 3.5A, lane 4)). When the 5 ^{o}C digestion is further evaluated over 90 mins at different time points it is evident that the dominant event is the removal of a small terminal peptide (Figure 3.5B) producing a large fragment (clipped product) that runs close to the intact protein. Smaller fragments that run close to the 20 and 15 kDa standards start appearing after 10 mins as subsequent minor events (Figure 3.5B). Analysis of the rate of the dominant event (Figure 3.5C) shows the difference between the mutant and control is either very little or not significant. Another observation that concerns the intact protein bands (Figures 3.5A and 3.5B, lanes 1 and 2) and the 20 kDa fragment (Figure 3.5B lanes 3 - 8) is mutant proteins ahead of control proteins as noted in Figure 3.2B.

At the higher temperature of 20 ^{o}C it is evident that control (Thr-77) Tpm1 (Figures 3.5D and 3.5E) undergoes extensive and accelerated breakdown, well beyond what is observed for the mutant. Within 2 min, the two smaller fragments, ~ 20 kDa and 15 kDa, are visible in the control digest (Figure 3.5D, lane 3). After 10 min 15 and 20 kDa fragments become prominent (Figure 3.5D, lane 5). Relative density reveals ~ 50% of the 'clipped' species remains at this time (Figure 3.5E). Thirty min later only a trace of clipped protein is visible (Figure 3.5D, lane 9, and Figure 3.5E). On the contrary, digestion of mutant (Lys-77) Tpm1 indicates a visible high-intensity intact protein band (M_r ~ 33 kDa) throughout the incubation accounting for ~ 80% of the starting amount (Figure 3.5E) with a faint appearance of smaller fragments (Figure 3.5D, lane 10).

As expected, further increasing the temperature to 37 ^{o}C accelerates the rate of proteolysis. The intact protein band corresponding to the control completely disappears by 20 min

(Figure 3.5F, lane 7, and Figure 3.5G). By comparison, the mutant intact band is visible even at 30 min (Figure 3.5F, lane 10, and Figure 3.5G) with the appearance of smaller fragments (Figure 3.5F, even-numbered lanes). Focusing on 18 kDa fragments, it is evident that they depict the same mobility shift shown by the intact proteins (Figure 3.1B). Furthermore, the mutant 18 kDa fragment is more stable and accumulates more compared to the control indicating the existence of Lys-77.

Based on the results of mass spectrometric peptide mapping (Table 3.3) the major fragments are assigned as CT1 (20 kDa) (residues 12 - 169), coverage 97.5%, and CT2 (15 kDa) (residues 170 - 284), coverage 94.7%. The assignments are identical to those of previous workers using rabbit Tpm1.1(α) (Pato et al., 1981). Furthermore, the mass analysis detected Lys-77-containing mutant peptides, specifically residues 66 - 77 (DAQEKLEVAEKK; measured mass, 1,387.74 Da) and 77 - 91 (KATDAEADVASLNRR; measured mass, 1616.84 Da) thereby validating the mutagenesis. Six cycles of N-terminal Edman sequencing complemented the mass spectrometric analysis and confirmed the origin of subfragments CT1, Lys-12-Leu-Asp-Lys-Glu-Asn-17 and CT2, Val-170-Ile-Ile-Glu-Ser-Asp-175 while establishing the points of chymotryptic cleavage of recombinant salmon Tpm1. Thus, putting all of the evidence together the main chymotryptic sites in recombinant salmon Tpm1 are found between (i) Leu-11 - Lys-12 (product, res. 12 - 284) and (ii) Leu-169 - Val-170 (product, res. 12 - 169 and 170 - 284) (illustrated in Figure 3.5H). Therefore, the effect of changing Thr-77 to Lys is pronounced in terms of its influence on proteolytic susceptibility of a site ~ 100 amino acids away that is equivalent to 1/3rd of the length of the molecule.

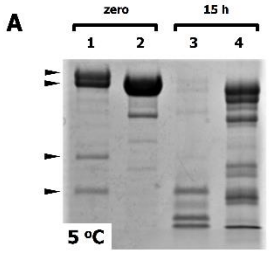
A
zero
15 h
1
2
3
4
5 °C

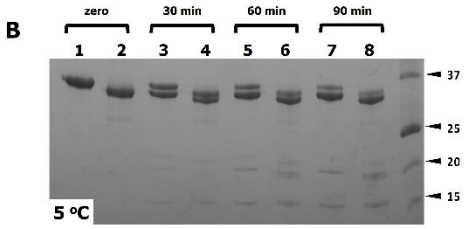
B
zero
30 min
60 min
90 min
1
2
3
4
5
6
7
8
37
25
20
15
5 °C

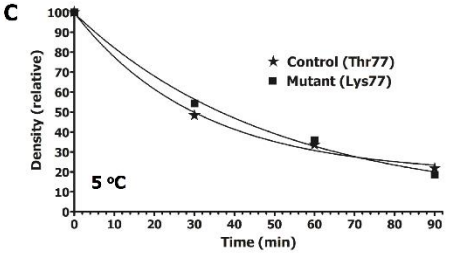
C
Density (relative)
Time (min)
Control (Thr77)
Mutant (Lys77)
5 °C

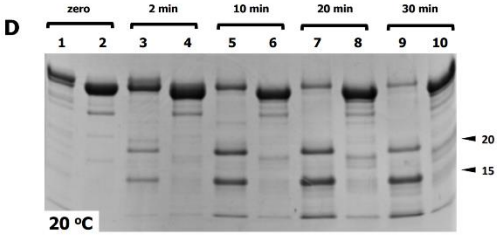
D
zero
2 min
10 min
20 min
30 min
1
2
3
4
5
6
7
8
9
10
20
15
20 °C

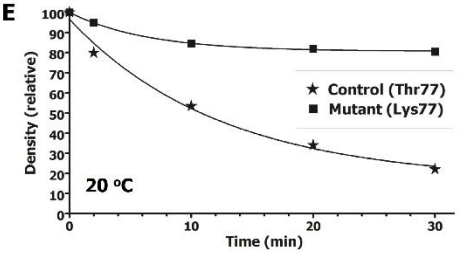
E
Density (relative)
Time (min)
Control (Thr77)
Mutant (Lys77)
20 °C

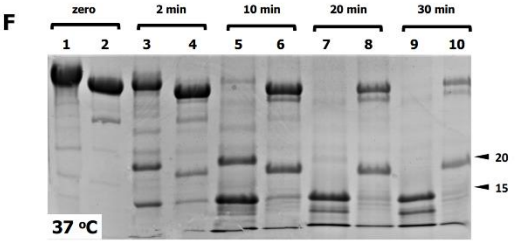
F
zero
2 min
10 min
20 min
30 min
1
2
3
4
5
6
7
8
9
10
20
15
37 °C

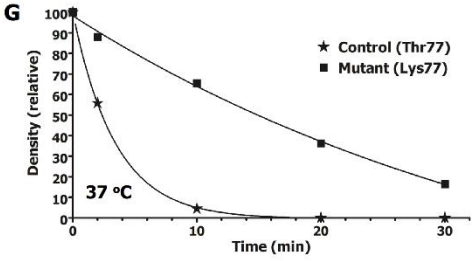
G
Density (relative)
Time (min)
Control (Thr77)
Mutant (Lys77)
37 °C

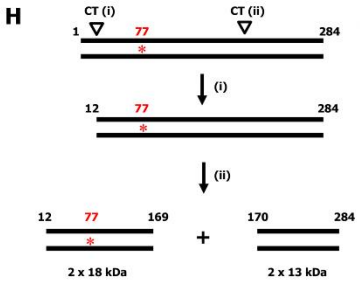
H
CT (i)
CT (ii)
1
77
284
(i)
12
77
284
(ii)
12
77
169
170
284
+
2 x 18 kDa
2 x 13 kDa

Figure 3.5. Effect of mutagenesis of residue-77 on the chymotrypsin susceptibility of Atlantic salmon Tpm1 (alpha-fast). Recombinant non-mutant (control, Thr-77) and mutant (Lys-77) full-length (33,000 g/mol) Tpm1s are digested side-by-side with chymotrypsin (substrate, 2 mg/mL). SDS-PAGE analyses show the decline in the protein chain and subsequent generation of peptide fragments. The mol:mol ratios of enzyme: substrate are, 1: 250 (5 ºC) and 1: 500 (20 ºC and 37 ºC). Extreme right-hand of (B), (D), and (F) Mr. markers. (A) 5 ºC, overnight (15 h). Control (Thr-77), odd-numbered lanes. Mutant (Lys-77) even-numbered lanes. Note evidence of a breakdown of control Tpm1 zero time (indicated by chevrons). The lower M_r band in lane 2 is an impurity. (B) 5 ºC, 90 min incubation. Control (Thr-77), odd-numbered lanes. Mutant (Lys-77) even-numbered lanes. **(**C) Densitometric analysis of B. Band intensities are relative to the starting (zero time) intensity. (D) 20 ºC, 30 min incubation. Control (Thr-77), odd-numbered lanes. Mutant (Lys-77), even-numbered lanes. (E) Densitometric analysis of D. (F) 37 ºC, 30 min incubation. Control (Thr-77), odd-numbered lanes. Mutant (Lys-77), even-numbered lanes. (G) Densitometric analysis of F. (H) Pathway of chymotryptic digestion. The preferred sites are CT(i) Leu-12 and CT (ii) Leu-169. Residue-77 is indicated by an asterisk (I) Digestion of CN1A. 25 ºC, 75 min incubation. Enzyme: substrate, 1: 250. Control (Thr-77) CN1A, odd-numbered lanes. Mutant (Lys-77) CN1A, even-numbered lanes. Extreme right-hand lanes in B, D, and F, M_r markers. Results of mass spectrometric tryptic peptide mapping are presented in Table 3.3. Reprinted with permission from Silva, A. M. M., Ige, T., Goonasekara, C. L., & Heeley, D. H. (2020a). Threonine-77 Is a Determinant of the Low-Temperature Conditioning of the Most Abundant Isoform of Tropomyosin in Atlantic Salmon. Biochemistry, 59(31), 2859–2869. https://doi.org/10.1021/acs.biochem.0c00416.

Table 3. 3. Tryptic peptide coverage by mass spectrometry analysis of chymotrypsin generated tropomyosin fragments 20 kDa (residues 11 - 169) and 15 kDa (residues 170 - 284).

Fragment	Fragment length	Sequence of the peptide
20 kDa coverage 97.5%	31-51	AAEDKSKQLEDDLVALQKKLK
	51-65	KGTEDELDKYSESLK
	66-77, confirmation of mutagenesis	DAQEKLEVAEK**K**
	77-91, confirmation of mutagenesis	**K**ATDAEADVASLNRR
	91-105	RIQLVEEELDRAQER
	106-125	LATALTKLEEAEKAADESER
	126-134	GMKVIENRA
	134-149	ASKDEEKMELQDIQLK
	153-168	HIAEEADRKYEEVAR
	Unconfirmed residues 150-152	
15 kDa fragment coverage 94.7%	168-182	KLVIIESDLERTEER
	182-198	RAELSEGKCSELEEELK
	199-205	TVTNNLK
	206-214	SLEAQAEK
	214-231	YSQKEDKYEEEIKVLTDK
	232-244	LKEAETRAEFAER
	249-266	LEKTIDDLEDELYAQKLK
	268-284	AISEELDNALNDMTSI
	Unconfirmed residues 245-248, 267, and 268.	

The Lys-77 residue in mutant peptide fragments are color-coded in red.

3.3.4.2 Chymotrypsin digestion of heat-treated mutant (Lys-77) protein

Previously, it had been noticed (Graceffa, 1992)that heat-treatment of gizzard tropomyosin caused irreversible chemical damage. One of the properties of tropomyosin that was affected was self-polymerization. Therefore, the author (Graceffa, 1992) cautioned against using high temperatures during the isolation procedure. In our protein unfolding studies (section 3.3.3.1), we noticed that a heating step alters the magnitude of the minor and major transitions of salmon Tpm1 (Figure 3.3C - 3.33D). To see the effects of a heating step on peptide bond accessibility, limited proteolysis is again carried out on the mutant (Lys-77) protein that was heated up to 65 ^{o}C following a gradual cool down to room temperature.

Following heat treatment, mutant (Lys-77) Tpm1 undergoes extensive and accelerated breakdown, well beyond what is observed for the unheated mutant protein when exposed to chymotrypsin (Figure 3.6). Within 5 min, the intensity of the heat-treated intact protein band almost disappears (Figure 3.6, lane 5). On the contrary, the unheated mutant (Lys-77) is more resistant to breakdown. It maintains a substantial amount of ~ 33 kDa protein band throughout the incubation (Figure 3.6, lane 10). Moreover, focusing on the gel, it is evident that 15 and 18 kDa fragments appear in both proteins within 2 min, but in the case of the heat-treated sample with a higher intensity.

The comparisons demonstrate the pronounced action of the enzyme on the heat-treated protein samples. Based on these results it is evident that heating of tropomyosin causes a permanent unfolding in the coiled-coil that is not reverted during a gradual cooling step. Therefore, as previous researchers (Graceffa, 1992) cautioned against using heat-treatment,

the current work also highlights the need for careful control of the isolation conditions for Atlantic salmon Tpm1.

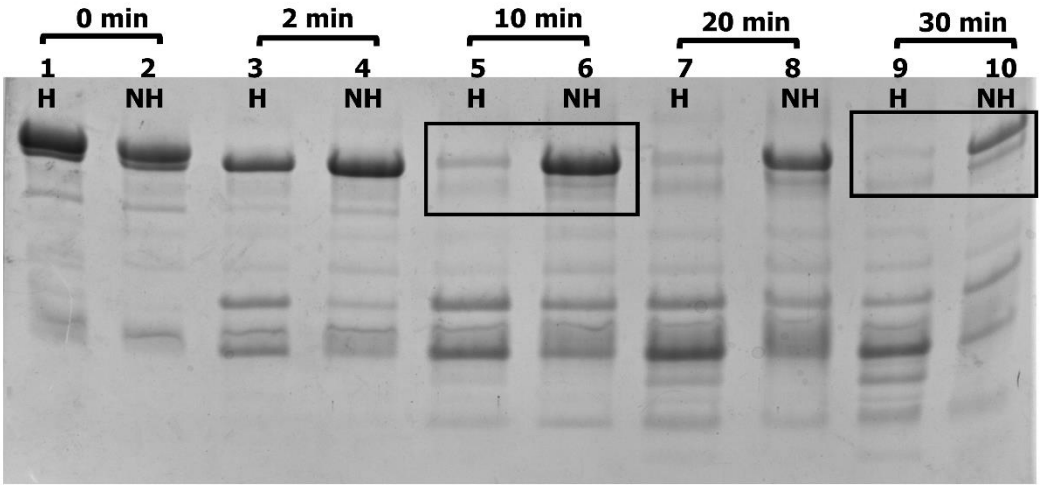

Figure 3.6. Chymotrypsin susceptibility of heat-treated mutant (Lys-77) Tpm1. Recombinant mutant (Lys-77) Tpm1 (33,000 g/mol) is digested side-by-side with chymotrypsin (substrate, 2 mg/mL). SDS-PAGE analyses show the decline in the protein chain and subsequent generation of peptide fragments. The mol: mol ratios of enzyme: substrate is 1:1000 incubated at 25 ºC. Odd-numbered lanes heated (H) sample. Even-numbered lanes non-heated (NH) samples. Note evidence of the increased breakdown of H samples at 10 and 30 min (indicated by boxes).

3.3.4.3 Chymotryptic digestion of CN1A fragments

The proteolytic susceptibility of the N-terminal cyanogen bromide fragment CN1A (residues 11 - 127) is analyzed in Figure 3.7.

When analyzed by SDS-PAGE both the control and mutant CN1A fragments appear as a doublet in the separating gel phase (Figure 3.7 lanes 1 and 2). This is likely due to incomplete cleavage at Met-10 or Met-141. Another observation that concerns the CN1A fragments is that they exhibit the same mobility shift as the intact control and mutant proteins (Figure 3.2B). Specifically, the mutant CN1A migrates slightly ahead of the control. Upon exposure to chymotrypsin, the control CN1A fragment is seen to deplete at a faster rate compared to that of the mutant, as indicated by the relative staining intensities of the 75 min time samples (Figure 3.7, lane 5 vs.. lane 6 see the boxed area). The subfragments reveal a corresponding difference in accumulation as indicated in lanes 3 and 4 (boxed area). Six cycles of Edman sequence yield a sequence corresponding to Asn-89-Arg-Arg-Ile-Gln-Leu-Val-95 residues revealing chymotryptic cleavage of CN1A at the peptide bond between Leu-88 and Asn-89. Despite the denaturing conditions (70% formic acid) used for chemical cleavage, these results are in line with those of the 20 kDa chymotryptic fragments (Figure 3.5F and Figure 3.6E) indicating the increased stability to the N-terminal half of the molecule contributed by Lys-77.

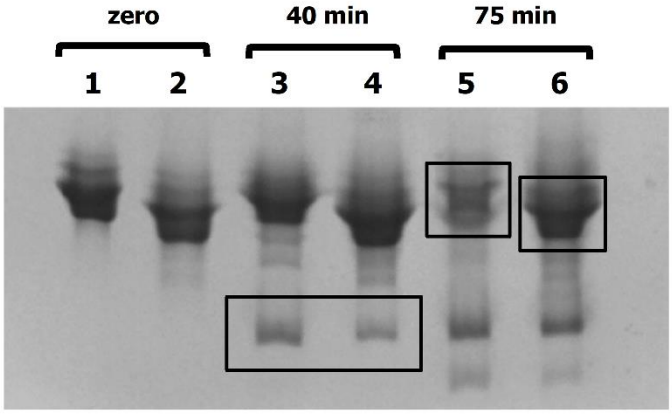

Figure 3.7. Effect of mutagenesis of residue-77 on the chymotrypsin susceptibility of CN1A (residues 11 - 127) fragments. Enzyme: substrate, 1: 250 mol: mol, temperature 25 ^{o}C and incubated for 75 min. Odd-numbered lanes, control CN1A (Thr-77) and even-numbered lanes, mutant CN1A (Lys-77). Note the differential breakdown of CN1A fragments at 75 min (lanes 5 and 6 boxed areas) and generation of more low molecular weight product at 40 min in the control CN1A sample compared to the mutant CN1A (indicated by boxes).

3.3.4.4 Trypsin digestion of non-heat treated intact proteins

Previous work has shown that Arg-133 is the primary site in rabbit Tpm 1.1(α) for trypsin digestion (Pato et al., 1981). Thus, trypsin is used to gauge the conformation of tropomyosin at a point that is ~ 35 amino acids farther upstream than Leu-169. Arginine-133 is conserved in salmon Tpm1 which also contains a susceptible site at Lys-6 (Goonasekara et al., 2007). To probe the accessibility of these residues in salmon Tpm1 the same approach is taken to that above (Figure 3.5 and Figure 3.6). For these incubations, the temperature is reduced to 10 ^{o}C owing to the large number of potential sites for trypsin.

In contrast to what is observed with chymotrypsin, trypsin digestion did not show a noticeable preference for the control Tpm1 vs. the mutant. Five time points are sampled over a 75 min period and similar rates of the breakdown of the two proteins are observed (Figures 3.8A and 3.8B). A number of peptides are detected on the gel, possibly due to the increased flexibility of salmon tropomyosin. At early times, a doublet is observed at the top of the gel (e.g., lanes 3 and 4) which is consistent with cleavage at Lys-6. But no attempt was made to sequence any of the products or to fine-tune the digestion conditions similar to what is presented in chapter 4, section 4.3.2.2 (comparison of phosphorylated and non-phosphorylated rabbit Tpm 1.1(α)).

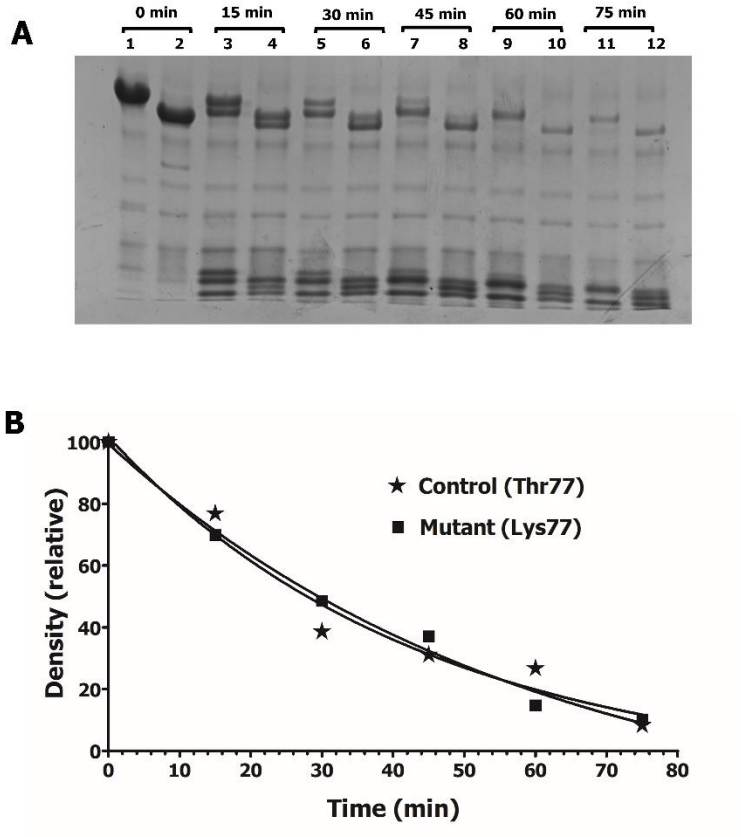

Figure 3.8. Effect of mutagenesis of residue-77 on the trypsin susceptibility of Atlantic salmon Tpm1. Recombinant non-mutant (control, Thr-77) and mutant (Lys-77) Tpm1s are digested side-by-side with trypsin (substrate, 2 mg/mL). SDS-PAGE shows the decline in the protein chain and subsequent generation of peptide fragments. The mol: mol ratio of enzyme: substrate, 1: 500 (10 ºC). (A) Control (Thr-77), odd-numbered lanes. Even-numbered mutant (Lys-77). (B) Densitometric analysis of A.

3.3.5 Interaction with Thin Filament Partners.

3.3.5.1 Troponin affinity chromatography

As established by previous researchers (Ohtsuki, 1979; Pearlstone & Smillie, 1982; Tanokura et al., 1983; Morris & Lehrer, 1984; Heeley et al., 1987; White et al., 1987; Yamada et al., 2020)**,** troponin T (TnT1) binds to either side of the overlap region of the tropomyosin filament (binding site 1) and troponin T (TnT2) to the central region of tropomyosin close to Cys-190 (binding site 2). Therefore, this lays the path to investigate the effect of the Thr-77 to Lys mutation on troponin binding (using affinity chromatography). In this regard in addition to non-mutant (control, Thr-77), mutant (Lys-77), and wild-type salmon Tpm1s, a double mutant with Gly-24 and Gly-27 replaced by Ala is used to further the understanding of the interaction at site 1.

Elution profiles from a troponin-Sepharose column are overlaid in Figure 3.9 for comparison. All experiments are carried out at 5 ^{o}C. Profiles are non-overlapping indicating differences in affinity. The conductivities of the fractions of peak A_{595} absorption, ~ 7.2 mS/cm (recombinant control (Thr-77) Tpm1) compared to 6.2 mS/cm (mutant (Lys-77) Tpm1), is equivalent to five fractions. Such a displacement represents a significant difference in elution behavior and by inference, the mutation is seen to weaken the interaction. Thus, recombinant control Tpm1 binds more tightly to troponin than mutant (Lys-77) Tpm1. Comparison of wild-type to the control reveals a peak A_{595} absorption, ~ 10.4 mS/cm with a noticeable rightwards shift (15 fractions compared to the recombinant control). This is suggestive of the crucial role of the only difference between the control and the wild-type, N-terminal acetylation. The protonated alpha-amino group of Met-1(a)

is thought to result in localized unfolding because the positive charge falls in a core position (Monteiro et al., 1994). In addition, it is possible that Gly-24 and Gly-27 of salmon Tpm1 further destabilize the coiled-coil at the N-terminus (possibly) close to binding site 1 in the absence of acetylation. Analysis of peak A_{595} absorption, ~ 7.8 mS/cm (three fractions compared to the control) of the double mutant (Ala-24 and Ala-27) reveals that the troponin affinity can be rescued by replacing the destabilizing Glys that are already located in a destabilized cluster Lys15-Ala18-Ala22-Ala25-Lys29-Ala32-Ser36.

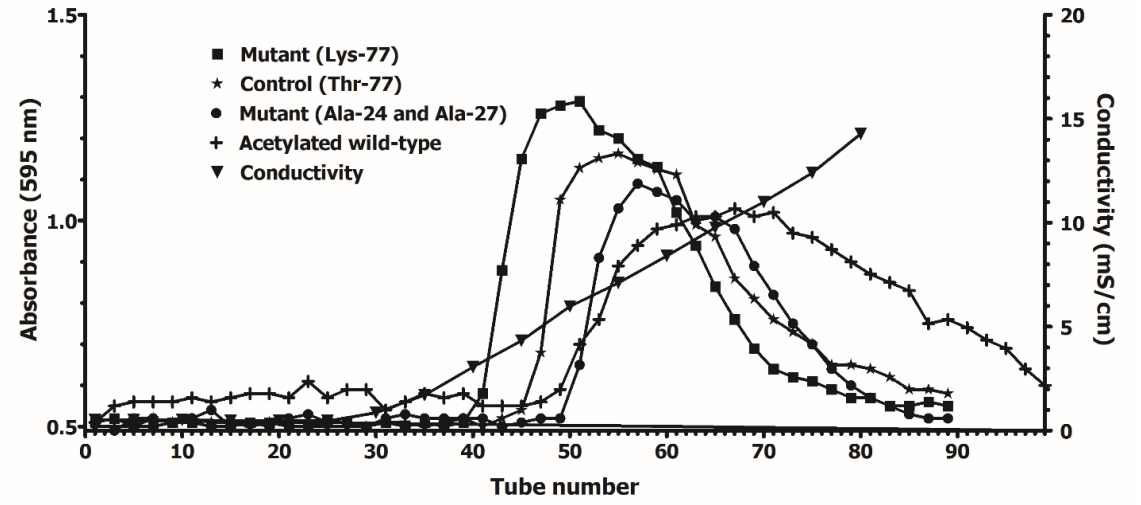

Figure 3.9. Affinity chromatography of Atlantic salmon Tpm1 on troponin-Sepharose 4B. All steps are carried out in a cold room (10 ^{o}C). The column was packed with rabbit skeletal troponin-Sepharose 4B and equilibrated in a low ionic strength buffer containing 1 mM EGTA. A given Tpm1 (either recombinant or wild-type) was separately passed through the same column on three consecutive days with one experiment per day. No protein is detected in the flow-through. Elution profiles are superimposed for comparison. Stars, control (Thr-77). Squares, mutant (Lys-77). Circles, double mutant (Ala-24 and Ala-27). Plus sign, acetylated wild-type. Triangles, conductivity (protein detection is by Bradford reagent A_{595}). The slope of the NaCl gradient expressed as the conductivity measured at room temperature is 0.34 mS/cm per fraction. Control (Thr-77): start of elution, 45th fraction; end 85th and conductivity at highest A_{595}, 7.2 mS/cm. Mutant (Lys-77): start of elution, 40th fraction; end 75th and conductivity at highest A_{595}, 6.2 mS/cm. Acetylated wild-type: start of elution, 50th fraction; ends beyond 100th and conductivity at highest A_{595}, ~10.4 mS/cm. The double mutant (Ala-24 and 27): start of elution, 50th fraction; end 85th and conductivity at highest A_{595}, 7.8 mS/cm. Fractions on either side of the fraction having the highest absorption reading were analyzed by SDS-PAGE. There is good agreement between the fraction that yielded the thickest gel band after staining with Coomassie and the results of the Bradford assay. Based on the peak absorbances, the displacement in elution compared to the control (Thr-77) : mutant (Lys-77), 1.8 mS/cm which is equivalent to five fractions or 9 mL; acetylated wild-type, 15 fractions or 27 mL and double mutant (Ala-24 and 27), three fractions or 5.4 mL. Adapted with permission from Silva, A. M. M., Ige, T., Goonasekara, C. L., & Heeley, D. H. (2020a). Threonine-77 Is a Determinant of the Low-Temperature Conditioning of the Most Abundant Isoform of Tropomyosin in Atlantic Salmon. Biochemistry, 59(31), 2859–2869. https://doi.org/10.1021/acs.biochem.0c00416. Copyright (2021) American Chemical Society.

3.3.5.2 F-actin affinity

The complexation of wild-type (acetylated) salmon Tpm1 (alpha-fast) and F-actin at 4 ^{o}C and 22 ^{o}C is investigated by sedimentation assay. Owing to the tight affinity between tropomyosin and F-actin, sub-maximal conditions of ionic strength (30mM KCl, 1mM $MgCl_2$, 0.1mM EGTA, 0.2mM ATP) are employed. The electrophoretic analysis of mixtures before and after centrifugation in a typical experiment is depicted in Figure 3.10A. Samples are paired to facilitate comparison. Analysis of the SDS-PAGE based on the intensity of staining of the actin-containing bands (Figure 3.10A lower gel) reveals that nearly all of the F-actin has sedimented. Further, it is demonstrated that a comparatively smaller fraction of tropomyosin remains in the supernatant at the lower temperature, i.e., for example, at a starting concentration of 0.25 µM (left-hand side of Figure 3.10A) no tropomyosin is detected in the 4 ^{o}C supernatant but it is present in the 22 ^{o}C supernatant. At twice the concentration, i.e. 0.5 µM, again a difference in the amount of unbound ligand is evident by visual inspection. Thus, the SDS-PAGE analysis provides a direct and clear illustration of the effect of temperature. Binding curves are presented in Figures 3.10B (non-normalized) and 3.10C (normalized) with the aid of a calibrated relationship (Figure 3.10C inset). The estimated apparent K_Ds are: 0.1 µM (4 ^{o}C) and 0.5 µM (22 ^{o}C), five-folds of a difference. Another observation concerning the two curves is that both plateau (~ 0.11 mole per mole) at a lower mole ratio than expected. This is attributed to the limitation of a densitometric method of determination (even with calibration). One advantage, however, is that it avoids radioactive labeling, which given the conformational sensitivity of salmon tropomyosin **(**Figure 3.10A**)** may have altered its actin-binding properties.

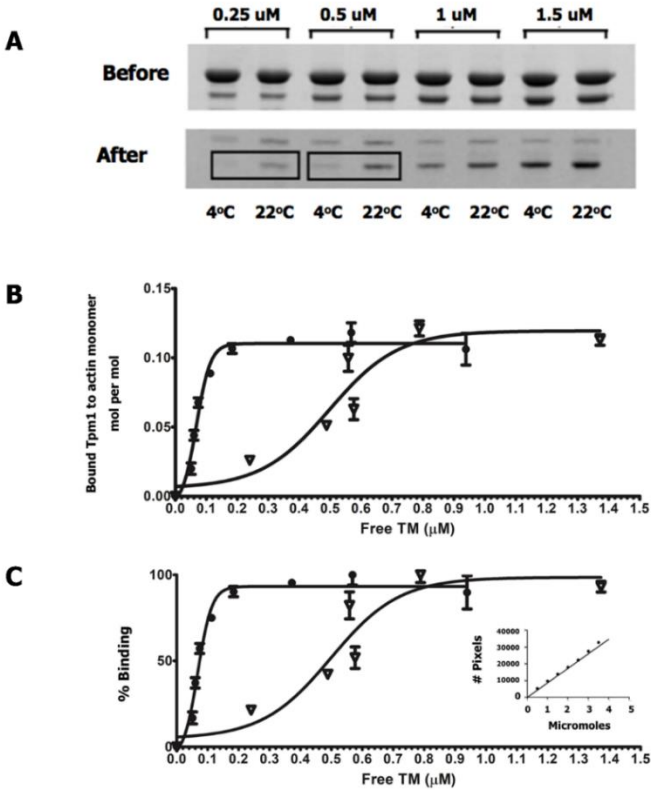

Figure 3.10. Effect of temperature on the affinity of wild-type Atlantic salmon Tpm1 (alpha-fast) for rabbit F-actin. Temperature (either 4 ^{o}C or 22 ^{o}C) and concentrations are indicated (buffer 10mM MOPS, 30mM KCl, 1mM $MgCl_2$, 0.1mM EGTA, 0.2mM ATP, 1mM DTT, pH 7). Binding mixtures were analyzed by SDS-PAGE. The concentration of tropomyosin is varied from 0.25 - 4 μM while F-actin is maintained at 10 μM. Proteins are wild-type (acetylated) salmon Tpm1 and rabbit skeletal actin, 10 μM. Rabbit skeletal actin and salmon fast skeletal actin (accession, AF304406) share four substitutions, residues 2, 278, 299, and 354. (A) SDS-PAGE of acto-tropomyosin 4 ^{o}C (lanes 1, 2, 5 and 6) and 22 ^{o}C (lanes 3, 4, 7 and 8) sedimentation. Upper band, actin. Lower band, tropomyosin. Highlighted lanes 1 vs. 2 and 3 vs. 4 demonstrate that a comparatively less amount of Tpm1 remains in the supernatant at 4 ^{o}C sedimentation indicating a greater degree of complexation. (B) Raw data. Circles, 4 ^{o}C; triangles, 22 ^{o}C. Stoichiometry is calculated assuming 100% sedimentation of F-actin and with the aid of a calibration relationship. (C) Normalized binding curves from B. Inset, calibrated densitometric relationship constructed using wild-type salmon Tpm1. The apparent K_Ds are: 0.1 μM (4 ^{o}C) and 0.5 μM (22 ^{o}C). Each data point is the average of two experiments. Adapted with permission from Silva, A. M. M., Ige, T., Goonasekara, C. L., & Heeley, D. H. (2020a). Threonine-77 Is a Determinant of the Low-Temperature Conditioning of the Most Abundant Isoform of Tropomyosin in Atlantic Salmon. Biochemistry, 59(31), 2859–2869. https://doi.org/10.1021/acs.biochem.0c00416. Copyright (2021) American Chemical Society.

3.2.6 Molecular Visualization

3.2.6.1 Ion-pairing interactions involving residue-77

Of those species surveyed in Table 1, only Atlantic salmon tropomyosin possesses a neutral side-chain, threonine, instead of lysine in position-77. As recognized in the first tropomyosin sequence (Stone & Smillie, 1978) the ‘inner’ heptad positions contain a high proportion of negatively charged “e” and positively charged “g” groups. A parallel arrangement of helices allows for ionic interactions between such groups on opposing helices (Parry, 1975). In this vein, the expectation is that residue-77(g) is juxtaposed with the “e” residue in the next heptad, which is Glu-82 (Figure 3.11). Significantly, Glu-82(e) are conserved as is Asp-80(c) (Table 3.1). Thus, favorable electrostatic interactions between (Parry, 1975) and within helices (Sano et al., 2020) are expected to be missing from the protein in Atlantic salmon.

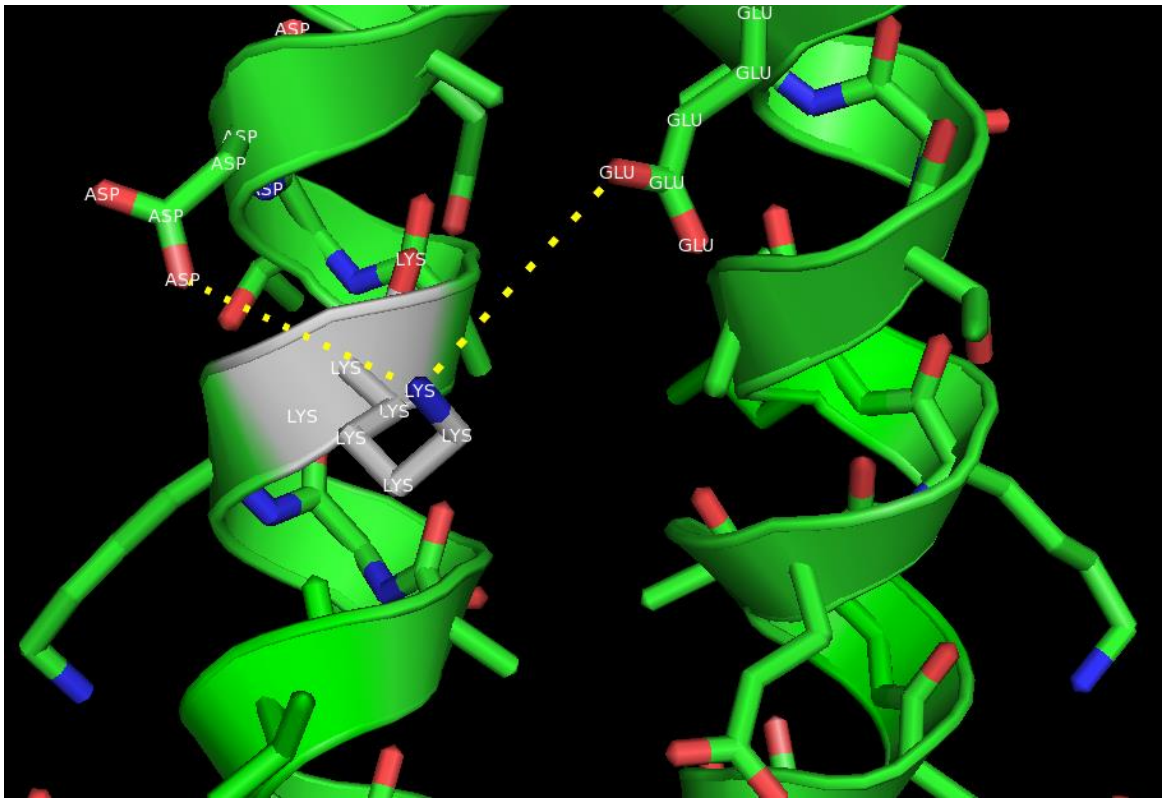

Figure 3.11. Putative ion-pairing interactions involving Lys-77(g), Asp-80(c), and Glu-82(e). The model is based on the 7 Angstrom structure (Whitby and Phillips 2000). Interatomic distances are not presented due to values being less than the resolution. Adapted with permission from Silva, A. M. M., Ige, T., Goonasekara, C. L., & Heeley, D. H. (2020a). Threonine-77 Is a Determinant of the Low-Temperature Conditioning of the Most Abundant Isoform of Tropomyosin in Atlantic Salmon. Biochemistry, 59(31), 2859–2869. https://doi.org/10.1021/acs.biochem.0c00416. Copyright (2021) American Chemical Society.

3.2.6.2 Comparison of the N-terminal destabilized cluster.

The alpha isoform of tropomyosin in fast skeletal muscle is the most plentiful form of protein in every vertebrate studied to date. According to the previously determined structure of a fragment of tropomyosin (Brown et al., 2001) and analysis of stabilizing and destabilizing amino acids in the core (Kwok & Hodges, 2004), a major destabilized cluster Lys15-Ala18-Ala22-Ala25-Lys29-Ala32-Ser36 was identified close to the N-terminus (conserved in the rabbit, human, and chicken sequences). Analysis of the salmon sequence (Heeley et al., 1995) reveals two Gly residues, namely Gly-24 and Gly-27 that fall into this region (Figure 3.12) which are missing from the other counterparts. Such positioning of Glys can induce further destabilization in the cluster that may be favorable at a lower temperature.

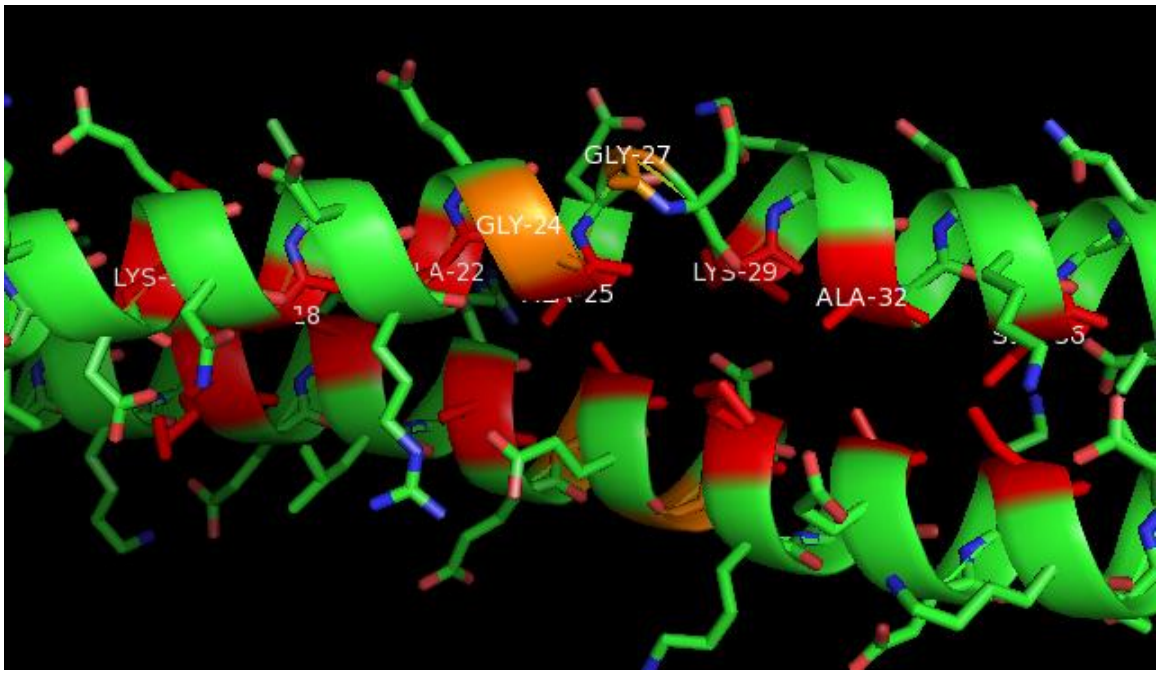

Figure 3.12. PyMOL visualization of destabilized cluster Lys15-Ala18-Ala22-Ala25-Lys29-Ala32-Ser36 region of Atlantic salmon Tpm1. Destabilized cluster highlighted in red. The Gly-24 and Gly-27 are highlighted in orange showing a localized unraveling in the helical structure.

3.4 Chapter 3 Discussion

Flexibility goes hand-in-hand with tropomyosin being a thin filament building block and a mobile regulator (Pirani et al., 2005; Risi et al., 2017 and references therein). But how is this property maintained in psychrophilic homologs? The question allows the identification of those regions in tropomyosin where flexibility is most needed (Hayley et al., 2011). In this regard, the Atlantic salmon *(Salmo salar)* serves as a very good model. The heat-induced unfolding of the most abundant tropomyosin isoform, Tpm1 (alpha-fast), occurs over a lower range of temperatures compared to warm-blooded homologs. This includes non-cooperative as well as cooperative processes (Figure 3.3A), and points to the presence of an additional set of destabilizing amino acids. In this regard, the sole core substitution threonine-179(a) and more surprisingly, a unique glycyl pair at residues 24 and 27 have been identified (Fudge & Heeley, 2015). Presented here is the investigation of a third source of instability that involves an amino acid with a neutral side-chain, threonine-77(g), in the second alanine cluster (Singh & Hitchcock-DeGregori, 2003), that can annul ionic interactions with proximal carboxylates (Figure 3.11) that would otherwise instigate a long-distance molecular rearrangement that reaches into the fifth Ala cluster (Singh & Hitchcock-DeGregori, 2007). The main results of this chapter are as follows. The presence of a neutral side chain at residue-77: (i) destabilizes the N-terminal half of Atlantic salmon Tpm1; (ii) affects the rate of proteolysis at a site ~100 amino acids away at, Leu-169 and (iii) assists in the maintenance of the quaternary structure necessary for regulatory function. These findings will now be discussed in turn.

Mesophilic tropomyosins are broadly divided into an N-domain of higher stability and a C-domain of lower stability (Woods, 1977; Edwards and Sykes, 1980; Phillips et al., 1980; Smillie et al., 1980; Morris & Lehrer, 1984; Ishii & Lehrer, 1986) which is demonstrated by the difference between the melting temperatures of the respective CNBr fragments, ΔT_m = 15 ^oC (Williams & Swenson, 1981). On the contrary, salmon CN1A and CN1B exhibit a much narrower ΔT_m (Table 3.2) (Goonasekara & Heeley, 2008), which is largely attributed to the natural replacement of lysine-77 by threonine (Table 3.1). For example, the reversal of this substitution raises the melting temperature of salmon CN1A (Lys-77) by 13 ^oC (Figure 3.4 & Table 3.2) bringing it into line with that of rabbit CN1A (Williams & Swenson, 1981). As the mutation affects the regions of salmon Tpm1 that are observed to unfold cooperatively (Figure 3.4A), it can be inferred that the effect of residue-77 extends over more than just the CN1A portion of the molecule.

Of the two cooperative unfolding domains observed for salmon Tpm1, the main transition, which is also the more stable of the two, can be assigned to sequences within the CN1A and aromatic-rich regions (residues 162 - 267) of the molecule. The heterogeneity (Table 3.1) has also created a minor transition with the lowest melting temperatures documented for vertebrate sarcomeric tropomyosin at neutral pH (0.1 M KCl, reducing conditions). Barely stable at room temperature, this part of salmon Tpm1 does not fully reform after heat-denaturation. At the present in combination with calorimetry results of mutant Ala-24 and Ala-27 (Figure 3E), it is assumed that the instability arises from the major destabilized cluster Lys15-Ala18-Ala22-Ala25-Lys29-Ala32-Ser36 along with the two closely-spaced glycines at 24 and 27 that add further destabilization perhaps in combination with effect

from Thr-77. Either way, this is a simplified view of a multi-step process consisting of non-cooperative and cooperative phases (Edwards & Sykes, 1980; Ishii & Lehrer, 1986; Potekhin & Privalov, 1982; Williams & Swenson, 1981), both of which may be sensitive to destabilizing amino acids.

Long-range communication within the molecule is observed with the help of limited proteolysis. The method allows the identification of peptide bonds whose solvent exposure is sensitive to amino acid substitutions. Leucine-169(a) is the primary chymotrypsin digestion site in mammalian Tpm (Pato et al., 1981), due to its situation in a conserved tetrapeptide that contains four bulky side-chains, Leu-169-Val-Ile-Ile-172, that is flanked by the repulsive pairing of Asp-175(g) and Glu-180(e) (Stone & Smillie, 1978). Other contributing factors include its proximity to residue 179(a) - Ala in the mammal, Thr in salmon (Fudge & Heeley, 2015; Heeley et al., 1995), and the charged core residue Asp-137(d). On the contrary, the preferred chymotrypsin cleavage site in recombinant salmon Tpm1 (alpha-fast) is Leu-11 - Lys-12 followed by Leu-169 - Val-170 (Figure 3.5H). The shift in the primary digestion site is explained by the two glycines mentioned above as well as by the lack of amino-terminal acetylation (Goonasekara et al., 2007). While the rate of scission at Leu-11, some 65 residues upstream, is insensitive to the presence of a positive charge in position 77 (Figures 3.5B and 3.5C), the downstream site, Leu-169 that is ~ 90 amino acids away, is intensely sensitive (Figures 3.5A, 3.5D - 3.5G). Astonishingly, the mutation (Thr-77 to Lys) has a profound effect on a scission site that is more than 90 amino acids away. The region between residues 77 - 169 incorporates the stability control region (residues 97 - 118) (Hodges et al., 2009; Kirwan & Hodges, 2010) and infiltrates into the

primary actin-binding period 5 (residues 166 - 189) (Singh & Hitchcock-DeGregori, 2007) as well as the site of troponin core attachment (White et al., 1987). In combination with the results of thermal unfolding, it can be concluded that the influence of residue-77 will almost certainly extend farther in the sequence. The results from trypsin digestion show no comparable differences in breaking down (Figure 3.8), compared to the differences in the rate of digestion observed for phosphorylated and unphosphorylated rabbit Tpm 1.1(α) (chapter 4 results section 4.3.2.2 for comparison of phosphorylated and non-phosphorylated rabbit Tpm 1.1(α) with trypsin). The above observations suggest that salmon Tpm1 has a higher flexibility and a greater temperature sensitivity compared to the mesophilic homolog,

Tropomyosin provides binding sites for the T subunit of troponin in two locations. Troponin T (TnT1) stretches across the tropomyosin overlap region (binding site 1) and troponin T (TnT2) binds to the central region close to Cys-190 (binding site 2) (Ohtsuki, 1979; Pearlstone & Smillie, 1982; Tanokura et al., 1983; Morris & Lehrer, 1984; Heeley et al., 1987; White et al., 1987; Yamada et al., 2020 and Oda et al., 2020). The TnT structure is highly elongated and extends from Gly-199 of TnT1 (199 - 272) across the actin filament down towards the tropomyosin molecule on the other actin strand to form an α-helical cross brace with the head-to-tail junction (Yamada et al., 2020 and Oda et al., 2020). Similar to tropomyosin, the troponin complex also spans seven actin monomers, where the upper four actin units bind to the C-terminal part of TnI and the troponin core while the lower three of the opposite actin strand bind to the N-terminal part of TnT (Yamada et al., 2020). Attachment at tropomyosin binding site 1 involves residues 59 - 97 in the N-terminal

section and recent cryo-EM structures reveal that binding site 2 involves the C-terminal third of TnT, notably residues 159 - 259 (numbering system for rabbit fast skeletal isoform) (Jin & Chong, 2010). Since a large number of Lys and Arg contribute to the amino acid content in these sections of TnT (Jin & Chong, 2010), interaction with tropomyosin is expected to involve a significant number of electrostatic components, which is also evident through the NaCl gradient involved in elution from troponin-Sepharose (Figure 3.9). Noticeably, Atlantic salmon contains every positive charge conserved in the corresponding section of rabbit fast skeletal TnT (accession, AF072687). The observed tighter binding of control Tpm1 (Thr-77) to the affinity medium compared to the mutant (Lys-77) (Figure 3.4) is consistent with the middle of salmon (Thr-77) Tpm1 adopting a more open configuration, one that is less resistant to protease (Figure 3.5) and heat (Figure 3.3D). Increased affinity of the wild-type Tpm1 demonstrates the crucial role of acetylation in stabilizing the N-terminal part of the molecule which is lacking in the recombinant proteins. The two glycines at residues 24 and 27 are a mode of additional flexibility (destabilization), which is consistent with the helix breaking properties of this amino acid (Richardson & Richardson, 1988). This feature would not be needed in the mesophilic tropomyosins which function at > 30 ^{o}C. Additionally, it is shown that in the presence of Gly-24 and Gly-27, and the absence of acetylation, flexibility increases to the extent that there is a reduction in the specificity of troponin binding. This result highlights the importance of optimum flexibility where too much flexibility otherwise will be detrimental to the function of the molecule. In view of the results presented in Figure 3.9, the affinity of troponin for site 1 on tropomyosin is influenced by beneficial destabilization of the N-terminal coiled-coil structure (Figure 3.9).

In the winter, the ambient temperature encountered by Atlantic salmon is more than 30 ^{o}C lower than that of mammals. Such frigid conditions present a potential problem for the formation as well as for the function of thin filaments because molecules lose mobility with decreasing temperature and become more rigid. The tight association of salmon Tpm1 with F-actin that is demonstrated in Figure 3.10 is strong evidence for salmon Tpm1 not being overly rigid at 4 ^{o}C. For optimum interaction, it is necessary for the coiled-coil to adopt a gently undulating shape in order to match the helical curvature of actin (Phillips, 1986; Orzechowski et al., 2014). To acquire this at lower temperatures, tropomyosin must possess the requisite flexibility. Of the amino acids that make this practicable, the present findings point to Thr-77 as playing a prominent role. Significantly, residue-77 falls in the second alanine cluster and as inferred by mutation is capable of inducing a long-range rearrangement that reaches the fifth alanine cluster, (as evidenced by a change in proteolytic susceptibility at Leu-169, Figure 3.5). Additionally, these alanine clusters merge with the residues in the 2nd (47 - 88) and 5th (166 - 189) actin-binding periods (Yamauchi-Takihara et al., 1996; Tobacman & Butters, 2000; Singh & Hitchcock-DeGregori, 2007). The weaker binding which is observed at 22 ^{o}C (Figure 3.10), a temperature near to the minor transition (Table 3.2), again is indicative of excessive flexibility which reduces the conformational specificity of the respective binding sites.

Interestingly, over the same temperature range, the affinity of mammalian tropomyosin for F-actin decreases with decreasing temperature (Drabikowski & Gergely, 1962) which is a beneficial feature during enrichment, pointing out the fact that the destabilizing alanine clusters (Brown et al., 2001; Kwok & Hodges, 2004) alone are insufficient to overcome the

cold-induced rigidity. Lacking the additional set of irregularities that exist in the Atlantic salmon counterpart, rigidity hinders the winding of mammalian tropomyosin around actin at low temperatures. Atlantic salmon tropomyosin additionally possessing Ala179Thr and Lys77Thr presents a broader set of flexibility-enhancing amino acids. Hence, we propose that these residues, both locally and remotely, aid the formation, and functioning, of thin filaments at temperatures below 10 ^{o}C.

Additionally, residue-77 can be used in understanding clinical manifestations of cardiomyopathies. The natural replacement of Lys-77 by Thr bears resemblance with a human missense cardiomyopathy mutation, one heptad unit upstream, Lys70(g)Thr (Heller et al., 2003). In that case, a neutral side-chain leads to destabilization (Hilario et al., 2004; Zheng et al., 2016), decreased affinity for F-actin (Yamauchi-Takihara et al., 1996), changed Ca^{2+} dependent activation of the thin filament as well as a severe clinical outcome (Heller et al., 2003). The current study brings a better understanding of the fact that an exchange of amino acid deleterious in one vertebrate group could be advantageous in another (Hayley et al., 2011), once more asserting the delicate balance between tropomyosin stability and function (Hitchcock-DeGregori & Singh, 2010).

In summary, experiments in this chapter demonstrate an additional strategy, specifically the insertion of a threonine instead of lysine in residue position 77, to preserve the flexibility of a simple coiled-coil protein. As a result, the most abundant isoform of tropomyosin in Atlantic salmon deviates slightly from its blueprint in order to transmit the beneficial structural perturbations over a long-range. As demonstrated before (Fudge & Heeley, 2015) and in the current study (Figure 3.9), the influence of glycines 24 and 27 extend to the

merger and that of Thr-77 reaches at least to Leu-169 (Figure 3.5) spanning through essential actin-binding periods 2 (Heald & Hitchcock-DeGregori, 1988) and 5 (Singh & Hitchcock-Degregori, 2006).

3.5 Chapter 3 Future directions

1) The basis of the low-temperature affinity of salmon Tpm1 for F-actin (Figure 3.10) can be investigated additional by mutagenesis. Firstly, a short N-terminal extension is needed to deal with the problem of unacetylation which disrupts the self-polymerization of tropomyosin and drastically weakens its affinity for actin (Hitchcock-DeGregori & Heald, 1987). Both properties are restored by fusion of a di- or tripeptide (Monteiro et al., 1994; Urbancikova & Hitchcock-DeGregori, 1994) as proposed in Figure 3.13. Incorporation of the N-terminal extension to the following mutations - Gly24,27Ala and Thr77Lys will allow a greater understanding of their effect on self-polymerization at different temperatures that can be analyzed using capillary flow viscometry (Heeley et al., 1995). Such measurements would go hand-in-hand with reemploying our established protocol (section 3.2.6) to measure the F-actin affinity of the extended mutant Tpm1s.

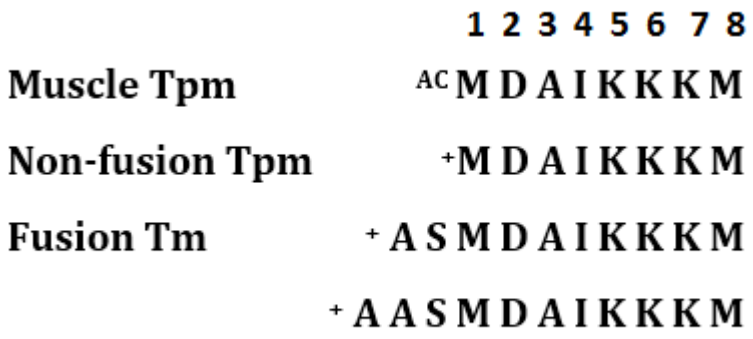

Figure 3.13. Schematic diagram of di and tri peptide fusions to the N-terminal region.

2) Since the mutations Thr77Lys, Gly24,27Ala and Thr179Ala affect the interaction of salmon Tpm1 with troponin (Figure 3.9) it will also be interesting to look at thin filament regulation. Specifically, to measure the steady-state MgATPase activity of reconstituted muscle systems (actin+troponin+tropomyosin+myosin S1) as a function of protein concentration and Ca(II) and rigor-myosin concentrations.

3) The greater stability of the Lys-77 Tpm1 mutant compared to the control (Thr-77) (Figure 3.3A and Table 3.3) is proposed to be the outcome of electrostatic interactions between Lys-77(g) and Glu-82(e) and to a lesser extent Asp-80(c). One way to test this postulate would be to annul (by alanine replacement) pairings between Lys-77 and residue-80(c) on the same strand and Lys-77 and residue-82(e) on the adjacent chain. This would involve generating double mutants of Tmp1 namely Thr77Lys + Asp80Ala and Thr77Lys + Glu82Ala and a triple mutant in which both carboxylates are switched, specifically Thr77Lys + Asp80Ala + Glu82Ala. Analysis of the thermal and proteolytic stabilities of the mutants, as described previously in this chapter, would shed light on the interactions that Lys-77 participates in and which are so influential.

3.6 Chapter 3 References

Bone, Q., Marshall, N. B., & Blaxter, J. H. S. (1995). *Biology of Fishes* (2nd ed.). Chapman & HaU in 1995. https://doi.org/10.1007/978-1-4615-2664-3

Bradford, M. M. (1976). A rapid and sensitive method for the quantitation of microgram quantities of protein utilizing the principle of protein-dye binding. *Analytical Biochemistry*, *72*(1), 248–254. https://doi.org/https://doi.org/10.1016/0003-2697(76)90527-3

Brisson, J. R., Golosinska, K., Smillie, L. B., & Sykes, B. D. (1986). Interaction of tropomyosin and troponin T: a proton nuclear magnetic resonance study. *Biochemistry*, *25*(16), 4548–4555. https://doi.org/10.1021/bi00364a014

Brown, J. H., Kim, K. H., Jun, G., Greenfield, N. J., Dominguez, R., Volkmann, N., Hitchcock-DeGregori, S. E., & Cohen, C. (2001). Deciphering the design of the tropomyosin molecule. *Proceedings of the National Academy of Sciences of the United States of America*, *98*(15), 8496–8501. https://doi.org/10.1073/pnas.131219198

Cambillau, C., & Claverie, J. M. (2000). Structural and genomic correlates of hyperthermostability. *The Journal of Biological Chemistry*, *275*(42), 32383–32386. https://doi.org/10.1074/jbc.C000497200

Crick, F. H. C. (1953). The packing of α-helices: simple coiled-coils. *Acta Crystallographica*, *6*(8), 689–697. https://doi.org/10.1107/s0365110x53001964

D'Amico, S., Claverie, P., Collins, T., Georlette, D., Gratia, E., Hoyoux, A., Meuwis, M. A., Feller, G., Gerday, C., Marahiel, M. A., Russell, R., Warren, G., & Davies, P. L. (2002). Molecular basis of cold adaptation. *Philosophical Transactions of the Royal Society B: Biological Sciences*, *357*(1423), 917–925. https://doi.org/10.1098/rstb.2002.1105

Davail, S., Feller, G., Narinx, E., & Gerday, C. (1994). Cold adaptation of proteins. Purification, characterization, and sequence of the heat-labile subtilisin from the Antarctic psychrophile Bacillus TA41. *The Journal of Biological Chemistry*, *269*(26), 17448–17453. https://doi.org/10.1016/s0021-9258(17)32460-2

Deniz, A. A. (2018). Remote wiggling helps cold enzymes work seas affect each other. *Nature*, *558*(2016), 195–196.

Drabikowski, W., & Gergely, J. (1962). The Effect of the Temperature of Extraction on the Tropomyosin Content in Actin. *The Journal of Biological Chemistry*, *237*(11), 3412–3417. https://doi.org/10.1016/s0021-9258(19)70831-x

Edwards, B. F. P., and Sykes, B. D. (. (1980). Nuclear magnetic resonance evidence for the coexistence of several conformational states of rabbit cardiac and skeletal tropomyosins. *Biochemistry*, *19*, 2577 – 2583.

Edwards, B. F. P., & Sykes, B. D. (1981). Analysis of Cooperativity Observed in pH Titrations of Proton Nuclear Magnetic Resonances of Histidine Residues of Rabbit Cardiac Tropomyosin. *Biochemistry*, *20*(14), 4193–4198. https://doi.org/10.1021/bi00517a037

Fudge, K. R., & Heeley, D. H. (2015). Biochemical characterization of the roles of glycines 24 and 27 and threonine 179 in tropomyosin from the fast skeletal trunk muscle of the Atlantic salmon. *Biochemistry*, *54*(17), 2769–2776. https://doi.org/10.1021/acs.biochem.5b00156

Gianese, G., Bossa, F., & Pascarella, S. (2002). Comparative structural analysis of psychrophilic and meso- and thermophilic enzymes. *Proteins: Structure, Function and Genetics*, *47*(2), 236–249. https://doi.org/10.1002/prot.10084

Goonasekara, C. L., Gallivan, L. J., Jackman, D. M., & Heeley, D. H. (2007). Some binding properties of Omp T digested muscle tropomyosin. *Journal of Muscle Research and Cell Motility*, *28*(2–3), 175–182. https://doi.org/10.1007/s10974-007-9114-9

Goonasekara, C. L., & Heeley, D. H. (2008). Conformational properties of striated muscle tropomyosins from some salmonid fishes. *Journal of Muscle Research and Cell Motility*, *29*(2–5), 135–143. https://doi.org/10.1007/s10974-008-9148-7

Goonasekara, C. L., & Heeley, D. H. (2009). Effect of Removing the Amino-Terminal Hexapeptide of Tropomyosin on the Properties of the Thin Filament. *Biochemistry*, *48*(15), 3538–3544. https://doi.org/10.1021/bi802004j

Graceffa, P. (1992). Heat-treated smooth muscle tropomyosin. *Biochim. Biophys. Acta.*, *1120*, 205–207.

Greaves, R. B., & Warwicker, J. (2009). Stability and solubility of proteins from extremophiles. *Biochemical and Biophysical Research Communications*, *380*(3),

581–585. https://doi.org/10.1016/j.bbrc.2009.01.145

Greenfield, N. J., & Hitchcock-DeGregori, S. E. (1995). The Stability of Tropomyosin, a Two-Stranded Coiled-Coil Protein, Is Primarily a Function of the Hydrophobicity of Residues at the Helix-Helix Interface. *Biochemistry*, *34*(51), 16797–16805. https://doi.org/10.1021/bi00051a030

Greenfield, N. J., Palm, T., & Hitchcock-DeGregori, S. E. (2002). Structure and interactions of the carboxyl terminus of striated muscle α-tropomyosin: It is important to be flexible. *Biophysical Journal*, *83*(5), 2754–2766. https://doi.org/10.1016/S0006-3495(02)75285-5

Hayley, M., Chevaldina, T., & Heeley, D. H. (2011). Cold adaptation of tropomyosin. *Biochemistry*, *50*(30), 6559–6566. https://doi.org/10.1021/bi200327g

Heald, R. W., & Hitchcock-DeGregori, S. E. (1988). The structure of the amino terminus of tropomyosin is critical for binding to actin in the absence and presence of troponin. *Journal of Biological Chemistry*, *263*(11), 5254–5259. https://doi.org/10.1016/s0021-9258(18)60708-2

Heeley, D.H., Bieger, T., Waddleton, D.M., Hong, C., Jackman, D.M., McGowan, C., Davidson, W.S. and Beavis, R. C. (1995). Characterisation of fast, slow and cardiac muscle tropomyosin from salmonid fish. *Eur J. Biochem.*, *232*, 226 – 234.

Heeley, D.H., Golosinska, K., Smillie, L. B. (1987). The effects of troponin-T fragments T1 and T2 on the binding of non-polymerisable tropomyosin to F-actin in the presence and absence of troponins - I and -C. *J. Biol. Chem.*, *262*, 9971 –9978.

Heeley, D. H., Bieger, T., Waddleton, D. M., Hong, C., Jackman, D. M., McGowan, C., Davidson, W. S., & Beavis, R. C. (1995). Characterisation of fast, slow and cardiac muscle tropomyosins from salmonid fish. *European Journal of Biochemistry*, *232*(1), 226–234. https://doi.org/10.1111/j.1432-1033.1995.tb20803.x

Heeley, D. H., & Lohmeier-Vogel, E. M. (2016). Biochemical Comparison of Rabbit Skeletal Muscle Alpha and Beta Tropomyosin Isoforms. *Biophysical Journal*, *110*(3), 276a. https://doi.org/10.1016/j.bpj.2015.11.1497

Heller, M. J., Nili, M., Homsher, E., & Tobacman, L. S. (2003). Cardiomyopathic Tropomyosin Mutations that Increase Thin Filament Ca^{2+} Sensitivity and Tropomyosin N-domain Flexibility. *The Journal of Biological Chemistry*, *278*(43), 41742–41748. https://doi.org/10.1074/jbc.M303408200

Hilario, E., da Silva, S. L. F., Ramos, C. H. I. and Bertolini, M. C. (2004). Effects of cardiomyopathic mutations on the biochemical and biophysical properties of the human alpha-tropomyosin. *European Journal of Biochemistry*, *271*, 4132 – 4140.

Hitchcock-DeGregori, S. E., & Heald, R. W. (1987). Altered actin and troponin binding of amino-terminal variants of chicken striated muscle alpha-tropomyosin expressed in *Escherichia coli. The Journal of Biological Chemistry*, *262*(20), 9730–9735.

Hitchcock-DeGregori, S. E., & Singh, A. (2010). What makes tropomyosin an actin binding protein? A perspective. *Journal of Structural Biology*, *170*(2), 319–324. https://doi.org/10.1016/j.jsb.2009.12.013

Hodges, R.S., Sodek, J., Smillie, L.B. and Jurasek, L. (1972). Tropomyosin: Amino acid

sequence and coiled-coil structure. *Cold Spring Harbor Symp. Quant. Biol.*, *37*, 299 – 310.

Hodges, R. S., Mills, J., McReynolds, S., Kirwan, J. P., Tripet, B., & Osguthorpe, D. (2009). Identification of a Unique "Stability Control Region" that Controls Protein Stability of Tropomyosin: A Two-stranded α-Helical Coiled-coil. *Journal of Molecular Biology*, *392*(3), 747–762. https://doi.org/10.1016/j.jmb.2009.07.039

Houk, T. W., & Ue, K. (1974). The measurement of actin concentration in solution: A comparison of methods. *Analytical Biochemistry*, *62*(1), 66–74. https://doi.org/https://doi.org/10.1016/0003-2697(74)90367-4

Ishii, Y., & Lehrer, S. S. (1986). Effects of the state of the succinimido-ring on the fluorescence and structural properties of pyrene maleimide-labeled alpha alpha-tropomyosin. *Biophysical Journal*, *50*(1), 75–80. https://doi.org/10.1016/S0006-3495(86)83440-3

Jin, J. P., & Chong, S. M. (2010). Localization of the two tropomyosin-binding sites of troponin T. *Archives of Biochemistry and Biophysics*, *500*(2), 144–150. https://doi.org/10.1016/j.abb.2010.06.001

Kirwan, J. P., & Hodges, R. S. (2010). Critical interactions in the stability control region of tropomyosin. *Journal of Structural Biology*, *170*(2), 294–306. https://doi.org/10.1016/j.jsb.2010.01.020

Kwok, S. C., & Hodges, R. S. (2004). Stabilizing and destabilizing clusters in the hydrophobic core of long two-stranded α-helical coiled-coils. *The Journal of*

Biological Chemistry, *279*(20), 21576–21588. https://doi.org/10.1074/jbc.M401074200

Laemmli, U. K. (1970). 227680a0. *Nature*, *227*, 680–685.

Lehrer, S. S. (1978). Effects of an interchain disulfide bond on tropomyosin structure: Intrinsic fluorescence and circular dichroism studies. *Journal of Molecular Biology*, *118*(2), 209–226. https://doi.org/https://doi.org/10.1016/0022-2836(78)90413-8

Mak, A. S., & Smillie, L. B. (1981). Structural interpretation of the two-site binding of troponin on the muscle thin filament. *Journal of Molecular Biology*, *149*(3), 541–550. https://doi.org/https://doi.org/10.1016/0022-2836(81)90486-1

Manning, E. P., Tardiff, J. C., & Schwartz, S. D. (2011). A model of calcium activation of the cardiac thin filament. *Biochemistry*, *50*(34), 7405–7413. https://doi.org/10.1021/bi200506k

Matthews, B. W., Nicholson, H., & Becktel, W. J. (1987). Enhanced protein thermostability from site-directed mutations that decrease the entropy of unfolding. *Proceedings of the National Academy of Sciences of the United States of America*, *84*(19), 6663–6667. https://doi.org/10.1073/pnas.84.19.6663

Minakata, S., Maeda, K., Oda, N., Wakabayashi, K., Nitanai, Y., & Maéda, Y. (2008). Two-crystal structures of tropomyosin C-terminal fragment 176-273: Exposure of the hydrophobic core to the solvent destabilizes the tropomyosin molecule. *Biophysical Journal*, *95*(2), 710–719. https://doi.org/10.1529/biophysj.107.126144

Monteiro, P. B., Lataro, R. C., Ferro, J. A., & Reinach, F. D. C. (1994). Functional α-

tropomyosin produced in *Escherichia coli*. A dipeptide extension can substitute the amino-terminal acetyl group. *The Journal of Biological Chemistry*, *269*(14), 10461–10466. https://doi.org/10.1016/s0021-9258(17)34082-6

Morris, E. P., & Lehrer, S. S. (1984). Troponin-Tropomyosin Interactions. Fluorescence Studies of the Binding of Troponin, Troponin T, and Chymotryptic Troponin T Fragments to Specifically Labeled Tropomyosin. *Biochemistry*, *23*(10), 2214–2220. https://doi.org/10.1021/bi00305a018

Oda, T., Yanagisawa, H., & Wakabayashi, T. (2020). Cryo-EM structures of cardiac thin filaments reveal the 3D architecture of troponin. *Journal of Structural Biology*, *209*(3), 107450. https://doi.org/10.1016/j.jsb.2020.107450

Ohtsuki, I. (1979). Molecular arrangement of troponin-T in the thin filament. *The Journal of Biochemistry*, *86*(2), 491–497. https://doi.org/10.1093/oxfordjournals.jbchem.a132549

Orzechowski, M., Li, X. E., Fischer, S., & Lehman, W. (2014). An atomic model of the tropomyosin cable on F-actin. *Biophysical Journal*, *107*(3), 694–699. https://doi.org/10.1016/j.bpj.2014.06.034

Parry, D. A. D. (1975). Analysis of the primary sequence of α-tropomyosin from rabbit skeletal muscle. *The Journal of Molecular Biology*, *98*(3), 519–535. https://doi.org/10.1016/S0022-2836(75)80084-2

Pato, M. D., Mak, A. S., & Smillie, L. B. (1981). Fragments of rabbit striated muscle α-tropomyosin. I. Preparation and characterization. *The Journal of Biological*

Chemistry, *256*(2), 593–601. https://doi.org/10.1016/s0021-9258(19)70014-3

Pearlstone, J. R., & Smillie, L. B. (1982). Binding of troponin-T fragments to several types of tropomyosin. Sensitivity to Ca^{2+} in the presence of troponin-C. *The Journal of Biological Chemistry*, *257*(18), 10587–10592. https://doi.org/10.1016/S0021-9258(18)33862-6

Perrie, W. T., & Perry, S. V. (1970). An electrophoretic study of the low-molecular-weight components of myosin. *The Biochemical Journal*, *119*(1), 31–38. https://doi.org/10.1042/bj1190031

Phillips, G. N. J. (1986). Construction of an atomic model for tropomyosin and implications for interactions with actin. *Journal of Molecular Biology*, *192*(1), 128–131. https://doi.org/10.1016/0022-2836(86)90469-9

Phillips, G. N. J., Fillers, J. P., & Cohen, C. (1980). Motions of tropomyosin. Crystal as metaphor. *Biophysical Journal*, *32*(1), 485–502. https://doi.org/10.1016/S0006-3495(80)84985-X

Pirani, A., Xu, C., Hatch, V., Craig, R., Tobacman, L. S., & Lehman, W. (2005). Single particle analysis of relaxed and activated muscle thin filaments. *Journal of Molecular Biology*, *346*(3), 761–772. https://doi.org/10.1016/j.jmb.2004.12.013

Potekhin, S. A., & Privalov, P. L. (1982). Co-operative blocks in tropomyosin. *Journal of Molecular Biology*, *159*(3), 519–535. https://doi.org/10.1016/0022-2836(82)90299-6

Potter, J. D. (1982). Preparation of troponin and its subunits. *Methods in Enzymology*, *85 Pt B*, 241–263. https://doi.org/10.1016/0076-6879(82)85024-6

Rasband, W. (2018). *ImageJ* (imagej 1.52a). U. S. National Institutes of Health. https://imagej.nih.gov/ij/

Richardson, J. S., & Richardson, D. C. (1988). Amino acid preferences for specific locations at the ends of alpha helices. *Science*, *240*(4859), 1648–1652. https://doi.org/10.1126/science.3381086

Risi, C., Eisner, J., Belknap, B., Heeley, D. H., White, H. D., Schröder, G. F., & Galkin, V. E. (2017). Ca^{2+} induced movement of tropomyosin on native cardiac thin filaments revealed by cryoelectron microscopy. *Proceedings of the National Academy of Sciences of the United States of America*, *114*(26), 6782–6787. https://doi.org/10.1073/pnas.1700868114

Saavedra, H. G., Wrabla, J. O., Andersona, J. A., Lia, J., and Hilser, V. J. (2017). Dynamic allostery can drive cold adaptation in enzymes. *Physiology & Behavior*, *176*(1), 139–148. https://doi.org/10.1038/s41586-018-0183-2.Dynamic

Sano, K. I., Yuki, T., Nomata, Y., Nakayama, N., Iida, R., Mitomo, H., Ijiro, K., & Osada, Y. (2020). Intrahelical Interactions in an α-Helical Coiled Coil Determine the Structural Stability of Tropomyosin. *Biochemistry*, *59*(23), 2194–2202. https://doi.org/10.1021/acs.biochem.0c00203

Silva, A. M. M., Ige, T., Goonasekara, C. L., & Heeley, D. H. (2020b). Threonine-77 Is a Determinant of the Low-Temperature Conditioning of the Most Abundant Isoform of Tropomyosin in Atlantic Salmon. *Biochemistry*, *59*(31), 2859–2869. https://doi.org/10.1021/acs.biochem.0c00416

Silva, A. M. M., Kennedy, L. S., Hasan, S. C., Cohen, A. M., & Heeley, D. H. (2020c). Demonstration of beta-tropomyosin (Tpm2) and duplication of the alpha-slow tropomyosin gene (TPM3) in Atlantic salmon (*Salmo salar*). *Comparative Biochemistry and Physiology Part - B: Biochemistry and Molecular Biology*, *245*(January), 110439. https://doi.org/10.1016/j.cbpb.2020.110439

Singh, A., & Hitchcock-DeGregori, S. E. (2003). Local Destabilization of the Tropomyosin Coiled Coil Gives the Molecular Flexibility Required for Actin Binding. *Biochemistry*, *42*(48), 14114–14121. https://doi.org/10.1021/bi0348462

Singh, A., & Hitchcock-Degregori, S. E. (2006). Dual requirement for flexibility and specificity for binding of the coiled-coil tropomyosin to its target, actin. *Structure*, *14*(1), 43–50. https://doi.org/10.1016/j.str.2005.09.016

Singh, A., & Hitchcock-DeGregori, S. E. (2007). Tropomyosin's periods are quasi-equivalent for actin binding but have specific regulatory functions. *Biochemistry*, *46*(51), 14917–14927. https://doi.org/10.1021/bi701570b

Smillie, L B. (1982). Preparation and identification of alpha- and beta-tropomyosins. *Methods in Enzymology*, *85 Pt B*, 234–241. https://doi.org/10.1016/0076-6879(82)85023-4

Smillie, L.B., Pato, M. D., Pearlstone, J. R., & Mak, A. S. (1980). Periodicity of α-helical potential in tropomyosin sequence correlates with alternating actin binding sites. *The Journal of Molecular Biology*, *136*(2), 199–202. https://doi.org/10.1016/0022-2836(80)90314-9

Spudich, J. A., & Watt, S. (1971). The regulation of rabbit skeletal muscle contraction. I. Biochemical studies of the interaction of the tropomyosin-troponin complex with actin and the proteolytic fragments of myosin. *The Journal of Biological Chemistry*, *246*(15), 4866–4871. https://doi.org/10.1016/S0021-9258(18)62016-2

Stone, D., & Smillie, L. B. (1978). The amino acid sequence of rabbit skeletal α-tropomyosin. The NH2-terminal half and complete sequence. *The Journal of Biological Chemistry*, *253*(4), 1137–1148. https://doi.org/10.1016/s0021-9258(17)38122-x

Sumida, J. P., Wu, E., & Lehrer, S. S. (2008). Conserved Asp-137 imparts flexibility to tropomyosin and affects function. *The Journal of Biological Chemistry*, *283*(11), 6728–6734. https://doi.org/10.1074/jbc.M707485200

Tanokura, M., Tawada, Y., Ono, A., & Ohtsuki, I. (1983). Chymotryptic subfragments of troponin t from rabbit skeletal muscle. interaction with tropomyosin, troponin I and troponin C1. *Journal of Biochemistry*, *93*(2), 331–337. https://doi.org/10.1093/oxfordjournals.jbchem.a134185

Tobacman, L. S., & Butters, C. A. (2000). A new model of cooperative myosin-thin filament binding. *The Journal of Biological Chemistry*, *275*(36), 27587–27593. https://doi.org/10.1074/jbc.M003648200

Urbancikova, M., & Hitchcock-DeGregori, S. E. (1994). Requirement of amino-terminal modification for striated muscle alpha-tropomyosin function. *The Journal of Biological Chemistry*, *269*(39), 24310–24315.

http://europepmc.org/abstract/MED/7929088

Whitby, F. G., & Phillips, G. N. (2000). Crystal structure of tropomyosin at 7 angstroms resolution. *Proteins: Structure, Function and Genetics*, *38*(1), 49–59. https://doi.org/10.1002/(SICI)1097-0134(20000101)38:1<49::AID-PROT6>3.0.CO;2-B

White, S. P., Cohen, C., & Phillips, G. N. (1987). Structure of co-crystals of tropomyosin and troponin. *Nature*, *325*(6107), 826–828. https://doi.org/10.1038/325826a0

Williams, D. L., & Swenson, C. A. (1981). Tropomyosin Stability: Assignment of Thermally Induced Conformational Transitions to Separate Regions of the Molecule. *Biochemistry*, *20*(13), 3856–3864. https://doi.org/10.1021/bi00516a029

Woods, E. F. (1977). Stability of Segments of Rabbit α-Tropomyosin. *Australian Journal of Biological Sciences*, *30*(6), 527–542. https://doi.org/10.1071/BI9770527

Yamada, Y., Namba, K., & Fujii, T. (2020). Cardiac muscle thin filament structures reveal calcium regulatory mechanism. *Nature Communications*, *11*(1), 153. https://doi.org/10.1038/s41467-019-14008-1

Yamauchi-Takihara, K., Nakajima-Taniguchi, C., Matsui, H., Fujio, Y., Kunisada, K., Nagata, S., & Kishimoto, T. (1996). Clinical implications of hypertrophic cardiomyopathy associated with mutations in the α-tropomyosin gene. *Heart*, *76*(1), 63–65. https://doi.org/10.1136/hrt.76.1.63

Zheng, W., Hitchcock-DeGregori, S. E., & Barua, B. (2016). Investigating the effects of tropomyosin mutations on its flexibility and interactions with filamentous actin using

molecular dynamics simulation. *Journal of Muscle Research and Cell Motility*, *37*(4–5), 131–147. https://doi.org/10.1007/s10974-016-9447-3

Chapter 4. Further investigation into the biochemical effects of phosphorylation of tropomyosin Tpm1.1(α); Serine-283 is in communication with the mid-region.

Abstract

The major isoform of tropomyosin, Tpm 1.1(α), in the skeletal and cardiac muscles of mammals and birds is phosphorylated at the penultimate C-terminal residue, serine-283. The degree of phosphorylation in tropomyosin is age-related: a high level is found in the mammal fetal heart muscle ~ 0.7 mole per mole that drops to ~ 0.3 in the adult. It is thought that phosphorylation functions in favor of the assembly of filaments. The current study investigates the effect of phosphorylation on the conformational stability of tropomyosin and its interaction with F-actin. Phosphorylated and non-phosphorylated forms of rabbit Tpm1.1(α) are chromatographically separated and analyzed using electrophoresis, limited proteolysis, circular dichroism, F-actin binding, and PyMOL. The rate of proteolytic digestion is investigated by densitometry of the Coomassie-stained electrophoretic gel band containing intact protein (33,000 g/mole) vs. time. Phosphorylated Tpm1.1(α) is more susceptible to cleavage by chymotrypsin (at Leu-169) and trypsin (at Arg-133) than unphosphorylated Tpm1.1(α). The points of cleavage are confirmed by mass spectrometric peptide mapping as well as by Edman sequencing. Phosphorylation also destabilized chymotryptic fragment CT2 (residues 170 - 284). Non-superimposable global unfolding profiles are observed using circular dichroism in the 25 and 42 ^{o}C temperature range in agreement with the results of the limited proteolysis experiments. Phosphorylation increases the affinity of Tpm1.1(α) for F-actin (30 mM KCl, 1mM $MgCl_2$, pH 7.5) at 4 ^{o}C

(K_D, 0.16 μM vs. 0.28 μM) as demonstrated in a co-sedimentation binding assay. The findings of this section are: (i) phosphorylation at serine-283 of Tpm1.1(α) increases the rate of scission by chymotrypsin and trypsin, indicative of an induced opening of the center of the molecule >150 amino acids away from the phosphorylation site and a long-range communication and (ii) phosphorylation tightens the interaction between Tpm1.1(α) and F-actin indicating that the two bound phosphate groups, in addition to strengthening the interaction between contiguous molecules of tropomyosin, increase the exposure of actin-binding periods 4 (residues 124 - 147) and 5 (N -terminal residues 166 - 189) which are known to be required for optimal actin binding.

4.1 Introduction

As described in chapter 2, the tropomyosin isoforms that occur in the skeletal and cardiac muscles of mammals and birds undergo reversible covalent modification by phosphorylation. The extent to which tropomyosin is phosphorylated does not change short-term (Bárány et al., 1979) but is age-related with the amount of the phosphorylated form falling from a high level in the fetus (~ 0.7 mole: mole) to ~ 0.3 in the adult rat heart (Heeley et al., 1982). Developmental surveys (Heeley et al., 1989) infer that phosphorylation works in favor of filament assembly, strengthening both the self-polymerization of Tpm1.1(α) as well as the interaction of Tpm1.1(α) with troponin (Heeley et al., 1989). Although phosphorylation was expected to increase affinity for F-actin this was not observed (Heeley et al., 1989), a mystery that is re-investigated herein.

The stronger end-to-end association of phosphorylated tropomyosin is explained by the ion-pairing ability between the Ser-283 phosphate group and positive side chains of Lys-5, Lys-6, Lys-7, and Lys-12 in the N-terminus (Greenfield et al., 2006). Evidence suggests that the ε-amino group of Lys-7 and 12 allow the formation of stabilizing ion-pairs to the phosphate group (Williams & Swenson, 1981; Greenfield et al., 2006). A study involving soluble fragments of troponin T (Heeley, 1994) demonstrated a comparatively stronger affinity of the C-terminal 100 amino acid fragment (TnT2) to Tpm1.1(α) with a bound phosphate group at Ser-283 even though TnT2 binds to a central region of tropomyosin, namely binding site 2 (close to Cys-190) (Ohtsuki, 1979; Pearlstone & Smillie, 1982b; Tanokura et al., 1983; Morris & Lehrer, 1984), that is well removed from the C-terminus. Studies involving troponin-T (TnT1) on the other hand demonstrated that its ability to arch

over consecutive tropomyosins, binding site1 (the overlap region of the tropomyosin) (Mak & Smillie, 1981; Brisson et al., 1986; White et al., 1987; Heeley et al., 1989; Goonasekara & Heeley, 2009), was significantly weakened when tropomyosin was fully phosphorylated (Heeley, 1994).

Research with transgenic animals has produced a number of interesting results. For example, a lower level of tropomyosin phosphorylation was observed in a mouse line synthesizing tropomyosin Glu54Lys which is a disease mutation (Warren et al. 2008). Alanine replacement (i.e., Ser283Ala) was found to provide protection against the familial hypertrophic cardiomyopathy mutation, Glu180Gly (Schulz et al. 2013). In a more recent study, pseudo phosphorylation (Ser283Asp) has been shown to be detrimental (post-birth) depending upon the proportions of the mutant and endogenous tropomyosins (Rajan et al. 2019). These observations indicate that the phosphorylation of tropomyosin is influential in both immature and mature muscles. At the same time, it is worth recognizing the limitations of mutagenesis. Specifically, a carboxylate group is not an exact match in terms of size and charge at pH 7 for a phosphate group.

The current study attempts to further understand the effect which phosphorylation has on the properties of tropomyosin, specifically the conformational stability of the molecule as well as its interaction with F-actin. In this regard, the issue of conformational stability is assessed by susceptibility to the proteases chymotrypsin (preferred site, Leu-169) and trypsin (Arg-137) and thermal denaturation using circular dichroism. An increased rate of scission of the phosphorylated form of tropomyosin by chymotrypsin (by two-fold) and, to a lesser extent (< two folds), trypsin compared to the unphosphorylated control is observed

pointing to an induced-opening of tropomyosin's mid-region. This is in excellent agreement with circular dichroism ellipticity measurements between 25 - 42 ^{o}C, where the unfolding of the C-terminal half of rabbit Tpm1.1(α) is known to occur (Williams & Swenson, 1981; Ishii et al., 1992).

The effect of tropomyosin phosphorylation on F-actin binding was re-investigated at sub-optimal ionic strength and temperature using unlabeled (non-radioactive) native proteins (α-acetylated). Under these conditions, phosphorylated Tpm1.1 (α) displays a higher affinity for F-actin compared to the control (K_D, 0.16 μM vs. 0.28 μM) suggesting that phosphorylation can influence critical actin-binding periods (4^{th} and 5^{th}) (Singh & Hitchcock-DeGregori, 2007) as well as the end-to-end polymerization of tropomyosin in the absence of troponin T.

4.2 Materials and Methods

4.2.1 Protein Isolation

4.2.1.1 Tropomyosin

Tropomyosin extracted from rabbit cardiac acetone powder as mentioned in Chapter 2 was further separated into phosphorylated and unphosphorylated forms using Q-Sepharose Fast Flow chromatography (GE Healthcare) (Hayley et al., 2008) (column, 2.5 cm x 15 cm (volume, ~ 75 mL). Freshly prepared start buffer, containing 6 M urea, 50 mM NaCl, 50 mM tris(hydroxymethyl)aminomethane (Tris), and 1 mM dithiothreitol, pH 8.0 was passed through 8.0 μm (Millipore) (linear salt gradient, 0.05 - 0.5 M NaCl, volume of 800 mL). Elution of each tropomyosin form was detected using ultraviolet (UV) absorbance (A_{280}) and conductivity measurement followed by alkaline urea-PAGE confirmation. Protein fractions were pooled together and dialyzed against ~ 20 - 24 L of total deionized water (dH_2O) volume for two days in the presence of ~ 2 mM β-mercaptoethanol and ~ 5 mM NH_4HCO_3 with three (8 L) water changes each day. The dialysates were freeze-dried and stored in a refrigerator (8 ^oC). Tropomyosin concentration was determined by UV absorbance with A_{280} according to the formula $[\ tropomyosin] = \frac{A280nm - 1.5A320nm}{0.25}$ with 1.5 A_{320} scatter correction.

4.2.1.2 Actin

Actin was prepared from rabbit skeletal muscle acetone powder by cycles of polymerization and depolymerization (White et al., 1987). G-actin was prepared as an actin-sucrose solution (sugar concentration, 2 mg/ml), freeze-dried, and stored at -20 ^{o}C. For binding assays actin-sucrose was dissolved in a binding buffer containing 5 mM 3-morpholinopropanesulfonic acid (MOPS), 30 mM KCl, 1 mM $MgCl_2$, 0.1 mM EGTA, 1 mM dithiothreitol at pH 7.5 with 0.5 mM MgATP and dialyzed overnight. The stock solution was stored refrigerated and used within two weeks. Actin concentration was measured by UV absorbance with A_{280} using the following formula $[F-actin] = \frac{A290nm - 1.34A320nm}{0.69}$ (Houk & Ue, 1974) with appropriate correction for light scattering at A_{320}.

4.2.2 Electrophoresis

Sodium dodecyl sulfate-polyacrylamide electrophoresis (SDS-PAGE) (Laemmli, 1970) and alkaline urea PAGE were carried out as outlined in Sano et al., 2000 and Goonasekara & Heeley, 2009 respectively. Alkaline urea gels were briefly pre-ran (15 mins at 160 V) before sample loading. Electrophoresis was carried out using 10 - 12 % (m/v) polyacrylamide slabs (thickness. 0.75mm, acrylamide/ N, N'-methylene-bis-acrylamide (BioRad) (m/v) ratio of 30 : 0.8). The gels were photographed in ImageQuant LAS400/chemiImager^{TM}. A duplicate SDS gel with identical sample loadings was electroblotted onto polyvinylidene difluoride (PVDF) using 10 mM N-cyclohexyl-3-aminopropanesulfonic acid (CAPS), 10% (v/v) methanol at pH 11.0 at 180 V for 2 hrs (total

VH ~ 400) with the gel tank surrounded in ice to prevent overheating. The membrane was briefly stained with 0.025% (m/v) Coomassie Brilliant Blue R-250, 40% methanol, and distained with 50% ethanol before being air-dried overnight.

4.2.3 Limited Proteolysis

Digestion with chymotrypsin (Worthington) and trypsin (Worthington) followed the same procedure as described (Pato et al., 1981). 10 mg of the freeze-dried enzyme prepared in 2 mM HCl was refrigerated at 8 ^{o}C. The same stock solution was used for each side by side comparison. Digestion buffer consisted of 50 mM NH_4HCO_3, 0.1 M NaCl, 1mM dithiothreitol at pH 8.0. For 33,000 g/mol of Tpm 1.1 (α) monomer, the following enzyme: substrate mole ratios were used: chymotrypsin; 1: 500 (20 and 30 ^{o}C) and 1: 100 (0 ^{o}C) and trypsin; 1: 250 (0 ^{o}C) and 1: 1000 (30 ^{o}C). Samples of phosphorylated and unphosphorylated Tpm1.1(α) derived from the same column batch were digested side-by-side at a concentration of 2 mg/mL. The reaction was initiated by the addition of protease and immediate mixing. Aliquots were withdrawn at set times and were quenched with 10 M urea containing 1 mM dithiothreitol. At the end of the experiment, the samples were analyzed together by SDS-PAGE with the boiling step omitted. The intensity of the Coomassie-stained band corresponding to intact tropomyosin was measured by densitometry by fitting data into the following equation for a single exponential process:

$$Y = (Yo - Plateau)^{\mathrm{T}(-K\mathrm{T}X)} + Plateau$$

Y^0, Y value when X (time) is zero.

Plateau, Y value at infinite times

K, the rate constant

T, time

Photographed gels were analyzed using ImageJ 1.52a. Selected gel bands were excised using a new scalpel, dried, and sent to the Proteomics and Mass Spectrometry Core Facility at Dalhousie University for peptide mapping. Fragments of interest were transferred onto PVDF membrane for Edman sequencing and sent to Tufts University Core Facility, Boston, USA, for Edman sequencing

4.2.4 Circular dichroism

Measurements were recorded using a Jasco J-810 instrument. 10 mg of phosphorylated and unphosphorylated Tpm1.1(α) were separately dissolved in 1 mL of 0.1 M NaCl, 20 mM sodium phosphate, 1 mM dithiothreitol, pH 7.0 and dialyzed against 500 mL of the same buffer overnight in the cold. Sample unfolding (concentration, 1.5 mg/mL; light path, 0.1 mm) was induced by a linear temperature gradient of 5 to 65 °C whilst recording the 222 nm (far UV) ellipticity change at 0.1 °C increments. The temperature of the cell was controlled by a circulating thermostated water bath. The unfolding profile was normalized by taking the average of the first and last 10 ellipticity readings in the ramp and applying

the following formula to obtain the ellipticity at a given temperature. The procedure was repeated three times for each protein.

$$\theta T = \frac{\theta T \ - \ \theta \text{ end}}{\theta \text{ start} \ - \ \theta \text{ end}} \times 100$$

θ start, average of first 10 ellipticity readings in the ramp (from 5 to 6 °C) as 100%

θ end, average of last 10 ellipticity readings in the ramp (from 64 to 65 °C) as 0%

θ T, the ellipticity at temperature T

θ T, normalized ellipticity at temperature T

4.2.5 F-actin binding

Mixtures of F-actin and tropomyosin were centrifuged at 4 ºC for 40 min at 40,000 rpm (70Ti rotor at 20,000 x g force). Binding buffer consisted of 30 mM KCl, 1 mM $MgCl_2$, 5 mM MOPS, 0.1 mM EGTA, 1 mM dithiothreitol (added from solid) and was set to pH 7.5 at room temperature. Actin was polymerized by dialysis against the binding buffer which also contained 0.2 mM MgATP and 0.01 % (m/v) NaN_3. The F-actin was refrigerated and the same stock was used within two weeks. F-actin was prepared daily by diluting an aliquot from the stock solution (assay conditions; actin concentration 10 µM, tropomyosin concentration from 0 – 3.5 µM). Components were combined in the order tropomyosin > buffer > F-actin, gently mixing using a P200 Gilson Pipetman with a truncated tip and incubated for 1 hr at 4 ºC temperature. Aliquots were taken before and after sedimentation

for analysis by SDS-PAGE. Each gel was stained using a standardized procedure consisting of 50 mL of 0.25% (m/v) unused Coomassie R-250 for 1 hr with constant shaking and then destained until clear. The intensity and the size of the tropomyosin-containing bands were estimated using densitometry as outlined below in ImageJ 1.52a (Rasband, 2018). After back-ground reduction, the moles of bound tropomyosin were determined from the difference in band intensity of loaded (pre-sedimentation) and free-unbound (post-sedimentation supernatant) tropomyosin in conjunction with a calibration relationship of quantified area of the bands of known amounts of tropomyosin. Binding curves were generated using GraphPad Prism 5 using the Sigmoidal dose-response (variable slope) equation (below) to obtain the best fit curve.

$$Y = Bottom + \frac{(Top - Bottom)}{1 + 10^{(LogEC50 - X) - Hill\ Slope}}$$

Bottom, Y value at the bottom plateau

Top, Y value at the top plateau

Log EC50 (K_D), X value when the response is halfway between Bottom and Top

Hill Slope, Hill coefficient

4.2.6 Molecular Visualization

The effect of the phosphate group on Ser-283 on the C-terminus was examined using PyMOL (DeLano Scientific, California). All structures were downloaded from the Research Collaboratory for Structural Bioinformatics Protein Data Base (RCSB PDB). The NMR structure of rat striated tropomyosin (DOI: 10.2210/pdb1MV4/pdb) was used to analyze the spatial arrangement of the C-terminus. The N and C-terminal complex of tropomyosin was analyzed using the 2.2 Å X-ray crystallography structure of tropomyosin overlap complex from chicken smooth muscle (Frye et al., 2010) DOI: 10.2210/pdb3MUD/pdb. Amino acid residues of the original structure were mutated using wizard → mutagenesis function at residues 249, 258 - 263, 265 - 273, 276, 277, and 279 - 284 in the C-terminus to the respective amino acid in the rabbit cardiac Tpm 1.1(α), and the N-terminal Met-Ala-Ser tripeptide was deleted.

4.3 Results

4.3.1 Chromatography

In Figure 4.1, rabbit cardiac tropomyosin, consisting almost totally of isoform Tpm1.1 (α) is chromatographically separated into the fully unphosphorylated (peak 1) and phosphorylated (peak 2) forms using Q Sepharose. Alkaline urea PAGE confirms the identity and enrichment of the fractions in Figure 4.1 (see inset). The discrepancy in conductivity of the elution peaks corresponding to unphosphorylated Tmp1.1(α) ~ 15 mS/cm vs. phosphorylated Tmp1.1(α) ~ 17 mS/cm and the differential migration (Figure 4.1 inset) is explained by the comparatively greater net negative charge of the phosphorylated protein at alkaline and neutral pH. Thus, the Q Sepharose chromatography sets the stage for a biochemical investigation using tropomyosin having a true phosphate moiety in the 283rd residue position. The trailing peak at the end of the profile is due to the less abundant kappa isoform, Tpm 1.2 which is not considered in this study. A yield of approximately 20 mg of phosphorylated Tmp1.1(α) was obtained from a column loading consisting of 200 mg of rabbit cardiac tropomyosin. The comparisons that are described below are carried out using samples from the same column that have been treated identically.

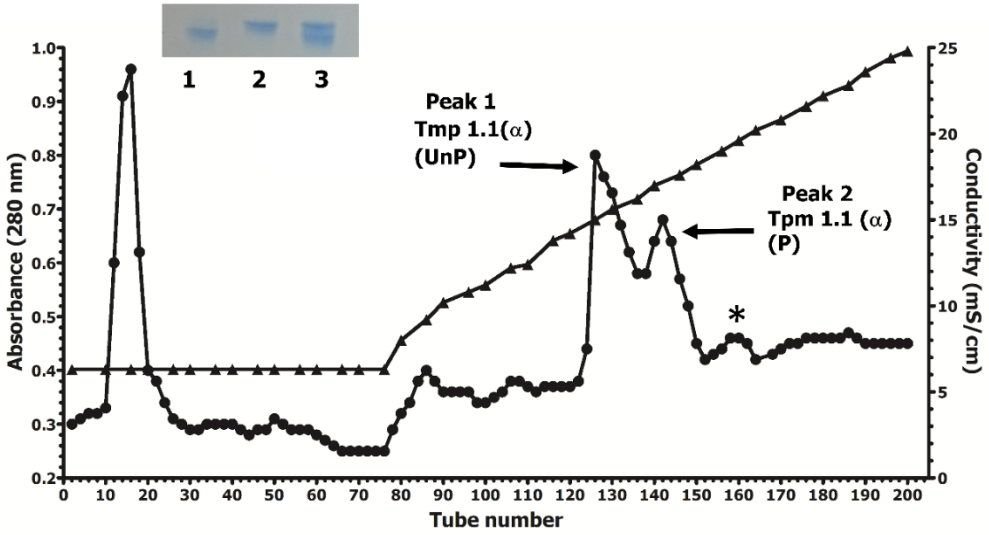

Figure 4.1. Q Sepharose Fast Flow separation of rabbit cardiac tropomyosin, Tpm 1.1 (α). Peak 1 containing the unphosphosphorylated (UnP) and peak 2 containing phosphorylated (P) forms are indicated by arrows. Asterisk, the trailing peak possibly containing a trace amount of Tpm1.2 (kappa) tropomyosin isoform (Denz et al., 2004; Rajan et al., 2010). Conductivity at room temperature is measured in milliSiemen (mS) per cm. The inset is from an alkaline urea polyacrylamide gel: lane 1, P; lane 2, UnP and lane 3, the mix of P + UnP. The gel is stained with Coomassie R-250. Reprinted with permission from Silva, A. M. M., Goonasekara, C. L., Hayley, M., & Heeley, D. H. (2020). Further Investigation into the Biochemical Effects of Phosphorylation of Tropomyosin Tpm1.1(α). Serine-283 Is in Communication with the Midregion. Biochemistry, 59(50), 4725–4734. https://doi.org/10.1021/acs.biochem.0c00882. Copyright (2021) American Chemical Society.

4.3.2 Effect of phosphorylation on the proteolytic susceptibility of tropomyosin.

4.3.2.1 Chymotrypsin

Previous research has shown that Leu-169 is the preferred site of chymotryptic cleavage in rabbit Tpm1.1(α) (Pato et al., 1981). Therefore, chymotrypsin serves as a tool by which to assess the solvent exposure of this particular amino acid. With this intent, limited proteolysis is performed on P-Tpm1.1(α) and UnP-Tpm1.1(α) acquired by peak 2 and peak 1 column fractions in Figure 4.1 respectively. The results of this section are presented in Figure 4.2.

When attention is focused on the intact protein band it migrates between the 37,000 and 24,000 kDa markers (Figures 4.2A and 4.2C) with an apparent Mr of 33,000. By comparing the intensity of the time-dependent change in the intensity of the intact protein bands over the considered digestion period (Figures 4.2A, 4.2B and 4.2C), it is evident that phosphorylation affects the rate of initial cleavage. For the experiment in Figure 4.2A (temperature 20 ^{o}C), the starting amount of the phosphorylated protein is set intentionally higher than that of the control (P-Tpm > UnP-Tpm in lanes 1 and 2 dashed inset), but after 5 min the opposite is true (P-Tpm < UnP-Tpm in lanes 3 and 4). The initial amount of intact protein reaches near complete digestion around 30 min (Figure 4.2A), with no significant difference in staining intensity between the two full size bands there onwards. To further, investigate this result the experiment was repeated at a higher temperature, 30 ^{o}C (Figures 4.2B and 4.2C). In Figure 4.2B, the amount of phosphorylated protein is set intentionally higher than that of the control, i.e., P-Tpm > unP-Tpm (lanes 1 and 2) as in Figure 4.2A. A reversed pattern is observed at 5 min, i.e., P-Tpm < unP-Tpm (lanes 3 and 4). From an

inspection of the entire time course in Figure 4.2C, it is evident that some of the undigested control (UnP-Tpm) remains at 15 min whereas little, if any, of the phosphorylated version can be detected at this time (Figure 4.2C, upper dashed area). Based on the plot of the relative density of the intact protein vs. time (Figure 4.2D) there is an approximately two-fold difference in the time required to deplete 50% of the starting material: 5 mins (P-Tpm1.1(α)) vs. 11 mins (control). The fragmentation pattern (Figure 4.2C) consists of a doublet that aligns with the 20 kDa standard, and a band that migrates slightly ahead of the 15 kDa marker, (Figure 4.2C). Based on the results of mass spectrometric peptide mapping (Table 1) the major fragments are assigned as CT1 (upper band) (residues 1 - 169), coverage 79%, and clipped versions of CT1 and CT2 (residues 170 - 284). The assignments are identical to those of previous workers using a mixture of unphosphorylated and phosphorylated Tpm1.1(α) (Pato et al., 1981). Further, six cycles of N-terminal Edman sequencing of CT2 (Val-170-Ile-Ile-Glu-Ser-Asp-175) complemented the mass spectrometric analysis and confirmed the origin of CT2. In this study, the clipped CT1 and other minor and low abundance species are not investigated. An important observation that concerns the CT2 fragment (residues 170 - 284) as noted by previous researchers (Pato et al., 1981) is that CT2 does not accumulate to the same extent as CT1. Considering the band intensities (Figure 4.2C, lower dashed area), it appears that this part of the molecule becomes even more susceptible to further protease action when phosphorylated than not. But the main conclusion is that the covalently bound phosphate accelerates the rate of scission of peptide bond 169 (Leu-169-Val-170) of P-Tpm1.1 (α). The distance between the two sites is striking: greater than 110 amino acids, which is ~ 1/3rd of the distance of

the molecule. An overnight digestion experiment carried out at 0 ^{o}C over 15 hrs did not show a difference in the banding pattern of the final products (Figure 4.2E).

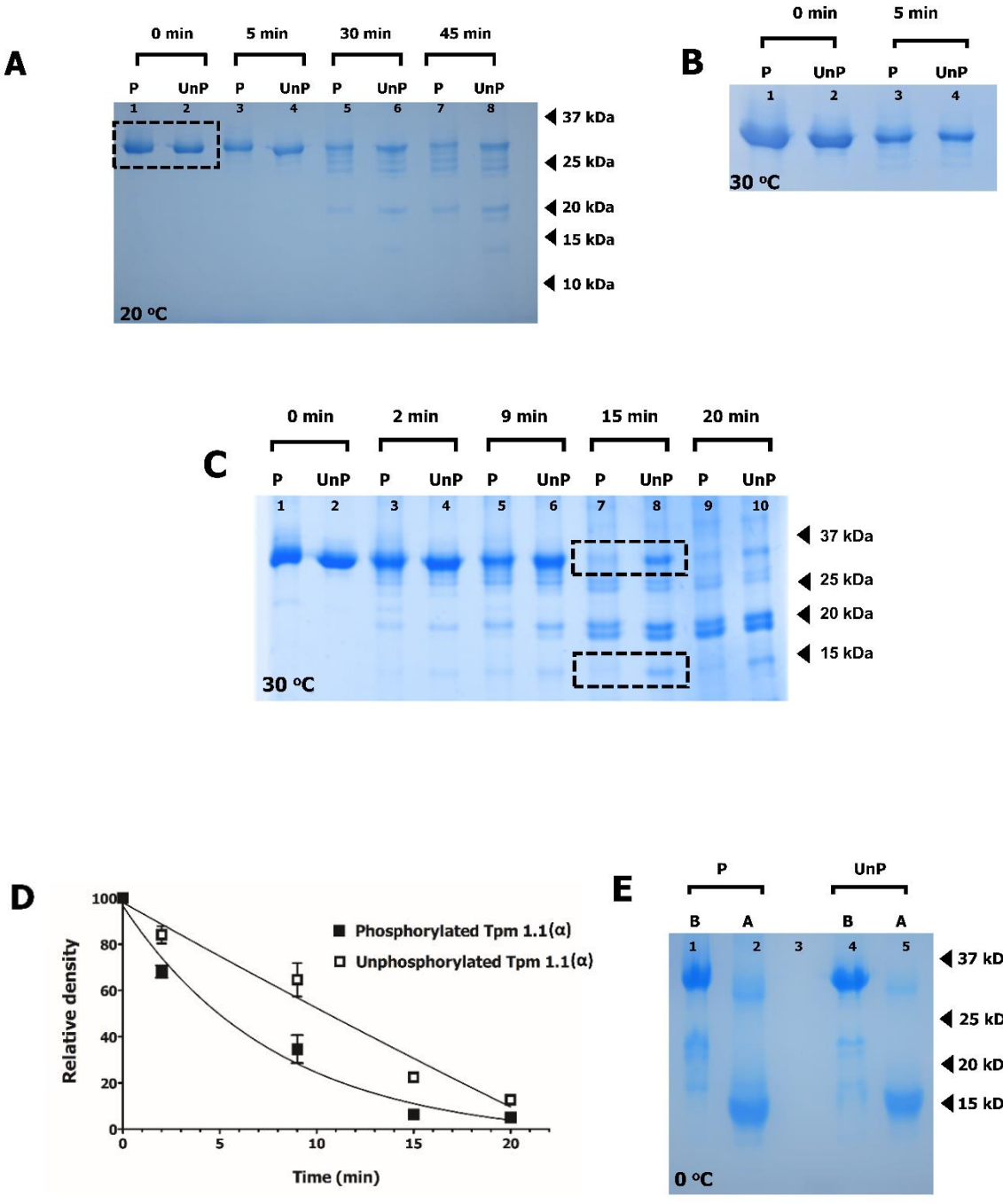
A
0 min
5 min
30 min
45 min
P
UnP
1
2
3
4
5
6
7
8
37 kDa
25 kDa
20 kDa
15 kDa
10 kDa
20 °C
B
0 min
5 min
30 °C
C
0 min
2 min
9 min
15 min
20 min
9
10
30 °C
D
Relative density
Time (min)
Phosphorylated Tpm 1.1(α)
Unphosphorylated Tpm 1.1(α)
E
B
A
0 °C

Figure 4.2. Chymotryptic digestion of P-Tpm1.1(α) and UnP-Tpm1.1(α). SDS-PAGE analyses showing the decline in 33,000 g/mol protein chain and subsequent generation of peptide fragments. P - Phosphorylated Tpm1.1(α) and UnP - Unhosphorylated Tpm1.1 (α). The mol: mol ratios of enzyme : substrate are: 1:500 (20 ºC and 30 ºC) and 1:1000 (0 ºC). Extreme right-hand of (A), (B), and (C) Mr markers. (A) Whole gel image at 20 ºC digestion. The upper dashed area highlights the intact protein 33 kDa and loadings of P-Tpm > UnP-Tpm in lanes 1 and 2, after 5 min lanes 3 and 4 P-Tpm < UnP-Tpm. (B) Section of the gel showing the change of intact protein at 30 ºC for 5 min incubation. The starting amounts set intentionally as P-Tpm > UnP-Tpm. After 5 min P-Tpm < UnP-Tpm. (C) Whole gel at 30 ºC. The upper highlighted area in (C) demonstrates the presence of intact protein band (33 kDa) remaining after 15 min in the control digest but not that of phosphorylated Tpm1.1 (α). The lower dashed area of (C) highlights the presence of fragment CT2 (residues 170 - 284) in a higher intensity, in the control digest compared to phosphorylated Tpm1.1 (α). (D) Densitometric analysis of (C). (E) Overnight (15 h) digestion, lanes 1and 2 and UnP, lanes 4 and 5. B - 0 min, A -15 hrs later. There is no observable difference in the breakdown of P and unP at 0 ºC. n=2. Adapted with permission from Silva, A. M. M., Goonasekara, C. L., Hayley, M., & Heeley, D. H. (2020). Further Investigation into the Biochemical Effects of Phosphorylation of Tropomyosin Tpm1.1(α). Serine-283 Is in Communication with the Midregion. Biochemistry, 59(50), 4725–4734. https://doi.org/10.1021/acs.biochem.0c00882.

Table 4. 1. Mass spectrometric tryptic peptide mapping of CT1 and CT2 chymotryptic fragments of rabbit cardiac Tmp1.1(α)

Fragment	Fragment length	Sequence of the peptide
CT1 **20 kDa** (residues 1 - 169) coverage 79%	13-21	AEQAEADKK
	22-30	KGTEDELDKYSESLK
	36-48	SKQLEDELVSLQK
	52-70	GTEDELDKYSEALKDAQEK
	66-76	DAQEKLELAEK
	77-91	KATDAEADVASLNRR
	92-105	IQLVEEELDRAQER
	106-112	LATALQK
	113-118	LEEAEK
	134-149	AQKDEEKMEIQEIQLK
	153-160	HIAEDADR
	161-167	KYEEVAR
CT2 **15 kDa** (residues 170 - 284) coverage 63%	170-182	VIIESDLERAEER
	190-198	CAELEEELK
	206-213	SLEAQAEK
	214-226	YSQKEDKYEEEIK
	252-264	SIDDLEDELYAQK
	269-284	AISEELDHALNDMTSI

4.3.2.2 Trypsin

Previous work has shown that the primary site in Tpm1.1(α) for trypsin is Arg-133 (Pato et al., 1981). Thus, trypsin can be used to gauge the conformation of tropomyosin at a point that is some 35 amino acids farther upstream than Leu-169. With this intention, an approach that is similar to chymotrypsin (Figure 4.2) is taken. The mol: mol ratios of enzyme: substrate is reduced in these experiments as tropomyosin contains more potential digestion sites than chymotrypsin.

For the 0 ^{o}C experiment (Figure 4.3A), carried out for 4 hrs, it is evident that phosphorylation again affects the rate of initial cleavage, although the difference is smaller than what is observed with chymotrypsin (Figure 4.2). Experiments carried out at 30 ^{o}C (Figures 4.3B and 4.3C) show a similar trend with a faster rate of cleavage of P-Tpm1.1(α) compared to the control (UnP-Tpm1.1(α)). The disparity in the rates of initial cleavage seen in Figure 3B is mirrored in Figure 3C. The reaction extending up to 30 min (Figure 4.3B) starts showing a small difference after 1 min and after 5 min the difference becomes very noticeable (Figure 4.3B, upper dashed area). The detectable amounts of phosphorylated version drop between 20 - 30 min compared to the unphosphorylated control (Figures 4.3B and 4.3D). Based on the plot of the relative density of the intact protein band vs. time, compared to the chymotrypsin digestion there is not a substantial difference in the time required to deplete 50% of the starting material (Figure 4.3D). The decay of P-Tpm1.1(α) is not shown beyond 5 min due to undetectable amounts of intact protein by the quantification method employed here.

At 0 ^{o}C the digestion pattern consists of two major fragments, one around 17 kDa and another slightly ahead of the 15 kDa marker (Figure 4.3A). With mass spectrometric peptide mapping (Table 2) the identities of the two fragments can be assigned T2 (17kDa) sub-fragment (residues 134 - 284), coverage 72%, and T1 (15kDa) sub-fragment (residues 1 - 133), coverage 92%. The assignments are identical to those of previous workers using a mixture of unphosphorylated and phosphorylated Tpm1.1(α) (Pato et al., 1981). The digestion carried out at 30 ^{o}C (Figure 4.3B) shows a different fragmentation pattern compared to 0 ^{o}C with two other additional fragments appearing. Previous researchers identified the appearance of additional bands similar to Figure 4.3B at extended digestions times (~ 24 hr) at 0 ^{o}C under similar conditions, T4 (a clipped product of T2) and T3 (a clipped product of T1) (Pato et al., 1981). In this study, the clipped T3, T4, and other minor and low abundance species are not investigated.

The main conclusion of this set of experiments is that the covalently bound phosphate groups accelerate the rate of scission of the peptide bond between Arg-133 and Ala-134 of Tpm1.1 (α) but to a smaller extent than is observed by chymotrypsin at peptide bond 169. The distance between the cleavage and phosphate site is half of the length of the molecule. We conclude that the diminished rate of scission shown by trypsin compared to chymotrypsin is most possibly due to the increased distance from the phosphate site, 150 vs. 115 amino acids (Figure 4.3E).

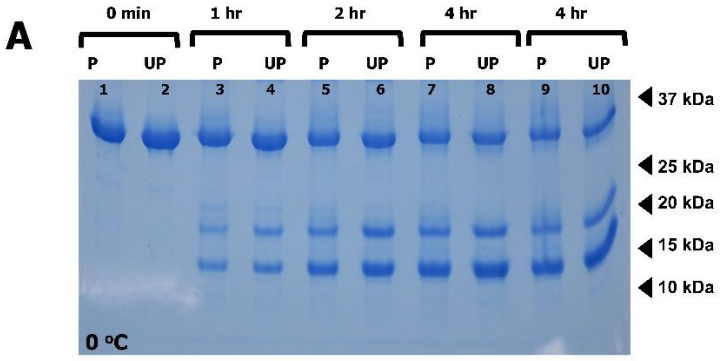
A
0 min
1 hr
2 hr
4 hr
4 hr
P UP P UP P UP P UP P UP
1 2 3 4 5 6 7 8 9 10
37 kDa
25 kDa
20 kDa
15 kDa
10 kDa
0 °C

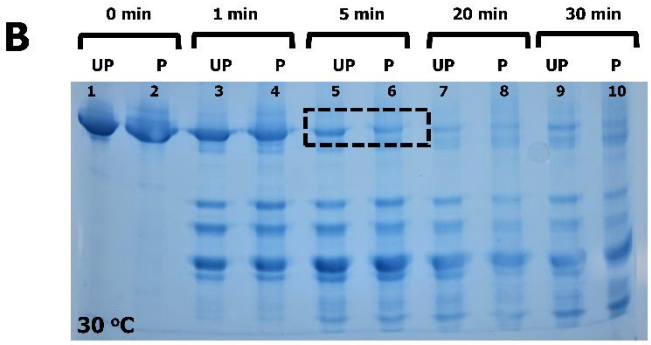
B
0 min
1 min
5 min
20 min
30 min
UP P UP P UP P UP P UP P
1 2 3 4 5 6 7 8 9 10
30 °C

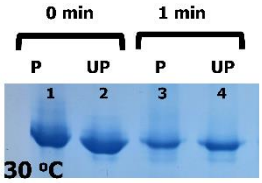
C
0 min
1 min
P UP P UP
1 2 3 4
30 °C

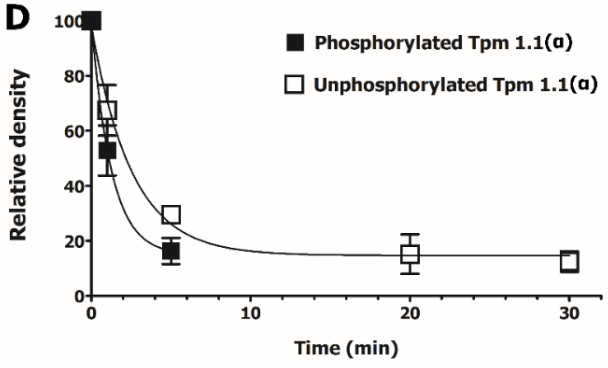
D
Relative density
100
80
60
40
20
0
0
10
20
30
Time (min)
Phosphorylated Tpm 1.1(α)
Unphosphorylated Tpm 1.1(α)

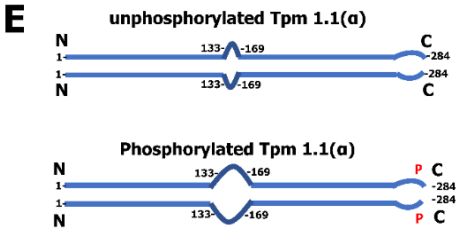
E
unphosphorylated Tpm 1.1(α)
N
C
1
133
169
284
Phosphorylated Tpm 1.1(α)
P

Figure 4.3. Tryptic digestion of P-Tpm1.1(α) compared to the control. The gels of 0 and 30 ^{o}C digestions are shown. P - Phosphorylated Tpm1.1(α) and UP - Unphosphorylated Tpm1.1(α). The mol: mol ratios of enzyme: substrate are: 1:250 (0 ^{o}C) and 1:1000 (30 ^{o}C). (A) 4-hour digestion at 0 ^{o}C. Extreme right of (A) Mr markers. (B) 30 min digestion at 30 ^{o}C. The upper highlighted area in (B) illustrates the differential abundance of the intact (33 kDa) band. (C) Short incubation with unequal amounts of the substrate, P > UP at time zero. Note the staining intensity of P < UP after 1 min. (D) Densitometric analysis of (B). Note: Phosphorylated Tpm1.1(α) is not measurable beyond 5 min (B and D). n=2. (E) Schematic representation of the effect of phosphorylation on the exposure of chymotryptic and tryptic digestion sites on the Tpm1.1 (α).

Table 4. 2. Mass spectrometric tryptic peptide mapping of T1 and T2 tryptic fragments of rabbit cardiac Tmp1.1(α).

Fragment	Fragment length	Sequence of the peptide
T1 **15 kDa** (residues 1 - 133) coverage 92%	1-6	MDAIKK
	7-12	KMQMLK
	12-21	LDKENALDR
	22-35	AEQAEADKKAAEDR
	38-56	LEDELVSLQK
	50-65	LKGTEDELDKYSEALK
	62-70	GTEDELDKYSEALKDAQEK
	66-76	DAQEKLELAEK
	71-91	LELAEKKATDAEADVASLNR
	91-105	RIQLVEEELDRAQER
	106-118	LATALQKLEEAEK
	112-125	AADESER
T2 **17 kDa** (residues 134 - 284) coverage 72%	134-150	AQKDEEKMEIQEIQLK
	153-160	HIAEDADR
	161-167	KYEEVAR
	167-182	KLVIIESDLERAEER
	190-205	CAELEEELKTVTNNLK
	199-213	TVTNNLKSLEAQAEK
	227-233	VLSDKLK
	245-251	SVTKLEK
	248-264	LEKSIDDLEDELYAQK

4.3.3 Effect of phosphorylation on conformational stability.

In this section, the global unfolding of tropomyosin is monitored circular dichroism. The ionic conditions, 0.1 M KCl, 1 mM dithiothreitol, pH 7.0, are such that both phosphorylated and unphosphorylated forms of tropomyosin will exist as units of 66,000 g/mole (reduced monomeric form) as in the case in the digestion experiments described above. The raw (non-derivatized) data are plotted in the normalized form in Figure 4.4. Although phosphorylation shows no significant effect on the recorded ellipticities at the start (~ 100 mdeg) and end (~ 10 mdeg) of a cycle relative to the error of concentration, the normalized profiles are not superimposable. In the middle portion of the temperature ramp, the curve corresponding to the phosphorylated protein is displaced slightly leftward showing reduced helical content between 25 and 42 ^{o}C compared to the unphosphorylated form (Figure 4.4)The unfolding that occurs in this temperature range can be assigned to sequences between the center and C-terminus of mammalian tropomyosin (Figure 4.6) (Ishii et al., 1992; Ly & Lehrer, 2012). As the temperature increases to 45 ^{o}C the two curves converge (Figure 4.4). At 50% ellipticity, the global melting temperatures differ by less than a degree: 43.5 ^{o}C (phosphorylated) and 44.3 ^{o}C (control). At this point, the difference in the melting temperatures reaches the limit of resolution. These observations are consistent with a subtle, but extended structural change emanating from the bound phosphates at one end of the molecule.

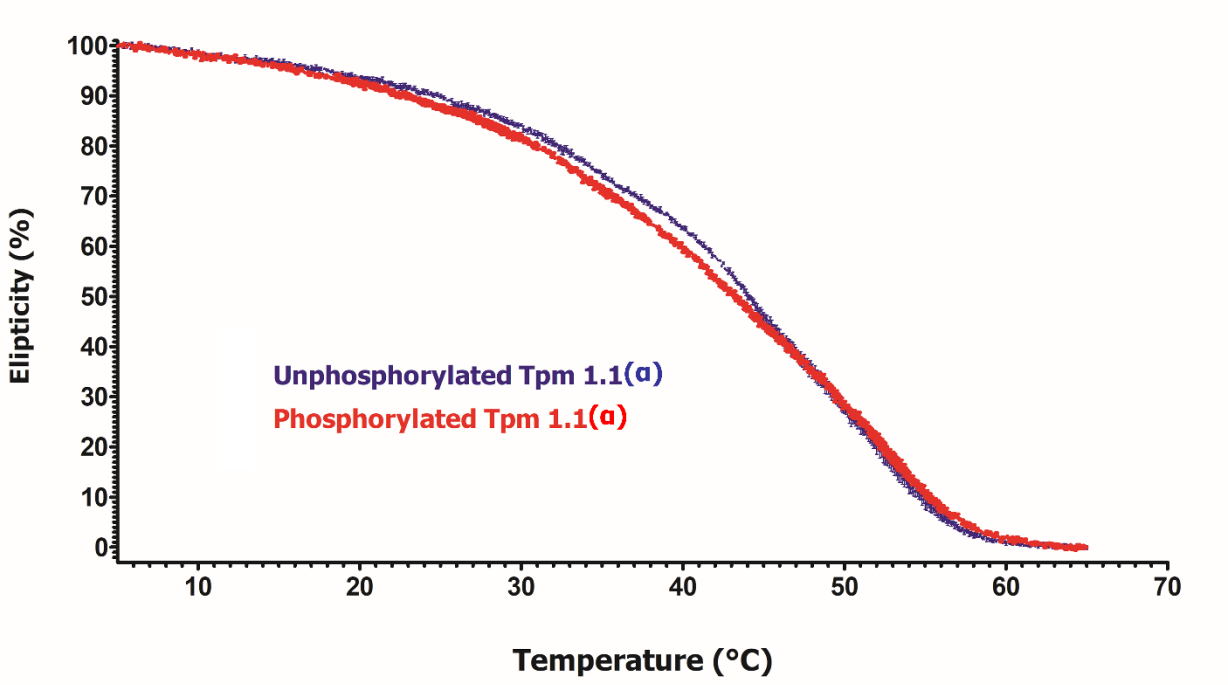

Figure 4.4. Comparison of the normalized unfolding profiles of phosphorylated and unphosphorylated rabbit tropomyosin Tpm1.1(α). The % ellipticity is calculated according to the formula in Materials and Methods (protein concentration, 1.5 mg/mL. Buffer conditions: 0.1 M NaCl, 20 mM sodium phosphate, 1 mM dithiothreitol, pH 7.0). Phosphorylated Tpm1.1(α) in red. Unphosphorylated control in blue. The curves, containing error bars every 0.1 ºC are the average of three separate experiments, N=3, in which a given sample is unfolded once only. Starting 222 nm ellipticities at 5 ºC, ~ 100 milli degrees. Ending 222 nm ellipticities at 65 ºC, ~ 10 millidegrees. Reprinted with permission from Silva, A. M. M., Goonasekara, C. L., Hayley, M., & Heeley, D. H. (2020). Further Investigation into the Biochemical Effects of Phosphorylation of Tropomyosin Tpm1.1(α). Serine-283 Is in Communication with the Midregion. Biochemistry, 59(50), 4725–4734. https://doi.org/10.1021/acs.biochem.0c00882. Copyright (2021) American Chemical Society.

4.3.4 Effect of phosphorylation on the F-actin affinity of unlabeled tropomyosin

In this section, the effect of phosphorylation on F-actin binding is assessed. In the process of actin-binding, a tropomyosin dimer (66,000 g/mole) interacts with seven actin monomers (Figure 4.5A). Owing to the tight interaction between tropomyosin and F-actin, sub-maximal conditions of ionic strength (30 mM KCl, 1 mM $MgCl_2$) and low temperature (Silva et al., 2020a) are employed to improve the chances of detecting a difference in affinity. It should be noted that no extrinsic modification is used. Titrations are performed by maintaining the F-actin concentration at 10 μM and varying the tropomyosin concentration between 0 - 3.5 μM. Presented in Figure 4.5B is an electrophoretic analysis of pre-and post-sedimentation mixtures of the two lowest concentrations, 0.25 and 0.50 μM. Based on the staining intensity of the tropomyosin-containing bands (Figure 4.5B, lanes 3, 4, 7, and 8) it is evident that phosphorylation alters the extent of complex formation. At both of the considered concentrations, the amount of phosphorylated Tpm1.1 (α) remaining in the supernatant is lower than that of the control (Figure 4.5B highlighted inset areas: lane 3 vs. lane 4 and lane 7 vs. lane 8). The binding curves in Figures 4.5C (non-normalized) and 4.5D (normalized) are generated in conjunction with a calibrated relationship (Figure 4.5C inset). The apparent binding constants obtained from the concentration of free tropomyosin at 50% saturation are 0.16 μM (phosphorylated Tpm1.1(α)) and 0.26 μM (control).

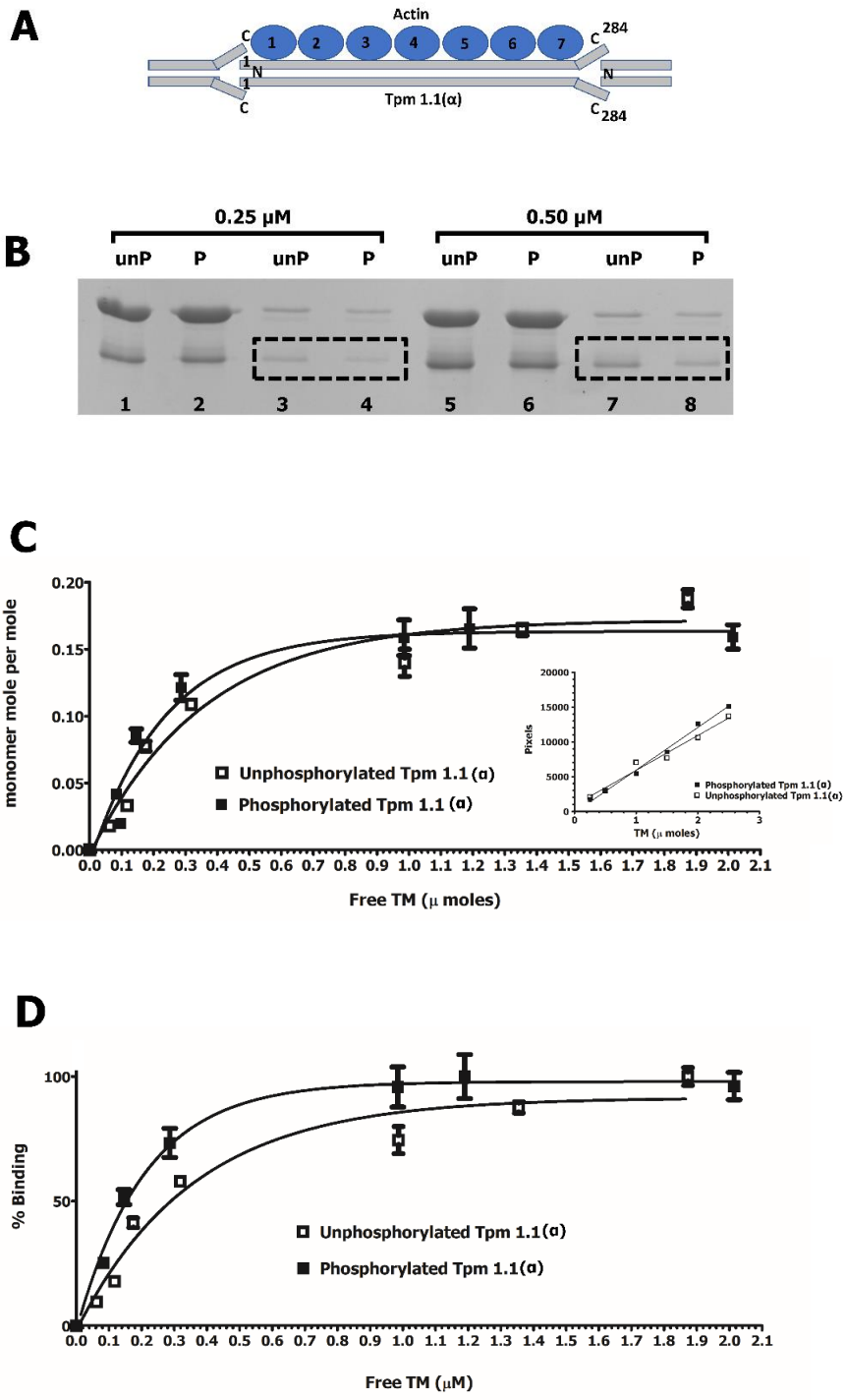
A
Actin
1
2
3
4
5
6
7
C
284
N
Tpm 1.1(α)
B
0.25 μM
0.50 μM
unP
P
unP
P
unP
P
unP
P
1
2
3
4
5
6
7
8
C
Bound Tpm 1.1(α) to actin monomer mole per mole
Free TM (μ moles)
Unphosphorylated Tpm 1.1 (α)
Phosphorylated Tpm 1.1 (α)
Pixels
TM (μ moles)
Phosphorylated Tpm 1.1(α)
Unphosphorylated Tpm 1.1(α)
D
% Binding
Free TM (μM)
Unphosphorylated Tpm 1.1(α)
Phosphorylated Tpm 1.1(α)

Figure 4.5. Effect of phosphorylation of rabbit tropomyosin Tpm1.1(α) on its interaction with F-actin. (A) Schematic representation of the acto-tropomyosin complex. Seven actin monomers (in blue) span across one molecule of tropomyosin which polymerizes via a merger of C- and N-termini. The concentration of tropomyosin is varied from 0 - 3.5 μM while F-actin is maintained at 10 μM. (B) SDS-PAGE of acto-tropomyosin mixtures before (lanes 1,2, 5, and 6) and after (lanes 3, 4, 7, and 8) sedimentation (stain, Coomassie R-250). Upper band, actin. Lower band, tropomyosin. UnP, unphosphorylated control. P, phosphorylated Tpm1.1(α). Highlighted lanes 3 vs. 4 and 7 vs. 8 demonstrate that comparatively less phosphorylated Tpm1.1(α) remains in the supernatant after sedimentation indicating a greater degree of complexation. (C) and (D) Tropomyosin concentration dependence of F-actin binding. (C) Raw data. Inset, calibrated densitometric relationships. (D) Normalized curves from (C). Apparent K_{DS} 0.16 μM (phosphorylated Tpm1.1(α), closed squares) and 0.28 μM (unphosphorylated control, open squares). Adapted with permission from Silva, A. M. M., Goonasekara, C. L., Hayley, M., & Heeley, D. H. (2020). Further Investigation into the Biochemical Effects of Phosphorylation of Tropomyosin Tpm1.1(α). Serine-283 Is in Communication with the Midregion. Biochemistry, 59(50), 4725–4734. https://doi.org/10.1021/acs.biochem.0c00882. Copyright (2021) American Chemical Society.

4.3.5 Molecular Visualization

The special arrangement of the N- and C-termini merger region was analyzed using PDB: 3MUD X-ray crystallography structure (Frye et al., 2010). According to the structure, ~ 10 amino acid residues from the N-terminus and ~ 12 from the C-terminus overlap with each other (Figure 4.6A). In this state, the C-terminal opening (distance between Ile-284s) is 22.7 Å (Figure 4.6B) which is ~ 4 times wider apart compared to the non-polymerized state. Neighboring Lys residues 5, 6, 7, 12, and 15 (Figure 4.6A highlighted in blue) are important in terms of their ability to introduce stabilization to the junction through ionic interactions to phosphate groups. Measuring the distance from phosphate groups to the Lys residues indicated that the closest possible interactions are caused by Lys-7 and Lys-12 residues on opposite strands which is in agreement with Lehman et. al 2015. In the case of Lys-7, the distances are 5.8 and 10.3 Å whereas for Lys-12 the values are 9.4 and 10.2 Å. When the distance between the two C-termini (Ile residues) is measured using PDB ID: 1MV4 in the non-polymerized state, rotamer 2 (out of the 10 rotamer structures provided) indicated a distance of 6.4 Å in the most favourable state (the lowest number of clashes with the neighboring residues).

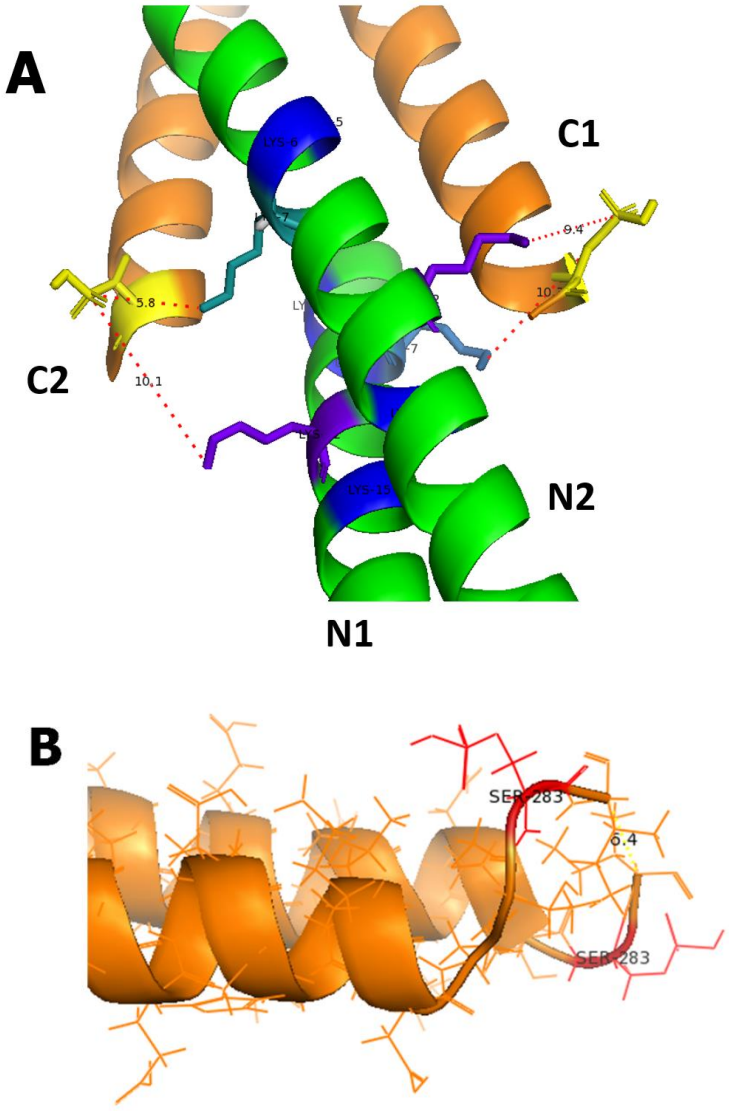

Figure 4.6. PyMOL visualization of the effect of phosphorylated serine-283 on the arrangement of N- and C-terminal residues of Tpm 1.1(α). C-terminus - orange, Ser-283 and the bound phosphate group - yellow, N-terminus - green, and Lys-5,6 and 15 - blue, Lys-7 - ash blue, Lys -12 – purple. C-terminal strands were labeled C1, C2 and N-terminal strands were labeled N1 and N2. (A) Interactions of N- and C-terminal junction residues (PDB ID: 1MUD). The distance of the C-terminal opening (distance between Ile-284s) 22.7 Å. Predicted distance between C-terminal phosphate C1 to Lys-7 on N-terminal strand N2 (5.8 Å) and Lys-12 on N-terminal strand N1 (10.2 Å). Similarly, C-terminal phosphate C2 to Lys-7 N-terminal strand N2 (10.3 Å) and Lys-12 on N-terminal strand N1 (9.4 Å). (B) C-terminal opening 6.4 Å in the monomeric state (PDB ID: 1MV4) of the most favorable rotamer structure (state two) with the lowest number of clashes with the neighboring residues.

4.4 Chapter 4 Discussion

Presented in this chapter is a further biochemical investigation into the effects of phosphorylation of Tpm1.1(α), the dominant isoform of tropomyosin in mammalian heart and skeletal muscle. The main findings are: (i) phosphorylation destabilizes sequences in the central region and the C-termini and (ii) phosphorylation tightens the interaction between Tpm1.1(α) and F-actin. These findings will now be discussed in turn.

Phosphorylation of serine-283 increases the susceptibility of Tpm1.1(α) to attack by chymotrypsin and trypsin, suggestive of an induced opening of the mid-region ~150 amino acids away from the phosphorylation site, and long-range communication. Although Leu-169 occupies a core "a" position, it is the preferred primary site in mammalian Tpm1.1(α) for chymotrypsin (Figure 4.2 and Pato et al., 1981). Such susceptibility to proteolysis is explained by the three adjoining bulky side-chains Val-170, Ile-171, and Ile-172 (Pato et al., 1981) and two carboxylates, Asp-175(g) and Glu-180(e), that disrupt electrostatic attraction between "e" (normally positive at pH 7) and "g" (negative at pH 7) residues (Stone & Smillie, 1978). Additional sources of instability are Asp-137(d) (Sumida et al., 2008) and Gly-126 (Nevzorov et al., 2011). Similarly, the susceptibility to trypsin at Arg-133 is explained by the neighboring residues in the sequence (Nevzorov et al., 2011). Occupation of the 137th core "d" position by a charged aspartic acid is expected to generate a local destabilization that increases the solvent exposure of Arg-133 (Pato et al., 1981). Therefore, it is reasonable to conclude that the corresponding section in tropomyosin adopts a more open configuration when phosphorylation occurs at the 283rd residue (Figure 4.3E). The accelerated rates of proteolysis (Figures 4.2 and 4.3) are in excellent agreement with

the melting experiments (Figure 4.4). Although we do not observe a drastic difference between the global melting temperatures of phosphorylated, 43.5 ^{o}C, and unphosphorylated, 44.3 ^{o}C (less than 1 ^{o}C apart) tropomyosin, the unfolding profiles are not superimposable between the temperatures 25 - 42 ^{o}C (Figure 4.4). Unfolding in this temperature range is known to arise from the destabilized sequences within the C-terminal half of tropomyosin (Williams & Swenson, 1981; Ishii et al., 1992; Ly & Lehrer, 2012).

The long-range effect of phosphorylation which we propose here leads to an increased rate of proteolysis by chymotrypsin (Figure 4.2), trypsin (Figure 4.3), and non-superimposable melting profiles (Figure 4.4) following the pattern of communication that has been demonstrated to occur between cysteine-190, the sole thiol group in Tpm1.1(α), and the C-terminal region (Graceffa & Lehrer, 1980; Clark & Burtnick, 1990). In the context of phosphorylation, the structural connectivity encompasses an even longer length of the molecule, from residue-283 to residue-133 (Figures 4.2 and 4.3). Co-sedimentation experiments (Figure 4.5) reveal that phosphorylation tightens the interaction between Tpm1.1(α) and F-actin. This is evident with the increased F- actin affinity (K_D, 0.25 μM) of the phosphorylated form as opposed to the non-phosphorylated form (0.5 μM, Figure 4.5). Although the complexation with F-actin depends on the ends of tropomyosin, the center also plays an important role by serving as actin-binding sites (Tobacman & Butters, 2000). Critical in this regard is the 4th and 5th actin-binding periods, especially residues 124 - 147 (4^{th} period) and 166 - 189 (5^{th} period N-terminal residues) (Hitchcock-DeGregori & Singh, 2010) which notably include the susceptible Arg-133 and Leu-169 peptide bonds.

PyMOL (Figure 4.6A) indicates the involvement of several ionic interactions between C-terminal Ser-283 phosphate groups and the N-terminal Lys-5, Lys-6, Lys-7, Lys-12, and Lys-15 residues (shortest to Lys-7 and Lys-12) that stabilize the merger as observed by Lehman et. al., 2015. The analysis of the C and N-terminal merger also suggests an enlargement in the opening of the C-termini (22.7 vs. 6.4 Å) as opposed to the non-polymerized states (Figure 4.6B). These findings suggest that phosphorylation stabilizes the merger region via the formation of extra salt-bridges (Lehman et. al 2015). The network of such interactions could be further investigated by mutagenic replacement of Lys-7 and Lys-12 to alanine, followed by phosphorylation of Ser-283 using the appropriate kinase (Montgomery & Mak 1984; Rajan et al., 2019), and measurement of polymerization (Heeley et al., 1989).

Combining the various strands of evidence, the current results add weight to the idea that a high proportion of phosphorylated tropomyosin, as occurs in immature striated muscle of mammals and birds (Montarras et al., 1981; Heeley et al., 1982; Heeley, 2013), favors thin filament formation by facilitating the interaction between connecting tropomyosins (Heeley et al., 1989), tropomyosin and troponin (Heeley et al., 1989; Heeley, 1994) and tropomyosin and F-actin (Figure 4.5). However, as needed during the muscle filament during development. However, this cannot be applied to all vertebrate species (e.g. Salmonidae) for which no evidence of phosphorylation has been found (Heeley et al., 1995; Silva et al., 2020a). It is also fascinating that a covalent modification that is advantageous early in life, can be, depending on the circumstances, detrimental later on (Rajan et al., 2019).

In summary, with the observations from this Chapter, we suggest that Ser-283 is in communication with the mid-region of tropomyosin (Silva et al., 2020a). Although the mechanism of transmission is unknown, the results are consistent with phosphorylation of this amino acid further destabilizing the ‘weak spot’ of the molecule (Sumida et al., 2008) and (Figure 4.3E), which is the location of two proteolytically susceptible peptide bonds (Figures 4.2 and 4.3) as well as binding sites for F-actin (Figure 4.3E and 4.5A) and troponin (Heeley et al., 1982; Heeley, 2013). The outcome can explain the possible important role that tropomyosin phosphorylation plays in embryogenesis, specifically in facilitating interactions between the various proteins of the thin filament.

4.5 Chapter 4 Future Directions

1) An obvious next step will be to compare the proteolytic susceptibility of phosphorylated and unphosphorylated Tpm 1.1(α) (Figures 4.2 and 4.3) when in complexed with actin. The results of co-sedimentation (Figure 4.5) suggest that the comparatively greater openness (solvent exposure) of the phosphorylated molecule as illustrated schematically in Figure 4.3E, does persist in the polymerized state. The digestion conditions of Ly and Lehrer (2012), where actin is resistant to trypsin, will be followed. Performing limited proteolysis on the acto-tropomyosin complex together with cleavage site identification will further reveal the actin-binding regions of the coiled-coil that are sensitive to phosphorylation.

2) All of the biochemical investigations into the effect of tropomyosin phosphorylation on thin filament function have been performed using skeletal muscle proteins (Heeley et al., 1989; Heeley 1994; Silva et al., 2020a). It will be interesting, therefore, to repeat these previous studies with cardiac proteins. These will include: (i) cardiac troponin-Sepharose to compare the binding affinities of P-Tpm 1.1(α) and UnP-Tpm 1.1(α) and (ii) tropomyosin-Sepharoses (phosphorylated and control) to compare the binding affinities of different isoforms of cardiac troponin-T. Further, phosphorylated and control thin filaments will be reconstituted with cardiac troponin for use in myosin ATPase assays as suggested in section 3.5.

4.6 Chapter 4 References

Bárány, K., Bárány, M., Gillis, J. M., & Kushmerick, M. J. (1979). Phosphorylation-dephosphorylation of the 18,000-dalton light chain of myosin during the contraction-relaxation cycle of frog muscle. *The Journal of Biological Chemistry*, *254*(9), 3617–3623. https://doi.org/https://doi.org/10.1016/S0021-9258(18)50806-1

Brisson, J. R., Golosinska, K., Smillie, L. B., & Sykes, B. D. (1986). Interaction of tropomyosin and troponin T: a proton nuclear magnetic resonance study. *Biochemistry*, *25*(16), 4548–4555. https://doi.org/10.1021/bi00364a014

Clark, I. D., & Burtnick, L. D. (1990). Coupled responses of the regions near cysteine-190 and the carboxy terminus of rabbit cardiac tropomyosin: fluorescence and circular dichroism studies. *Biochemistry*, *29*(48), 10842–10846. https://doi.org/10.1021/bi00500a018

Denz, C. R., Narshi, A., Zajdel, R. W., & Dube, D. K. (2004). Expression of a novel cardiac-specific tropomyosin isoform in humans. *Biochemical and Biophysical Research Communications*, *320*(4), 1291–1297. https://doi.org/10.1016/j.bbrc.2004.06.084

Frye, J., Klenchin, V. A., & Rayment, I. (2010). Structure of the tropomyosin overlap complex from chicken smooth muscle: Insight into the diversity of N-terminal recognition. *Biochemistry*, *49*(23), 4908–4920. https://doi.org/10.1021/bi100349a

Goonasekara, C. L., & Heeley, D. H. (2009). Effect of Removing the Amino-Terminal Hexapeptide of Tropomyosin on the Properties of the Thin Filament. *Biochemistry*,

48(15), 3538–3544. https://doi.org/10.1021/bi802004j

Graceffa, P., & Lehrer, S. S. (1980). The excimer fluorescence of pyrene-labeled tropomyosin. A probe of conformational dynamics. *The Journal of Biological Chemistry*, *255*(23), 11296–11300. https://doi.org/https://doi.org/10.1016/S0021-9258(19)70290-7

Greenfield, N. J., Huang, Y. J., Swapna, G. V. T., Bhattacharya, A., Rapp, B., Singh, A., Montelione, G. T., & Hitchcock-DeGregori, S. E. (2006). Solution NMR Structure of the Junction between Tropomyosin Molecules: Implications for Actin Binding and Regulation. *The Journal of Molecular Biology*, *364*(1), 80–96. https://doi.org/10.1016/j.jmb.2006.08.033

Greenfield, N. J., Swapna, G. V. T., Huang, Y., Palm, T., Graboski, S., Montelione, G. T., & Hitchcock-DeGregori, S. E. (2003). The structure of the carboxyl terminus of striated α-tropomyosin in solution reveals an unusual parallel arrangement of interacting α-helices. *Biochemistry*, *42*(3), 614–619. https://doi.org/10.1021/bi026989e

Hayley, M., Chevaldina, T., Mudalige, W. A. K. A., Jackman, D. M., Dobbin, A. D., & Heeley, D. H. (2008). Shark skeletal muscle tropomyosin is a phosphoprotein. *Journal of Muscle Research and Cell Motility*, *29*(2–5), 101–107. https://doi.org/10.1007/s10974-008-9143-z

Heeley, D.H., Bieger, T., Waddleton, D.M., Hong, C., Jackman, D.M., McGowan, C., Davidson, W.S. & Beavis, R. C. (1995). Characterisation of fast, slow and cardiac

muscle tropomyosin from salmonid fish. *European Journal of Biochemistry.*, *232*, 226 – 234.

Heeley, D. H., Moir, A. J. G., & Perry, S. V. (1982). Phosphorylation of tropomyosin during development in mammalian striated muscle. *FEBS Letters*, *146*(1), 115–118. https://doi.org/10.1016/0014-5793(82)80716-3

Heeley, D. H. (1994). Investigation of the effects of phosphorylation of rabbit striated muscle αα-tropomyosin and rabbit skeletal muscle troponin-T. *European Journal of Biochemistry*, *221*(1), 129–137. https://doi.org/10.1111/j.1432-1033.1994.tb18721.x

Heeley, D. H., Watson, M. H., Mak, A. S., Dubord, P., & Smillie, L. B. (1989). Effect of phosphorylation on the interaction and functional properties of rabbit striated muscle αα-tropomyosin. *Journal of Biological Chemistry*, *264*(5), 2424–2430. https://doi.org/10.1016/S0021-9258(19)81630-7

Heeley, D. H., Smillie, L. B., & Lohmeier-Vogel, E. M. (1989). Effects of deletion of tropomyosin overlap on regulated actomyosin subfragment 1 ATPase. *The Biochemical Journal*, *258*(3), 831—836. https://doi.org/10.1042/bj2580831

Heeley, D. H. (2013). Phosphorylation of tropomyosin in striated muscle. *Journal of Muscle Research and Cell Motility*, *34*(3), 233–237. https://doi.org/10.1007/s10974-013-9351-z

Hitchcock-DeGregori, S. E., & Singh, A. (2010). What makes tropomyosin an actin binding protein? A perspective. *Journal of Structural Biology*, *170*(2), 319–324. https://doi.org/10.1016/j.jsb.2009.12.013

Houk, T. W., & Ue, K. (1974). The measurement of actin concentration in solution: A comparison of methods. *Analytical Biochemistry*, *62*(1), 66–74. https://doi.org/https://doi.org/10.1016/0003-2697(74)90367-4

Ishii, Y., Hitchcock-Degregori, S., Mabuchi, K., & Lehrer, S. S. (1992). Unfolding domains of recombinant fusion αα-tropomyosin. *Protein Science*, *1*(10), 1319–1325. https://doi.org/10.1002/pro.5560011011

Ly, S., & Lehrer, S. S. (2012). Long-range effects of familial hypertrophic cardiomyopathy mutations E180G and D175N on the properties of tropomyosin. *Biochemistry*, *51*(32), 6413–6420. https://doi.org/10.1021/bi3006835

Mak, A. S., & Smillie, L. B. (1981). Structural interpretation of the two-site binding of troponin on the muscle thin filament. *Journal of Molecular Biology*, *149*(3), 541–550. https://doi.org/https://doi.org/10.1016/0022-2836(81)90486-1

Montarras, D., Fiszman, M. Y., & Gros, F. (1981). Characterization of the tropomyosin present in various chick embryo muscle types and in muscle cells differentiated in vitro. *The journal of Biological Chemistry*, *256*(8), 4081–4086. https://doi.org/10.1016/s0021-9258(19)69568-2

Montgomery, K., & Mak, A. S. (1984). In vitro phosphorylation of tropomyosin by a kinase from chicken embryo. *The Journal of Biological Chemistry*, *259*(9), 5555–5560.

Morris, E. P., & Lehrer, S. S. (1984). Troponin-Tropomyosin Interactions. Fluorescence Studies of the Binding of Troponin, Troponin T, and Chymotryptic Troponin T

Fragments to Specifically Labeled Tropomyosin. *Biochemistry*, *23*(10), 2214–2220. https://doi.org/10.1021/bi00305a018

Nevzorov, I. A., Nikolaeva, O. P., Kainov, Y. A., Redwood, C. S., & Levitsky, D. I. (2011). Conserved noncanonical residue Gly-126 confers instability to the middle part of the tropomyosin molecule. *The Journal of Biological Chemistry*, *286*(18), 15766–15772. https://doi.org/10.1074/jbc.m110.209353

Ohtsuki, I. (1979). Molecular arrangement of troponin-T in the thin filament. *Journal of Biochemistry*, *86*(2), 491–497. https://doi.org/10.1093/oxfordjournals.jbchem.a132549

Pato, M. D., Mak, A. S., & Smillie, L. B. (1981). Fragments of rabbit striated muscle α-tropomyosin. I. Preparation and characterization. *The Journal of Biological Chemistry*, *256*(2), 593–601. https://doi.org/10.1016/s0021-9258(19)70014-3

Pearlstone, J. R., & Smillie, L. B. (1982). Binding of troponin-T fragments to several types of tropomyosin. Sensitivity to Ca^{2+} in the presence of troponin-C. *The Journal of Biological Chemistry*, *257*(18), 10587–10592. https://doi.org/10.1016/s0021-9258(18)33862-6

Rajan, S., Jagatheesan, G., Karam, C. N., Alves, M. L., Bodi, I., Schwartz, A., Bulcao, C. F., D'Souza, K. M., Akhter, S. A., Boivin, G. P., Dube, D. K., Petrashevskaya, N., Herr, A. B., Hullin, R., Liggett, S. B., Wolska, B. M., Solaro, R. J., & Wieczorek, D. F. (2010). Molecular and functional characterization of a novel cardiac-specific human tropomyosin isoform. *Circulation*, *121*(3), 410–418.

https://doi.org/10.1161/CIRCULATIONAHA.109.889725

Rajan, S., Jagatheesan, G., Petrashevskaya, N., Biesiadecki, B. J., Warren, C. M., Riddle, T., Liggett, S., Wolska, B. M., Solaro, R. J., & Wieczorek, D. F. (2019). Tropomyosin pseudo-phosphorylation results in dilated cardiomyopathy. *The Journal of Biological Chemistry*, *294*(8), 2913–5835. https://doi.org/10.1074/jbc.RA118.004879

Rasband, W. (2018). *ImageJ* (imagej 1.52a). U. S. National Institutes of Health. https://imagej.nih.gov/ij/

Sano, K., Maeda, K., Oda, T., & Maéda, Y. (2000). The effect of single residue substitutions of serine-283 on the strength of head-to-tail interaction and actin binding properties of rabbit skeletal muscle alpha-tropomyosin. *Journal of Biochemistry*, *127*(6), 1095–1102. https://doi.org/10.1093/oxfordjournals.jbchem.a022703

Silva, A. M. M., Goonasekara, C. L., Hayley, M., & Heeley, D. H. (2020a). Further Investigation into the Biochemical Effects of Phosphorylation of Tropomyosin Tpm1.1(α). Serine-283 Is in Communication with the Midregion. *Biochemistry*, *59*(50), 4725–4734. https://doi.org/10.1021/acs.biochem.0c00882

Silva, A. M. M., Kennedy, L. S., Hasan, S. C., Cohen, A. M., & Heeley, D. H. (2020c). Demonstration of beta-tropomyosin (Tpm2) and duplication of the alpha-slow tropomyosin gene (TPM3) in Atlantic salmon (*Salmo salar*). *Comparative Biochemistry and Physiology Part - B: Biochemistry and Molecular Biology*,

245(January), 110439. https://doi.org/10.1016/j.cbpb.2020.110439

Singh, A., & Hitchcock-DeGregori, S. E. (2007). Tropomyosin's periods are quasi-equivalent for actin binding but have specific regulatory functions. *Biochemistry*, *46*(51), 14917–14927. https://doi.org/10.1021/bi701570b

Stone, D., & Smillie, L. B. (1978). The amino acid sequence of rabbit skeletal α-tropomyosin. The NH2-terminal half and complete sequence. *The Journal of Biological Chemistry*, *253*(4), 1137–1148. https://doi.org/10.1016/s0021-9258(17)38122-x

Sumida, J. P., Wu, E., & Lehrer, S. S. (2008). Conserved Asp-137 imparts flexibility to tropomyosin and affects function. *The Journal of Biological Chemistry*, *283*(11), 6728–6734. https://doi.org/10.1074/jbc.M707485200

Tanokura, M., Tawada, Y., Ono, A., & Ohtsuki, I. (1983). Chymotryptic subfragments of troponin t from rabbit skeletal muscle. interaction with tropomyosin, troponin I and troponin C1. *Journal of Biochemistry*, *93*(2), 331–337. https://doi.org/10.1093/oxfordjournals.jbchem.a134185

Tobacman, L. S., & Butters, C. A. (2000). A new model of cooperative myosin-thin filament binding. *The Journal of Biological Chemistry*, *275*(36), 27587–27593. https://doi.org/10.1074/jbc.M003648200

White, S P, Cohen, C., & Phillips, G. N. J. (1987). Structure of co-crystals of tropomyosin and troponin. *Nature*, *325*(6107), 826–828. https://doi.org/10.1038/325826a0

Williams, D. L., & Swenson, C. A. (1981). Tropomyosin Stability: Assignment of Thermally Induced Conformational Transitions to Separate Regions of the Molecule. *Biochemistry*, *20*(13), 3856–3864. https://doi.org/10.1021/bi00516a029

Chapter 5. General discussion

5.1 Fish beta and alpha-1 chain-like isoform X1 tropomyosin isoforms

Chapter 2 of this thesis demonstrates the existence of beta (Tpm2) and alpha-1 chain-like isoform X1 tropomyosin isoforms at the protein level in Atlantic salmon (*Salmo salar*) and for the first time in any fish species. Tpm2 is identified in the skeletal muscles of the tongue, jaw, and pectoral fin (as well as in the slow muscle in the trunk (Silva et al., 2020c)) where it contributes to half of the total tropomyosin, collectively making it the second-most abundant isoform of tropomyosin in Atlantic salmon after Tpm1 (alpha fast). The identity of salmon Tpm2 was confirmed by phylogenetic analysis. Compared to the chicken and rodent homologues, salmon Tpm2 contains 29 and 30 amino acid differences, respectively. Unique features of the salmonid Tpm2 isoform are a reduced number of cysteine (one vs. two) and tyrosine (five vs. six) residues (Figure 2.4), and differences in the C-terminal portion of the overlap region. Between salmon Tpm2 and Tpm1, there are 32 amino acid differences which are found in clusters located within troponin binding sites and the C- and N-terminal regions (Figure 2.4). The only charge substitution, Lys-77 in Tpm2 and Thr-77 in Tpm1 generates the opposite of the mobility-isotype relationship that was originally reported by Cummins & Perry, 1973; Tpm1 (slower migration) and Tpm2 (faster migration) (Figure 3.2). Comparison of salmon Tpm2 to the homologs in pufferfish and zebrafish shows fewer than 10 substitutions. Tpm2 and alpha-1 chain-like isoform X1 (XP_013996655) differ by 32 substitutions (Figure 2.6 legend). These include alterations in group charge and size. A unique feature of salmon tropomyosin isoforms is the presence of closely spaced pairs of glycines between residues 20 - 90, specifically, Gly-24 and Gly-

27 in Tpm1; Gly-27 and Gly-31 in Tpm2; Gly-45 and Gly-52 in alpha-1 chain-like isoform X1 and Gly-83 and Gly-87 in Tpm4 (cardiac) (Figure 2.4). This thesis proposes that such pairings help tropomyosin to achieve additional flexibility which is needed to inhabit a polar niche in the ocean where the temperture is sustained at single digits throughout most of the year.

5.2 Cold adaptations in Tpm1 of Atlantic salmon

Chapter 3 of this thesis demonstrates two strategies used by tropomyosin to adjust to low temperature: 1) the insertion of a neutral side-chain, threonine-77(g) instead of lysine, the residue found in other vertebrate Tpm1s, in the second alanine cluster (Singh & Hitchcock-DeGregori, 2003), that annuls ionic interactions with proximal carboxylates (Figure 3.11) and 2) a unique glycyl pair at residues at positions 24 and 27 which are conspicuous in regard to the helix breaking properties of this amino acid (Richardson & Richardson, 1988). Chapter 3 demonstrates that these features have long-range and localized effects on the conformation of salmon Tpm1. Reinstating lysine at residue position 77 (i.e., Thr-77 to Lys-77) produces a significant increase in melting temperature compared to wild type salmon Tpm1. (Chapter 3 Table 3.2). A similar result is obtained by double mutation of the two glycines (i.e., Gly-24 and Gly-27 to Ala) (Figures 3A and 3E). In both instances, the effect of the mutation infers that the wild type amino acids, Gly-24, Gly-27 and Thr-77, are sources of instability. Results from Chapter 3 suggest that the induced-molecular flexibility combines with that which is produced by alanine clusters (especially nos. 1 and 2) in order to maintain the binding of salmon tropomyosin to its targets, actin and troponin. The

mutation Thr-77 to Lys-77 generates a marked resistance to chymotrypsin digestion at Leu-169 (Figure 3.5), more than 90 amino acids downstream, highlighting the long-range (2^{nd} to 5^{th} alanine cluster) communication within the molecule. The influence of Thr-77 is also evident in the tighter binding of control Tpm1 (Thr-77) to a troponin affinity medium compared to the mutant (Lys-77) (Figure 3.4), which again indicates that the middle of salmon Tpm1 adopts a more open configuration when it contains a neutral 77^{th} amino acid.

Binding experiments (Figure 3.10) demonstrate that salmon Tpm1 possesses the requisite flexibility to wind around F-actin and thereby form a tight association at 4 ^{o}C, unlike mammalian tropomyosin whose greater rigidity deters interaction at low temperature (Drabikowski & Gergely, 1962). In the case of the salmon protein, which contains destabilizing side-chains at positions 24, 27, and 77, the weaker binding which is observed at 22 ^{o}C (Figure 3.10), a temperature near to the first unfolding transition (Table 3.2), is indicative of too much flexibility which reduces the conformational specificity of binding sites.

Additionally, the replacement of Lys-77 by Thr in the human missense cardiomyopathy mutation, Lys70(g)Thr (Heller et al., 2003) demonstrates (the fact) that an exchange of an amino acid deleterious in one vertebrate group could be advantageous in another (Hayley et al., 2011) highlighting the delicate balance between stability and function (Hitchcock-DeGregori & Singh, 2010).

5.3 Phosphorylation of Ser-283 of Tpm1.1(α)

Chapter 4 investigates the effects of phosphorylation of Tpm1.1 (α), the dominant isoform of tropomyosin in the mammalian heart and skeletal muscle. Phosphorylation increases the susceptibility of Tpm1.1(α) to attack by chymotrypsin (between Leu-169-Val-170) and trypsin (between Arg-133-Ala-134), indicative of an induced opening of the mid-region (Figure 4.3E), and structural connectivity that encompasses ~150 amino acids away from the phosphorylation site (Figures 4.2 and 4.3) (Silva et al., 2020a). A similar pattern of communication is known to occur between cysteine-190 and the C-terminal region (Graceffa & Lehrer, 1980; Clark & Burtnick, 1990). The modification also causes the thermal unfolding profiles of phosphorylated and non-phosphorylated forms to be non-superimposable between the temperatures 25 - 42 ^{o}C (Figure 4.4), in excellent agreement with the proteolysis results (Figures 4.2 and 4.3).

Co-sedimentation experiments (Figure 4.5) reveal that phosphorylation tightens the interaction between tropomyosin and F-actin consistent with an effect on the 4th (residues 124 - 147) and 5th (N-terminal residues 166 - 189) actin-binding periods (Hitchcock-DeGregori & Singh, 2010) which notably include the susceptible Arg-133 and Leu-169 peptide bonds (‘weak spot’ of the molecule (Sumida et al., 2008)) (Figures 4.2, and 4.3E). PyMOL indicates ionic interactions between Ser-283 phosphate groups and the N-terminal Lys-5, Lys-6, Lys-7, Lys-12, and Lys-15 residues (Figure 4.6A) show the involvement of several cross strand salt-bridges (Lys-7 and Lys-12 generating the shortest) that stabilize the merger as reported by Lehman et. al., 2015. Further, analysis of the C- and N-terminal

merger in the polymeric tropomyosin shows an enlargement in the opening of the C-terminus compared to the monomer (22.7 vs. 6.4 Å) (Figure 4.6B). The current results add weight to the idea that a high proportion of phosphorylated tropomyosin, favors thin filament formation by facilitating the associations between the various constituents, namely tropomyosin with itself (Heeley et al., 1989), tropomyosin, and troponin (Heeley et al., 1989; Heeley, 1994) and tropomyosin and F-actin (Figure 4.5 and Silva et al., 2020b) as would be needed during muscle development.

5.4 Conclusion

This thesis provides a biochemical explanation as to how tropomyosin acquires the additional-flexibility needed to interact with other proteins in the thin filament without deviating from its blueprint. Although the most abundant form of tropomyosin from mesophiles (rabbit) and psychrophiles (salmon) share more than 90 % identity, a small number of amino acid changes in key positions (Perutz, 1983) have created an isoform in salmon that is optimized for function at low temperature.

Proteomic analyses of tropomyosins existing in the head and trunk (white) muscles of Atlantic salmon demonstrate the existence of other, previously unstudied, isoforms including beta that contain features (i.e., closely situated pairs of glycine residues) suited to maintaining flexibility in a cold ocean niche.

Additionally, the post-translational modification process of phosphorylation, which occurs at Ser-283, is another mode used by the molecule to fine-tune its structural and functional characteristics.

5.5 Chapter 5 References

Clark, I. D., & Burtnick, L. D. (1990). Coupled responses of the regions near cysteine-190 and the carboxy terminus of rabbit cardiac tropomyosin: fluorescence and circular dichroism studies. *Biochemistry*, *29*(48), 10842–10846. https://doi.org/10.1021/bi00500a018

Cummins, P., & Perry, S. V. (1973). The subunits and biological activity of polymorphic forms of tropomyosin. *Biochemical Journal*, *133*(4), 765–777. https://doi.org/10.1042/bj1330765

Drabikowski, W., & Gergely, J. (1962). The Effect of the Temperature of Extraction on the Tropomyosin Content in Actin. *The Journal of Biological Chemistry*, *237*(11), 3412–3417. https://doi.org/10.1016/s0021-9258(19)70831-x

Graceffa, P., & Lehrer, S. S. (1980). The excimer fluorescence of pyrene-labeled tropomyosin. A probe of conformational dynamics. *The Journal of Biological Chemistry*, *255*(23), 11296–11300. https://doi.org/https://doi.org/10.1016/S0021-9258(19)70290-7

Hayley, M., Chevaldina, T., & Heeley, D. H. (2011). Cold adaptation of tropomyosin. *Biochemistry*, *50*(30), 6559–6566. https://doi.org/10.1021/bi200327g

Heeley, D. H. (1994). Investigation of the effects of phosphorylation of rabbit striated muscle αα-tropomyosin and rabbit skeletal muscle troponin-T. *European Journal of Biochemistry*, *221*(1), 129–137. https://doi.org/10.1111/j.1432-1033.1994.tb18721.x

Heeley, D. H., Watson, M. H., Mak, A. S., Dubord, P., & Smillie, L. B. (1989). Effect of phosphorylation on the interaction and functional properties of rabbit striated muscle αα-tropomyosin. *The Journal of Biological Chemistry*, *264*(5), 2424–2430. https://doi.org/10.1016/S0021-9258(19)81630-7

Heller, M. J., Nili, M., Homsher, E., & Tobacman, L. S. (2003). Cardiomyopathic Tropomyosin Mutations that Increase Thin Filament Ca^{2+} Sensitivity and Tropomyosin N-domain Flexibility. *The Journal of Biological Chemistry*, *278*(43), 41742–41748. https://doi.org/10.1074/jbc.M303408200

Hitchcock-DeGregori, S. E., & Singh, A. (2010). What makes tropomyosin an actin binding protein? A perspective. *Journal of Structural Biology*, *170*(2), 319–324. https://doi.org/10.1016/j.jsb.2009.12.013

Perutz, M. F. (1983). Species adaptation in a protein molecule. *Molecular Biology and Evolution*, *1*(1), 1–28. https://doi.org/10.1093/oxfordjournals.molbev.a040299

Richardson, J. S., & Richardson, D. C. (1988). Amino acid preferences for specific locations at the ends of alpha helices. *Science*, *240*(4859), 1648–1652. https://doi.org/10.1126/science.3381086

Silva, A. M. M., Goonasekara, C. L., Hayley, M., & Heeley, D. H. (2020a) Further Investigation into the Biochemical Effects of Phosphorylation of Tropomyosin Tpm1.1(α). Serine-283 Is in Communication with the Midregion. *Biochemistry*, *59*(50), 4725–4734. https://doi.org/10.1021/acs.biochem.0c00882

Silva, A. M. M., Kennedy, L. S., Hasan, S. C., Cohen, A. M., & Heeley, D. H. (2020c).

Demonstration of beta-tropomyosin (Tpm2) and duplication of the alpha-slow tropomyosin gene (TPM3) in Atlantic salmon (*Salmo salar*). *Comparative Biochemistry and Physiology Part - B: Biochemistry and Molecular Biology*, *245*(January), 110439. https://doi.org/10.1016/j.cbpb.2020.110439

Singh, A., & Hitchcock-DeGregori, S. E. (2003). Local Destabilization of the Tropomyosin Coiled Coil Gives the Molecular Flexibility Required for Actin Binding. *Biochemistry*, *42*(48), 14114–14121. https://doi.org/10.1021/bi0348462

Sumida, J. P., Wu, E., & Lehrer, S. S. (2008). Conserved Asp-137 imparts flexibility to tropomyosin and affects function. *The Journal of Biological Chemistry*, *283*(11), 6728–6734. https://doi.org/10.1074/jbc.M707485200

Appendix

Copyright Licenses 1

Demonstration of beta-tropomyosin (Tpm2) and duplication of the alpha-slow tropomyosin gene (TPM3) in Atlantic salmon Salmo salar

Author:
A. Madhushika M. Silva,Luke S. Kennedy,Stephanie C. Hasan,Alejandro M. Cohen,David H. Heeley

Publication:
Comparative Biochemistry and Physiology Part B: Biochemistry and Molecular Biology

Publisher: Elsevier

Date: July 2020

Journal Author Rights

Please note that, as the author of this Elsevier article, you retain the right to include it in a thesis or dissertation, provided it is not published commercially. Permission is not required, but please ensure that you reference the journal as the original source. For more information on this and on your other retained rights, please visit: https://www.elsevier.com/about/our-business/policies/copyright#Author-rights

BACK CLOSE WINDOW

Copyright Licenses 2

Threonine-77 Is a Determinant of the Low-Temperature Conditioning of the Most Abundant Isoform of Tropomyosin in Atlantic Salmon

Author: A. Madhushika M. Silva, Tolulope Ige, Charitha L. Goonasekara, et al

Publication: Biochemistry

Publisher: American Chemical Society

Date: Aug 1, 2020

PERMISSION/LICENSE IS GRANTED FOR YOUR ORDER AT NO CHARGE

This type of permission/license, instead of the standard Terms & Conditions, is sent to you because no fee is being charged for your order. Please note the following:

- Permission is granted for your request in both print and electronic formats, and translations.
- If figures and/or tables were requested, they may be adapted or used in part.
- Please print this page for your records and send a copy of it to your publisher/graduate school.
- Appropriate credit for the requested material should be given as follows: "Reprinted (adapted) with permission from (COMPLETE REFERENCE CITATION). Copyright (YEAR) American Chemical Society." Insert appropriate information in place of the capitalized words.
- One-time permission is granted only for the use specified in your request. No additional uses are granted (such as derivative works or other editions). For any other uses, please submit a new request.

BACK CLOSE WINDOW

Copyright Licenses 3

ACS Publications
Most Trusted. Most Cited. Most Read.

Further Investigation into the Biochemical Effects of Phosphorylation of Tropomyosin Tpm1.1(α). Serine-283 Is in Communication with the Midregion

Author: A. Madhushika M. Silva, Charitha L. Goonasekara, Michael Hayley, et al

Publication: Biochemistry

Publisher: American Chemical Society

Date: Dec 1, 2020

PERMISSION/LICENSE IS GRANTED FOR YOUR ORDER AT NO CHARGE

This type of permission/license, instead of the standard Terms & Conditions, is sent to you because no fee is being charged for your order. Please note the following:

- Permission is granted for your request in both print and electronic formats, and translations.
- If figures and/or tables were requested, they may be adapted or used in part.
- Please print this page for your records and send a copy of it to your publisher/graduate school.
- Appropriate credit for the requested material should be given as follows: "Reprinted (adapted) with permission from (COMPLETE REFERENCE CITATION). Copyright (YEAR) American Chemical Society." Insert appropriate information in place of the capitalized words.
- One-time permission is granted only for the use specified in your request. No additional uses are granted (such as derivative works or other editions). For any other uses, please submit a new request.

BACK CLOSE WINDOW